Isolation and Functional Analysis of *Xenopus* Ephrin-A3

Taslima Khan

A Thesis for the Degree of Doctor of Philosophy

1999

Division of Developmental Biology and
Division of Developmental Neurobiology,
National Institute for Medical Research,
The Ridgeway,
Mill Hill,
London, NW7 1AA.

University College, London,
Gower Street,
London, WC1E 6BT.

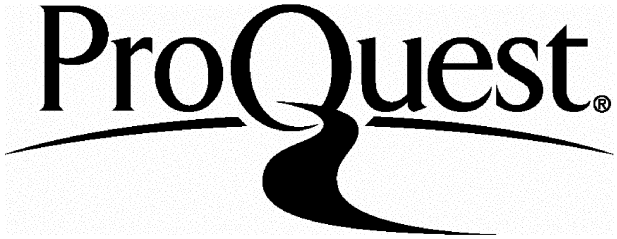

"We shall not cease from exploration
And the end of all our exploring
Will be to arrive where we started
And know the place for the first time.
Through the unknown, remembered gate
When the last of the earth left to discover
Is that which was the beginning;"

Little Gidding, T. S. Eliot.

To My Family
For Encouraging Me, Entertaining Me
and For Trying, So Often, To Understand This PhD

ABSTRACT

Segmentation is a primary requirement for the establishment of the vertebrate body plan and it is therefore of great interest to identify proteins involved in these patterning events. The Eph family is the largest sub-group of the Receptor Tyrosine Kinases (RTKs), and several Eph family members have been shown to have important roles in development, including maintenance of segmental boundaries and as guidance cues within the nervous system. Ligands of the Eph family, known as ephrins, have been identified in many vertebrate species where they have been shown to be expressed in many tissues during development and in the adult.

A PCR based strategy was used to isolate members of the ephrin-A class in *Xenopus*. RNAase protection analysis indicated that at two of the ephrins are expressed during gastrula and/or neurula stages. A library screen isolated XLIG4, one of these putative ephrins. Sequence analysis shows that XLIG4 is an ephrin-A3 homologue. Whole mount *in situ* hybridisation and RNAase protection in *Xenopus* embryos, revealed that Xephrin-A3 expression occurs throughout gastrulation, neurulation and tailbud stages, with dynamic expression in the migrating crest.

Functional analysis was carried out by overexpression of soluble and full length forms of Xephrin-A3 in the *Xenopus* embryo. Since Xephrin-A3 has expression within specific neural crest streams, it was possible Xephrin-A3 had a role in these cells. Utilising whole mount *in situ* analysis with molecular markers, it was found that both ephrin forms disrupted the migration pattern of neural crest, the severity of which depended on the concentration of ectopic Xephrin-A3 expressed. Ephrin-A class ligands interact EphA class receptors of which EphA4 is expressed in the third arch neural crest and EphA2 in the second arch neural crest in *Xenopus*. It is proposed that complementary and overlapping expression of ephrin-A3 and EphA receptors is involved in the targeted migration of branchial neural crest.

TABLE OF CONTENTS

	PAGE
Title	1
Dedication	2
Abstract	3
Table of Contents	4
List of Figures	10
List of Tables	13
Abbreviations	14
CHAPTER ONE: INTRODUCTION	
1.1 Introduction	17
1.2 Mesoderm Induction and Dorsalisation	18
1.3 Signalling Proteins and Neural Induction	18
1.4 TGF-β Superfamily	20
1.4.1 Activin	20
1.4.2 BMP4	21
1.4.3 Noggin, Follistatin and Chordin	21
1.5 Receptor Tyrosine Kinases	23
1.5.1 Structure	24
1.5.2 Signalling	27
1.5.3. SH2 and SH3 Domains	28
1.6 The Eph Receptor Family	28
1.6.1 Structure of Eph Receptors	29
1.6.2 Ligands of the Eph Receptor Tyrosine Kinase Family	33
1.6.3 Ephrin Structure and Binding Specificity Classes	33
1.6.4 Receptor and Ephrin Binding Analysis	33
1.6.5 Biochemistry of Eph Receptors	34

1.6.6 Cytoskeletal Associations 38
1.6.7 Signalling Through Ephrins 42
1.6.8 Eph Family Developmental Expression Patterns 45
1.6.9 Roles in Axonal Pathfinding in the Retinotectal System 46
1.6.10 Axonal Repulsion and Axon Fasiculation 48
1.6.11 Signal Transduction Through an Ephrin 49
1.7 Hindbrain Segmentation 50
1.7.1 *Hox* genes 51
1.7.2 *Krox20* 51
1.7.3 *Kreisler* 54
1.8 Compartments and Boundaries 55
1.8.1 A Role for an Eph Receptor in Hindbrain Segmentation 57
1.9 Neural Crest 60
1.9.1 Segmentation of Branchial Neural Crest 61
1.9.2 Neural Crest Migration 62
1.10 Cell Adhesion Molecules 63
1.11 Expression of Eph Receptors and Ligands in Neural Crest 64
1.11.1 Roles of Eph Receptors in Neural Crest Pathfinding 65
1.12 Roles in Angiogenesis 66
1.13 Roles in Adhesion 71
1.14 Aims of the Project 68
1.14.1 Hypothesis 72

CHAPTER TWO: MATERIALS AND METHODS

2.1 Standard Solutions: 74
2.2 Cloning and DNA Manipulation 75
2.2.1 Preparation of Competent Cells for Plasmid Transformation 76
2.2.2 Subcloning and Ligation 76
2.2.3 Bacterial Transformation 76
2.2.4 Isolation of Plasmid DNA in a Mini-Preparation 76
2.2.5 Maxi-Preparation of Plasmid DNA 77
2.2.6 Restriction Endonuclease Digests of DNA 77
2.2.7 Electrophoretic Separation of DNA and RNA 78

2.3 Embryo Culture and Manipulations 78
2.3.1 Microinjection of *Xenopus* Embryos 78
2.4 RNA Isolation 78
2.4.1 RT-PCR Cloning of Ephrins 79
2.4.2 Gel-Purification of DNA 80
2.5 DNA Sequence Analysis 80
2.5.1 Sequence Comparisons 80
2.6 Library Screening 81
2.6.1 Obtaining DNA from λgt10 Phage Library 81
2.6.2 Southern Blot 82
2.7 RNAase Protection 82
2.7.1 Preparation of Probe 82
2.7.2 Probe Purification 83
2.7.3 Hybridisation 83
2.7.4 Degradation of Non-Protected RNA 84
2.8 Whole Mount *in situ* Hybridisation 84
2.8.1 Preparation of Probe 84
2.8.2 Preparation of Embryos and Hybridisation 85
2.8.3 Post-Hybridisation Washes 85
2.8.4 Antibody Washes and RNA Detection 86
2.8.5 Fluorescein Dextran Detection 86
2.8.6 Clearing Embryos 87
2.8.7 Sectioning Embryos 87
2.9 *In vitro* Transcription and Translation 87
2.9.1 Creation of Truncated Xephrin-A3 87
2.9.2 *In vitro* Translation Reaction 88
2.9.3 *In vitro* Transcription Reaction 89
2.10 Northern Blotting Analysis 89
2.10.1 Preparation of Gel and RNA Samples 89
2.10.2 Preparation of Probe and Hybridisation 90

CHAPTER THREE: THE CLONING OF *XENOPUS* EPHRINS

3.1 Introduction 91

3.2 Results 91

3.2.1 RT-PCR Procedure 91

3.2.2 PCR Clone Analysis 97

3.2.3 PCR Class Categorisation 100

3.2.4 Sequence Comparisons of XLIG Class Clones 100

3.2.5 Analysis of XLIG1-5 Classes 105

3.2.6 Isolation and Sequence Analysis of an XLIG4 cDNA Clone 108

3.2.7 Analysis of XLIG4 cDNA Sequence 113

3.3 Discussion 113

3.3.1 XLIG Classes 123

3.3.2 The XLIG4 cDNA Analysis 124

3.3.3 Pseudotetraploidy 128

CHAPTER FOUR: THE EXPRESSION PATTERN OF *XENOPUS* EPHRINS

4.1 Introduction 129

4.2 Results 129

4.2.1 Temporal Profile of XLIG1-5 Classes 129

4.2.2 Expression Analysis of Xephrin-A3 132

4.2.3 Northern Blot Analysis 132

4.2.4 Whole Mount *in situ* Hybridisation 137

4.2.4.1 Early Neurula Stage Expression 137

4.2.4.2 Late Neurula to Tailbud Stage Expression 142

4.2.4.2.1 Summary 145

4.2.4.3 Late Tailbud Stage Expression 145

4.3 Discussion 145

4.3.1 Xephrin-A3 Expression in the Neural Crest 148

4.3.2 Role of the Eph Family in Neural Crest Migration 149

4.3.3 Xephrin-A3 in other species 152

4.3.4 Non-neuronal Xephrin-A3 expression 152

CHAPTER FIVE: FUNCTIONAL ANALYSIS OF XEPHRIN-A3

5.1 Introduction 153

5.2 Results 153

5.2.1 Subcloning the full length and soluble forms of Xephrin-A3 153

5.2.2 Microinjection of Full Length and Soluble Xephrin-A3 156

5.2.2.1 Microinjection of Full Length Xephrin-A3 156

5.2.2.1.1 *XKrox20* Analysis: Overexpression of 3-2ng Xephrin-A3 161

5.2.2.1.2 *XKrox20* Analysis: Overexpression of 2-1ng Xephrin-A3 164

5.2.2.1.3 *XKrox20* Analysis: Overexpression of 0.5-0.1ng Xephrin-A3 171

5.2.2.1.4 *XAP2* and EphA2 Analysis 171

5.2.2.2 Microinjection of Soluble Xephrin-A3 176

5.2.2.3 Targeted Blastomere Injections of Full Length and Soluble Xephrin-A3 182

5.2.2.4 Observations of Gastrulation 182

5.3 Discussion 186

5.3.1 The Effect of Ectopic Expression of Xephrin-A3 on Neural Crest Cell Migration 186

5.3.2 The Role Of Overlapping and Complementary Expression in Xephrin-A3 Function 190

5.3.2.1 The Role of Overlapping Expression in the Eph Family 190

5.3.2.2 The Potential Role of Xephrin-A3 Expression in the First Arch Neural Crest Cells 192

5.3.2.3 The Role of Complementary Expression in the Eph Family 193

5.3.3 The Effects of Lower Ectopic Xephrin-A3 Expression 194

5.3.4 Soluble Xephrin-A3 Ectopic Expression 195

5.3.5 Gastrulation Defects 196

5.3.5.1 Xephrin-A3 Ectopic Expression 196

5.3.5.2 Targeted Injections of Xephrin-A3 197

5.3.5.3 Fate change of Injected Blastomeres 197

5.3.6 Similarity of Full Length and Soluble Xephrin-A3 Overexpression Phenotypes 198

5.3.7 Comparing and Contrasting the Effect of Dominant-Negative EphA Receptors in *Xenopus* Neural Crest Migration with Xephrin-A3 198

CHAPTER SIX: DISCUSSION

6.1 Neural Crest Cell Migration 200

6.1.1 Generating Neural Crest Free Zones 200

6.1.2 Neural Crest Cell Guidance 200

6.1.3 The Role of the Eph Family 201

6.2 General Roles of Eph Receptors and Ephrins 202

6.3 Xephrin-A3 Expression Patterns 203

6.4 General Summary 204

6.5 Future Directions 206

BIBLIOGRAPHY 209

ACKNOWLEDGEMENTS 230

LIST OF FIGURES

PAGE

CHAPTER ONE: INTRODUCTION

Figure 1.1
Molecular phylogeny of the vertebrate members of the RTK family 26

Figure 1.2
Structure of Eph receptors and ephrins 32

Figure 1.3
Binding specificity classes of Eph receptor and ephrins 36

Figure 1.4
Summary model of Eph receptor signalling 41

Figure 1.5
Signalling through ephrins: predicted model for ephrin-B proteins 44

Figure 1.6
The branchial *Hox* code 53

Figure 1.7
Eph family receptor and ephrin hindbrain expression 59

Figure 1.8
The migration of *Xenopus* neural crest 68

Figure 1.9
Eph family receptor and ephrin expression in *Xenopus* branchial neural crest 70

CHAPTER THREE: THE CLONING OF *XENOPUS* EPHRINS

Figure 3.1
The primers chosen to amplify ephrins in *Xenopus* 93

Figure 3.2
Representative PCR gel obtained from ephrin isolation 96

Figure 3.3
An example of T-tracks obtained for several putative ephrin clones 99

Figure 3.4
The classes of clone obtained from the PCR analysis 103

Figure 3.5
Ephrin phylogenetic tree with the XLIG classes 107

Figure 3.6
A diagrammatic representation of the Xephrin-A3 cDNA 110

Figure 3.7
The nucleotide sequence and protein translation of the open reading frame of XLIG4 112

Figure 3.8
PileUp between vertebrate ephrins and Xephrin-A3 115

Figure 3.9
Vertebrate ephrin phylogenetic tree with Xephrin-A3 117

Figure 3.10
Peptide alignment of XLIG4 with murine ephrin-A3 120

Figure 3.11
Nucleotide alignment of XLIG4 with murine ephrin-A3 122

CHAPTER FOUR: THE EXPRESSION PATTERN OF *XENOPUS* EPHRINS

Figure 4.1
Temporal profile of Xephrin-A3 and XLIG5 131

Figure 4.2
Spatial localisation of Xephrin-A3 transcripts 134

Figure 4.3
Developmental RNAase protection 136

Figure 4.4
Northern Blot 139

Figure 4.5
Whole mount *in situ* hybridisation of Xephrin-A3 at early neurula stages 141

Figure 4.6
Whole mount *in situ* hybridisation of Xephrin-A3 during branchial neural crest migration 144

Figure 4.7
Whole mount *in situ* hybridisation of Xephrin-A3 at late tailbud stages 147

Figure 4.8
Eph family expression in *Xenopus* branchial neural crest 151

CHAPTER FIVE: FUNCTIONAL ANALYSIS OF XEPHRIN-A3

Figure 5.1
The amino acid sequences of the full length and soluble Xephrin-A3 injection constructs 155

Figure 5.2
In vitro translation of full length and soluble Xephrin-A3 158

Figure 5.3
XKrox20 analysis: Overexpression of 3-2ng Xephrin-A3 160

Figure 5.4
Serial sections indicating the absence of third arch neural crest cell migration 163

Figure 5.5
XKrox20 Analysis: Overexpression of 2ng Xephrin-A3 166

Figure 5.6
Horizontal sections of *XKrox20* hybridised third arch neural crest cells of 2ng injected embryo 168

Figure 5.7
XKrox20 Analysis: Overexpression of 1ng Xephrin-A3 170

Figure 5.8
XKrox20 Analysis: Overexpression of 0.5-0.1ng Xephrin-A3 173

Figure 5.9
XAP2 Analysis of Xephrin-A3 injected embryos 175

Figure 5.10
Ectopic soluble Xephrin-A3 expression 179

Figure 5.11
Targeted injections in the 32 cell stage *Xenopus* embryo 184

Figure 5.12
Ectodermal lesions in gastrula stage embryos 187

CHAPTER SIX: DISCUSSION

Figure 6.1
Eph Family Overlapping and Complementary Interactions in *Xenopus* Branchial Neural Crest 205

LIST OF TABLES

PAGE

CHAPTER ONE: INTRODUCTION

Table 1
Eph receptor and ephrin nomenclature 30

CHAPTER THREE: THE CLONING OF *XENOPUS* EPHRINS

Table 2
The breakdown of the classes obtained from the PCR analysis 101

Table 3
Peptide identities between the XLIG Classes and their closest homologues 104

Table 4
Peptide Identities between the XLIG4 cDNA clone and all other cloned ephrin-A ligands 118

Table 5
Peptide Identities between murine ephrin-A5 and all other cloned ephrin-A ligands 125

Table 6
Peptide Identities between *Xenopus* ephrin-A1 and all other cloned ephrin-A ligands 126

CHAPTER FIVE: FUNCTIONAL ANALYSIS OF XEPHRIN-A3

Table 7
Composite table of injections performed in 1 cell of the 2 cell stage *Xenopus* embryo 180

Table 8
Data for a typical injection experiment with reference to gastrula stage embryo death 181

Table 9
Data for the targeted overexpression injections 185

Table 10
Xbra expression in stage 10 embryos ectopically expressing full length and soluble Xephrin-A3. 189

ABBREVIATIONS

A-P	anterioposterior
ATP	adenosine-5'-triphosphate
bp	base pair
BMP	bone morphogenic protein
BSA	bovine serum albumin
cDNA	complementary DNA
C-terminal	carboxy-terminal
CNS	central nervous system
CTP	cytosine-5'-phosphate
DEPC	diethylpyrocarbonate
DMSO	dimethylsulpoxide
DNA	deoxyribonucleic acid
dpc	days post coitum
DTT	dithiothreitol
EDTA	diaminoethanetetraacetic acid
EGF	epidermal growth factor
EGFR	epidermal growth factor receptor
Eph	erythropoietin-producing hepatoma cell line
Fig.	figure
FGF	fibroblast growth factor
FRL1	FGF related factor
GPI	glycosylphosphatidylinositol
GTP	guanosine-5'-triphosphate
HOX	homeobox
IC	inferior colliculus
IgG	immunoglobulin G
JNK	Jun N-terminal Kinase
Kb	kilobase
kDa	kilodalton
LacZ	β-galactosidase
LMW-PTP	low molecular weight phosphotyrosine phosphatase
M	molar

ml	millilitre
mM	millimolar
mRNA	messenger RNA
MW	molecular weight
N-terminal	amino-terminal
NCAM	neural cell adhesion molecule
ng	nanogram
Ng-CAM	neuron-glia cell adhesion molecule
nl	nanolitre
OD	optical density
ODC	ornithine decarboxylase
PAGE	polyacrylamide gel electrophoresis
PCR	polymerase chain reaction
PDGF	platelet-derived growth factor
PDGFR	platelet-derived growth factor receptor
PDZ	post-synaptic density protein
PEG	polyethylene glycol
PH	pleckstrin homology
PI3	phosphatidylinositol 3 kinase
PLCγ	phospholipase C
PNA	peanut agglutinin
PNS	peripheral nervous system
PY	phosphotyrosine
r	rhombomere
RNA	ribonucleic acid
RNAase	ribonuclease
RPTK	receptor protein tyrosine kinase
RTK	receptor tyrosine kinase
SAM	sterile alpha motif
SDS	sodium dodecyl sulphate
SH2	Src homology 2 domain
SH3	Src homology 3 domain
SLAP	Src-like adaptor protein
St.	stage
TGF-β	transforming growth factor
Tris	2-amino-2-(hydroxymethyl)-propane-1,3-diol

UV	ultraviolet
µg	microgram
µl	microlitre
µm	micromolar
WASP	Wiskott-Aldrich Syndrome protein
XLIG4	*Xenopus* ligand 4
Y	tyrosine residue

CHAPTER ONE

1.1 INTRODUCTION

Embryonic development begins with the fertilisation of the egg. Development of this single cell gives rise to many cell types creating both tissues and organs, a result of highly ordered and specific cellular arrangements. These patterns are due to several concurrent processes including: cell proliferation and cell death; cell differentiation to generate many different cell types; pattern formation where specific cell types are arranged into specific spatial arrangements; and morphogenesis in which the physical form of tissues arises.

During early vertebrate development a series of processes establishes the major tissues and organisation of the body plan. One of the first morphogenic events is the process of gastrulation in which mesodermal cells are induced to form, migrate and differentiate. Neuralising signals induce presumptive epidermis to become neural ectoderm, leading to the establishment of the vertebrate central nervous system. *Xenopus* has provided many of the clues followed to understand the role of signals and their action in neural induction.

The source of signals that ultimately lead to the specification of neural fate, known as neural induction, arise in *Xenopus* from a region of tissue known as Spemann's organiser (reviewed by (Harland and Gerhart, 1997)). In the mouse and chick, this region is called the node. I shall describe the origin of the organiser and its roles with special attention to the primary neural induction signals in *Xenopus laevis.*

The *Xenopus* embryo provides an excellent system to study patterning. Firstly, it develops outside the mother allowing easy access to all stages of development. Secondly, the embryo is large and robust making injection and dissection straightforward. And thirdly, *Xenopus* development is well characterised from oogenesis to later stages of differentiation, allowing body plan pattern defects to be easily analysed.

1.2 Mesoderm Induction and Dorsalisation

The fertilised *Xenopus* embryo consists of the uppermost, darkly pigmented animal hemisphere and the lightly pigmented vegetal hemisphere. These regions harbour two cell types: prospective ectoderm in the animal hemisphere and prospective endoderm in the vegetal hemisphere. Mesoderm arises from inductive interactions in which vegetal cells act on cells in the equatorial region (the marginal zone) of the embryo causing them to form mesoderm rather than ectoderm (reviewed by (Smith, 1995)). The vegetal cells provide two signals: ventral vegetal cell signals induce ventral mesoderm and dorso-vegetal cells induce the formation of dorsal mesoderm (dorsal marginal zone), also known as the organiser. These two signals form part of the three signal model (Smith and Slack, 1983). The third signal emanates from the organiser, which imposes more dorsal and intermediate fates on neighbouring ventral mesoderm in the gastrula stage embryo.

The organiser is a population of cells comprising of 5% of the gastrula. Three of its main roles include; induction, self-differentiation. and morphogenesis. Inductive signalling affects the mesoderm, ectoderm and endoderm. The signals that dorsalise the mesoderm give rise to the heart, kidney and somites, (from which the sclerotome, bone and cartilage; myotome, muscle; and dermotome, dermis; derive from secondary inductions). Neural induction of the ectoderm utilises organiser signals and anterior endoderm, such as the pancreas and liver, seem to require signals form the organiser.

The organiser cells self-differentiate into mesodermal and endodermal derivatives including notochord and prechordal head plate mesoderm, and pharyngeal endoderm and anterior gut tissues respectively.

Organiser-dependent morphogenesis consists of movements of the organiser cells themselves and the movements they induce in neighbours such as: posterior organiser cells (prospective notochord cells) engaging in convergent extension, leading to the backward extension of the forming notochord (reviewed in (Harland and Gerhart, 1997)).

1.3 Signalling Proteins and Neural Induction

In *Xenopus*, the first interaction of the naive ectoderm with the organiser results in neural induction, a process that is believed to begin at stage 10, the onset of gastrulation and

continues to stage 12.5 (Albers, 1987); (reviewed by (Harland and Gerhart, 1997; Harland, 1994; Hemmati-Brivanlou and Melton, 1997; Kessler and Melton, 1994)).

The induction of neural plate is believed to be the result of two steps; the first is neuralisation of the naive ectoderm and the second, the posteriorisation of the neuralised ectoderm. The neuralisation step leads to the differentiation of the anterior neural tissue alone such as fore- and midbrain, pituitary gland and perhaps the cement gland. Caudalisation of the neural plate leads to the development of the hindbrain and spinal cord. The second effect modifies the actions of the first and has no neuralising effect of its own. The initial neuralisation signals are suggested to be presented vertically from the first involuted part of the organiser, that can then be spread both anteriorly and laterally due to propagated planar signalling within the ectoderm (Nieuwkoop and Koster, 1995). It is further suggested that the location of the border of the neural plate is determined by the loss of competence of the cells concerned to respond to the planar signals, rather than the signal being too low for response at the end of a gradient. Caudalisation continues until the closure of the neural tube at stage 16 (Nieuwkoop and Albers, 1990). The caudalisation signals are also thought to both be vertical and planar.

Several neural specific marker genes have been cloned which reveal events of early neural induction. The *Xotx2* gene is expressed in the mid-gastrula embryo, in the approximate regions of the neural plate (Blitz and Cho, 1995). *En* (*engrailed*), is already expressed as a stripe delimiting the boundary between the midbrain and hindbrain in the late gastrula (Hemmati-Brivanlou *et al.,* 1991). As broad domains refine into distinct rostro-caudal regions, patterning in the regions of the fore-, mid- and hindbrain and the spinal cord takes place. Genes such as *Krox20* in the hindbrain and *Hox* genes are expressed in a rostro-caudal sequence from the hindbrain to the spinal cord. *Sox-2* is the earliest marker of neuralised cells in the early *Xenopus* embryo (Mizuseki *et al.,* 1998). In addition, *Xslu* (*slug*) and twist homologues are expressed at the borders of the neural plate where neural crest cells appear (Hopwood *et al.,* 1989; Mayor *et al.,* 1995).

The concept of neural induction was introduced when it was shown that the transplantation of the blastopore lip (the organiser) from one salamander gastrula, to the ventral side of another gastrula stage embryo, caused formation of a second nervous system (Spemann and Mangold, 1924). Ordinarily, the ventral ectoderm that was induced to become the second nervous system, becomes epidermis. This suggested that the

organiser was inducing and organising a patterned nervous system on neighbouring dorsal ectoderm, which without these signals would be epidermis.

Signalling candidates have been identified that appear to have either a) direct roles in the induction of neural tissue, b) inhibition of their signalling promotes neural induction or c) their signalling induces neural tissue indirectly. The principle soluble signalling proteins that have been identified, known as morphogens, include activin, the growth factor BMP4 (bone morphogenic protein) and the neural inducers noggin, follistatin and chordin.

1.4 TGF-β Superfamily

1.4.1 Activin

Several growth factors with mesoderm-inducing activity such as activin, a member of the TGF-β growth factor superfamily, and Vg-1, cause the formation of neural tissue when added to animal caps, the prospective ectoderm of the animal pole of the gastrula. This ability is indirect since they initially induce mesoderm formation that mimics the action of the organiser to induce neural tissue. In one such experiment the animal cap of either the late blastula or gastrula was removed. The animal caps were then either cultured in buffer or exposed to activin (Green and Smith, 1990). Animal caps placed in buffer formed epidermis. However, the blastula animal cap exposed to activin is induced to form mesodermal tissues; dorsal mesoderm then secondarily induced ectoderm, which without further access to activin became neural tissue. The gastrula cap has lost its ability to respond to activin and therefore forms epidermis.

However, further experiments involving the activin type II receptor suggested that the prevention of activin signalling contributed to neuralisation (Hemmati-Brivanlou and Melton, 1992). In experiments originally intended to test for a requirement for activin in mesoderm induction, animal caps resulting from the injection of a truncated type II activin receptor, where found to express NCAM (neural cell adhesion molecule), a pan neural marker. This expression was observed in the presence of little or no mesoderm. Therefore, an inhibition of activin signalling was associated with an inhibition of mesoderm induction leading to direct neuralisation (Hemmati-Brivanlou and Melton, 1992). This observation coupled with experiments indicating the animal cap is

predisposed to form neural tissue, suggests that neuralisation is a default state (Hemmati-Brivanlou and Melton, 1994).

1.4.2 BMP4

Further evidence for the default state was provided by experiments with BMP4. It had been noted that the truncated activin type II receptor was found to inhibit not only the type II activin receptor but other TGF-β members including BMP's and the processed form of Vg-1 (Hemmati-Brivanlou and Thomsen, 1995; Schulte-Merker *et al.,* 1994). Therefore, BMP signalling may have a role in neural induction. A complementation assay was set up were cells of the animal cap were dissociated and incubated in the presence of or absence of activin or BMP4, both ligands of the TGF-β family previously shown to be inhibited by the truncated activin type II receptor. Ectopic expression of BMP4 is known to cause ventralisation of *Xenopus* embryos (Dale *et al.,* 1992; Jones *et al.,* 1992) and expression of a truncated BMP4 receptor in the early *Xenopus* embryo causes the embryo to become dorsalised (Schmidt *et al.,* 1995). Activin was found to inhibit the neuralisation of the dissociated ectodermal cells by inducing mesodermal tissue, however, the expression of epidermal markers was not induced. In contrast, BMP4 inhibited neuralisation and induced epidermal fate (Wilson and Hemmati-Brivanlou, 1995). This ability of BMP4 to suppress neuralisation and induce epidermal induction, suggested that neuralisation is a default state which is prevented by positive signalling amongst ectodermal cells to produce epidermis. This action is favoured in the Wilson *et al* (1995) neuralisation model (Wilson and Hemmati-Brivanlou, 1995).

These experiments suggested that the inhibition of BMP4 expression contributes to neuralisation. Additionally, antagonists of BMP4 signalling lead to neuralisation. For example, the dominant negative type I receptor for BMP4/2, which does not inhibit Vg-1 or activin signalling, induces neural tissue in animal caps and dominant negative forms of the BMP4 and BMP7 ligands directly induce neural tissue in animal caps (Hawley *et al.,* 1995).

1.4.3 Noggin, Follistatin and Chordin

Several molecules have been identified that have neural inducing activity in various assays: these soluble proteins include noggin, follistatin and chordin, all of which are expressed in the organiser. Noggin and chordin satisfy at least two of the three (see later)

requirements for putative neural inducers; the first, they are present at the right time and place in the embryo to elicit their actions and secondly, the purified protein, when presented to the normal responsive tissue, elicits a normal response (Bouwmeester *et al.,* 1996; Lamb *et al.,* 1993; Piccolo *et al.,* 1996; Sasai *et al.,* 1994; Smith *et al.,* 1993).

Noggin was found to directly induce neuralisation in late blastula or gastrula animal caps, without the induction of mesoderm (Cunliffe and Smith, 1994; Knecht *et al.,* 1995). Similarly, animal caps expressing follistatin will directly turn on neural markers (Hemmati-Brivanlou *et al.,* 1994). Follistatin can function as an inhibitor by binding activin, and therefore possibly function by interfering with activin receptor signalling, aiding the formation of neural plate. Chordin (Chd) is able to rescue UV-ventralised embryos and dorsalise mesoderm. It shares strong sequence homology with *Drosophila sog* (*short gastrulation*) gene and has direct neural inducing ability (Sasai *et al.,* 1995). Noggin and chordin specifically bind BMP4 *in vitro* (Piccolo *et al.,* 1996; Zimmerman *et al.,* 1996), but have not been shown to bind activin or TGF-β1. Therefore, endogenous BMP4 present in the mesoderm, is removed from the organiser (Fainsod *et al.,* 1995; Schmidt *et al.,* 1995). This would suggest that antagonistic binding of BMP4 by noggin and chordin allows neural fate induction on the dorsal side. However, there is no *in vivo* evidence for any of these molecules binding BMP4. Recent work investigating the role of chordin and BMP4 in the chick has discovered that the ectopic expression of BMP4 in the presumptive neural plate does not interfere with neural induction and chordin is not sufficient to induce neural tissue; misexpression in regions outside the future neural plate does not induce early neural markers (Streit *et al.,* 1998). Therefore, neural induction in the chick is not as proposed in *Xenopus*; the chordin/BMP system may work downstream of, or in conjunction with, other factors produced by the organiser.

A third criterion for a neural inducer holds that if the protein is essential, its removal will disrupt neural induction for example. Presently three knockout examples have been characterised: during early neuralisation the *noggin*$^{-/-}$ knockout mouse has an essentially normal neural tube and somites. This indicates successful neural induction and dorsalisation. However, older mutants develop severe neural patterning and skeletal defects (McMahon *et al.,* 1998). Therefore, noggin may not be involved in primary neural induction but in dorso-ventral patterning of the neural tube. The *chordino* mutant in zebrafish, is a chordin mutant; it is partially ventralised, with a reduced neural tube,

small somites and an expanded ventral region (Schulte-Merker *et al.,* 1997). The role of follistatin is not clear: the *follistatin*$^{-/-}$ knockout mouse has few alterations in early development (Matzuk *et al.,* 1995) and in comparative studies it is expressed in the lateral plate mesoderm and not the node (Albano *et al.,* 1994). Therefore, noggin and chordin partially meet the third requirement.

It is possible that the functions of noggin and chordin partially overlap. Both proteins dorsalise and neuralise mesoderm (Knecht *et al.,* 1995; Sasai *et al.,* 1994; Smith *et al.,* 1993), anteriorise endoderm (Sasai *et al.,* 1996) and bind BMPs (Piccolo *et al.,* 1996; Zimmerman *et al.,* 1996). They differ mostly in their diffusibility: noggin can dorsalise the entire embryo when it is expressed locally in a small ventral sector whereas chordin acts more locally (Sasai *et al.,* 1994; Smith and Harland, 1992). Therefore compound knockouts would provide an improved environment to study the function of these genes.

Four further candidates for neural inducers are Cerberus (Bouwmeester *et al.,* 1996), Xnr3 (Smith and Harland, 1992) Smith, 1995), FGF (Kengaku and Okamoto, 1993) and FRL1 (an FGF related factor) (Harland, 1994; Kinoshita *et al.,* 1995). Cerberus appears to block mesoderm formation, induce anterior neural tissue and act as a antagonist of nodal, BMP and Wnt signalling (Bouwmeester *et al.,* 1996; Piccolo *et al.,* 1999). Xnr3 (*Xenopus* nodal related) is a TGF-β family member that is expressed in the organiser and has direct neural inducing activity that is mediated through BMP4 inhibition (Hansen *et al.,* 1997). If cells are dissociated and cultured in low amounts of FGF, several neural cell types are produced but it is likely that FGF serves as a neural differentiating agent (Amaya *et al.,* 1993). Indeed, FGF has been shown to induce all neural markers tested.

Further cell signalling interactions have been shown to have a role in cell type differentiation, proliferation, survival and migration. The cell-cell communication necessary to relay these signals can be carried out by many classes of receptors including GPI-anchored receptors, cytoplasmic receptors such as hormone and retinoic acid receptors and a large family known as the Receptor Tyrosine Kinase family.

1.5 Receptor Tyrosine Kinases

One form of cell-cell communication involves the transduction of an extracellular signal to within the cell by cell surface receptors. These receptors are a diverse class of

membrane spanning proteins to which are attributed many cellular responses, including cell proliferation (Derynck, 1994; Marikovsky *et al.,* 1995), cell differentiation (Miettinen *et al.,* 1994) and cell survival (Glass *et al.,* 1991). Examples of extracellular signalling molecules include the FGFs (fibroblast growth factors) and PDGFs (platelet-derived growth factors), secreted molecules that have been implicated in vertebrate embryogenesis. One of the largest cell surface receptor families is the Receptor Tyrosine Kinase (RTK) family, (reviewed by (Schlessinger and Ullrich, 1992; Ullrich and Schlessinger, 1990; van der Geer *et al.,* 1994)), of which over fifty members have been identified in vertebrates.

1.5.1 Structure

Structurally, the RTKs consist of three major domains; an extracellular domain that binds the growth factor ligand and is connected, via a single membrane-spanning domain, to a cytoplasmic domain. The intracellular cytoplasmic domain contains tyrosine residues which become phosphorylated upon receptor activation. The activated tyrosine residues bind cytosolic proteins which themselves become activated and propagate the intracellular signal(s) further.

The RTKs can be organised into 14 distinct sub-families based on their ligand-binding domains (see Fig. 1.1) (van der Geer *et al.,* 1994). The mode of interaction of the RTKs with ligand can be divided into four classes. The goal of the interaction is to achieve receptor dimerisation, a process believed to be achieved by a ligand-induced conformational change. The juxtaposition of the cytoplasmic domains induces a conformational change that stimulates catalytic activity. Transphosphorylation of specific tyrosine residues then takes place between the dimerised receptors (reviewed in (van der Geer *et al.,* 1994)). The dimerisation of the

EGFR (epidermal growth factor receptor), a class I member, is not completely understood. The single EGF (epidermal growth factor) molecule binds to a single EGFR. EGF binding is believed to induce a conformational change, that stabilises the interaction between two adjacent EGFRs, allowing dimerisation (Schlessinger and Ullrich, 1992). The insulin receptor is a class II member. A single insulin growth hormone molecule will bind two receptors and induce receptor dimerisation by bridging the two receptor molecules. The PDGFR (platelet-derived growth factor receptor) is a class III member

Figure 1.1

Molecular phylogeny of the vertebrate members of the RTK family

This tree divides the members of the RTK family into subfamilies. The relatedness between the subfamilies, and individual members within those subfamilies, is indicated by tree branch length. The upper region of the figure is taken van der Geer and Hunter (1994). It was constructed using phylogenic tree software as described by Hanks and Quinn (1988).

The lower part of the figure was taken from Flanagan and Vanderhaeghen (1998). It was constructed using the Clustal programme.

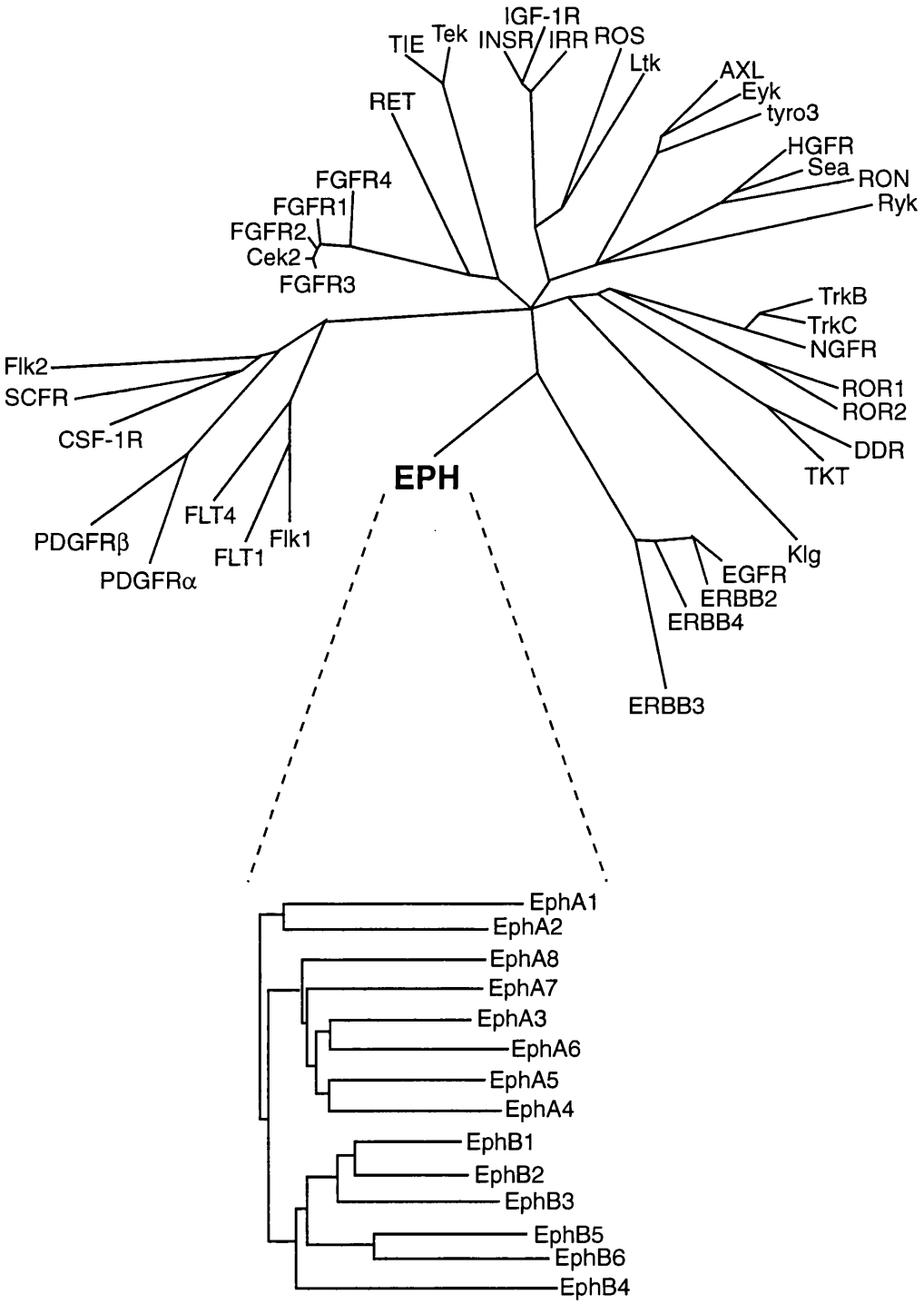
IGF-1R
INSR
IRR
TIE
Tek
ROS
Ltk
AXL
Eyk
tyro3
RET
HGFR
Sea
RON
Ryk
FGFR4
FGFR1
FGFR2
Cek2
FGFR3
TrkB
TrkC
NGFR
Flk2
SCFR
ROR1
ROR2
CSF-1R
DDR
TKT
EPH
FLT4
Flk1
FLT1
PDGFRβ
PDGFRα
Klg
EGFR
ERBB2
ERBB4
ERBB3
EphA1
EphA2
EphA8
EphA7
EphA3
EphA6
EphA5
EphA4
EphB1
EphB2
EphB3
EphB5
EphB6
EphB4

that binds the PDGF growth factor which is a dimeric molecule. PDGF bridges across two receptor molecules so bringing them together for dimerisation (Ullrich and Schlessinger, 1990). Eph receptors constitute the fourth class of receptor tyrosine kinases (Flanagan and Vanderhaeghen, 1998; van der Geer *et al.,* 1994). They will be discussed later.

1.5.2 Signalling

Cytoplasmic domain tyrosine residues (Y) phosphorylated due to receptor dimerisation, are able to bind cytosolic signalling molecules (reviewed in (Kazlauskas, 1994; van der Geer *et al.,* 1994)). RPTK (receptor protein tyrosine kinase) mutants demonstrate that RPTK signalling is absolutely dependent on the phosphorylation of specific cytoplasmic substrates, which have an increased affinity for the autophosphorylated receptors (Margolis *et al.,* 1990) and (reviewed by (Schlessinger and Ullrich, 1992; Ullrich and Schlessinger, 1990)).

There are many signalling substrates that interact with activated RTKs and they include enzymes, adaptor proteins and structural proteins (van der Geer *et al.,* 1994). The enzyme activity of PLCγ (Nishibe *et al.,* 1990), RasGAP (Vogel *et al.,* 1988) and PI3 kinase p85/p110 (Carpenter *et al.,* 1990), can be altered directly by phosphorylation or they can gain access to their substrates by translocation to the plasma membrane. Adaptor proteins include Nck (Meisenhelder and Hunter, 1992), Crk (Birge *et al.,* 1992), Grb2 (Lowenstein *et al.,* 1992), Grb10 (Ooi *et al.,* 1995) and Shc (Pelicci *et al.,* 1992); they have no obvious catalytic domain and are believed to serve as intermediates between RPTK's and downstream signalling molecules. The phosphorylation of structural proteins including cortactin, cadherins and F-actin binding protein can be responsible for membrane and cytoskeletal rearrangements, common on activation of a RPTK. Other signalling proteins such as p190 RhoGAP (Holland *et al.,* 1997) and $p62^{dok}$ (Yamanashi and Baltimore, 1997) are present. p190 RhoGAP, is a negative regulator of the small GTPase Rho (Holland *et al.,* 1997) and $p62^{dok}$, is a pleckstrin homology domain-containing protein that provides docking sites for phosphotyrosine (PY)-binding proteins (Yamanashi and Baltimore, 1997).

1.5.3 SH2 and SH3 Domains

Signalling proteins often contain a region of approximately 100 amino acids termed Src homology 2 domains (SH2) with which they interact with the activated RPTK. The SH2 domains represent recognition motifs for specific tyrosine-phosphorylated peptide sequences. The binding of SH2 domain-containing proteins to the activated RPTK can affect the protein in at least three ways, which are not necessarily mutually exclusive: First, the binding to the activated RPTK may cause tyrosine phosphorylation of the SH2 domain-containing protein resulting in activation or inhibition effects; second, binding may cause allosteric activation of the binding protein; and third, the localisation of the SH2-containing proteins and proteins that bind to this SH2 domain-containing protein, in close proximity to their substrates on the inner face of the plasma membrane. SH2 domains are often accompanied by SH3 domains, conserved domains of approximately 60 amino acids in length. These domains are also involved in protein-protein interactions (van der Geer *et al.,* 1994).

A less understood role is that of the pleckstrin-homology (PH) domain, which is a third domain found in many signalling proteins. *In vitro*, the pleckstrin homology domain is shown to interact with inositol phospholipids to aid their cellular translocation (Irvine, 1998) and it is involved in protein-protein interactions such as serving as a binding site for the G protein βγ subunit on the βARK protein kinase (Koch *et al.,* 1993).

1.6 The Eph Receptor Family

The Eph family is the largest subfamily of the RTKs with at least 14 vertebrate members identified to date (see Fig 1.1) (Friedman, *et al.,* 1996; Muller *et al.,* 1996; Pandey *et al.,* 1995b; van der Geer *et al.,* 1994; Drescher, 1997; Flanagan and Vanderhaeghen, 1998; Orioli and Klein, 1997; Pasquale, 1997). The archetype of this family, EphA1 (Harai *et al.,* 1987), was isolated during a search for gene sequences homologous to the tyrosine kinase domain of the viral oncogene *v-fps*, and was found to be over-expressed in the human erythropoietin-producing hepatoma cell line, ETL-1. Further members of this family have been isolated in a variety of ways: mouse EphA4 (Gilardi-Hebenstreit *et al.,* 1992; Neito *et al.,* 1992), for example, was found by polymerase chain reaction (PCR) amplification of cDNA from 9.5-day-old mouse embryo hindbrains using redundant oligonucleotides corresponding to protein kinase catalytic domain-coding sequences.

This method and cross-hybridisation techniques allowed other receptors of this family to be isolated (Fox *et al.,* 1995; Ganju *et al.,* 1994; Maisonpierre *et al.,* 1993; Valenzuela *et al.,* 1995). Many receptors were initially identified using anti-phosphotyrosine antibodies; a monoclonal antibody to a lymphoid cell surface antigen was used to identify EphA3 (Boyd *et al.,* 1992) and an Eph receptor, *vab-1*, has recently been identified in a screen of *Caenorhabditis elegans* (*C.elegans*) epidermal mutants (George *et al.,* 1998). The identification of many members of the family in a short period of time, resulted in multiple names for the same genes, therefore, a new nomenclature was established to systemise the naming of Eph family receptors and their ligands as shown in Table 1 (Eph Nomenclature Committee, 1997).

1.6.1 Structure of Eph Receptors

All members of this sub-family are characterised by extracellular domains: a 'globular' domain at the amino terminus (Labrador *et al.,* 1997), which consists of a jellyroll folding topology (Himanen *et al.,* 1998), followed by a cysteine rich region and two fibronectin type III repeats (see Fig. 1.2) (Connor and Pasquale, 1995; Flanagan and Vanderhaeghen, 1998; Kenny *et al.,* 1995; Wilkinson, 1999). These domains are followed by a single transmembrane domain and an intracellular cytoplasmic region consisting of a tyrosine kinase domain flanked by a juxtamembrane region and a carboxy-terminal (C-terminal) tail. Variant forms of the receptors exist. They do not conform to the prototypical receptor structure mostly due to domain deletions and truncations (Ciossek *et al.,* 1995; Connor and Pasquale, 1995; Maisonpierre *et al.,* 1993; Sajjadi *et al.,* 1991; Sajjadi and Pasquale, 1993; Tang *et al.,* 1998; Valenzuela *et al.,* 1995). EphB6 lacks kinase activity: its kinase domain contains amino acid substitutions within conserved consensus motifs known to be crucial for kinase activity. However, the ligand binding domain is intact and predicted to bind ligand (Gurniak and Berg, 1996).

The Eph receptor family represents the fourth class of receptor-ligand interactions in the RTK family. It is known that ligand clustering is required for receptor activation as discussed later (Davis *et al.,* 1994). Recently, a series of deletion and domain substitution mutants have shown that the N-terminal domain of the Eph receptor is sufficient for ligand binding (Labrador *et al.,* 1997). Additionally, distinct subdomains within the N-terminal region of the extracellular domain of the EphA3 receptor have been identified as mediators of ligand binding and receptor dimerisation (Lachmann *et al.,* 1998).

Receptors		Ligands	
New Name	Previous Names	New Name	Previous Names
EphA1	Eph, Esk	ephrin-A1	B61; LERK-1, EFL-1
EphA2	Eck, Myk2, Sek2	ephrin-A2	ELF-1; Cek7-L, LERK-6
EphA3	Cek4, Mek4, Hek, Tyro4; Hek4	ephrin-A3	Ehk1-L, EFL-2, LERK-3
EphA4	Sek, Sek1, Cek8, Hek8, Tyro1	ephrin-A4	LERK-4; EFL-4
EphA5	Ehk1, Bsk, Cek7, Hek7; Rek7	ephrin-A5	AL-1, RAGS; LERK-7, EFL-5
EphA6	Ehk2; Hek12		
EphA7	Mdk1, Hek11, Ehk3, Ebk, Cek11		
EphA8	Eek; Hek3		
EphB1	Elk, Cek6, Net; Hek6	ephrin-B1	LERK-2, Elk-L, EFL-3, Cek5-L; STRA-1
EphB2	Cek5, Nuk, Erk, Qek5, Tyro5, Sek3; Hek5, Drt	ephrin-B2	Htk-L, ELF-2; LERK-5, NLERK-1
EphB3	Cek10, Hek2, Mdk5, Tyro6, Sek4	ephrin-B3	NLERK-2, Elk-L3, EFL-6, ELF-3; LERK-8
EphB4	Htk, Myk1, Tyro11; Mdk2		
EphB5	Cek9; Hek9		
EphB6	Mep		

Table 1

Eph receptor and ephrin nomenclature

Many members of the Eph family were identified in a short period of time which resulted in multiple names for the same genes. Therefore a new nomenclature was established to systemise the naming of the Eph family receptors and their ligands.

The names are listed by publication date with full-length sequences shown first. Names after a semicolon indicate hypothetical orthologs or proposals to rename a sequence that had previously been published. (Eph Nomenclature Committee, 1997).

Figure 1.2

Structure of Eph receptors and ephrins

Left: A schematic representation of the Eph receptor family is shown. The main extracellular features include: the N-terminal ligand-binding domain, cysteine-rich domain and two fibronectin type III repeats. These domains are followed by a single transmembrane domain and an intracellular cytoplasmic region consisting of a tyrosine kinase domain flanked by a juxtamembrane region and a carboxy-terminal (C-terminal) tail.

Right: The ephrins fall into two structural classes based upon the nature of their membrane attachment. The ephrin-A class ligands contain a glycosylphosphatidylinositol (GPI) linkage at the C-terminus, which anchors the protein in the plasma membrane. The ephrin-B class have a transmembrane and C-terminal cytoplasmic domain.

Figure adapted from Wilkinson (1999).

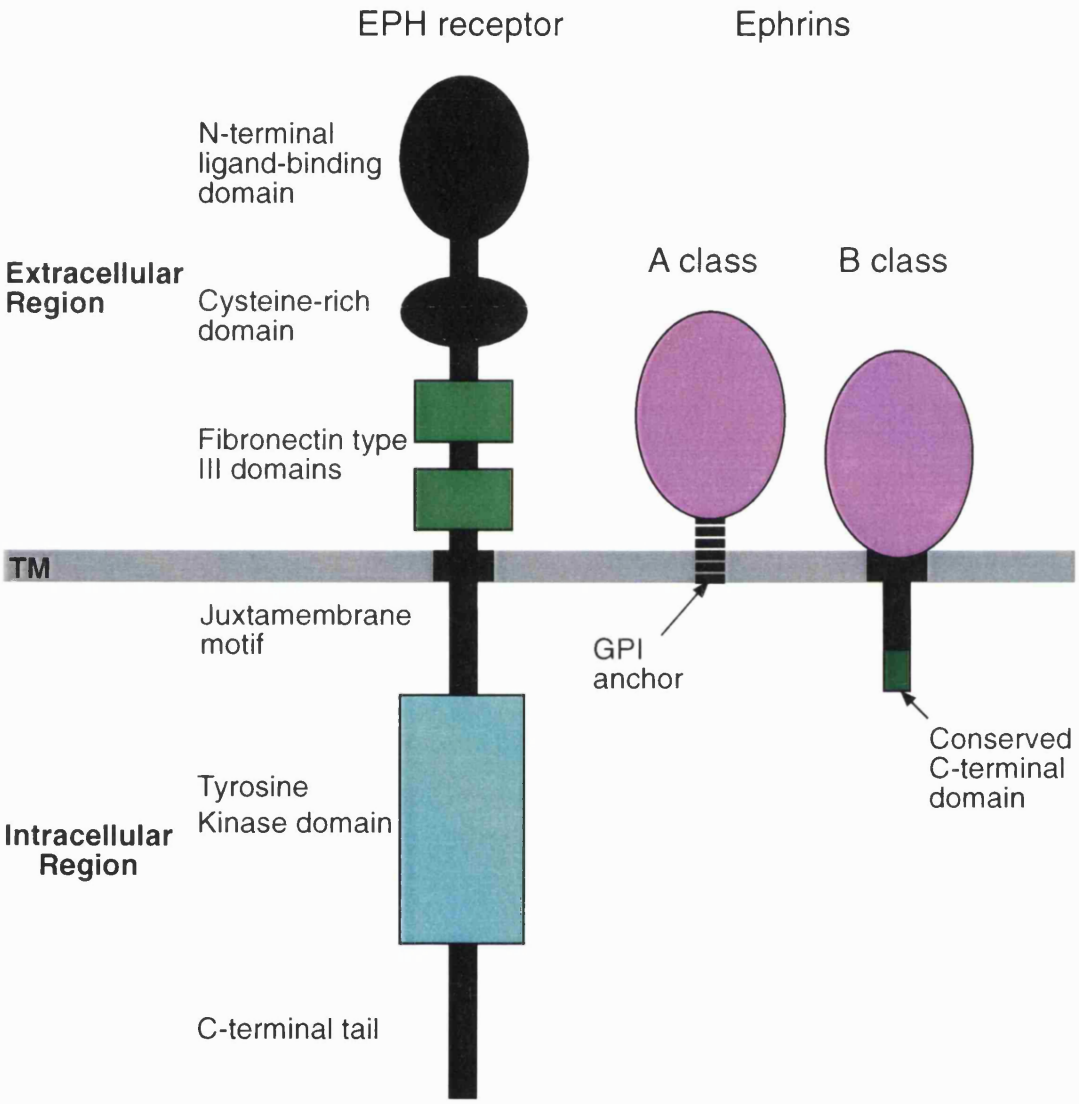
EPH receptor
Ephrins
N-terminal ligand-binding domain
Extracellular Region
Cysteine-rich domain
A class
B class
Fibronectin type III domains
TM
Juxtamembrane motif
GPI anchor
Conserved C-terminal domain
Tyrosine Kinase domain
Intracellular Region
C-terminal tail

1.6.2 Ligands of the Eph Receptor Tyrosine Kinase Family

The Eph family of RTKs was an orphan receptor family until 1994 when ephrin-A1, a protein that was previously cloned as a tumour necrosis factor-inducible sequence named B61 in endothelial cells (Holtzman *et al.,* 1990), was subsequently identified by others as a ligand for EphA2. Its role as a ligand was uncovered when a group (Bartley *et al.,* 1994), covalently bound the extracellular domain of the receptor to dextran for use in affinity chromatography. Cell culture supernatants were screened and supernatant proteins that bound to the column were assessed for receptor binding activity.

Of the proteins isolated, a single sequence was revealed which matched that of B61, now named ephrin-A1. Since then, eight ligands of this ephrin family (Eph Nomenclature Committee, 1997), in various species, have been published. The ephrins have largely been identified by screening of expression libraries with fusion proteins between receptor extracellular domain and Fc portions of IgG or alkaline phosphatase. In addition, several orthologues of ephrins in different species have been obtained by screening libraries or by PCR (Beckmann *et al.,* 1994; Bennett *et al.,* 1995; Bergemann *et al.,* 1995; Cerretti *et al.,* 1995; Cheng and Flanagan, 1994; Drescher *et al.,* 1995; Kozlosky *et al.,* 1995; Shao *et al.,* 1994; Shao *et al.,* 1995; Weinstein *et al.,* 1996; Winslow *et al.,* 1995). Ephrin-A5 was identified independently in a screen for molecules involved in retinotectal development (Drescher *et al.,* 1995).

1.6.3 Ephrin Structure and Binding Specificity Classes

All ephrins have a core sequence of approximately 125 amino acids which includes a potential receptor binding region that contains four conserved cysteine residues, and a membrane attachment region (Fig. 1.2) (Pandey *et al.,* 1995b; Wilkinson, 1999). The ephrins can be sub-divided into two classes based upon the nature of their membrane attachment which can be via a transmembrane domain, for the three members of the ephrin-B class or a glycosylphosphatidylinositol (GPI) linkage for the five members of the ephrin-A class.

1.6.4 Receptor and Ephrin Binding Analysis

Receptor binding studies reveal that the Eph-related receptors can be divided into two classes: those receptors that preferentially bind the transmembrane ephrins, the EphB

class, or the GPI-anchored ephrins, the EphA class (Gale *et al.,* 1996b). Within each ephrin-receptor binding class, interactions are promiscuous. For example, the receptors EphB1, EphB2 and EphB3 all interact with ephrin-B1 *in vitro* (Brambilla *et al.,* 1995). EphA4 is an exception to the binding classes since it interacts with ephrins of both sub-classes (Gale *et al.,* 1996a; Gale *et al.,* 1996b). The receptor-ephrin interactions are shown in Fig. 1.3 (O'Leary and Wilkinson, 1999). There are differences of affinity between receptors and specific ephrins which may be functionally important. The affinity studies all utilised one partner in an artificial soluble form however, when the receptors and ligands are present in interacting cell surfaces, *in vivo* binding is likely to be multivalent and co-operative. Therefore, the lowest affinities as well as the highest affinities observed between receptors and ligands, may be biologically significant (Flanagan and Vanderhaeghen, 1998; Gale *et al.,* 1996b).

Several experiments were conducted to determine the nature of ephrin-induced Eph receptor activation (Davis *et al.,* 1994). Taking receptor-expressing reporter cells and stimulating them with COS cells overexpressing membrane-bound ephrin (EphB1/ephrin-B1 or EphA5/ephrin-A1), they found Eph receptor activation, as judged by phosphorylation. Repeating the experiment with soluble monomeric ephrin, no receptor phosphorylation was evident. It was reasoned that the membrane attachment might facilitate ligand dimerisation or clustering, or both, which would subsequently promote receptor multimerisation and activation. Therefore, if the soluble ligands were artificially clustered, receptor activation should be observed. Using epitope tagged secreted forms of the ephrin, where antibodies to the tags could be used to aggregate the ephrins, it was confirmed that clustering was necessary for receptor activation (Davis *et al.,* 1994). In addition to ligand clustering, the requirement for membrane attachment suggested that the ephrin-expressing cells had to be in direct cell to cell contact with their receptor-expressing cells to allow Eph receptor activation. Subsequently, has been shown that ephrin-A5 binds to the EphA3 extracellular domain as a one-to-one interaction (Lackmann *et al.,* 1997), therefore ligand clustering appears to facilitate receptor clustering.

1.6.5 Biochemistry of Eph Receptors

The signalling pathways downstream of the Eph receptor family have not been fully elucidated, however, several interacting cytosolic signalling proteins have been identified

Figure 1.3

Binding specificity classes of Eph receptor and ephrins

Receptor binding studies reveal that the Eph-related receptors can be divided into two classes: those receptors that preferentially bind the transmembrane ephrins, the EphB class, or the GPI-anchored ephrins, the EphA class (Gale *et al.,* 1996). Within each ephrin-receptor binding class, interactions are promiscuous. One exception to this subdivision is EphA4 which binds members of both ephrin classes. The interacting ephrin for EphB5 is unknown.

Figure reproduced from O'Leary and Wilkinson (1999).

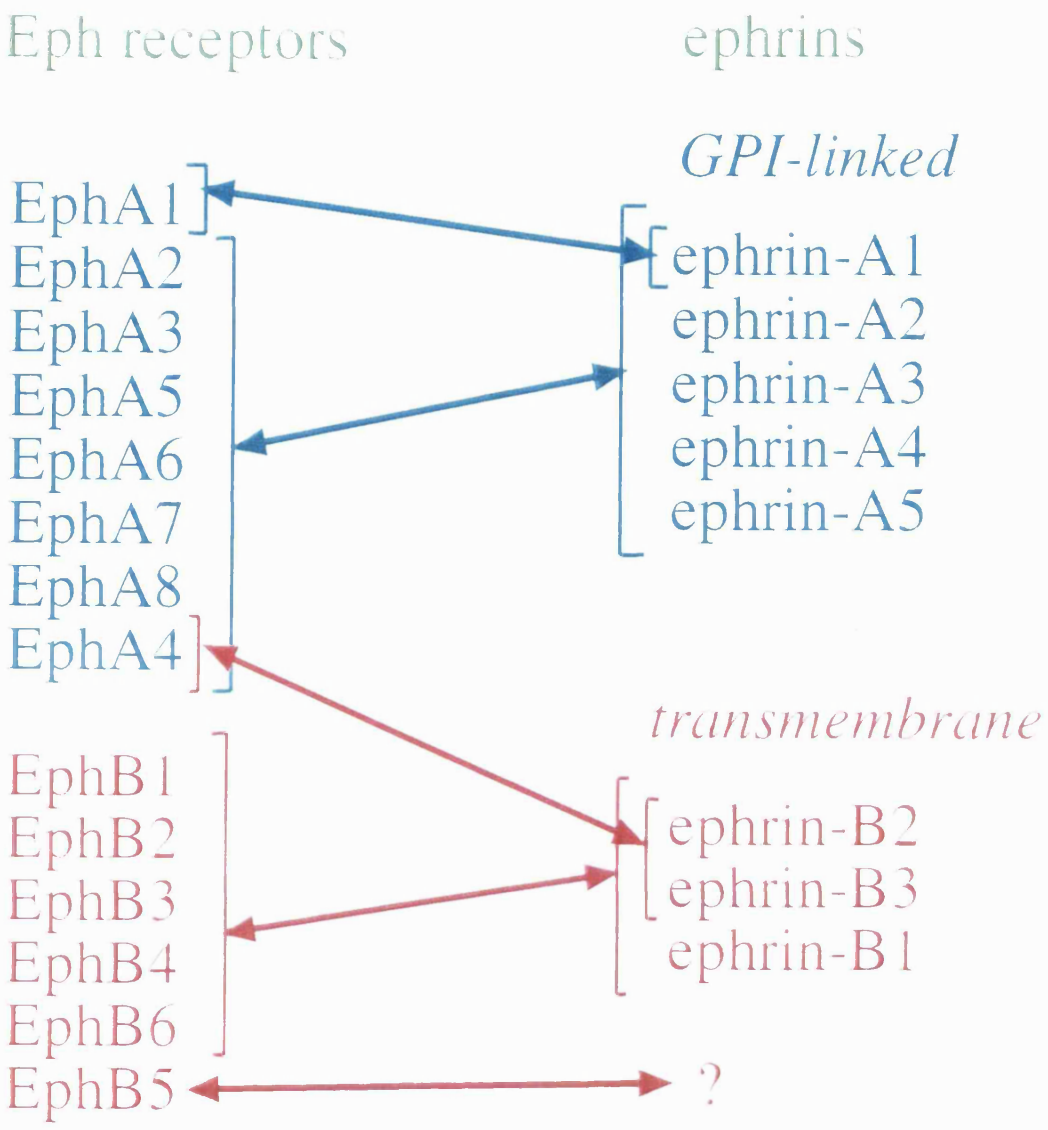
Eph receptors
ephrins
GPI-linked
EphA1
EphA2
EphA3
EphA5
EphA6
EphA7
EphA8
EphA4
ephrin-A1
ephrin-A2
ephrin-A3
ephrin-A4
ephrin-A5
transmembrane
EphB1
EphB2
EphB3
EphB4
EphB6
EphB5
ephrin-B2
ephrin-B3
ephrin-B1
?

(reviewed by (Bruckner and Klein, 1998; Holland *et al.*, 1998; Pasquale, 1997)). Eph receptor cytoplasmic domain interactions have been identified with the following signalling molecules; the p85 subunit of PI3-kinase (Pandey *et al.*, 1994), SLAP (Pandey *et al.*, 1995a), Src (Zisch, 1998), p120RasGAP (Holland *et al.*, 1997), Nck (Stein *et al.*, 1998a), LMW-PTP (low molecular weight phosphotyrosine phosphatase) (Stein *et al.*, 1998a), Fyn (Zisch, 1998), Yes (Zisch, 1998), Crk and RasGAP (Hock *et al.*, 1998a; Holland *et al.*, 1997), Grb10 and Grb2 kinases (Stein *et al.*, 1996). These proteins bind to activated receptors by interaction with specific tyrosine residues located either within the kinase region, the C-terminal tail or the juxtamembrane region where two phosphotyrosine residues have been identified as major regions of autophosphorylation and are conserved in all Eph receptors (Pasquale, 1997). For example in the juxtamembrane region, it has been shown that the second of the phosphorylated tyrosine residues is a major site for EphA4 to bind p59fyn (Ellis *et al.*, 1996) and mutation of both these residues in EphB2, substantially reduces ligand-induced tyrosine phosphorylation (Holland *et al.*, 1997).

The majority of the signalling proteins that interact with the Eph receptors were identified by the two-hybrid system and biochemical assays. Nck, Crk, Grb2, Grb10 and Src-like adaptor protein (SLAP) are adaptor molecules which contain an SH2 domain and one or more additional protein regions, often SH3 domains. The adaptor molecules have no catalytic domain. They bind to an activated receptor with their SH2 domain allowing their additional protein domains free to bind to other cytosolic proteins. This facilitates the cotranslocation of effector molecules that may interact with the activated receptor too (van der Geer *et al.*, 1994). It has been found that Grb2, Grb10 and Nck, bind to EphB1 (Stein *et al.*, 1996; Stein *et al.*, 1998a), Crk to EphB3 (Hock *et al.*, 1998a) and SLAP to EphA2 (Pandey *et al.*, 1995a). The binding of Grb2 for instance cotranslocates SOS, a guanine nucleotide exchange factor, bringing it to the cytoplasmic face of the plasma membrane, a process that results in the activation of Ras (van der Geer *et al.*, 1994); Nck has been shown to act as an intermediary linking EphB1 signalling to JNK (Jun N-terminal Kinase), a stress responsive kinase. SLAP is a negative regulator of mitogenesis which potentially acts as a negative regulator of signalling initiated by growth factors (Roche *et al.*, 1998). Eph receptors do not exert pronounced mitogenic or

transforming activities (Brambilla *et al.,* 1995) and therefore, an association with SLAP may explain these observations.

PI3 kinase, Src family kinases Fyn Src and Yes, and p120RasGAP have intrinsic catalytic activities (van der Geer *et al.,* 1994). PI3 kinase associates with EphA2 (Pandey *et al.,* 1994), Fyn with EphA4 and EphA3 (Ellis *et al.,* 1996; Zisch, 1998) Src with EphA3, EphA4 and EphB2 and Yes with EphA3, EphA4 and EphB2. EphB2 also binds to RasGap. It is known that the activation of EphA2 increases the activity of PI3 kinase (Pandey *et al.,* 1994) a protein that feeds into signalling pathways associated with neurite outgrowth, cell migration and cytoskeletal organisation, as discussed below (Holland *et al.,* 1997; Pandey *et al.,* 1994; Zisch, 1998).

The localisation of receptor interacting proteins may be aided by the SAM domain (sterile alpha motif), a conserved motif found in the C-terminal tail of the Eph receptor family (Thanos *et al.,* 1999), and many other proteins (reviewed in (Schultz *et al.,* 1997)). The SAM domain appears to mediate protein-protein interactions, for example, serving as a docking site for Grb10 which interacts with phosphorylated Y929 present in the SAM domain of EphB1 (Stein *et al.,* 1996). In addition the C-termini of several Eph receptors of both sub-classes bind to the PDZ domain of the ras-binding protein AF6 (Hock *et al.,* 1998b). As previously mentioned, PDZ domains mediate protein-protein interactions often as an aid to clustering (Craven and Bredt, 1998; Sheng, 1996) and in this capacity, AF6 may aid the location of ras to EphB3-bound RasGAP (Hock *et al.,* 1998b). Recently further evidence to support these possibilities has been obtained: PDZ-containing proteins were shown to specifically bind and cluster both Eph receptors and ephrin-B ligands in heterologous cells (Torres *et al.,* 1998).

1.6.6 Cytoskeletal Associations

Regions have been identified within the Eph receptor structure which suggest further links with cytoskeletal associations; roles to mediate clustering, the localisation of membrane proteins or associations with scaffolding proteins to aid the assembly of signalling complexes.

The cytoskeleton is the structural framework of the cell. Its flexibility underlies processes such as cell movement and the formation and retraction of filopodia. One of the main components of the cytoskeleton is actin which can exist as filaments whose

polymerisation and de-polymerisation leads to changes in cell shape. Several of the signalling proteins previously shown to interact with members of the Eph receptor family are also associated with signalling pathways that affect actin. The responses resulting from these interactions include growth cone collapse and axon guidance (Suter and Forscher, 1998; Van Vactor, 1998).

Several of the main protagonists linking the Eph receptor family to the cytoskeleton are p120RasGAP, $p62^{dok}$ a protein that provides docking sites for phosphotyrosine binding proteins, and Nck. Amongst the Eph receptor family, they all associate with EphB2 (Holland *et al.,* 1997). It has been shown that p120RasGAP forms a complex with a tyrosine-phosphorylated form of p190RhoGAP, a negative regulator of the small GTPase Rho (see Fig. 1.4) (Bruckner and Klein, 1998). Rho cycles between active and inactive states with two further members of the small GTPase family, Rac1 and Cdc42 (Hall, 1998). Their action has placed them as candidates for signalling agents linking extracellular guidance cues and the regulation of the actin cytoskeleton in growth cones (Luo *et al.,* 1997). Mutations of Rho, have been shown to lead to defects in cell migration and axon outgrowth in *Drosophila* (Luo *et al.,* 1994; Zipkin *et al.,* 1997). Furthermore, guidance and targeting of photoreceptor cell axons in *Drosophila* requires dreadlocks (*dock*), the homologue of Nck (Garrity *et al.,* 1996). $p62^{dok}$ is believed to be a scaffolding protein that allows the assembly of multiprotein complexes at the membrane (Yamanashi and Baltimore, 1997). $p62^{dok}$ associates with RasGap and Nck in ephrin-B1-stimulated NG-EphB2 cells (Holland *et al.,* 1997). The possible complex formed between RasGap, Nck and $p62^{dok}$ may allow their positioning to sites involved in cytoskeletal regulation. A further example for the close ties between Eph receptor signalling and cytoskeletal regulation is provided by PI3 kinase activity, which was shown to be increased by the activation of EphA2 (Pandey *et al.,* 1994). Work on mammalian Ras showed that Ras regulates membrane ruffling, through Rac, a process that is entirely dependent on normal PI3 kinase function (Rodriguez-Viciana *et al.,* 1997).

Further downstream effectors linked to cytoskeletal reorganisation include PAK, a family of serine/threonine kinases (Lu *et al.,* 1997), WASP (Wiskott-Aldrich Syndrome protein) (Rivero-Lezcano *et al.,* 1995) and SOS (son of sevenless) (Hu *et al.,* 1995) an activator of Ras and Rho. Nck interacts with PAK, WASP and SOS. PAK and WASP associate

Figure 1.4

Summary model of Eph receptor signalling

This figure is a summary model of all the Eph receptor/signalling protein interactions known to take place. Not all Eph receptors may mediate all the interactions shown.

The activated Eph receptor binds SH2 domain-containing proteins indicated by the concavity on the left of the designated proteins e.g. Grb2 and Nck. These proteins then interact with other cytosolic proteins linking the receptor to signalling cascades as described in the text. The Eph receptor-bound Nck may mediate the same interactions as the Nck shown associated with p62.

The dark grey arrow represents the hypothesised overall effect of Eph signalling on the cytoskeleton. The light grey arrow indicates that Eph receptors do not directly trigger mitogenic responses.

Figure reproduced from Bruckner and Klein (1998).

Y-tyrosine residue, V-valine residue

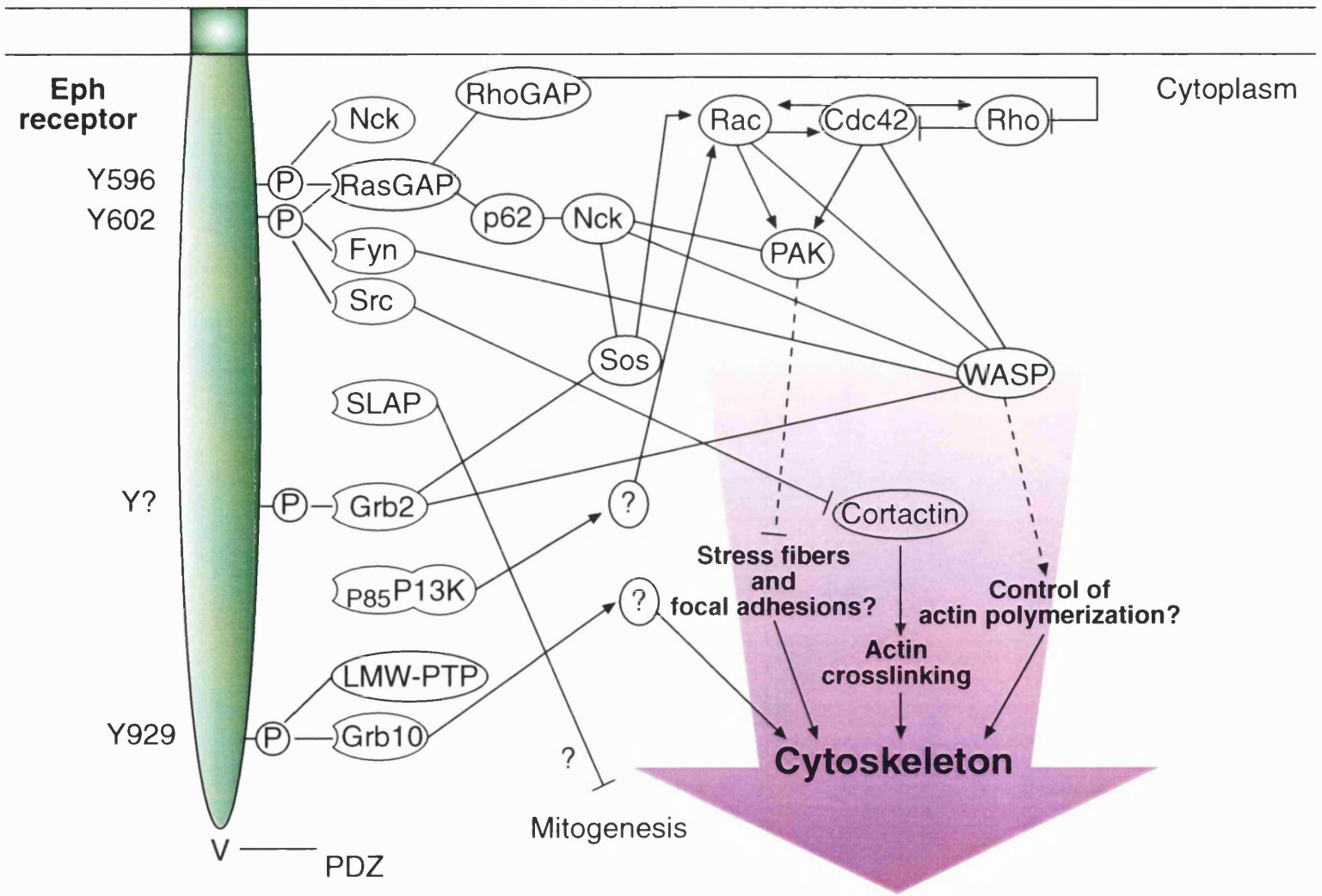
Eph receptor
Cytoplasm
Y596
Y602
Y?
Y929
V
PDZ
Nck
RhoGAP
RasGAP
p62
Nck
Rac
Cdc42
Rho
PAK
Fyn
Src
Sos
WASP
SLAP
Grb2
?
Cortactin
P85P13K
?
Stress fibers and focal adhesions?
Control of actin polymerization?
Actin crosslinking
LMW-PTP
Grb10
?
Mitogenesis
Cytoskeleton

with activated Cdc42/Rac and possibly provides a link to the actin cytoskeleton (Li, 1997; Manser *et al.,* 1997; Symons *et al.,* 1996).

Src and Fyn also have roles in the cytoskeleton. One physiological substrate for Src is cortactin, an actin binding protein which mediates cross-linking of filamentous (F-) actin into bundles (Huang *et al.,* 1997), as found in growth cones (Suter and Forscher, 1998). Fyn can interact with WASP, a further association that advocates an involvement of the Eph receptor family in cytoskeletal regulation (Banin *et al.,* 1996).

1.6.7 Signalling Through Ephrins

The cytoplasmic domains of ephrin-B1, ephrin-B2 and ephrin-B3, the three members of the ephrin-B class, where found to have strong sequence conservation of the 33 amino acids at the C-terminal end. These sequences contain five potential tyrosine-phosphorylation sites, some of which were surrounded by amino acid residues that could be recognised as substrates by receptor and non-receptor tyrosine kinases. Members of the ephrin-B family were found to be phosphorylated on tyrosine when EphB2, a receptor known to be activated by the ephrin-B subgroup, was not only phosphorylated itself when cocultured with cells carrying of ephrin-B1 or ephrin-B2, but also induced phosphorylation of these ligands when presented to them as a clustered ectodomain (Bruckner *et al.,* 1997; Holland *et al.,* 1996). Therefore, in the ligand-expressing cell, there is activation of an endogenous tyrosine kinase which phosphorylates ephrin-B1 and ephrin-B2. These findings were extended when it was found that serum or PDGF growth factor treatment leads to phosphorylation of ephrin-B1 (Bruckner *et al.,* 1997). The rapid phosphorylation of tyrosine residues suggested that ephrin-B2 is a direct target of the PDGFR tyrosine kinase. Therefore, ephrin-B1 can be phosphorylated independent of Eph receptor contact. Both papers conclude that the EphB/ephrin-B subclass interaction triggers bidirectional signalling: that is phosphorylation of both an EphB class receptor and its interacting ligand. Additionally, cross-talk by other activated receptor tyrosine kinase members can occur (see Fig. 1.5) (Bruckner and Klein, 1998).

The cytoplasmic tails of the transmembrane ephrins contain a four amino acid motif that binds PDZ domains (Bruckner *et al.,* 1997; Lin *et al.,* 1999; Songyang *et al.,* 1997). Proteins that contain PDZ domains have been shown to play a general role in the localisation of channels, downstream signal-transducing enzymes and adhesion

Figure 1.5

Signalling through ephrins: predicted model for ephrin-B proteins

Left: Cell-cell contact between the EphB2 receptor and ephrin-B ligands mediates bidirectional signalling. Autophosphorylation of EphB2 and tyrosine phosphorylation of the ephrin cytoplasmic domain takes place.

Right: Cross talk between PDGFR and ephrin-B1 takes place when both proteins are expressed in the same cell. PDGFR activation results in ephrin-B1 tyrosine phosphorylation which may trigger further downstream events.

Figure adapted from Bruckner and Klein (1998).

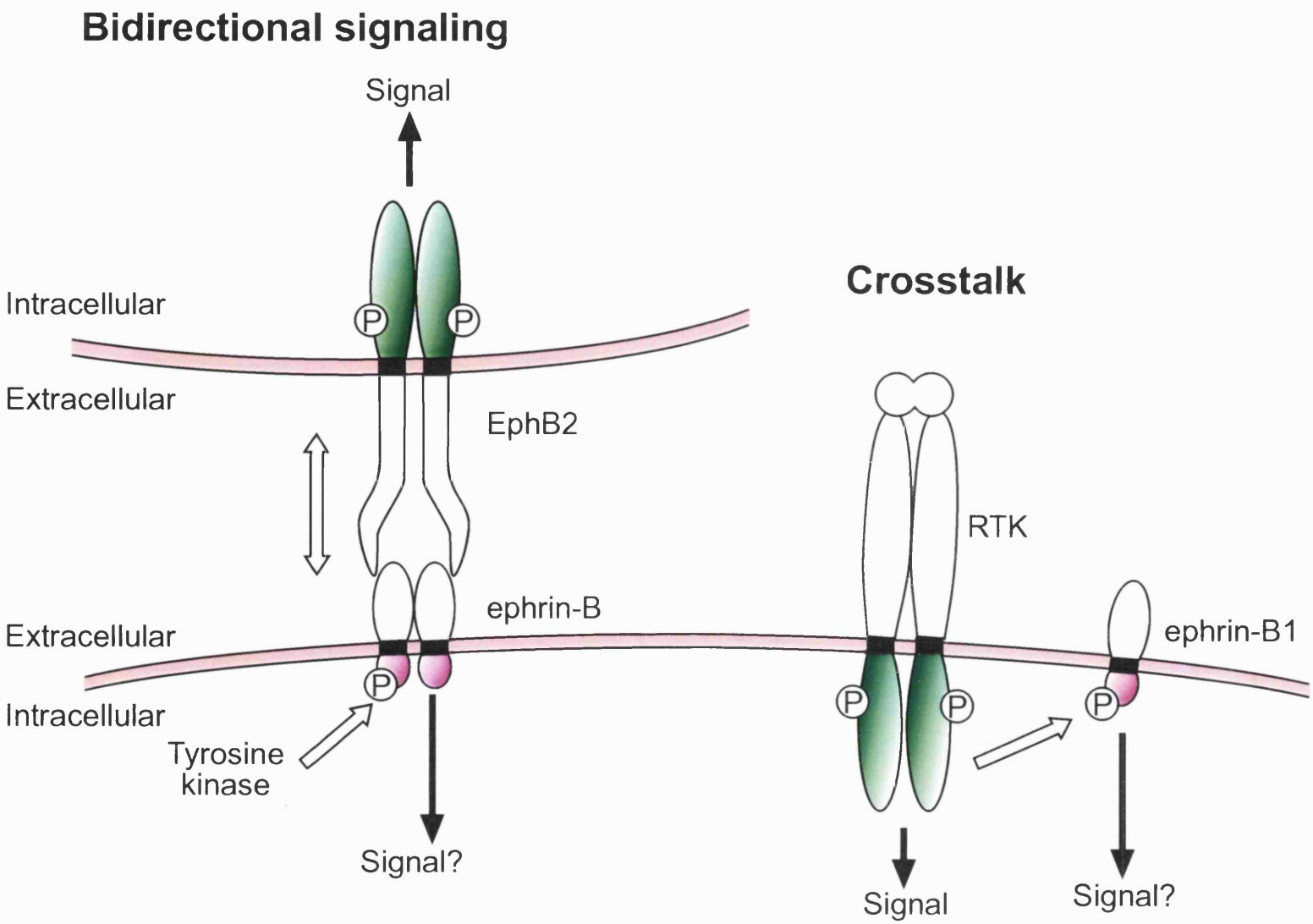
Bidirectional signaling
Signal
Intracellular
Extracellular
EphB2
ephrin-B
Extracellular
Intracellular
Tyrosine kinase
Signal?
Crosstalk
RTK
ephrin-B1
Signal
Signal?

molecules to sites of cell-cell contact, (reviewed by (Craven and Bredt, 1998)). The domains themselves mediate protein-protein interactions usually by binding to specific motifs in the C-termini of interacting proteins or, by linking themselves together to create a concatamer of PDZ domain-containing proteins, mediating clustering (Craven and Bredt, 1998; Sheng, 1996). The properties of PDZ domain proteins suggest that they may play a role in ephrin-B signalling.

1.6.8 Eph Family Developmental Expression Patterns

Many studies have revealed the expression of Eph receptors and ephrins in a variety of tissues in both the adult and embryo. In order to investigate the expression patterns *in vivo*, within an entire class, rather than with the individual ephrin or receptor, fusion proteins were constructed where the extracellular portion of the receptors or ephrins were fused to the Fc domain of IgG.

Two studies utilised IgG-Fc tagged ligands and receptors in whole mount *in situ* staining, so that the receptor fusion indicates regions of ligand expression and the ligand fusion proteins reveals the receptor expressing tissues (Flenniken *et al.*, 1996; Gale *et al.*, 1996). Since GPI-anchored subclass of the Eph ligand family bind Eph-A receptors whereas the ephrin-B ligands bind to Eph-B receptors, these reagents will detect the entire binding specificity class. It was found that the composite distributions of each subclass subdivided the embryonic day 10.5 mouse embryo into domains of mutually exclusive expression of a receptor subclass and its corresponding ligands. For example, the expression of ephrin-B ligands occurred in the ventral hindbrain/midbrain (Becker *et al.*, 1994; Flenniken *et al.*, 1996; Gale *et al.*, 1996b; Nieto *et al.*, 1992) whereas the corresponding receptor expression occurred in the dorsal midbrain/tectum (Cheng *et al.*, 1995; Drescher *et al.*, 1995; Gale *et al.*, 1996b; Monschau *et al.*, 1997). Similarly, complementary regions of expression are found in the limb buds, the branchial arches, the spinal cord and the somites.

However, Flenniken *et al* (1996), found that in addition to complementary expression, there are overlaps between corresponding classes of receptors and ligands (Flenniken *et al.*, 1996). As found previously (Gale *et al.*, 1996), Fc fusion reagents reveal complementary distributions of receptors and ligands, but when individual ligands are analysed by *in situ* hybridisation in embryonic day 9.5 mice, it was clear that overlaps

exist. The reason for this discrepancy was that the ephrin bound to its receptor was masked and was therefore not detected by the receptor Fc fusion reagent (Sobiesczcuk and Wilkinson, 1999). For example, several ligands and receptors are expressed in the somites with ephrin-A4 throughout the somites overlapping with the receptors EphA4 (Neito *et al.,* 1992), EphB3 (Becker *et al.,* 1994) and EphA7 (Ellis *et al.,* 1995).

In summary, ephrins and their receptors therefore have both complementary and overlapping domains of expression. The roles for these features in the Eph family are discussed below and in several reviews concentrating on the developing nervous system (Barinaga-M, 1995; Harris and Holt, 1995; Orioli *et al.,* 1996) and (reviewed by (Drescher, 1997; Flanagan and Vanderhaeghen, 1998; Muller *et al.,* 1996b; Orioli and Klein, 1997; Tessier-Lavigne, 1995; Xu *et al.,* 1996)).

1.6.9 Roles in Axonal Pathfinding in the Retinotectal System

During development, topograpically organised neuronal connections in the brain are established by molecular guidance cues. Initially, axons must find their target regions guided by target and pathway-derived cues and then their local spatial organisation in the target area (Harris and Holt, 1995; Holt and Harris, 1998; Orike and Pini, 1996; Tessier-Lavigne, 1995). Topographic projection of neurons is crucial in the retinotectal system. Here, visual information from the retina is carried via retinal axons to the tectum in the chick (the superior colliculus in mammals). Axons of retinal ganglion cells arising from the anterior (nasal) retina project to the posterior tectum and retinal axons arising from the posterior (temporal) retina project to the anterior tectum.

Insights into the nature of the molecular cues were provided by stripe assays. A "membrane stripe assay" was devised where the migration of retinal axons to the tectum could be analysed (Walter *et al.,* 1987b). The assay allows axons to choose whether to grow along anterior or posterior tectal membranes. The nasal axons that project from the anterior retina to the posterior tectum were shown to have no tectal membrane preference but temporal retinal axons were found only to grow along anterior tectal membranes (Walter *et al.,* 1987a). This behaviour was due to repulsion of the axons by posterior tectum membranes. A collapse assay confirms these observations. The addition of posterior membranes to growing cultures of temporal axons caused axon growth cones to

become paralysed and retract. When anterior tectal membranes were added, there was no observed effect (Cox *et al.,* 1990).

It was found that surface molecules on the posterior tectum lead to the collapse of the temporal axons. These repulsive molecules were GPI-anchored and had a graded distribution across the tectum, being most highly expressed in the posterior tectum.

Recently it has been shown that members of the Eph family contribute to guidance in the retinotectal system, (reviewed by (Flanagan and Vanderhaeghen, 1998; Tessier-Lavigne, 1995)). In assay systems, the chick homologue of ephrin-A5 has been shown to induce growth cone collapse and repulsion of retinal ganglion cell axons (Drescher *et al.,* 1995). *In situ* hybridisation and binding studies using receptor or ligand affinity probes show that ephrin-A5 and ephrin-A2, are expressed in a graded distribution across the developing tectum (Cheng *et al.,* 1995; Drescher *et al.,* 1995). The highest concentration of ephrin is present in the posterior tectum, and the lowest concentration in the anterior tectum. Messenger RNA for EphA3, a receptor for ephrin-A2 and ephrin-A5, has a complementary gradient, where highest expression is in the temporal retinal ganglion axons (Cheng *et al.,* 1995). These axons project to the anterior tectum, where there are low levels of ephrin expression. Nasal retinal ganglion axons, which express low levels of EphA3, project to the posterior tectum where there are high levels of ephrin expression. The membrane stripe assay (Walter *et al.,* 1987a; Walter *et al.,* 1987b), was used to show *in vitro*, that ephrin-A2 is repellent for temporal but not nasal axons and ephrin-A5, is repellent for both nasal and temporal axons but to different degrees (Monschau *et al.,* 1997; Nakamoto *et al.,* 1996).

Further experiments involving retroviral overexpression of ephrin-A2 in the chick tectum have shown that retinal axons avoid ectopic patches of ephrin-A2 expression (Nakamoto *et al.,* 1996), which leads the axons to map to abnormally anterior positions. These data suggest that high levels of EphA3 expression in the temporal retinal ganglion cells causes the axons to be repelled away from posterior tectum where high levels of ephrin are expressed. These observations are consistent with those observed in zebrafish where COS cells expressing an ephrin-A2 homologue are avoided by temporal but not nasal axons (Brennan *et al.,* 1997). Therefore, Eph receptor members and ephrins are expressed in complementary gradients that control the topographic targeting of retinal axons by repulsion (Monschau *et al.,* 1997; Muller *et al.,* 1996a).

Recent work has also addressed the role of Eph receptors in the retinotectal system in mammals, namely mouse and rat (Davenport *et al.,* 1998; Frisen *et al.,* 1998). Frisen and colleagues generated an ephrin-A5 homozygous knockout in the mouse. They found that retinal axons are present at topographically incorrect sites in the superior colliculus, their major target in the midbrain, correlating to locations of low ephrin-A2 expression. Some of the axons also overshoot their target and extend aberrantly into the inferior colliculus (IC). Therefore, ephrin-A5 is essential for proper retinal axon guidance and topographic mapping in the mammalian visual system.

1.6.10 Axonal Repulsion and Axon Fasiculation

Ephrin-A5 was initially identified as a human ephrin which activated EphA5, an Eph-related tyrosine kinase receptor that is expressed in the nervous system with highest levels in the hippocampus and cortex (Winslow *et al.,* 1995). To find a biological role for this receptor, a culture system was used in which axons of cortical neurons grow over astrocytes, and interactions between these populations leads to axon bundling. On addition of soluble EphA5-IgG fusion protein to the culture system, axon bundling between the cortical neurons was prevented. Similarly, soluble ephrin-A5 caused a block of axon bundling. Further evidence for a role of Eph receptors was shown, when defective axon bundling was observed in EphB2 and EphB3 double homozygous mouse mutants (Orioli *et al.,* 1996). Axon fasciculation defects were found in a pair of axon bundles running along the anterior/posterior axis called the habenular-interpeduncular tract, within the midbrain.

Utilising the collapse assay, Meima *et al* (1997) asked if the axon bundle formation was due to an avoidance mechanism: did bundling enable axons to avoid the ephrin-A5-rich repellent surfaces of the astrocytes? When ephrin-A5-IgG was added to rat cortical axons, growth cones collapsed and there was extensive retraction of the neurite (Meima *et al.,* 1997). Therefore, the agonistic interaction of ephrin-A5-IgG with Eph-A5, caused growth cone collapse. The loss of cytoskeletal F-actin which is normally enriched in spreading growth cones, resulted in the neurite retraction. Therefore, ephrin-A5 via EphA5 is possibly causing perturbation of the actin cytoskeleton, leading to growth cone collapse.

The transmembrane ligands, ephrin-B1 and ephrin-B2 have been shown to have a role in motor axon migration (Wang and Anderson, 1997). These ligands are expressed in trunk regions of the embryo that act as barriers to motor axon outgrowth, including the caudal half of the somite. Their receptors are expressed on the axons themselves. To test if the ephrin expression was inhibiting axon outgrowth, motor axons were grown in culture. To these cultures, preclustered ligand-Fc proteins at various concentrations were added and it was found that growth cones of the axons collapsed. The ephrins were also tested to see if they caused repulsive axon guidance activity in the stripe assay (Walter *et al.*, 1987b). The motor axons avoided the stripes expressing the ephrins, therefore implicating ephrin-B ligands in inducing growth cone collapse and providing repulsive guidance cues to trunk motor axons.

1.6.11 Signal Transduction Through an Ephrin

Indirect *in vivo* evidence for signal transduction through an ephrin was provided by work investigating the role of EphB2 (Henkemeyer *et al.*, 1996). Two mutations were introduced into the mouse EphB2 gene, and their effects were studied in the nervous system. The first mutation, $EphB2^{1}$, produced by homologous recombination was a protein null allele. The second mutation, $EphB2^{lacZ}$, encoded a fusion protein encoding the extracellular, transmembrane and juxtamembrane domains of EphB2 linked to b-galactosidase. Transgenic mice resulting from the second mutation aided the characterisation of EphB2 expression: the most intense $EphB2^{lacZ}$ was restricted to ventral structures including the preoptic area, hypothalamus of the forebrain, the ventral cells of the neural tube and within axons of the PNS (peripheral nervous system). Histological analysis of homozygous null mutants ($EphB2^{1}/EphB2^{1}$), revealed that the pathfinding of axons forming the posterior tract of the anterior commissure was abnormal (acP tract). The acP tract defect was due to the failure of temporal cortical neurons to extend axons laterally towards the midline and subsequently into the contralateral cortex. The acP tracts were well formed in the +/+, $EphB2^{1}/+$ mice and the $EphB2^{lacZ}$ homozygous mice; this suggested that a truncated EphB2 receptor lacking a kinase domain retains the functions necessary for the pathfinding of temporal cortical axons. The axons themselves migrate along a pathway defined by EphB2 expression but not into regions of EphB2 expression. However, in the $EphB2^{1}/EphB2^{1}$ homozygotes, the axons migrate inappropriately into regions that would normally express EphB2. The axons

forming the acP tract were shown to express ephrin-B1, suggesting that in wildtype mice, EphB2 may act as a repulsive signal to ephrin-B1, a signal which is not received in the double mutants. Therefore, ephrin-B1 may itself function as a receptor molecule: interaction of ephrin-B1 with the EphB2 extracellular domain causes a repulsive reaction in the acP axons in which ephrin-B1 is expressed. The elimination of EphB2 in the $EphB2^{1}/EphB2^{1}$ mice therefore prevented correct anterior commissural axon migration.

1.7 Hindbrain Segmentation

The vertebrate hindbrain is divided into seven segments termed rhombomeres which are transient bulges in the neuroepithelium. Hindbrain segmentation is important since it underlies the patterning of neurones and neural crest which arise from the rhombomeres (Guthrie, 1996). For example, in the chick, the branchial motor neurones arise from two adjacent rhombomeres: rhombomeres 2 and 3 give rise to the V^{th} nerve, rhombomeres 4 and 5 to the VII^{th} nerve and rhombomeres 6 and 7 to the IX^{th} nerve (Lumsden and Keynes, 1989). In zebrafish, the serially repeated pattern of reticulospinal neurones in the hindbrain reflect its segmental organisation (Kimmel *et al.*, 1985; Metcalfe *et al.*, 1986). The reticulospinal neurons are found in seven bilateral clusters which are periodically spaced. Each cluster contains several different types of reticulospinal neurones with morphologically similar cells being found at rhombomeric intervals along the rostrocaudal axis (Metcalfe *et al.*, 1986). In the chick it has been shown that each rhombomere contains the same set of basic neuronal types but some contain more of one particular neuronal type than another (Clarke and Lumsden, 1993). It therefore seems that the initial neuronal development of each rhombomere is conserved and the differences arise from variations of this repeated pattern.

Genes have been identified which are expressed prior to segmentation of the hindbrain suggesting that these gene products may underlie patterning (Wilkinson, 1995). These genes include the *Hox* family of transcription factors, the zinc finger gene *Krox20* and the leucine zipper gene, *Kreisler*. *Hox* genes are implicated in segment identity whereas *Krox20* and *Kreisler* are implicated in segmentation of the hindbrain.

1.7.1 *Hox* genes

The *Hox* genes are the vertebrate homologues of the *Drosophila* HOM-C genes and they encode DNA binding proteins which have been conserved throughout animal evolution. Vertebrate *Hox* genes are arranged in four separate clusters: *Hoxa*, *Hoxb*, *Hoxc* and *Hoxd* (Scott, 1992). The genes are expressed from the posterior part of the CNS to anterior limits of expression in the spinal cord or hindbrain, correlating with their position in the cluster such that the 5' genes have the most posterior limits of expression and the 3' genes, the most anterior. This is known as "colinearity", a conserved feature of *Hox*/HOM gene expression. An example can be taken from paralogous genes: here, the paralogous group 3 has an expression domain up to the rhombomere 4/5 boundary and the more 5' set, paralogous group 4, are expressed up to the rhombomere 6/7 boundary.

The transfer of patterning information from the rhombomeres to the branchial arches is believed to take place via the neural crest cells (Hunt *et al.*, 1991b; Hunt *et al.*, 1991a). These cells migrate from specific rhombomeres to specific destinations. The prespecification of the cranial neural crest cells is believed to be due to the overlapping expression of the *Hox* genes, which creates a *Hox* code (Hunt *et al.*, 1991b). The neural crest cell expresses a *Hox* code which is maintained during migration (Hunt *et al.*, 1991d; Hunt *et al.*, 1991c) and subsequently observed in the adjacent branchial arch (Hunt *et al.*, 1991b; Hunt *et al.*, 1991a). Therefore, it appears that the migration of neural crest cells to their correct branchial arch is important in branchial arch patterning. Figure 1.6 indicates the patterns of mouse *Hox* subfamily gene expression in the branchial region after neural crest migration (Hunt and Krumlauf, 1992).

1.7.2 *Krox20*

Krox20 is a transcription factor that contains three zinc fingers capable of binding to specific sequences of DNA. It has conserved expression in rhombomeres 3 and 5 and in the third arch neural crest in *Xenopus* (Bradley *et al.*, 1992), chick (Nieto *et al.*, 1991), mouse (Wilkinson *et al.*, 1989) and zebrafish embryos (Oxtoby and and Jowett, 1993), suggesting a conserved role.

Krox20 expression is initially seen prior to the morphological segmentation of the hindbrain as two fuzzy stripes coinciding with presumptive rhombomeres 3 and 5. This expression sharpens as the rhombomeres boundaries form (Irving *et al.*, 1996).

Figure 1.6

The branchial *Hox* code

This schematic figure indicates the patterns of mouse *Hox* subfamily gene expression in the branchial region after neural crest migration.

The arrows are shaded according to the combination of *Hox* families expressed and they indicate the migration of mesenchymal and neurogenic neural crest from specific rhombomeres into the branchial arches. The branchial arch ectoderm subsequently adopts an identical pattern of *Hox* subfamily expression, as indicated by the shaded arrows. The open arrows represent first arch crest which do not have a *Hox* label.

Figure adapted from Hunt and Krumlauf (1992).

r-rhombomere, B-branchial arch.

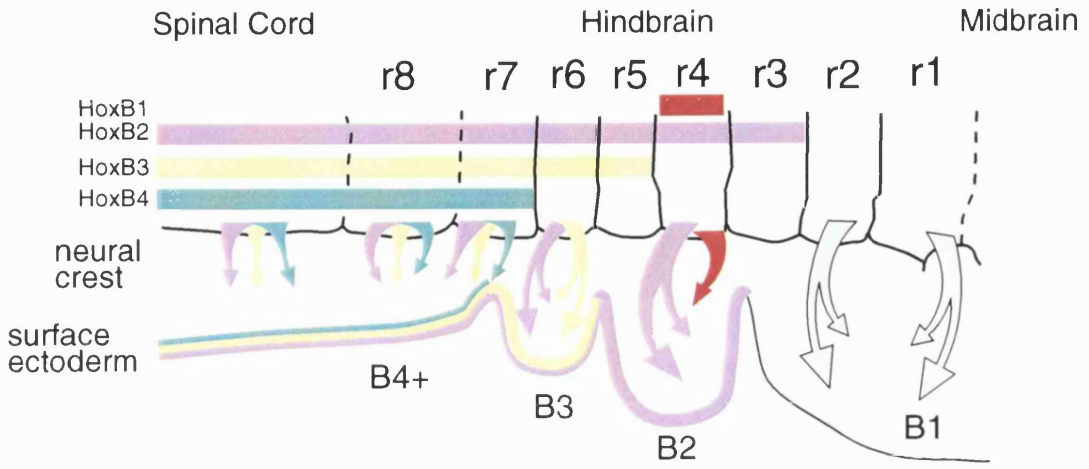
Spinal Cord
Hindbrain
Midbrain
r8
r7
r6
r5
r4
r3
r2
r1
HoxB1
HoxB2
HoxB3
HoxB4
neural crest
surface ectoderm
B4+
B3
B2
B1

Disruption of the *Krox20* gene causes the loss of rhombomeres 3 and 5 indicating the vital role for *Krox20* in hindbrain segmentation (Schneider-Maunoury *et al.*, 1993; Swiatek and Gridley, 1993). *Krox20* is also found in third arch branchial neural crest that migrates posterior to the otic vesicle. In contrast, in homozygous embryos which have a LacZ reporter gene inserted to disrupt *Krox20* expression, there is LacZ expression in neural crest cells rostral and caudal to the otic vesicle (Schneider-Maunoury *et al.*, 1993). This suggests that *Krox20* may regulate genes required for the correct migration of the third arch neural crest cells.

Regulation of *Hox* gene expression by *Krox20* has been shown in mice (Nonchev *et al.*, 1996; Schneider-Maunoury *et al.*, 1993; Sham *et al.*, 1993; Swiatek and Gridley, 1993). *Hoxb-2* is initially expressed in a uniform domain up to the presumptive r2/r3 boundary, and is then upregulated in r3, r4 and r5 coincident with the expression of *Krox20* (Sham *et al.*, 1993; Wilkinson *et al.*, 1989). A regulatory interaction between *Hoxb-2* and *Krox20* was suggested when it was found that in *Krox20* null mutants *Hoxb-2* expression was absent in the position of rhombomere 3, and at reduced levels in rhombomere 5 (Schneider-Maunoury *et al.*, 1993; Swiatek and Gridley, 1993). Further analysis has shown that an enhancer of the *Hoxb-2* gene contains two *Krox20* binding sites and that *Krox20* is involved in the transcriptional regulation of *Hoxb-2* in rhombomeres 3 and 5 (Sham *et al.*, 1993).

1.7.3 *Kreisler*

The *Kreisler* gene encodes a leucine zipper transcription factor of the MAF superfamily which is expressed in presumptive r5/r6 during hindbrain segmentation (Cordes and Barsch, 1994). Initial studies suggested that in homozygous *Kreisler* mutants at E9.5, r5 and r6 are absent. However at E8.5, the expression of *Hox* genes and *Krox20* are altered in homozygous *Kreisler* mutant mice. For example, *Krox20* is expressed in rhombomere 3 and absent from rhombomere 5 (Frohman *et al.*, 1993; McKay *et al.*, 1994). The expression pattern of *Hoxb-1* which is usually within the boundaries of rhombomere 4, has expanded to cover a region broader than the entire rhombomere, suggesting that the disruption to segmentation has led to an abnormal encroachment of cells into adjacent regions. *Hox*b-4 expression is seen to coincide with the posterior limit of *Hoxb-1* rather than ceasing at the 6/7 boundary (McKay *et al.*, 1994). In addition, binding sites for *Kreisler* protein have been identified within *Hoxb-3* enhancers while investigating the

upstream mechanisms for the regulation of *Hoxb-3* in r5 (Manzanares *et al.,* 1997). The binding sites were required for r5 activity since mutation of either of these sites abolishes *Hoxb-3* expression. The results show that *Hoxb-3* is a direct target of *Kreisler* and that *Kreisler* plays a primary role in regulating segmental identity through *Hox* genes. Recently, it has been shown that *Kreisler* mutant mice do form r6 (Manzanares *et al.,* 1999). It is believed the original homozygous *Kreisler* mutant is due to mutations in an r5/r6 regulatory element (Manzanares *et al.,* 1999). Therefore, the complete absence of r5 in *Kreisler* mutants indicates that it has an early role in the specification of this segment.

The zebrafish homologue of *Kreisler* is *Valentino* (Moans *et al.,* 1996). Mutations in *Valentino* disrupt the expression of *Krox20* in rhombomere 5 and mutant embryos display an absence of visible rhombomere boundaries and boundary specific rhombomere gene expression posterior to the rhombomere 3/4 boundary. The hindbrain of the mutant embryos is shortened by one rhombomere. This observation suggested, that the region between rhombomeres 4 and 7 has failed to expand, and become subdivided to form rhombomeres 5 and 6, creating a distinct but developmentally earlier "protosegment". Although there are differences between the mammalian *Kreisler* and fish *Valentino* mutants, their phenotypes indicate that this gene is important in the segmentation of the hindbrain.

1.8 Compartments and Boundaries

The rhombomeres of the hindbrain are established by the progressive formation of rhombomere boundaries in the neural plate. Fraser *et al* (1990), provided evidence as to how precise segment-specific patterns of cell organisation are established and maintained (Fraser *et al.,* 1990). Chick cells were labelled with a vital fluorescent dye at various stages during development; before, during and after rhombomere boundary formation. Initially, when the boundaries are not established, cells can spread into neighbouring pre-rhombomere territory. However, once boundaries are formed, most cells cannot cross these partitions, yet they can move freely within their own rhombomere. The boundaries restrict mass cell movement between rhombomeres, but the lineage restriction of rhombomeres has been shown to be violated by approximately 5% of cells (Birgbauer and Fraser, 1994).

The restriction of cell movement between adjacent rhombomeres could be due to two possibilities: the first could be a result of intrinsic differences between the adjacent segments or second, the formation of a barrier at rhombomere boundaries. The rhombomere boundary cells are different from cells found at the centre of rhombomeres (Heyman *et al.,* 1995). They have different rates of cell division, which cumulatively results in a static population of cells at the boundaries (Guthrie *et al.,* 1991). The space between boundary cells is increased with higher levels of chrondroitin sulphate proteoglycan in the extracellular spaces (Heyman *et al.,* 1995). Gene expression also differs between the boundary cells and those within the rhombomeres. Vimentin, an intermediate filament protein has increased expression in the rhombomere boundary cells a feature also found with NgCAM (Lumsden and Keynes, 1989) and peanut lectin-binding glycoprotein (Layer and Alber, 1990). The mature rhombomere boundary cells show decreased expression of *Krox20* and *Hoxb-1* but an increase in the expression of *PLZF*, a zinc-finger containing transcription factor (Cook *et al.,* 1994), *Fgf-3* (Mahmood *et al.,*1995) and *Pax-6* (Heyman *et al.,* 1995). These properties of boundary cells suggest the possibility that the cells serve to prevent intermingling between adjacent rhombomeres.

Another possibility is that the cells of rhombomeres have different cell surface properties. To investigate this possibility, rhombomere transplantation experiments were performed. In the chick, fluorescently pre-labelled rhombomere fragments were grafted from into various positions along the anterioposterior axis. These experiments showed that extensive cell mixing occurs between cells of even numbered origin placed into even numbered rhombomeres (Guthrie *et al.,* 1993). This behaviour is reciprocated between cells of odd numbered origin placed in odd numbered rhombomeres. If cells of even-numbered origin are placed into an odd numbered rhombomere, cell mixing does not take place. Additionally increased cell mixing is apparent between r3/r3 grafts than r3/r5 grafts. Therefore it is possible that an adhesive hierarchy exists which serves to dissuade intermingling of odd and even-rhombomere cells but additionally, can discourage intermingling between non-identical odd/odd or even/even rhombomeric cells (Guthrie *et al.,* 1993).

Wizenmann and Lumsden (1997), provided further evidence to address this possibility (Wizenmann and Lumsden, 1997). Chick cells from even- and odd-numbered

rhombomeres were mixed in all combinations from the time of rhombomere formation through to later stages. An aggregation assay showed that odd-numbered rhombomere cells sort out from adjacent even-numbered rhombomere cells; even (or odd) rhombomere cells selectively re-aggregate when mixed with other even (or odd) rhombomere cells but cells from the same rhombomere will remain mixed. It was found that of the two major adhesion molecules groups classified by virtue of being Ca^{2+}-independent or Ca^{2+}-dependent, that the latter were implicated as molecules providing adhesive differences that restrict the mixing of adjacent rhombomeric cells (Wizenmann and Lumsden, 1997). These collective findings suggest that differential cell affinity may be involved in restricting cell intermingling.

1.8.1 A Role for an Eph Receptor in Hindbrain Segmentation

A number of Eph receptor family members and their ligands have been shown to exhibit segmentally restricted expression within the developing hindbrain (see Fig 1.7) (Becker *et al.*, 1994; Bergemann *et al.*, 1995; Flenniken *et al.*, 1996; Gale *et al.*, 1996a; Henkemeyer *et al.*, 1994; Nieto *et al.*, 1992; Wilkinson, 1999; Xu *et al.*, 1995). The expression of one of these members EphA4, is restricted to r3 and r5 with transient low level expression in r2 and r6 (Gilardi-Hebenstreit *et al.*, 1992; Neito *et al.*, 1992).

The role of EphA4 was investigated by using a dominant negative approach (Xu *et al.*, 1995). A form of EphA4 was expressed in embryos, which consisted of the extracellular and transmembrane domains, but lacking the kinase function. This truncated receptor is capable of dimerising with endogenous receptor but transphosphorylation will not occur, due to the absence of the kinase domain. The effects on segmentation in *Xenopus* and zebrafish embryos were assessed using *Krox20* and EphA4 as markers of r3/r5. It was found that expression of truncated EphA4 lead to ectopic r3/r5 gene expression in the even numbered rhombomeres r2, r4 and r6 in *Xenopus* and zebrafish. As previously noted, during hindbrain development cells are able to cross between rhombomeres prior to boundary establishment. Cell lineage labelling of rhombomeric cells have shown that there is little cell movement across rhombomere boundaries once they have formed (Birgbauer and Fraser, 1994; Fraser *et al.*, 1990). Therefore, this phenotype, where odd numbered rhombomere cells are present in even numbered rhombomeres, could be caused by increased cell mixing between rhombomeres. A second possibility is that there was normal intermingling at early stages, but that EphA4 cell signalling was required to

Figure 1.7

Eph family receptor and ephrin hindbrain expression

Upper part: The hindbrain neural epithelium is divided into rhombomeres (r).The cells within each individual rhombomere are prevented from intermingling with its neighbours. This restriction is due to distinct cellular properties of r2/r4/r6 compared with r3/r5.

Lower part: The expression patterns of the Eph receptors and ephrins within the rhombomeres are shown. The hatched shading indicates regions of lower expression. EphA7 is expressed only in the dorsal part of r2-r6.

Figure adapted from Sadaghiani and Thiebaud (1999).

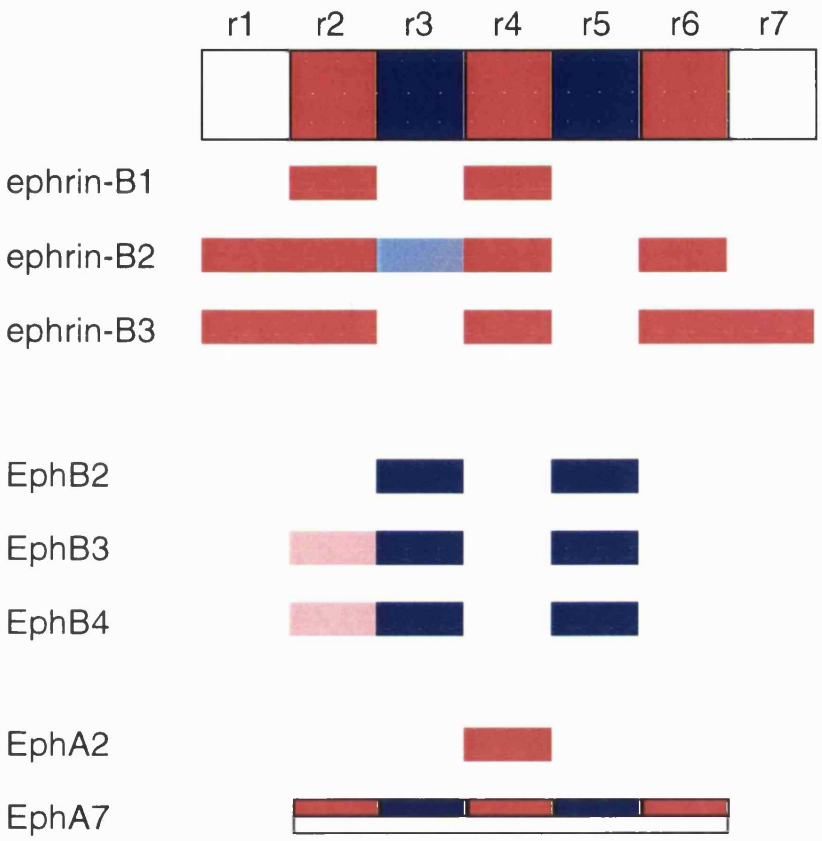

Eph family expression in r2, r4 or r6

Eph family expression in r3 or r5

switch r3 or r5 cells to even-numbered rhombomere fate in a community effect. Third, that the r2, r4 and r6 cells had switched fate *de novo* to those of r3 and r5. Therefore, EphA4 could be involved in regulating cell fate changes or cell movement (Xu *et al.*, 1995).

It has been shown in the zebrafish embryo that the expression of dominant negative EphA4 also causes a forebrain phenotype where there is an expansion of the retina and loss of diencephalic structures. These phenotypes suggest a role for EphA4 in regulating cell fate change or cell movement in the zebrafish forebrain (Xu *et al.*, 1996).

Recent work by mosaic analysis, has shown that Eph receptors mediate restriction of cell movement in the zebrafish embryo (Xu *et al.*, 1999). Cells expressing ephrin-B2, a ligand for EphA4 and EphB class receptors, were shown to segregate adjacent to the boundaries of rhombomeres 3 and 5, whereas they were randomly distributed in the even numbered rhombomeres. The expression of *Krox20* or EphA4 was not affected therefore, the expression of ephrin-B2 activates EphA4/EphB class receptors that leads to cell sorting and not a change in cell identity of the ligand expressing cells or their neighbours.

1.9 Neural Crest

The vertebrate neural crest is a migratory cell population that arises at the border between the neural plate and epidermis. These cells delaminate from the neuroepithelium in a rostro-caudal wave and migrate, forming many derivatives throughout the embryo. Neural crest cells form all epidermal pigment cells, much of the skull and with a contribution from ectodermal placodes, most of the peripheral nervous system (reviewed by (Le Douarin, 1982)). Specific derivatives include bone, cartilage, connective tissue, dermis, smooth muscle, melanocytes, glia, and sensory, sympathetic and enteric neurons.

At present there are three models proposed to explain neural crest cell induction: local interactions between neural and non-neural ectoderm; changes in ectodermal competence and the influence of signals from the mesoderm (reviewed by (Baker and Bronner-Fraser, 1997; Chitnis, 1999)). First, the induction of neural crest in *Xenopus* and the chick was suggested to be due to interactions between the neural plate and epidermis (Moury and Jacobson, 1990; Selleck and and Bronner-Fraser, 1995). *Slug*, a gene expressed in late gastrula prospective neural crest cells in *Xenopus* (Mayor *et al.*, 1995),and later in chick

neural induction (Nieto *et al.,* 1994), is also believed to be involved in neural crest formation (Mancilla and Mayor, 1996). Second, as previously mentioned, BMPs may also specify neural crest cell fates in a concentration-dependent manner (Wilson and Hemmati-Brivanlou, 1995). Recent experiments have extended this work to suggest that a gradient of BMP activity directly determines neural plate, neural crest and epidermal fate in the ectoderm (Marchant *et al.,* 1998; Nguyen *et al.,* 1998). In addition, it has been found that FGFs and Wnts are also provide signals for neural crest induction (LaBonne and Bronner-Fraser, 1998; Mayor *et al.,* 1997). Alternatively, the ability of epidermis to induce prospective neural plate to form neural crest cells may suggest a role for non-BMP related signalling. Third, signalling from the mesoderm may be important in neural crest induction as demonstrated in the chick (Selleck and Bronner-Fraser, 1995) and *Xenopus* (Bonstein *et al.,* 1998). A two signal model has been proposed by LaBonne *et al* (1998) where BMP provides an initial, weak specification of neural crest fate. Additional signals from adjacent non-neural ectoderm, the underlying mesoderm of both are required to attenuate and maintain neural crest induction (LaBonne and Bronner-Fraser, 1998).

Neural crest can be subdivided into cranial and trunk neural crest. Cranial neural crest tissue migrates in a segmental manner and plays a central role in the patterning of the vertebrate head (reviewed by (Bronner-Fraser, 1995)). The migration of the cranial neural crest can be subdivided for functional purposes, into four regions; caudal forebrain, midbrain, rostral hindbrain and caudal hindbrain (which overlaps with rostral vagal neural crest cells). Neural crest cells emanating from the caudal fore- and mid-brain, migrate primarily under the ectoderm as a broad, unsegmented sheet of cells (Bronner-Fraser, 1995). Derivatives of these cells are destined to become membrane bones of the face, the ciliary ganglion, part of the trigeminal ganglion, schwann cells, periocular skeleton and connective tissue of the eye.

1.9.1 Segmentation of Branchial Neural Crest

Neural crest cells emerging from the hindbrain, have segmentally restricted migration. These cranial neural crest cells migrate from rhombomere 2 to populate the mandibular (first) branchial arch and the trigeminal ganglion. Neural crest from rhombomere 4 fills the hyoid (second) arch and geniculate and vestibucochlear ganglia, and neural crest from

rhombomere 6 and more posterior regions fill the third and fourth branchial arches and the superior and petrosal ganglia of the glossopharyngeal nerve (Lumsden *et al.,* 1991).

Two questions that have been addressed in the chick are: what is the exact pathway of cranial neural crest migration and what are the factors that influence the directed migration of the neural crest cells? Cranial neural crest cells in the chick were suggested to emerge from r5 (Couly and LeDourin, 1990) an observation that contrasted with the findings of Lumsden *et al* (1991), who believed that r3 and r5 do not form neural crest cells, perhaps a result of cell death (Graham *et al.,* 1993; Lumsden *et al.,* 1991). To address these observations Graham *et al* (1993) showed elevated levels of apoptosis in the dorsal midline of r3 and r5 at a time when neural crest cells would be expected to emerge at these neuraxial levels (Graham *et al.,* 1993). The elevated apoptosis was noted to coincide with the expression of *msx-2* in a co-localised pattern. If the r3 and r5 cells where isolated or distanced from the even-numbered rhombomeres, they produced neural crest cells. *Msx-2* expression was downregulated in the transplanted rhombomeres. Therefore, the incidence of *msx-2* expression coincides with apoptosis of cranial neural crest cells in the hindbrain. Subsequently, Graham *et al* (1994) showed that the signalling molecule *Bmp4* is expressed in r3 and r5 (Graham *et al.,* 1994). This expression is dependent on the presence of neighbouring rhombomeres. The addition of recombinant BMP4 protein to explant cultures of r3 and r5 caused the expression of *msx-2* to be reinstated and apoptosis of the associated neural crest cells. Therefore, initial patterning of hindbrain cranial neural crest cells is due in part to apoptosis in r3 and r5, a result of the action of *msx-2* through BMP4.

1.9.2 Neural Crest Migration

The migratory pattern of cranial neural crest has also been shown to be influenced by their migratory environment. Contrasting with the results of Lumsden *et al* (1991) (Lumsden *et al.,* 1991), lineage tracer experiments reveal that r3 and r5 do produce a small number of neural crest cells (Sechrist, 1993). These cells migrate either rostrally or caudally to join the streams of neural crest emanating from adjacent rhombomeres; the cells fail to enter adjacent preotic mesoderm or otic vesicle region (Birgbauer, 1995). The neural crest-free zones are unlikely to be wholly due to apoptosis of the neural crest cells emanating from r3 and r5, since it has been shown that this cell death occurs after the main emanation of neural crest cells.

The exit points of the neural crest cells leaving r3 and r5 are different. Injections of lineage tracer show that the rostral region of r3 gives rise to neural crest cells that move predominantly rostrally, whereas the middle and caudal portions of r3 produce neural crest cells that migrate predominantly caudally. The migration of neural crest cells in r5 are both rostral and caudal, independent of their site of origin within the rhombomere (Birgbauer, 1995). Rhombomere rotation experiments where performed where rhombomere 3 was transplanted into the position of rhombomere 4 (Sechrist, 1994). This caused neural crest cells to preferentially exit at the r3/r4 border which indicated that either an attractive point or inhibitory signals are associated with rhombomere 3. Additionally, it was shown that transplanting rhombomere 4 into the position of rhombomere 3 caused neural crest cells to enter the mesenchyme adjacent to r3, and therefore, this mesenchyme may be inhibitory for the migration of neural crest cells of r3 origin but not those emanating from r4.

The direction of migration of neural crest can be disrupted if either the otic vesicle is transplanted to an ectopic position or is ablated, partially or fully. Neural crest cells will migrate towards the transplanted otic vesicle suggesting the presence of a selective attraction or pathway-derived cues (Sechrist, 1994). Rotation of mesoderm adjacent to r3 and r4 did not appear to alter the pattern of neural crest migration (Sechrist, 1994).

1.10 Cell Adhesion Molecules

In the chick, trunk neural crest cells migrate either in a dorsal or ventral pathway. In the dorsal pathway, neural crest cells migrate beneath the ectoderm and eventually give rise to pigment cells. The ventral pathway followed by neural crest cells, eventually gives rise to sensory and sympathetic ganglia (Rickmann *et al.,* 1985). Unlike the dorsal pathway, the ventral pathway is segmented: this is due to the presence of condensed paraxial mesoderm cells, the somites. The mature somite consists of three distinct tissues: the dermomyotome, the myotome and the sclerotome. It was found that if rostral halves of chick somites are placed adjacent to one another, the resulting ganglia are abnormally large (Kalcheim and Teillet, 1989) but if two caudal halves of chick somites are placed adjacent to each other, the resulting ganglia are smaller than normal. Therefore, the size and morphology of the ganglia resulting from the ventral migration of trunk neural crest is somite imposed. This is because ventral pathway neural crest cells only migrate

through the rostral half of the sclerotome (Bronner-Fraser and Stern, 1991) These observations suggested that an inhibitory factor found in the caudal half of the sclerotome, prevents neural crest migration or, the rostral sclerotome has an attractive factor that facilitates neural crest migration along the ventral pathway.

A possible candidate molecule shown to be involved in the segmental migration of trunk neural crest, is a peanut lectin binding glycoprotein (PNA). PNA-binding molecules have been shown to be localised to the caudal sclerotome. When PNA is applied, trunk neural crest cells migrate though the whole somite (Krull, 1995). It seems that the segmental migration of trunk neural crest cells is due to the presence of PNA-binding molecules in the caudal sclerotome, which prevents neural crest migration (Krull, 1995). Further inhibitory molecules that inhibit neural crest cell migration include collagen IX, a chrondroitin sulphate proteoglycan which is present in the caudal sclerotome (Ring *et al.*, 1996) and F-spondin which is expressed in the caudal half of the avian somite (Debby-Brafman *et al.*, 1999) Therefore, the localisation of inhibitory molecules can affect the migration of trunk neural crest. *(Stern et al., 1986)

1.11 Expression of Eph Receptors and Ligands in Neural Crest

Several receptors and ligands of the Eph family have been shown to be expressed in pre-migratory and migratory neural crest. In the mouse these include: EphA3 and EphB3 in first and second arch neural crest streams (Becker *et al.*, 1994; Cheng and Flanagan, 1994), EphA4 in the third arch neural crest streams (Nieto *et al.*, 1992) and ephrin-A class ligands such as ephrin-A4 and ephrin-A5 are associated with the ectodermal component of all visceral arches (Flenniken *et al.*, 1996). Additionally, ephrin-B1 and ephrin-B3 are expressed within the mesenchyme of visceral arches during mouse embryogenesis (Bergemann *et al.*, 1995; Flenniken *et al.*, 1996). In *Xenopus*, the expression of EphA4, as in the mouse, is found in the third arch neural crest (Winning and Sargent, 1994; Xu *et al.*, 1995). *Xenopus* EphB1 expression is observed in the third and posterior arches' neural crest (Jones *et al.*, 1995; Scales *et al.*, 1995; Smith *et al.*, 1997). Additionally, Smith *et al* (1997) have shown that *Xenopus* ephrin-B2 expression is present in the second arch neural crest and mesoderm (Smith *et al.*, 1997), an expression pattern shared with EphA2 (Helbling *et al.*, 1998). Therefore, the expression of several members of the Eph family are present in the cranial neural crest.

These findings are not exhaustive however, since precise neural crest expression analysis has only been carried out with the aforementioned Eph receptors and ligands in *Xenopus* and the mouse. Other ephrins and Eph receptors reported to be expressed in the neural crest have only been studied by northern blot analysis. The expression of these additional genes by whole mount *in situ* hybridisation has not been published.

1.11.1 Roles of Eph Receptors in Neural Crest Pathfinding

Evidence for the role of the Eph family in trunk and cranial neural crest migration have been provided by three groups (Krull *et al.*, 1997; Smith *et al.*, 1997; Wang and Anderson, 1997). It was observed that ephrin-B2 was expressed in the caudal half of rat somites (Wang and Anderson, 1997) and that the trunk neural crest predominantly expresses EphB2. Two assays were used to assess the significance of the expression of ephrin-B2 and neural crest cell migration. Rat trunk neural tubes were cultured in the presence of alternating stripes of ephrin-B2-Fc fusion protein. The neural crest cells were found to avoid ligand containing stripes. When all stripes were coated with either ligand-Fc fusion proteins or Fc alone, the neural crest cells migrated uniformly. The interpretation of these findings is that neural crest cell migration is restricted at boundaries between ligand-containing and ligand-free regions *in vitro*. The second assay utilised a transfilter chemotaxis assay which tested the effects of ligands on neural crest cell migration. It was shown that there was a concentration-dependent reduction of migration due to preclustered ephrin-B2. This supported the previous findings suggesting that the inhibition of neural crest cell migration *in vitro* requires a discontinuous or graded presentation of ligand. These findings were confirmed by work in the chick (Krull *et al.*, 1997). They found that EphB3 localises to the rostral half-sclerotome and the trunk neural crest and ephrin-B1 localises to the caudal half-sclerotome. In order to test the functional significance of this complementary expression two assays were used: an *in vivo* system using whole trunk explants or an *in vitro* system using neural crest cells. The tissue/cells from each assay were cultured on stripes of ephrin-B1. Soluble ephrin-B1 was then added to the cultures in order to disrupt receptor-ligand interactions. This caused the neural crest cells to migrate through rostral and caudal sclerotome.

In *Xenopus* embryos, cranial neural crest cells migrate from the hindbrain along specific pathways towards the visceral arches (Sadaghiani and Thiebaud, 1987). Neural crest cells

migrate from adjacent to r2 to the first branchial arch and from adjacent to r4 to the second arch. The third and fourth arch crest, emanating from adjacent to rhombomeres 5 and 6, initially migrates as one stream posterior to the otic vesicle. At first, the second, third and fourth arch neural crest cells migrate in contact with each other and during migration the third arch crest segregates into two: the third and fourth arch neural crest streams. Physical barriers between the migrating streams of crest only arise when the cells migrate deep into the forming arches where they are permanently separated by the branchial clefts (see Fig 1.8) (Sadaghiani and Thiebaud, 1987).

Xenopus EphA4 and EphB1 are expressed in third arch neural crest and mesoderm of the third arch, and third and fourth arch neural crest, respectively. Ephrin-B2, an interacting ligand of EphA4/EphB1, is expressed in the adjacent second arch neural crest and mesoderm (see Fig. 1.9) (Wilkinson, 1999). To investigate the function of these receptors in neural crest migration truncated forms of EphA4/EphB1, designed to inhibit the endogenous receptors, where injected into *Xenopus* embryos. Inhibition of EphA4/EphB1 caused aberrant migration of the third arch neural crest into the adjacent pathways: the second and fourth branchial arch territories. This is similar to the effects of the overexpression of ephrin-B2, where a scattering of third arch neural crest into adjacent territories occurs (Smith *et al.,* 1997). Targeted expression of ephrin-B2 or the truncated receptors was performed by microinjecting the A1/A2 blastomeres of the *Xenopus* embryo at the 32-cell stage. These blastomeres make a major contribution to cranial neural crest. These injections produced similar phenotypes in the neural crest indicating that the disruption of receptor-ligand interactions in neural crest leads to defects in third arch neural crest migration. In summary, these data indicate that complementary expression of EphA4/EphB1 receptors and ephrin-B2 is involved in restricting the intermingling of the third and second arch neural crest cells and in targeting the migration of the third arch neural crest to its correct destination.

1.12 Roles in Angiogenesis

Further roles for ephrins have been shown in the process of angiogenesis (Pandey *et al.,* 1995c; Wang *et al.,* 1998). A major aspect of angiogenesis is the invasive, migratory behaviour of endothelial cells which leads to the generation of blood vessels. It had been shown that ephrin-A1 was a cytokine-inducible molecule in endothelial cells, but its role

Figure 1.8

The migration of *Xenopus* neural crest

In *Xenopus* embryos, cranial neural crest cells migrate from the hindbrain along specific pathways towards the visceral arches.

Initially at stage 15, all the neural crest cells are in contact with each other. By stage 22, the second (green colour), third (red colour) and fourth (blue colour) arch neural crest cells continue to migrate in contact with each other. Neural crest cells from adjacent to r2 migrate to the first branchial arch and those adjacent to r4 migrate to the second arch. The third and fourth arch crest emanate from adjacent to rhombomeres 5 and 6: they initially migrate as one stream posterior to the otic vesicle. By stage 26, neural crest cells from r2 and r4 continue to occupy the first and second branchial arches respectively. The third arch crest segregates into two, creating the third and fourth arch neural crest streams.

Figure reproduced from Sadaghiani and Thiebaud (1987).

1-first branchial arch, 2-second branchial arch, 3-third branchial arch, 4-fourth branchial arch, St.-stage.

Stage 15

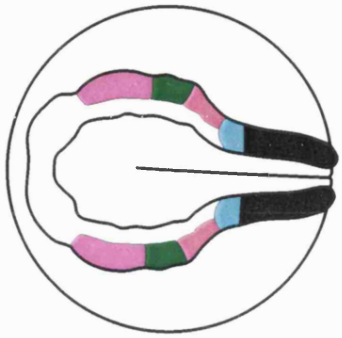

Stage 22

Stage 26

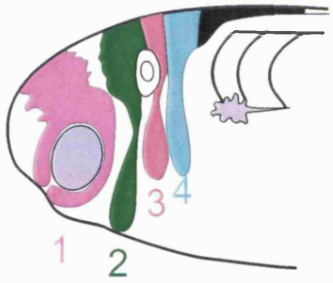

Figure 1.9

Eph family receptor and ephrin expression in *Xenopus* branchial neural crest

Several members of the Eph receptor and ephrin family are expressed in *Xenopus* branchial neural crest. EphA4 and EphB1 are expressed in third arch neural crest and mesoderm of the third arch, and third and fourth arch neural crest, respectively. Ephrin-B2, an interacting ligand of EphA4 and EphB1, is expressed in the adjacent second arch neural crest and mesoderm. EphA2 is expressed in second arch neural crest and mesoderm. It was shown that ephrin-A ligands are expressed in all branchial arches (Helbling *et al.*, 1998).

Figure adapted from Wilkinson (1999).

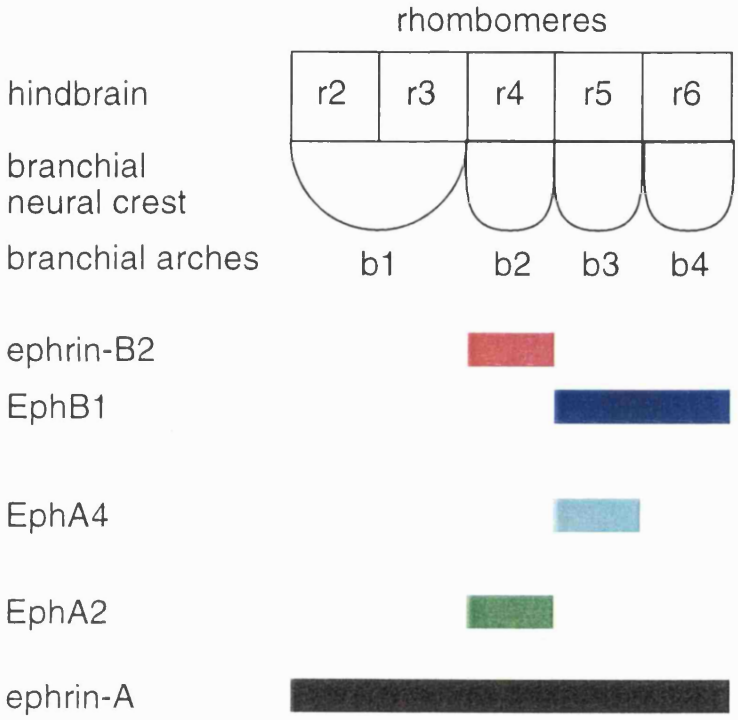
rhombomeres
hindbrain
r2
r3
r4
r5
r6
branchial
neural crest
branchial arches
b1
b2
b3
b4
ephrin-B2
EphB1
EphA4
EphA2
ephrin-A

remained unknown (Holtzman *et al.,* 1990) Chemotaxis assays were employed to test the effect of ephrin-A1 on endothelial cell migration (Pandey *et al.,* 1995c). Ephrin-A1 was shown to be a chemoattractant *in vitro* by inducing the migration of endothelial cells. Furthermore, pellets impregnated with ephrin-A1-Ig induced an angiogenic response in the normally avascular rat cornea.

Recently, ephrin-B2 was shown to be expressed in arterial endothelial cells complementary to its receptor EphB4, which is expressed in venous endothelial cells (Wang *et al.,* 1998). Analysis of ephrin-B2 knockout mice found that in the head, there is a block in the branching of the internal carotid artery and in the remodelling of the capillary bed of the anterior cardinal vein. This implicates ephrin-B2 and its receptor EphB4 in distinguishing the vascular boundary between the artery and vein and remodelling the capillary network. It is possible that ephrin-B2 provides a signal from arteries to remodel the veins. In the yolk sac, venous remodelling defects are also evident, but they are coupled with an arterial network blockage too. Therefore, a reciprocal signal from veins to arteries is also necessary for arterial angiogenesis. It can be proposed that reciprocal signalling between arteries and veins is crucial for capillary bed morphogenesis and that signalling interactions between ephrin-B class and an interacting receptor EphB4, influence the endothelial cell migration involved in vasculogenesis.

1.13 Roles in Adhesion

There are several lines of evidence that implicate Eph receptor members in cell adhesion related activities. EphB/ephrin-B interactions have been shown to induce cell adhesion in a heterologous system and in primary cultures (Bohme *et al.,* 1996; Holash *et al.,* 1997). A cellular attachment response has also been elicited by autophosphorylation of EphB receptors in endothelial-derived and teratocarcinoma-derived cell lines (Stein *et al.,* 1998b). It was found that stimulation of the cell lines with ephrin-B1 dimers and multimers (tetramers) caused phosphorylation of EphB1 and EphB2 receptors. Only multimers produced increased cell attachment between receptor and ligand expressing cells. The recruitment of LMW-PTP (low molecular weight phosphatase protein) was coincident with the attachment response but the mechanistic role of LMW-PTP with Eph signalling has not been defined. This is also true in the case of Ng-CAM (neuron-glia cell

adhesion molecule), a member of the L1 family of cell adhesion molecules which have been shown to be involved in control of cell migration, axonal outgrowth, axon fasciculation and are known to mediate cell-cell contact (Cohen *et al.,* 1997) and (reviewed by (Brummendorf *et al.,* 1998; Van Vactor, 1998)). EphB2 directly phosphorylates Ng-CAM indicating a possible regulation of adhesive properties (Zisch *et al.,* 1997).

In contrast, a role for Eph receptors in de-adhesion is shown by other experiments. An activated form of EGFR-XEphA4 was injected into *Xenopus* embryos (Winning *et al.,* 1996). There was a kinase-dependent dissociation of embryonic tissue believed to be a result of interference with the adhesive properties of the cells. Additionally, it has been shown that the injection of the *Xenopus* form of ephrin-B1 causes disaggregation of blastomeres (Jones *et al.,* 1998; Jones *et al.,* 1997). This effect was prevented by incubation of full length ephrin-B1 injected animal caps with FGF or attenuated, by the removal of the carboxy-terminal 19 amino acids of ephrin-B1. Therefore, a transmembrane ligand affects cell adhesion properties in the early *Xenopus* embryo.

1.14 Aims of the Project

The aim of this project was to clone and characterise ephrin-A ligand family members in *Xenopus laevis.*

Segmentation is a fundamental feature of the body plan. Its role is crucial in embryonic patterning in that it provides the frame work on which the body plan is established (Wilkinson, 1995). However, little is known about the signals and interactions that occur during this process. Members of the Eph family have been previously shown to have segmentally restricted expression (van der Geer *et al.,* 1994). My work addressed this problem by looking at the ligands, ephrins, for this RTK family.

1.14.1 Hypothesis

At the start of the project, the role of the Eph family was not defined. By cloning ligands, characterising them and carrying out functional experiments it was hoped to increase our knowledge for the role of the family. It had been shown that EphA4 was dynamically expressed during mesoderm formation and neurulation in the early *Xenopus* embryo (Neito *et al.*, 1992). Early functional experiments with truncated EphA4, caused the loss

of segmentally restricted expression in the hindbrain (Xu *et al.*, 1995). It was postulated that EphA4 could be involved in regulating cell fate changes or cell movement.

As the project began, four ephrins were identified (Davis *et al.*, 1994; Cheng *et al.*, 1994). They too, like EphA4, had dynamic expression in many tissues, especially neural tissues. In addition, it was found that soluble forms of the ligands did not activate their Eph receptor partners. This indicated a role for ephrins in cell-cell contact interactions between ephrin and receptor. It was hoped by cloning ephrins in *Xenopus*, evidence for a role of the Eph family in mesoderm and neurulation might be found.

In my study, a PCR strategy identified five potential ephrin-A ligands. One of these ligands XLIG4, was subsequently cloned and characterised. This potential ephrin is expressed in the first, third and fourth arch neural crest. It had been previously shown in *Xenopus*, that the overexpression of truncated EphA4 and EphB1 receptors, which are expressed in the third arch neural crest and third arch mesoderm and third and fourth arch crest respectively, caused aberrant migration of the third arch neural crest (Smith *et al.*, 1997). Therefore, it was postulated that XLIG4 may also have a role in affecting the migration of neural crest.

The functional work on XLIG4 indicates a role for the ephrin in directing the migration of the third arch neural crest in the developing *Xenopus* embryo.

CHAPTER TWO

This chapter describes the methods I have used throughout my project. The compositions of all solutions are presented below. The laboratory chemicals were supplied by BDH, Boehringer Mannheim and Sigma. The oligonucleotides were produced at N.I.M.R., Mill Hill and by OSWELL, Southampton. All molecular biology protocols were carried out as described by Sambrook *et al.,* (1989). Any deviations are described in detail below.

2.1 Standard Solutions:

LB-agar: As LB broth but with the addition of 1.5% (w/v) bacto-agar. Supplied by N.I.M.R. media.

LB Broth: 1% (w/v) bacto-tryptone, 0.5% (w/v) bacto yeast extract, 0.5% NaCl. Supplied by N.I.M.R. media.

TSB: LB Broth containing 10% PEG (MW=3,350), 5% DMSO and 20 mM Mg^{++} (10 mM each of $MgCl_2$ and $MgSO_4$).

T4 DNA ligase:
T4 DNA buffer Supplied by Boehringer Mannheim.

TE: 10 mM Tris-HCl (pH 8.0), 100 mM NaCl, 1 mM EDTA (pH 8.0)

Loading Buffer: 50% glycerol, 20 mM Tris-HCl, 20 mM EDTA (pH 8.0), 0.1% Orange G.

NAM: 110 mM NaCl, 2 mM KCl, 1 mM $Ca(NO_3)_2$, 1 mM $MgSO_4$, 0.1 mM Na_2EDTA, 2 mM $NaPO_4$ (pH 7.0), 1 mM $NaHCO_3$, 50mg/ml gentamycin).

DEPC-treated:
water 0.05% (v/v) diethyl pyrocarbonate added to deionised water, shaken, left overnight and autoclaved.

10xTBE: 108g Tris Base, 55g Boric Acid, 40mls 0.5M EDTA (pH 8.0), water to 1L.

20 x SSC: 175.3g NaCl, 88.2g sodium citrate, pH 7.0, water to 1L.

SM: 5.8g NaCl, 2g $MgSO_4.7H20$, 50ml 1M Tris-HCl at (pH 7.5), 5mls of 2% gelatin solution, water to 1L, autoclave.

10% SDS: 10g SDS, 100mls H_2O. pH 7.2.

5xTranscription: Buffer	200 mM Tris (pH 7.5), 30 mM MgCl2, 10 mM Spermidine, 50 mM NaCl.
Elution Buffer:	0.1% SDS, 1 mM EDTA, 0.5M NH_4Ac, 10 mM MgAc.
10 x PIPES Buffer:	0.4M PIPES (pH 6.4), 4M NaCl, 10 mM EDTA.
RNA loading: Buffer	80% deionised formamide, 1 mM EDTA, 0.1% Bromophenol Blue, 0.1% Xylene Cyanol.
DIG Mix:	10 mM each of dGTP, dUTP, dATP, dCTP and 3.5 mM DIG-UTP.
MEMFA:	0.1 MOPS, 2 mM EDTA, 1 mM $MgSO_4$, 3.7% formaldehyde pH 7.4.
PBS:	Phosphate Buffered Saline Tablets (Oxoid), RNAase-Free water (Romil).
PBT:	1 x PBS, 0.1% Triton X-100.
Denhardt's: Solution	50 X: 5g Ficoll, 5g polyvinylpyrrolidone, 5g Bovine Serum Albumin, water to 500ml.
Hybridisation: Buffer	50% formamide, 5 x SSC, 1mg/ml Torula RNA, 100µg/ml heparin, 1 x Denhardt's solution, 0.1% Tween-20, 0.1% CHAPS, 5 mM EDTA (pH 8.0).
PBSTw:	PBS, 0.1% Tween-20.
MAB:	100 mM Maleic Acid, 150 mM NaCl (pH 7.5).
AP Buffer:	100 mM Tris-HCl pH 9.5, 50 mM $MgCl_2$, 100 mM NaCl, 0.1% Tween-20, 5 mM Levamisol.
10 x MOPS:	0.2M MOPS (pH 7.0), 80 mM NaOAc, 10 mM EDTA (pH 8.0).
Standard: Buffer	0.5 M sodium PO4 (pH 7.2), 7% SDS, 5% dextran sulphate.

2.2 Cloning and DNA Manipulation

The bacterial strain used was Escherichia coli K12 DH5α F'.

The plasmid vectors used were:

pBluescript KS+/-

pSP64T

2.2.1 Preparation of Competent Cells for Plasmid Transformation

K12 DH5αF' were streaked on an LB-agar plate and grown overnight at 37°C. A single colony was then placed in 50mls of LB broth and allowed to shake at 37°C overnight. 5mls of the culture was then placed in 45mls of fresh LB broth. This culture was grown again shaking at 37°C until the $O.D._{600}$ was 0.3-0.6. The culture was then spun in a 4°C bench-top centrifuge at 2,500rpm for 10 minutes. The pellet of cells was then placed on ice and resuspended in 1/10th the volume of transformation and storage buffer (TSB). The cells were incubated on ice for 10 minutes and were then ready for use. Unused cells were snap frozen in aliquots of 500µl and stored at -70°C until required (Chung and Miller, 1988).

2.2.2 Subcloning and Ligation

The T4 DNA ligase and buffer were used according to the manufacturers instructions. Ligations were performed with a ratio 10:1, insert:vector. Annealing reactions were carried out overnight at 16°C.

2.2.3 Bacterial Transformation

10µl of the ligation was placed into 100µl of competent cells which had been allowed to defrost on ice. The transformation was left on ice for 30 minutes and then heat shocked at 42°C for 90 seconds. It was then placed on ice for 2 minutes. 900µl of LB broth was then placed with the mixture and incubated at 37°C. After at least 40 minutes, the cells were spun down at 3000rpm for 3 minutes and 700µl of the broth was decanted off. The transformed cells were resuspended in the remainder LB-broth and plated out onto LB-agar plates containing 100µg/ml ampicillin. The plates were incubated overnight in a 37°C incubator.

2.2.4 Isolation of Plasmid DNA in a Mini-Preparation

A single plasmid colony was placed in 4mls of LB-broth. This was grown up overnight with shaking at 37°C. 1.5mls of this culture was then placed in a microfuge tube and spun down for 3 minutes at 13,000rpm. The supernatant was aspirated from the pellet which was then re-suspended in 100µl of TE. To this 100µl of phenol:chloroform:iso-amyalcohol (25:24:1), was added. The mixture was vortexed twice and then centrifuged at 13,000rpm for 10 minutes. The aqueous layer of the phenol/chloroform step was

removed and placed in 100µl chloroform. This solution was vortexed twice and centrifuged again at 13,000rpm for 10 minutes. The aqueous phase from this step was then placed into 300µl of 100% EtOH previously stored at -20°C. This solution was incubated on ice for 15 minutes. The solution was then centrifuged at 13,000rpm for 5 minutes. The resultant pellet was washed with 70% EtOH and left to air dry for 3-5 minutes. The pellet was resuspended in 50µl TE and stored at -20°C. When running out the plasmid DNA on a gel, the loading buffer contained RNAaseA at 10µg/ml. This digests any RNA contamination of the plasmid DNA.

2.2.5 Maxi-Preparation of Plasmid DNA

1ml of plasmid bacterial culture was placed in 100mls of LB-broth containing 100µg/ml ampicillin. The Qiagen maxi-prep kit (Hybaid) was then used to isolate the maxi-prep DNA. The DNA concentration was calculated by reading the optical density at 260 and 280nm.

2.2.6 Restriction Endonuclease Digests of DNA

All restriction digest were carried out in accordance with the manufacturers instructions.

In certain cases it was necessary to de-phosphorylate the ends of vectors to be used in cloning. This step aids cloning success by preventing vector-vector re-ligation. A 40µl complete restriction enzyme digest of a vector was carried out. 4µl of phosphatase buffer was added to the digest and 1µl of alkaline phosphatase enzyme was also added. This reaction was then placed at 37°C for a total of 15 minutes. A third of the reaction was removed at the 5 minute and 10 minute time points, in order to ensure I had a vector aliquot that had not been over-phosphatased. 2.5µl of 0.2M EGTA was added to the digest and incubated at 65°C for 10 minutes to inactivate the phosphatase enzyme. The digest was then vortexed with an equal volume of phenol:chloroform (1:1) and then centrifuged at 13,000rpm for 10 minutes. The resultant aqueous phase was placed in 2.5 x volume of 100% EtOH, 1/10th x volume of 3M NaOAc and 1µl glycogen (20µg/µl). The solution was precipitated on dry ice for 30 minutes and centrifuged at 13,000rpm for 15 minutes. The pellet was washed in 70% EtOH again centrifuging at 13,000rpm for 5 minutes. The final pellet was resuspended in TE.

2.2.7 Electrophoretic Separation of DNA and RNA

The DNA or RNA sample were separated using agarose gel electrophoresis with TBE buffer. The percentage of the agarose used depended on the size of bands to be visualised. The DNA or RNA sample was loaded after mixing the sample with a one tenth volume of Orange G buffer. The size of the band was determined by co-running a 1Kb ladder with the samples. Ethidium bromide was included in the gel preparation using 1µl of a 10mg/ml solution in 100mls of agarose gel solution, so that the DNA or RNA bands could be visualised with a UV transilluminator and subsequently photographed.

2.3 Embryo Culture and Manipulations

Xenopus embryos were obtained from adult females that had been injected 12 hours previously with 800 units of human chorionic gonadotrophin (HCG). The eggs were expelled by gentle peristalsis of the mother's ventrolateral surface. They were then fertilised by rubbing them with the dissected testes from a sacrificed male. After 10 minutes the eggs were flooded with 10% Normal Amphibian Medium (NAM). After they had rotated, the embryos were dejellied using 2% cysteine hydrochloride (pH 7.9-8.1) and were staged (Nieuwkoop and Faber, 1975).

2.3.1 Microinjection of *Xenopus* Embryos

Dejellied embryos were placed into 75% NAM solution containing 4% ficoll. One cell of the embryos at the 2 cell stage or 32 cell stage was injected using a using a glass needle and an air-driven injection system (Inject+matic). Volumes of 10nl were injected into the embryo.

2.4 RNA Isolation

RNA was isolated from embryos using the TRIzol™ Reagent (Total RNA Isolation Reagent) produced by GIBCO BRL. The embryos used in this procedure were obtained as described above. Once they had reached the desired stages for analysis, the embryos were placed in microtubes with all surrounding medium removed. They were then snap-frozen on dry ice and stored at -80°C until required.

The manufacturers instructions for TRIzol™ Reagent were followed. Briefly, this method uses a mono-phasic solution of acid phenol and guanidine isothiocyanate. The embryos were homogenised in the TRIzol™ Reagent. The homogenate was then left at room temperature for 5 minutes after which time an equal volume of chloroform was added. This solution was mixed and centrifuged and the aqueous layer was removed and precipitated with propan-2-ol and glycogen (20µg/µl). After being left at room temperature for 10 minutes the solution was re-centrifuged. The resulting RNA pellet was washed in 75% ethanol and left to air dry for 5 minutes. The pellet was re-suspended in DEPC-treated water (diethyl pyrocarbonate). As a further purification step this RNA was placed mixed together with an equal volume of 8M LiCL. This was then incubated on ice for 2 hours. The solution was then spun down for 15 minutes at 13,000rpm at 4°C. The pellet was left to air-dry for 2-5 minutes and resuspended in 50-100µl DEPC-treated water.

2.4.1 RT-PCR Cloning of Ephrins

RNA was isolated from embryos at stages 10 and 17. This was used to create cDNA using a Stratagene kit. Both oligo dT and random hexamer primers were used. These cDNA preparations were then both used for PCR.

Three degenerate oligonucleotides, two 5' and one 3' were designed based on conserved regions within the published sequences of ephrin-A1, ephrin-A2 and ephrin-A3, ligand members of the Eph receptor family. The peptide sequences of the primers are given below:

```
     EcoR1 (V/L) D   I (I/Y) C  P                    Oligo 1
5' gaattcTN  GAT ATT ATT TGT CC 3'                    1A
              C   C   C   C
                  A   A

5' gaattcTN  GAT ATT TAT TGT CC 3'                    1B
              C   C   C   C
                  A

  EcoR1 (V/L) D   I (I/Y) C   P   H  Y                Oligo 2
5'gaattcTN   GAT ATT ATT TGT CCN CAT TA 3'            2A
              C   C   C   C   C
                  A   A

5'gaattcTN   GAT ATT TAT TGT CCN CAT TA 3'            2B
              C   C   C   C   C
                  A

   BamH1                                              Oligo3
3' ggatccA NCT CTG GAA TTT CTC 5'   (antisense)      3A
           T   A   C   T
```

```
3' ggatccA CCT CTG GAA TTT CTC 5'    (antisense)        3B
          T   T   A   C   T
```

The N nucleotide represents any nucleotide. Each oligonucleotide was made in two forms e.g. 1A and 1B to avoid inappropriate codons at positions with alternative amino acids. These oligonucleotides were used in a 1:1 ratio A:B, in the PCR reactions. The oligo nucleotides are represented as capital letters (see above). Restriction sites were included at the oligonucleotide 5' ends (small letters).The combined degeneracy for 1A (36) + 1B(24) is 60; for 2A(72) +2B(48) is 120 and for 3A (16) + 3B(32) is 48.

These primers were used under the following PCR conditions: 1 cycle of 94°C for 3 minutes followed by 4 cycles of 94°C for 45 seconds, 42°C or 47°C or 51°C for 2 minutes, 68°C for 1 minute, 72°C for 1 minute, followed by 40 cycles of 94°C for 45 seconds, 60°C for 2 minutes, 68°C for 1 minute, 72°C for 1 minute and finally 1 cycle of 72°C for 10 minutes. The final $MgCl_2$ concentration used was 1.5 mM.

2.4.2 Gel-Purification of DNA

The PCR products were run on 2.5% agarose gels. The amplified sequences running at or round 200 bp were gel extracted (Qiaex II Agarose Gel Extraction, Qiagen). Recovered PCR fragments were then cut with BamHI and EcoRI (sites incorporated into the original PCR primers). The 200 bp DNA was subcloned into de-phosphorylated pBluescript KS+.

2.5 DNA Sequence Analysis

The sequences of the initial 104 recombinants and the full sequences of positive recombinants were obtained by using the Pharmacia Biotech Kit. The sequencing reactions were run on 5% denaturing acrylamide gels (Sequagel, National Diagnostics) at 60 watts for 2-3 hours.

2.5.1 Sequence Comparisons

These were obtained using the Seqed, BestFit, Translate, PileUp, Distance and GrowTree functions on the GCG programme.

2.6 Library Screening

To obtain longer cDNA clones of the putative ligands, a stage 17 *Xenopus* λgt10 cDNA library was plated with Y1090 cells. 800 000 clones were screened with 200 bp PCR fragment probes labelled using the Mega Prime Random Labelling Kit (Amersham). Briefly, 25ng of the PCR fragment was present in 29µl of double-distilled water. This solution was denatured by boiling for 2 minutes in the presence of 5µl of primer. The solution was left to cool to room temperature for 5 minutes. To this label reaction 10µl of label buffer, 5µl of ^{32}P-dCTP and 2µl of Klenow fragment were added. The reaction was then incubated at 37°C for 15-30 minutes. The probe was then purified by passing it through a G-50 spin column to remove all unincorporated nucleotides. The specific activity of 1µl of probe was measured by scintillation counting. The filters were placed in hybridisation buffer and incubated at 65°C for 1-2 hours. Probe at 1 x 10^6 cpm/µl was then boiled for 2 minutes and directly added to fresh 65°C warmed hybridisation buffer. The filters were then hybridised in this buffer at 65°C overnight. The following day the filters were washed as follows; 2 x 30 minute washes each at 2 x SSC, 1 x SSC and 0.1 x SSC at 65°C. Positive clones were picked which were purified through two more rounds of screening until the final positive clone was obtained.

2.6.1 Obtaining DNA from λgt10 Phage Library

DNA from positive library clones was obtained using a plate lysate method (Kuo *et al.*, 1982). Eight plates (13.7cm) were plated with the positive phage and left to grow overnight at 37°C. Once complete confluent lysis was achieved, each plate was overlain with 10mls SM. The plates were then placed on a rocker overnight at 4°C. The SM was harvested from the plates into 50ml falcon tubes. A further 3ml of SM was added to each plate and recovered. The SM fractions were then pooled. 0.5ml of chloroform was added to the cultures which were allowed to shake for 5 minutes at 37°C. The cultures were centrifuged at 4K for 20 minutes at room temperature. DNAase and RNAase each at a final concentration of 10mg/ml was added to the supernatant obtained from the lysed cultures. The supernatant was left at 37°C for 30 minutes and spun down (Sorvall SS34) for two hours at 16K. The supernatant was poured away and the remaining pellet re-suspended with 0.3ml 0.1M Tris-HCl (pH 7.9), 0.3M NaCl. This solution was then left at 4°C overnight. 50µl of Proteinase K (10mg/ml) was then added to the solution which was incubated at 37°C for 30 minutes. EDTA was then added to a final concentration of

10 mM. The DNA was extracted three times with Phenol-Chloroform-isoamyl alcohol preequilibrated with 1M NaCl, 20 mM Tris-HCl (pH 8.0) and 1 mM EDTA. The aqueous phase was precipitated in 2 volumes of 100% EtOH at -20°C overnight. The solution was aliquoted into eppendorf tubes and centrifuged at 13,000rpm for 15 minutes. The supernatant was aspirated and the pellet was allowed to air dry for 5-10 minutes and then resuspended in 400µl TE (pH 8.0). The DNA was excised from the phage λgt10 arms by restriction enzyme digestion with EcoRI.

2.6.2 Southern Blot

DNA obtained from the cDNA clone was digested with several restriction enzymes producing different numbers and sizes of bands on an agarose gel. To decide which of these bands should be subcloned Southern blot analysis was used. The protocol for Southern blot analysis described in (Sambrook *et al.,* 1989) was followed. A megaprime labelled probe, corresponding to the 200 bp PCR isolate that was positive for this DNA, was used to probe the blot. Conditions for post hybridisation washes each of 20 minutes were : 2 x SSC/0.1% SDS, 0.2 x SSC/0.1% SDS, 0.1 x SSC/0.1% SDS, all at 65°C . 3 bands, resulting from the *Eco*R1 digest of the clone DNA that hybridised with the blot, were subcloned into pBluescript KS+.

2.7 RNAase Protection

RNAase protection assays were performed essentially as described (Jones *et al.,* 1992). A detailed protocol is presented below. (The ephrin clones obtained from the PCR analysis were labelled and used as protection probes). All probes are approximately 200 bp in size.

2.7.1 Preparation of Probe

Each clone was directionally subcloned into pBluescript KS+ such that on linearisation with *Cla*I and transcription with T7 RNA polymerase, an anti-sense probe was created. To make the anti-sense riboprobe, the following *in vitro* transcription reaction was set up at room temperature: 1µl of DNA template (1µg/µl) was added to 4µl of 5x transcription buffer. 2µl 0.1M DTT, 1µl 0.5 mM UTP, 3µl rNTP mix (GAC) 3 mM of each, 1µl RNAsin, 5µl ^{32}P-UTP (800 Cu/mmol), 5µl dH20. The reaction mixture was pre-warmed for 5 minutes at 37°C. 1µl of RNA Polymerase (T3, T7 or SP6) was then added. The mix

was incubated at 37°C for 1 hour. To degrade the DNA template, 1µl RQ1 DNAase was added to the reaction. The mix was re-incubated at 37°C for 15 minutes. 10µl of RNA loading buffer was added for every 20µl of reaction mix.

2.7.2 Probe Purification

The probe was purified on an 6% sequencing gel (Sequagel) with TBE buffer. The gel was run at 25W until the xylene cyanol band of the loading buffer was two-thirds of the way down the gel. The gel was exposed for 10-15 seconds while it is still attached to one of the gel plates. The exposed film was placed beneath the gel plate, and using it as a template, the probe band was cut from the gel. The gel piece was placed in an eppendorf tube and cut into small pieces. 500µl of elution buffer was added to the gel pieces. This was incubated for 2 hours-overnight at 50°C.

The eppendorf was spun down for 20 seconds, 13,000rpm, at room temperature. 450µl of the supernatant was removed from the eppendorf, placed into a fresh eppendorf tube and spun down again. 400µl of the supernatant was added to 40µl NaOAc, 50µg tRNA (torula) and 1ml ice cold 100% EtOH. This was precipitated twice on dry ice. The mix was centrifuged for 30 minutes, 13,000rpm and washed with 70% ice cold EtOH. The pellet was allowed to dry for 3-5 minutes. The pellet was re-dissolved in 50µl DEPC-treated H_2O. 1µl of the probe was counted in the scintillation counter. All riboprobes were used with an activity of $5x10^5$ cpm/µl.

2.7.3 Hybridisation

30µg of total RNA from the chosen developmental stages 10, 13 or 17 was placed in a final volume of 15µl of DEPC-treated H_2O. To this was added 4µl of 10X PIPES buffer, 20µl of deionised formamide and 1µl of 32P-RNA probe ($5X10^5$ cpm/µl). A control sample consisted of the same mix but the same concentration of tRNA replacing the RNA used. To each tube 1µl of the loading control marker EF1-α which is expressed in all embryonic cells was added (Krieg *et al.,* 1989; Sargent, 1990). The mix was vortexed and heated at 85°C for 5 minutes. The eppendorf tube was quickly spun down for 20 seconds at 13,000rpm, and placed in a 50°C water-bath for 8 hours-overnight, to allow hybridisation to take place.

2.7.4 Degradation of Non-Protected RNA

The tubes were brought to room temperature. Protected fragments were digested with the following mix (for 10 eppendorf tubes): 30µl 1M Tris pH 7.4, 0.25M EDTA pH 8.0, 180µl 5M NaCl, 6µl T1 (10 units/µl) and 2.8mls dH_2O. 300µl of this mix was added to each protection sample which were placed at 37°C for 15 minutes. 20µl 10% SDS, 50µl Proteinase K (1mg/ml; freshly diluted), 1µl tRNA (torula 10mg/ml) and 800µl ice cold 100% EtOH were added to the samples that were precipitated twice on dry ice for 15 minutes. The samples were spun down for 30 minutes at 13,000rpm at room temperature. Pellets were washed with 200µl of ice cold 70% EtOH and left to dry for 3-5 minutes.

The pellets were dissolved by adding 1µl of dH_2O and 5µl of RNA loading buffer. The mix was heated at 80°C for 2 minutes. Samples were re-heated prior to separation on an 8% polyacrylamide sequencing gel which was subsequently fixed, dried and exposed on Kodak X-AR film overnight at -70°C with two intensifying screens.

The developmental RNAase protection followed the above protocol but 40µg of total RNA was used in the hybridisations.

2.8 Whole Mount in situ Hybridisation

RNA localisation was visualised using whole mount RNA in situ hybridisation (Wilkinson, 1994). The 727 bp fragment of Xephrin-A3 was subcloned into pBluescript (KS+) and was linearised with *Cla*I, which provided a template on which an anti-sense digoxygenin (DIG) labelled riboprobe could be transcribed. T7 RNA polymerase was used as the transcription enzyme. The sense probe was made by linearising the template with *Not*I, and transcribing with T3 RNA polymerase. The sense probe provides a control for non-specific hybridisation.

2.8.1 Preparation of Probe

The riboprobe was prepared using DIG Labelling Mix (Boehringer Mannheim). The probe was made as follows: 10µl 5 x Transcription buffer, 2.5µl Linearised plasmid template (1µg/µl), 0.5µl 1M DTT, 10µl DIG mix, 1µl RNAsin, 24µl RNAase-free water, 2µl RNA polymerase. The reaction was incubated for 2 hours at 37°C. 2µl of RNAase-free DNAase 1 was then added to the reaction and incubated at 37°C for a further 15 minutes. The probe was then purified using the RNAase-free Clontech column system.

This was followed by precipitation by addition of 0.5 volumes 10M NH4ACe, 2.5 volumes 100% EtOH and 1µl glycogen (20µg/µl) to the probe. This mix was placed in dry ice for 30 minutes. The probe was then centrifuged at 13,000rpm for 15 minutes at 4°C. The resulting probe pellet was washed with 70% EtOH and centrifuged again at 13,000rpm for 5 minutes at 4°C. The pellet was allowed to dry at room temperature for 2-5 minutes and it was then resuspended in 20-30µl of RNAase-free water.

2.8.2 Preparation of Embryos and Hybridisation

Embryos were obtained as detailed earlier. Once they had reached the desired stages for analysis, the embryos were placed directly in MEMFA and left for 30 minutes at room temperature. The embryos were then taken though a series of washes of 10 minutes each in PBT, 30% methanol in PBT, 70% methanol in PBT and 100% methanol. The embryos were then stored at -20°C. The embryos were rehydrated though this series of washes when they were required for the whole mount RNA in situ hybridisation procedure. Briefly the method is as follows; rehydrated embryos are treated with 10µg/ml proteinase K (Proteinase K solution, Boehringer Mannheim) in PBT for 5 minutes at room temperature. The embryos are then washed 2 x 5 minutes in 0.1M triethanolamine (pH 7-8). The embryos are then incubated with a solution containing 12.5µl acetic anhydride for every 5mls of triethanolamine, for 5 minutes. Another 12.5µl of acetic anhydride is added to the embryos again per 5mls of triethanolamine for a further 5 minutes. The embryos are then washed in PBT 2 x 5 minutes. The embryos are then re-fixed by placing them in a 4% solution of formaldehyde in PBT where they are washed for 20 minutes. After a further wash in PBT for 20 minutes the embryos are placed in 1ml of hybridisation buffer. The embryos are allowed to sink. The buffer is then replaced with another 1ml of fresh hybridisation buffer. The embryos are then left to prehybridise overnight at 60°C. The following day, fresh hybridisation buffer replaces the overnight buffer and the DIG labelled probe is then added to 1µg/µl. Hybridisation was also at 60°C overnight.

2.8.3 Post-Hybridisation Washes

All the following washes are done at 60°C. The hybridisation buffer was replaced with mock-hybridisation buffer (mock-hyb buffer). The embryos were washed in this buffer for 10 minutes. The embryos were then sequentially washed with the following solutions:

50% Mock-hyb buffer/ 50% 2 x SSC for 10 minutes, 25% mock-hyb buffer/ 75% 2 x SSC for 10 minutes, 2 x SSC/ 0.3% CHAPS for 2 x 20 minutes, 0.2 x SSC/ 0.3% CHAPS for 10 minutes, PBST/0.3% CHAPS for 2 x 10 minutes and PBST for 3 x 5 minutes at room temperature.

2.8.4 Antibody Washes and RNA Detection

The embryos were then prepared for antibody incubations. The embryos were washed in Maleic Acid Buffer (MAB) for 3 x 5 minutes at room temperature. They were then placed in MAB containing 20% heat-treated lamb serum and 2% blocking reagent (Boehringer Mannheim). The embryos are then incubated for 1 hour at room temperature to block the tissues. This solution was then replaced with MAB, lamb serum and blocking reagent containing anti-digoxygenin antibody coupled to alkaline phosphatase, at a dilution of 1:2000. The embryos are incubated in this solution overnight at 4°C. After 5 x 1 hour washes in MAB at room temperature and a final wash overnight at 4°C, the embryos were washed 2 x 5 minutes in alkaline phosphatase buffer. For colour development the embryos were developed using NBT/BCIP Tablets (Boehringer Mannheim). Once the colour reaction had developed sufficiently, the embryos were washed in for 10 minutes and then placed in MEMFA fix for 30 minutes at room temperature. The embryos are then placed in PBS at 4°C.

2.8.5 Fluorescein Dextran Detection

In some experiments, embryos were co-injected with RNA and dextran fluorescein. This was done in order to confirm the site of injection of synthetic RNA in the 1 in 2 cell stage injections and the 1 in 32 cell stage injections. After the embryos had been fixed in the MEMFA at the post-colour development step above, the embryos were washed for 2 x 20 minutes in PBS containing 0.1% Tween (PBSTw). They were then placed in PBST containing 10% heat-treated lamb serum and incubated in this solution for at least 1 hour at 4°C. This solution was then replaced but it also contained anti-fluorescein-AP Fab fragments at a 1:2000 dilution. The embryos were incubated in this solution overnight at 4°C. The following day, the embryos were washed 6 x 20 minutes in PBSTw. They were then washed for 2 x 5 minutes in 0.1M Tris-HCl pH 8.2, 0.1% Tween. This solution was replaced with Fast Red Tablets (Boehringer Mannheim) dissolved in 0.1M Tris-HCl solution and cooled on ice (1 tablet/2mls solution) which allows full penetration of the

staining solution into the embryos. The embryos were then placed on ice and kept in the dark. After 30 minutes to 1 hour the Fast Red colour had reached the desired intensity. The reaction was stopped by washing the embryos 2 x 10 minutes in PBSTw and then re-fixing in MEMFA for 30 minutes at room temperature. The embryos were then washed and stored in fresh PBSTw at 4°C.

2.8.6 Clearing Embryos

In some cases it was necessary to clear the embryos. In this procedure, the embryos are taken from the PBS solution and washed in methanol for 30 minutes at room temperature. They are then rinsed once in Murray's Clear (Benzyl Benzoate: Benzoic Acid in a 2:1 ratio). The embryos are then put into a glass dish containing fresh Murray's Clear and photographed using transmitted light.

2.8.7 Sectioning Embryos

For sectioning, the embryos are washed in methanol 2 x 5 minutes and then in propan-2-ol for 2 x 10 minutes. They are then placed in cedarwood oil (BDH/Merck, Poole, Dorset.) for 2 x 30 minutes and then overnight in fresh cedarwood oil. These embryos are transferred to a 1:1 mixture of cedarwood oil and wax in a 60°C embedding station. After 3 changes in wax lasting at least 30 minutes each and one overnight incubation, the embryos are oriented and embedded in fresh wax. 10µm sections were cut on a microtome. The resulting ribbon sections were placed onto water heated to 55°C. These sections were then captured onto Tespa (Rentrop, 1986) coated superfrost slides (BDH) and then left to dry overnight on a 47°C hot plate. To de-wax the sections, the slides were placed in 2 x 5 minutes of Histoclear. Excess Histoclear was allowed to drip off the slides and the sections were then mounted with DPX mountant (BDH 360294H).

2.9 *In vitro* Transcription and Translation

2.9.1 Creation of Truncated Xephrin-A3

Two constructs were used in the ectopic expression experiments (Chapter 5). Both constructs were subcloned into pSP64T vector to enable subsequent *in vitro* translation. The resultant RNA was injected into the *Xenopus* embryo. One construct encoded the full

coding region of Xephrin-A3 and the other encoded a deletion of the 3' hydrophobic region, creating a soluble form of the ligand.

The full coding region was previously cloned in pBluescript KS+. This region was excised from pBluescript KS+ and cloned into suitably cut pSP64T. The truncated Xephrin-A3 had to be created by PCR. Two primers were designed: the first encoded nucleotides in the initiating methionine region and the second, was designed to create a stop codon at the beginning of the 3' hydrophobic region.

The primers used are indicated below with the position along the coding region indicated by the bp (base pair) number.

```
      1                    10 bp
5'    GCGGATCATGGCTTTG

      594                  609 bp
3'    CTCCCTCGTGAATGTGATC
```

The primers were used in the following PCR reaction: 5µl 10 x PCR buffer, 1µl each of dATP, dTTP, dGTP and dCTP, 0.25µl of each primer at 1mg/ml and 5µl of Xephrin-A3 (1pg/µl). The reaction was made up to 50µl with DEPC-treated water. To increase the fidelity of base incorporation, 0.5µl of Vent DNA Polymerase was used (New England Biolabs) per 50µl PCR reaction.

The following PCR conditions were used: 2 cycles at 94°C for 45 seconds, 50°C for 30 seconds, 72°C for 1 minute, 20 cycles at 94°C for 20 seconds, 55°C for 30 seconds and 72°C for 1 minute. These PCR products were cloned into pSP64T vector. End sequencing of the resultant clones indicated that both constructs encoded correct forms of Xephrin-A3.

2.9.2 *In vitro* Translation Reaction

At room temperature the following *in vitro* transcription reaction was assembled:
10µl 5 x Transcription buffer, 6.3µl 0.25M DTT, 2µl each 25 mM ATP, CTP, UTP and 2.5 mM GTP, 5µl 5 mM GpppG (Cap analogue, New England Biolabs), 2.5µl RNAsin (Promega), 2.5µl RNA polymerase (Promega) and 5µl DNA (1µg/µl).

This reaction was mixed and incubated at 37°C for 1.5 hours. 2.5µl 10 mM GTP was then added to the reaction which was left to incubate for a further 30 minutes at 37°C. 5µl of RQ1 DNAase1 (Promega) was then added to the reaction which was further incubated at 37°C for 30 minutes. The reaction was then spun down in an R-50 spin column Clontech). The elutate was then precipitated by adding 0.5 volumes 10M NH4AC, 2.5 x volumes 100% EtOH. This precipitation was placed at -20°C overnight. It was then spun down at 13,000rpm at 4°C for 15 minutes. The pellet was washed with 75% EtOH and spun down again at 13,000rpm, at 4°C for 10 minutes. The ethanol was then removed and the pellet was left to dry on the bench for 2-4 minutes. The RNA was then resuspended in 20µl of sterile RNAase-free water. The concentration of RNA was measured with an $O.D._{260}$.

2.9.3 *In vitro* Transcription Reaction

To ensure the synthetic RNA was translated and produced a correct size protein, the rabbit reticulolysate system (Promega) was used. 400ng of synthetic RNA (*in vitro* translation product) was added to 8µl of reticulolysate, 0.5µl amino acid mix minus methionine, 0.5µl 35S methionine and 0.5µl RNAsin. This mix was incubated at 30°C for 1 hour. 11.5µl of 2x buffer was added to the mix which was then placed at -20°C. The translation reactions were placed in boiling water for 2 minutes and then run on a 15% SDS-PAGE, using the buffer system of Laemmli. Protein size was estimated by comparison to pre-stained "Rainbow" molecular weight markers (Amersham).

2.10 Northern Blotting Analysis

Northern analysis was carried out in order to determine the size of the full length gene of XLIG4. The intensity of the bands seen would also indicate the amount of the mRNA present at that particular embryonic stage of development.

2.10.1 Preparation of Gel and RNA Samples

All solutions used in this procedure are RNAase-free. An 1.2% agarose gel was run (1.8g agarose and 126.5ml sterile RNAase-free water). This solution was boiled using a hot plate. The solution was then removed from the heat and allowed to cool. 8.75mls of formaldehyde (30%) and 15mls of MOPS was then added to the solution which was then

poured into a gel apparatus previously treated with 0.2M NaOH overnight to ensure RNAase contamination was minimised.

The RNA loading samples consisted of: 6.75µl of 10mg of total RNA was added to 5.25µl formaldehyde (30%), 15µl formamide and 3µl 10 x MOPS. These mixes were then incubated at 65°C for 15 minutes. 5µl of loading dye was then added to each sample. These samples were then loaded on the denaturing gel. The RNA samples were also added to loading dye containing ethidium bromide. These samples can be visualised under the UV transilluminator and the extent of the migration of the component 18S and 25S of the RNA can be measured. This allows the size of the mRNA to be calculated.

The gel was run for 4 hours at 70V with 1 x MOPS buffer and a picture of the gel was taken. The gel was then immersed in 0.05M NaOH for 15 minutes. This solution was replaced with 20 x SSC and the gel was gently shaken for 30 minutes. Following the protocol in Sambrook *et al.,* (1989), a nylon membrane was placed onto the gel (Hybond N; Amersham) which was used to immobilise the size fractionated RNA. Using capilliarity and 20 x SSC buffer, the blot was set up and left overnight.

2.10.2 Preparation of Probe and Hybridisation

A photograph was taken of the gel to ensure the efficient RNA removal. The nylon Hybond N^+ membrane with the bound RNA was cross-linked by exposure to UV light in a Stratalinker (Stratagene) and then baked for 2 hours in an 80°C oven. The membrane was then prehybridised in standard buffer (modified Churches' buffer) at 60°C for 2-4 hours (Sambrook, 1989). A radiolabelled probe consisting of the 700 bp of the coding region of the Xephrin-A3 gene was made with the Mega prime kit as previously described. This probe at 5 x 10^5 cpm/ml was added to warmed, fresh standard buffer containing torula RNA (20µg/ml), in which the Northern Blot was placed. The blot was hybridised overnight at 60°C , washed for 2 x 10 minutes with 2 x SSC/ 0.1% SDS at room temperature and again washed with 2 x SSC/0.1% SDS but at 60°C for 30 minutes. The blot was then placed in saran wrap and exposed on Kodak X-OMAT film with intensifying screens for 2 days at -70°C and exposed.

CHAPTER THREE

3.1 INTRODUCTION

All members of the Eph family were initially identified as orphan receptors (Bennett *et al.,* 1995; Harai *et al.,* 1987; Maisonpierre *et al.,* 1993). When the first ligands were identified, it was found that they were members of a novel gene family. Sequence alignments of these so-called ephrins (ephrin-A1, ephrin-A2, ephrin-A3 and ephrin-B1), showed that they shared conserved regions including four conserved cysteine residues (Cheng and Flanagan, 1994; Davis *et al.,* 1994). The ephrin sequences also indicated that ephrin-B1 contained a transmembrane domain whereas the carboxy terminal ends of ephrin-A1, ephrin-A2 and ephrin-A3 encoded a glycosylphosphatidylinositol (GPI) linkage motif. Using this sequence information, I designed primers for use in a PCR-based strategy, based on regions of high homology between these ephrins.

This chapter describes the identification of ephrin-A ligands in the early *Xenopus* embryo by this PCR strategy. I will analyse the sequence data obtained from the PCR clones and compare them with ephrins previously cloned in other vertebrate species.

3.2 RESULTS

3.2.1 RT-PCR Procedure

The primer design was based only on the sequences of ephrin-A1, ephrin-A2 and ephrin-A3 since the ephrin-B1 sequence is divergent and a primer could not be designed that was long enough to accommodate amplification of both subclasses.

Three degenerate oligonucleotide primers were designed, two 5' and one 3', suitable for use in an RT-PCR based strategy. These primers were used to amplify a conserved region of 165 nucleotides in length, specific for members of the ephrin-A class. The region chosen for the screen is shown in Fig. 3.1. The amino acid sequences corresponding to the primers are shown below with their nucleotide sequences detailed in Chapter 2.

5'	(V/L)DI(I/Y)CP	**Oligo 1**
5'	(V/L)DI(I/Y)CPHY	**Oligo 2**
3'	EKFQR(F/Y)	**Oligo 3**

Figure 3.1

The primers chosen to amplify ephrins in *Xenopus*

The regions of homology between ephrin-A1, ephrin-A2 and ephrin A3 which were used to create degenerate oligonucleotide primers for the RT-PCR procedure are shown.

The arrows above the sequence indicate the 5' and 3' ends of the primer sequences. The sequence motifs are in bold. The boxed amino acids indicate sequence expected in ephrin clones. The conserved cysteine residues are high-lighted in red.

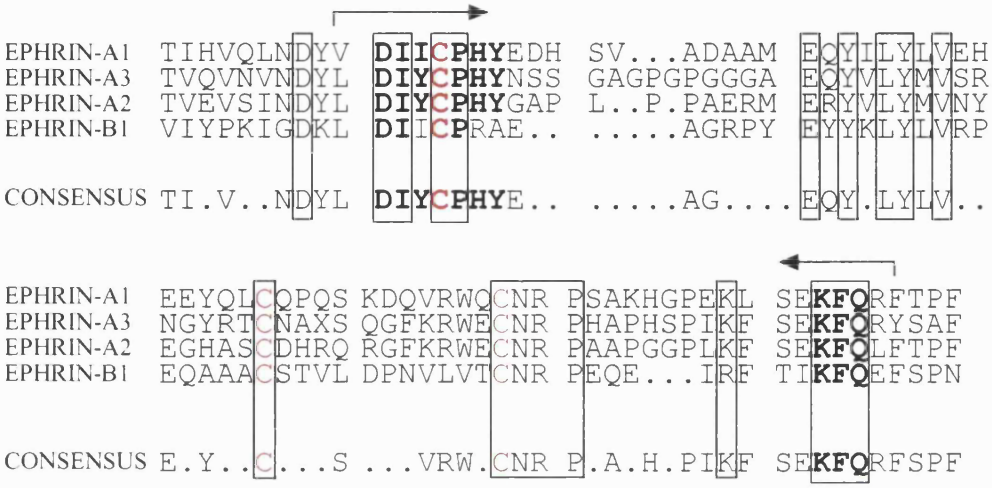
EPHRIN-A1 TIHVQLNDYV DIICPHYEDH SV...ADAAM EQYILYLVEH
EPHRIN-A3 TVQVNVNDYL DIYCPHYNSS GAGPGPGGGA EQYVLYMVSR
EPHRIN-A2 TVEVSINDYL DIYCPHYGAP L..P.PAERM ERYVLYMVNY
EPHRIN-B1 VIYPKIGDKL DIICPRAE.. .....AGRPY EYYKLYLVRP
CONSENSUS TI.V..NDYL DIYCPHYE.. .....AG....EQY.LYLV..
EPHRIN-A1 EEYQLCQPQS KDQVRWQCNR PSAKHGPEKL SEKFQRFTPF
EPHRIN-A3 NGYRTCNAXS QGFKRWECNR PHAPHSPIKF SEKFQRYSAF
EPHRIN-A2 EGHASCDHRQ RGFKRWECNR PAAPGGPLKF SEKFQLFTPF
EPHRIN-B1 EQAAACSTVL DPNVLVTCNR PEQE...IRF TIKFQEFSPN
CONSENSUS E.Y..C...S ...VRW.CNR P.A.H.PIKF SEKFQRFSPF

Each primer was also designed to incorporate a restriction site, such that the 5' primers, Oligo1 and Oligo2, included the restriction site for *Eco*R1 and the 3' primer, Oligo 3, a restriction site for *Bam*HI. These restriction enzyme sites would increase the likelihood that the subcloned *Eco*R1-*Bam*HI digested PCR products contained the correct 5' and 3' primers. With the addition of these restriction enzyme sites and the primers, the amplified PCR products would be approximately 212bp in size.

Total RNA was extracted from *Xenopus* embryos at stage 10, just after mesoderm induction and the beginning of gastrulation, and at stage 17, when neurulation is almost complete. The RNA was reverse transcribed using both oligo dT and random hexamer primers. In initial experiments PCR was carried out using a final $MgCl_2$ concentration of 3 mM, and an annealing temperature Tm (melting temperature) of 47°C. The Tm was calculated as indicated below, where the nucleotides are those encoding the primers.

$$4°C\ (G/C) + 2°C\ (A/T) = Tm$$

I was not able to see any PCR products on an agarose gel run with the resultant PCR products. It was possible either that the concentration of the $MgCl_2$ was not optimal or that the annealing temperature had to be changed. To address this problem, PCR reactions were set up at three final concentrations of $MgCl_2$ (4.5 mM, 3 mM and 1.5 mM) and at each of the following annealing temperatures: 42°C, 47°C and 51°C. PCR products of 212 bp in size were obtained at all three annealing temperatures when the $MgCl_2$ final concentration was 1.5 mM. Therefore, the $MgCl_2$ concentration had been sub-optimal.

The PCR reaction products were run on a 2% agarose preparative gel. DNA running at a position equivalent to 212 bp was extracted. A representative PCR gel shown in Fig. 3.2 indicates the close migration of the molecular weight bands representing 201bp and 220bp. PCR products present at, or near, the position of these migrated markers, were excised. This DNA was digested using the restriction enzymes *Eco*R1 and *Bam*HI and subcloned into similarly cut and de-phosphorylated pBluescript (KS+) vector. De-phosphorylation was used to decrease the occurrence of vector-vector re-ligation.

Figure 3.2

Representative PCR gel obtained from ephrin isolation

Several bands were obtained in the PCR procedure. Only bands migrating at 200 bp were subcloned.

The O and R letters represent the oligo dT and random primer PCR products. L1 and L2 are the 5' primers Oligo 1 and Oligo 2 respectively and L3 is the 3' primer Oligo 3.

The control lane represents products obtained when only the primers, L1, L2 and L3, were subjected to PCR. No products were seen.

MWM-Molecular Weight Marker.

This control is where no DNA has been added

A PCR gel obtained for putative ligand isolation.

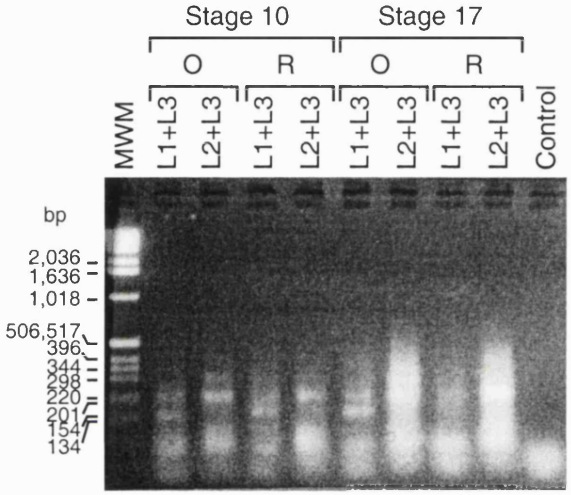

In order to obtain a representative sample of the ephrins expressed at the RNA stages chosen, I aimed to isolate and sequence at least one hundred clones. This would increase the probability of obtaining at least one clone of any ephrin-A class member in the *Xenopus* embryo.

A total of 20 PCR's were set up. As shown in Fig.3.2, a PCR consisted of eight separate PCR reactions: four each using stage 10 and stage 17 oligo dT and random hexamer reverse transcribed reaction products. Each of the four reactions would utilise either oligo1 and oligo3 or, oligo2 and oligo3. The PCR and the subsequent cloning procedures produced 301 bacterial colonies. Of these colonies, 104 appeared to contain inserts of approximately 212bp in length. These clones were T-tracked (see below).

3.2.2 PCR Clone Analysis

The 104 clones obtained from the PCR procedure were initially characterised by sequencing with the T-reaction of the Pharmacia Biotech Kit, in a procedure known as T-tracking. The T-reactions were run adjacent to each other on a 6% sequencing gel. The resultant T-tracks were compared to each other based on their nucleotide separation patterns, an example of which is shown in Fig. 3.3. This comparison allowed the clones be placed into groups dependent on their T-track similarity.

All the clones were analysed in this way and five classes, based on identical T-tracks, were obtained. Some of the clones had T-tracks that appeared to belong to a certain class, but they were not identical to that class, due to the presence of an additional 1-8 T residues. In these cases, the clones were fully sequenced and translated; their amino acid sequences were then compared to the amino acid sequence of each of the five classes. Some of the additional T-residues occurred in wobble positions leaving the amino acid sequence unchanged. Therefore, these clones could be placed directly into a class. In some clones, the extra T residues altered an amino acid sequence by 1-3 amino acids. However, specific conserved amino acid motifs representative of the different classes, were still present in these T-tracks. Therefore, these T-tracks were assigned to one of the five classes identified.

Figure 3.3

An example of T-tracks obtained for several putative ephrin clones

The numbers above each T-track represents the clone from which it was obtained. Five different T-tracks are shown.

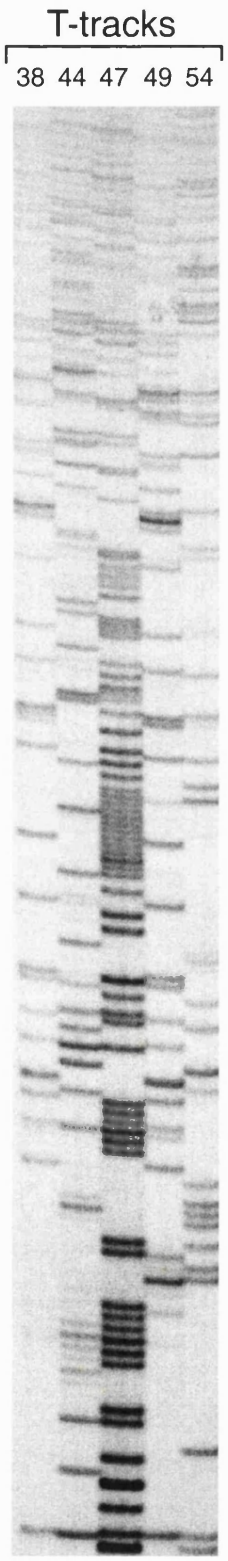
T-tracks
38 44 47 49 54

As a precautionary measure at least 4 or 5 members in a class which had identical T-tracks, were also completely sequenced. The 22 clones which were sequenced for this reason, were always identical.

Table 2 details the T-tracking results indicating which class of putative ephrin was obtained at the chosen annealing temperatures. Some of the T-tracks were vector sequences and others were not analysed because the primers used in the PCR could not be identified. The annealing temperature of 47°C was the most successful in the amplification of putative ephrin sequences.

3.2.3 PCR Class Categorisation

The classes obtained were provisionally given the names XLIG1-5 representing *Xenopus* ligand class 1-5. The ligand (ephrin) sequences are shown in Fig. 3.4.

The most common class obtained from the screen was XLIG1 present in both the stage 10 and stage 17 PCR products. XLIG2 was found in the stage 17 PCR products only. Clones of the XLIG3 class were only found in stage 10 PCR products. XLIG4 was the second most common class obtained and was found in both stage 10 and stage 17 PCR products. XLIG5 was represented once in the PCR screen. It was a stage 10 PCR product.

3.2.4 Sequence Comparisons of XLIG Class Clones

In order to compare the sequences of XLIG PCR fragments and ephrins present in the Genbank database, the GCG programme was used. The GCG PileUp function creates a multiple sequence alignment from a group of related sequences using progressive pairwise alignments. Using this information, the GrowTree function constructs phylogenetic trees enabling the familial relationship between the XLIG classes and other cloned ephrins to be visualised. Two methods were used to construct the phylogenetic trees: the Jukes-Cantor distance (Jukes and Cantor, 1969), which calculates evolutionary distances taking account of gaps in the protein sequence and the Kimura distance (Kimura, 1980), where gap distances are ignored and only exact matches contribute to the positioning of proteins in the resultant phylogenetic tree. Third, the BestFit function was used: this displays the optimal alignment between two peptide or DNA sequences. Table 3 summarises the highest peptide sequence identities between the XLIG classes and the 17 ephrin-A class ligands cloned so far.

PCR ANNEALING °C	42		47		51	
RNA STAGE	**10**	**17**	**10**	**17**	**10**	**17**
XLIG1	7	5	13	17	3	4
XLIG2	0	0	0	7	0	2
XLIG3	1	0	4	0	0	0
XLIG4	4	2	2	1	0	1
XLIG5	0	0	1	0	0	0
NOT ANALYSED[1]	2	8	4	4	1	0
VECTOR	0	0	2	2	4	3
T-TRACKS	**14**	**15**	**26**	**31**	**8**	**10**

Table 2

The breakdown of the classes obtained from the PCR analysis

This table shows the class of clone obtained from the PCR analysis with reference to the annealing temperature used and the T-track sequence comparisons.

[1] not determined since both primers could not be identified.

Figure 3.4

The classes of clone obtained from the PCR analysis

These are representative clones of each class obtained using the degenerate oligonucleotide primers.

From the 104 clones sequenced, five classes were found to contain ephrin motifs. The primers and conserved cysteine residues (C) are shown in bold and sequence motifs are in the red blocks.

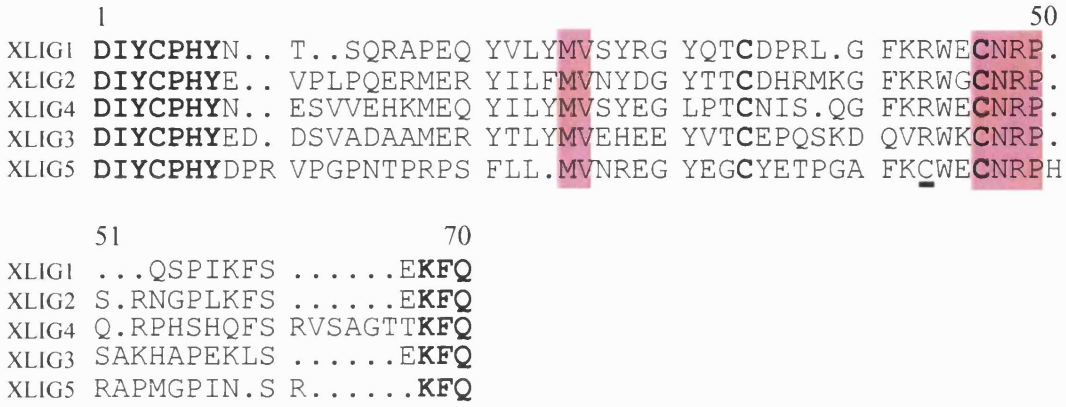
1 50
XLIG1 DIYCPHYN.. T..SQRAPEQ YVLYMVSYRG YQTCDPRL.G FKRWECNRP.
XLIG2 DIYCPHYE.. VPLPQERMER YILFMVNYDG YTTCDHRMKG FKRWGCNRP.
XLIG4 DIYCPHYN.. ESVVEHKMEQ YILYMVSYEG LPTCNIS.QG FKRWECNRP.
XLIG3 DIYCPHYED. DSVADAAMER YTLYMVEHEE YVTCEPQSKD QVRWKCNRP.
XLIG5 DIYCPHYDPR VPGPNTPRPS FLL.MVNREG YEGCYETPGA FKCWECNRPH
51 70
XLIG1 ...QSPIKFS ......EKFQ
XLIG2 S.RNGPLKFS ......EKFQ
XLIG4 Q.RPHSHQFS RVSAGTTKFQ
XLIG3 SAKHAPEKLS ......EKFQ
XLIG5 RAPMGPIN.S R......KFQ

PCR LIGAND CLASS	XLIG1	XLIG2	XLIG3	XLIG4	XLIG5
% Number of Clones	47	8.7	5.8	9.0	1.4
	P.I.%	P.I.%	P.I.%	P.I.%	P.I.%
Ephrin-A1	h54.5	m53.3	m90.3	h52.0 r52.0	r43.3
Ephrin-A2	c70.9	c80.0	c54.1	c63.3	c50.0
Ephrin-A3	h78.2	h59.3 x59.3	h55.7	h70.6	h56.7
Ephrin-A4	h50.0	h58.3	h39.7	m39.2	h48.9
Ephrin-A5	z70.9	z78.2	z55.7	c60.0 z60.0	z55.0 m55.0 h55.0

Table 3

Peptide identities between the XLIG Classes and their closest homologues

This table shows the peptide identities between the XLIG classes and their closest homologues indicated by the phylogenetic GrowTree results.

The percentage number of clones obtained from the screen for each class is shown.

P.I.% represents protein sequence identity.

h-human, m-mouse, c-chick, x-*Xenopus*, r-rat,
z-zebrafish

3.2.5 Analysis of XLIG1-5 Classes

The PileUp programme places XLIG3 adjacent to murine ephrin-A1. This placement is confirmed by the phylogenetic tree (Fig. 3.5), where XLIG3 is present within the ephrin-A1 group. BestFit sequence comparisons confirm that XLIG3 is highly homologous to murine ephrin-A1, where the peptide identity is 90.3% (see Table 3).

The tree places XLIG2 adjacent to chick ephrin-A2. The highest amino acid sequence identity is between chick ephrin-A2 and XLIG2 - it is 80.0%. However, XLIG2 also shares a high peptide sequence identity with zEphrin-A5. This identity is 78.3% (see Table 3).

XLIG1 lies between murine ephrin-A3 (Cerretti and Nelson, 1998) and XLIG4 in the PileUp analysis. The tree places XLIG1 in the ephrin-A3 grouping, suggesting that XLIG1 represents a *Xenopus* ephrin-A3 homologue (Table 3). XLIG1 has amino acid sequence homology to human ephrin-A3 which is 78.2%. This peptide homology was the highest achieved by XLIG1 when compared to all other cloned ephrins (see Table 3).

XLIG4 lies adjacent to XLIG1 in the pileup analysis. Similarly to XLIG1, XLIG4 is also placed in the ephrin-A3 grouping after phylogenetic tree analysis. This also suggests that XLIG4 is a *Xenopus* ephrin-A3. XLIG4 has a highest amino acid sequence identity with human ephrin-A3 of 70.6% (see Table 3).

The PileUp programme places XLIG5 within the ephrin-A class, a position confirmed by phylogenetic tree analysis methods where XLIG5 is placed in the ephrin-A3 group. Indeed, BestFit analysis indicated that the highest peptide identity of XLIG5 was to human ephrin-A3 at 56.7%. However, XLIG5 also has a peptide identity to zebrafish ephrin-A5 at 55%, as shown in Table 3. It is possible that under the tree construction conditions, XLIG5 has a slightly higher sequence similarity to the ephrin-A3 group, than to other ephrins, hence this position. Additionally, XLIG5 differs from the other XLIG classes due to the presence of an extra cysteine (C) amino acid within the clone. The C residue is found in the consensus sequence GAFKRW.CNRP (high-lighted in Fig. 3.4) where it replaces the arginine (R) amino acid normally found, which is underlined here.

Figure 3.5

Ephrin phylogenetic tree with the XLIG classes

The tree indicates that the XLIG3 class is most related to the ephrin-A1 family, the XLIG1, XLIG4 and XLIG5 classes to the ephrin-A3 family and the XLIG2 class to the ephrin-A2 family.

The vertebrate ephrin sequences were obtained from a Genbank search. The ephrins are written such that hephrin-A4 denotes human ephrin-A4. The following additional abbreviations were used: h-human, m-mouse, r-rat, X-*Xenopus*, c-chick and z-zebrafish.

The references for the sequences are listed below:

hephrin-A4 (Kozlosky *et al.,* 1995); mephrin-A4 (Flenniken *et al.,* 1996); mephrin-A1 (Takahashi and Ikeda, 1995); rephrin-A1 (Takahashi and Ikeda, 1995); hephrin-A1 (Kozlosky *et al.,* 1995); Xephrin-A1 (Weinstein *et al.,* 1996); hephrin-A3 (Kozlosky *et al.,* 1995); mephrin-A3 (Cerretti and Nelson, 1998); hephrin-A5 (Winslow *et al.,* 1995); mephrin-A5 (Flenniken *et al.,* 1996); rephrin-A5 (1996 Li/Feldman A.M.), submitted to Genbank), cephrin-A5 (Drescher *et al.,* 1995); zephrin-A5 (Brennan *et al.,* 1997); cephrin-A2 (Cheng *et al.,* 1995); mephrin-A2 (Shao *et al.,* 1995) and zephrin-A2 (Brennan *et al.,* 1997).

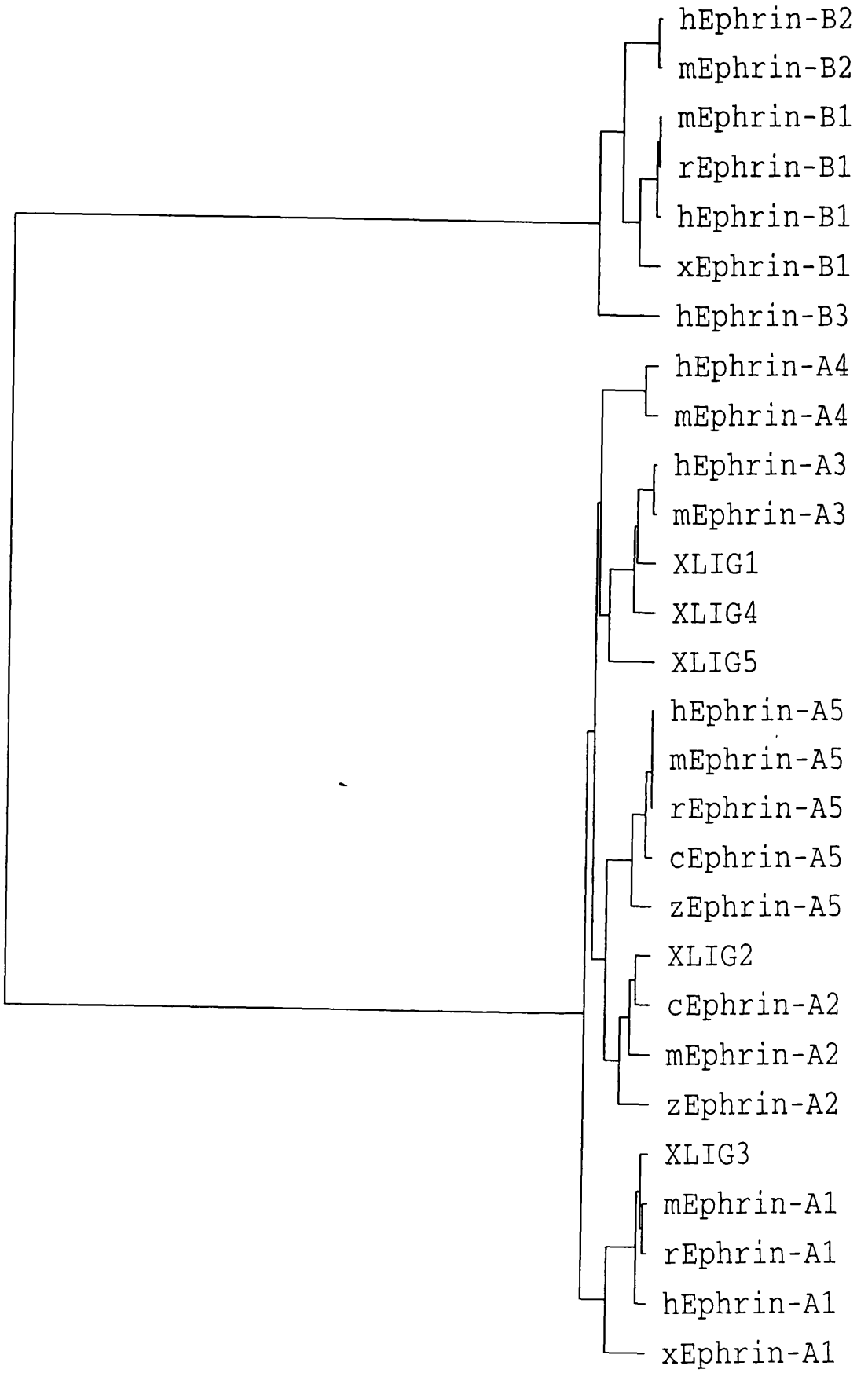
hEphrin-B2
mEphrin-B2
mEphrin-B1
rEphrin-B1
hEphrin-B1
xEphrin-B1
hEphrin-B3
hEphrin-A4
mEphrin-A4
hEphrin-A3
mEphrin-A3
XLIG1
XLIG4
XLIG5
hEphrin-A5
mEphrin-A5
rEphrin-A5
cEphrin-A5
zEphrin-A5
XLIG2
cEphrin-A2
mEphrin-A2
zEphrin-A2
XLIG3
mEphrin-A1
rEphrin-A1
hEphrin-A1
xEphrin-A1

3.2.6 Isolation and Sequence Analysis of an XLIG4 cDNA Clone

Preliminary expression data indicated that XLIG4 and XLIG5 had dynamic expression profiles during the development of the early *Xenopus* embryo, and the decision was taken to obtain longer cDNA clones of XLIG4 and XLIG5. 800,000 clones of a stage 17 λgt10 *Xenopus* cDNA library were plated out and screened with 32P DNA probes for the 212 bp PCR products of XLIG4 and XLIG5. From three library screens under stringent conditions with both ephrin probes, one positive clone was isolated using the XLIG4 PCR product.

To excise the cDNA clone from the phage λ arms of the λgt10 cDNA library, an *Eco*R1 digest was required. This digestion produced three bands on an agarose gel with approximate sizes of 2.1 Kb, 1.6 Kb and 700 bp. In order to ascertain which bands hybridised with an XLIG4 probe and represented a longer cDNA of the XLIG4 PCR product, a Southern Blot was performed.

Only the 2.1 Kb and the 700 bp bands hybridised to the XLIG4 PCR product and they were subcloned into *Eco*R1 cut pBluescript (KS+). The 700 bp cDNA was fully sequenced and it contained amino acid motifs indicative for an A-class ephrin. End sequencing of the 2.1 Kb cDNA indicated that one end of this DNA fragment had exactly the same sequence as the N-terminal end of the 700 bp cDNA. Therefore the 700 bp cDNA was part of the 2.1 Kb cDNA. The third DNA band seen on the agarose gel running at 1.6 Kb, did not hybridise with the Southern blot probe. Due to its size, the 1.6 Kb band is likely to be the other end of the 2.1 Kb clone and since it showed no homology to an ephrin sequence, it is assumed to be the 3' UTR (untranslated region) of the 2.1 Kb cDNA. Therefore the longest cDNA obtained was 2.1 Kb.

Sequencing of the 700 bp XLIG4 clone (found to be 727 bp in length) identified an open reading frame with an initiating methionine residue at 28 bp and a stop codon at 682 bp nucleotide positions respectively (Fig. 3.6). Comparisons of the protein translation of XLIG4 with other cloned vertebrate ephrins described below, suggests that the full coding region of XLIG4 is contained within this DNA clone. Figure 3.7 shows the DNA sequence and protein translation of XLIG4. High-lighted within the translation of the XLIG4 open reading frame are the four conserved cysteine residues and other conserved

Figure 3.6

A diagrammatic representation of the Xephrin-A3 cDNA

On release from the λgt10 arms (purple blocks), the approximate length of the XLIG4 cDNA is 2.1kb. Following EcoRI restriction enzyme digestion (⇑) the cDNA becomes three fragments: an incomplete digestion fragment of 2.1kb, a 727 bp fragment containing the ORF (green block) and a 1.6kb fragment assumed to be the 3' untranslated region (blue block). The positions of the initiating methionine residue (28 bp) and the stop codon (682 bp) within the ORF are indicated.


28
68
ORF
3' UTR
1←
→727 bp
1←
→2.1 kb

Figure 3.7

The nucleotide sequence and protein translation of the open reading frame of XLIG4

The cDNA sequence of XLIG4 is shown on the upper line. The protein translation is shown underneath.

Conserved cysteine residues are high-lighted in bold.

The underlined sequence represents the hydrophobic C-terminal domain of XLIG4

```
        10         20         30         40         50         60
ATGGCTTTGG TGTTCGCGCT TATCTTGCCG CTGCTCTCCC TGTTTCCCCG CTCCGGAGCC
 M  A  L   V  F  A  L   I  L  P   L  L  S   L  F  P  R   S  G  A

        70         80         90        100        110        120
                                        *
AACCGGCACT CGGTCTATTG GAACAGCTCC AACTACCACC TGCGGCGGGA CGGCTACACG
 N  R  H   S  V  Y  W   N  S  S   N  Y  H   L  R  R  D   G  Y  T

       130        140        150        160        170        180
GTGCAGGTGG ATGTGAACGA TTACCTGGAT ATCTATTGCC CCCACTACAA TGAGTCGGTG
 V  Q  V   D  V  N  D   Y  L  D   I  Y  C   P  H  Y  N   E  S  V>

       190        200        210        220        230        240
                   *
GTGGAGCACA AGATGGAGCA GTACATCCTC TATATGGTGA GCTACGAGGG GCTACCGACC
 V  E  H   K  M  E  Q   Y  I  L   Y  M  V   S  Y  E  G   L  P  T

       250        260        270        280        290        300
                                                              *
TGCAACATCA GCCAGGGCTT CAAGCGCTGG GAGTGTAACC GCCCCGCCCC CCACAGTCCA
 C  N  I   S  Q  G  F   K  R  W   E  C  N   R  P  A  P   H  S  P

       310        320        330        340        350        360
ATCAAATTCT CCGAGAAGTT CCAGCGGTAC AGTGCCTTCT CCTTGGGCTA CGAGTTCCAC
 I  K  F   S  E  K  F   Q  R  Y   S  A  F   S  L  G  Y   E  F  H

       370        380        390        400        410        420
                                        *
GCTCGCGGCC ACGAGTACTA CTATATCTCG ACAGGAACGC ACAATCACAG GCGCTCCTGT
 A  R  G   H  E  Y  Y   Y  I  S   T  G  T   H  N  H  R   R  S  C

       430        440        450        460        470        480
CTGAAGATGA AAGTGTTTGT GTCGTGCGCC AGCACTTCCC ACTCTGGAGA GAAACATTCC
 L  K  M   K  V  F  V   S  C  A   S  T  S   H  S  G  E   K  H  S

       490        500        510        520        530        540
                   *
CCGACCCTCC CCCAGTTCAC GATAGGCCCA GAGGTGAACA TACAGGATTT AGATAACTTC
 P  T  L   P  Q  F  T   I  G  P   E  V  N   I  Q  D  L   D  N  F

       550        560        570        580        590        600
                                                              *
AACCCGGAGA TCCCAAAGTT GGAGAAGAGC GATCAGTGGG AGCAGCCACA CAAGAGGGAG
 N  P  E   I  P  K  L   E  K  S   D  Q  W   E  Q  P  H   K  R  E

       610        620        630        640        650
CACTTACACC TGACAGTGGC AGTTTGTCTC ATTATAATGA CGCTCCTGGC TTCCTAG
 H  L  H   L  T  V  A   V  C  L   I  I  M   T  L  L  A   S
```

amino acid motifs indicative of an ephrin-A class ligand member. The hydrophobic C-terminal domain of XLIG4 is underlined.

3.2.7 Analysis of XLIG4 cDNA sequence

A PileUp comparison was made between the full length XLIG4 cDNA sequence and the ephrin sequences from the Genbank database.

This PileUp places the XLIG4 cDNA sequence between murine ephrin-A3 and human ephrin-A5 (Fig. 3.8). The tree constructed from the PileUp data (Fig. 3.9) places the full length XLIG4 sequence within the ephrin-A3 group, closest to murine ephrin-A3. This indicated that full length XLIG4 sequence is likely to be the *Xenopus* homologue of ephrin-A3. To clarify this observation, sequence comparisons were constructed at the peptide level with all the cloned ephrins (see Table 4). The highest peptide sequence identity was found between full length XLIG4 sequence and murine ephrin-A3 at 71.9% (see Fig. 3.10). The DNA sequence identity between full length XLIG4 sequence and murine ephrin-A3 is 78.7%, as shown in Fig. 3.11. With the similar BestFit peptide sequence identity of the XLIG4 cDNA sequence to human ephrin-A3, which is 71.8%, it is a strong possibility that the full length XLIG4 sequence is the *Xenopus* homologue the ephrin-A3 group.

3.3 DISCUSSION

I have described the cloning of *Xenopus* ephrins of the Eph RTK family using an RT-PCR based strategy. I have been able to identify five PCR product classes with homologies to previously cloned vertebrate A-ephrins.

Table 2 identifies the possible stages at which the ephrins are expressed in the embryo. For example, the XLIG1 and XLIG4, were isolated from both stage 10 and 17 RNA PCR products. The XLIG2 clones were present in only stage 17 PCR products. The XLIG3 and XLIG5, were found only in stage 10 PCR products. Since PCR amplification could favour certain sequences it is possible that the high percentage of XLIG1 obtained could be a mis-representation of the actual extent of the expression of this clone in the *Xenopus* embryo.

Figure 3.8

PileUp between vertebrate ephrins and Xephrin-A3

PileUp creates a multiple sequence alignment of a group of related sequences.

Xephrin-A3 is in bold and positioned between mephrin-A3 and hephrin-A5.

mephrin-A3 is mouse ephrin-A3

hephrin-A5 is human ephrin-A5

```
                1                                                   50
hephrin-A4  ~~~~~~~~~~ ~~~~~~~~MR LLPLLRTVLW AAFLGSPLRG GSSLRHVVYW
mephrin-A4  MLLRLGLIYP PTRPPAPPGP LVPLLRTVLW AALLGSRLPG CSSLRHPIYW
mephrin-A1  ~~~~~~~~~~ ~~~~~~~~~~ ~~~~~MEFLW APLLGLCCSL AAADRHIVFW
rephrin-A1  ~~~~~~~~~~ ~~~~~~~~~~ ~~~~~MEFLW APLLGLCCSL AAVDRHIVFW
hephrin-A1  ~~~~~~~~~~ ~~~~~~~~~~ ~~~~~MEFLW APLLGLCCSL AAADRHTVFW
xephrin-A1  ~~~~~~~~~~ ~~~~~MMELY RAAVQLIVGV GLGVGLWLRE AQGERHIVFW
hephrin-A3  ~~~~~~~~~~ ~~~MAAAPLL LLLLLVPVPL LPLLAQGPGG ALGNRHAVYW
Xephrin-A3  ~~~~~~~~~~ ~~~~~~~~~~ ~~~MALVFAL ILPLLSLFPR SGANRHSVYW
hephrin-A5  ~~~~~~~~ML HVEMLTLVFL VLWMCVFSQD PGSKAVADRY AVYWNSSNPR
mephrin-A5  ~~~~~~~~ML HVEMLTLLFL VLWMCVFSQD PGSKVVADRY AVYWNSSNPR
rephrin-A5  ~~~~~~~~ML HVEMLTLLFL VLWMCVFSQD PGSKVVADRY AVYWNSSNPR
cephrin-A5  ~~~~~~~~MP HVEMLLLAVA ALWVCVRGQE PGRKAVADRY AVYWNSTNPR
zephrin-A5  ~~~~~~~~ML QAEMIVFVGV ILWMCVFSQE PSSKVMADRY AVFWNRTNPR
cephrin-A2  ~~~~~~~~MP RWEAAALLAA IVGVCVWSDD PG.KVISDRY AVYWNRSNPR
mephrin-A2  ~~~~~~MAPA QRPLLPLLLL LLPLRARNED PA.RANADRY AVYWNRSNPR
zephrin-A2  ~~~~~~~~~~ ~~MELSLVVF TVVCWVSVWS DD.RIISDRH AVYWNSSNSR

                51                                                  100
hephrin-A4  NSSNPRL... ...LRGDAVV ELGLNDYLDI VCPHYE.... ....GPGPPE
mephrin-A4  NSSNPRL... ...LRGDAVV ELGFNDYLDI FCPHYE.... ....SPGPPE
mephrin-A1  NSSNPKFR.. ....EEDYTV HVQLNDYLDI ICPHYEDDSV ADAA......
rephrin-A1  NSSNPKFR.. ....EEDYTV HVQLNDYLDI ICPHYEDDSV ADAA......
hephrin-A1  NSSNPKFR.. ....NEDYTI HVQLNDYVDI ICPHYEDHSV ADAA......
xephrin-A1  NSSNYRFM.. ....QEDYTV QVQLNDYLDI VCPYYEEGSV AGHT......
hephrin-A3  NSSNQHLR.. ....REGYTV QVNVNDYLDI YCPHYNSSGV GPGAGPGPGG
mephrin-A3  ~~~~~~LR.. ....REGYTV QVNVNDYLDI YCPHYNSS.. ......GPGG
Xephrin-A3  NSSNYHLR.. ....RDGYTV QVDVNDYLDI YCPHYNESVV EHKM......
hephrin-A5  NSSNPRFQ.. ....RGDYHI DVCINDYLDV FCPHYEDSV. .......PED
mephrin-A5  NSSNPRFQ.. ....RGDYHI DVCINDYLDV FCPHYEDSV. .......PED
rephrin-A5  NSSNPRFQ.. ....RGDYHI DVCINDYLDV FCPHYEDSV. .......PED
cephrin-A5  NSTNPRFQ.. ....QGDYHI DVCINDYLDV FCPHYEDSV. .......PED
zephrin-A5  NRTNPRFQ.. ....RGDYHI DVCINDYLDV YCPHYEDSV. .......PEE
cephrin-A2  NRSNPRFH.. ....RGDYTV EVSINDYLDI YCPHYEEPL. .......PAE
mephrin-A2  NRSNPRFQVS AVGDGGGYTV EVSINDYLDI YCPHYGAPL. ......PPAE
zephrin-A2  NSSNSRF... ...WQGEYTV AVSINDYLDV YCPYYESP.. ......QPHS

                101          *                *                  150
hephrin-A4  LYMVDWPGYE SCQAEGPRAY KRWVCSL... .PFGHVQFSE KIQRFTPFSL
mephrin-A4  LYMVDWSGYE ACTAEGANAF QRWNCSMP.F APFSPVRFSE KIQRYTPFPL
XLIG3       LYMVEHEEYV TCEPQ.SKDQ VRWKCNRP.S AKHAPEKLSE KFQ-------
mephrin-A1  LYMVEHQEYV ACQPQ.SKDQ VRWNCNRP.S AKHGPEKLSE KFQRFTPFIL
rephrin-A1  LYMVEHQEYV TCEPQ.SKDQ VRVKCNQP.S AKHGPEKLSE KFQRFTPFTL
hephrin-A1  LYLVEHEEYQ LCQPQ.SKDQ VRWQCNRP.S AKHGPEKLSE KFQRFTPFTL
xephrin-A1  LFLVDYEEYE TCKPK.SKDQ VRWECNKP.F APHGPEKFCE KFQKFTPFTL
hephrin-A3  LYMVSRNGYR TCN.A.SQGF KRWECNRPH. APHSPIKFSE KFQRYSAFSL
mephrin-A3  LYM.NLSGYR TCN.A.SQGS KRWECNRQH. ASHSPIKFSE KFQRYSAFSL
XLIG1       LYMVSYRGYQ TCD.P.RLGF KRWECNR... .PQSPIKFSE KFQ-------
Xephrin-A3  LYMVSYEGLP TCN.I.SQGF KRWECNRP.. APHSPIKFSE KFQRYSAFSL
hephrin-A5  LYMVNFDGYS ACDHT.SKGF KRWECNRPH. SPNGPLKFSE KFQLFTPFSL
mephrin-A5  LYMVNFDGYS ACDHT.SKGF KRWECNRPH. SPNGPLKFSE KFQLFTPFSL
rephrin-A5  LYMVNFDGIS ACDHT.SKGF KRWECNRPH. SPNGPLKFSE KFQLFTPFSL
cephrin-A5  LYMVNFDGYS SCDHI.SKGF KRWECNRPH. SPNGPLKFSE KFQLFTPFSL
zephrin-A5  LYMVNYDGYS TCDHT.AKGF KRWECNRPH. SPNGPLKFSE KFQLFTPFSL
XLIG2       LFMVNYDGYT TCDHR.MKGF KRWGCNRP.. SRNGPLKFSE KFQ-------
cephrin-A2  LYMVNYEGHA SCDHR.QKGF KRWECNRPD. SPSGPLKFSE KFQLFTPFSL
mephrin-A2  LYMVNGEGHA SCDHR.QRGF KRWECNRPA. APGGPLKFSE KFQLFTPFSL
zephrin-A2  LFMVNHDGYL TCEHR.MRGF KRWECNRPQ. SPDGPLRFSE KFQLFTPFSL
XLIG5       LLMVNREGYE GCYET.PGAF KCWECNRPHR APMGPIN.SR KFQ-------

                151                *                  200
hephrin-A4  GFEFLPGETY YYISVPTPES SGQ.CLRLQV SVCCKERKS. .ESAHPVGSP
mephrin-A4  GFEFLPGETY YYISVPTPES PGR.CLRLQV SVCCKESGSS HESAHPVGSP
mephrin-A1  GKEFKEGHSY YYISKPIYHQ ESQ.CLKLKV TVNGKITHNP QAHVNPQEKR
rephrin-A1  GKEFKEGHSY YYISKPIYHQ ETQ.CLKLKV TVNGKITHSP HAHVNPQEKR
hephrin-A1  GKEFKEGHSY YYISKPIHQH EDR.CLRLKV TVSGKITHSP QAHVNPQEKR
xephrin-A1  GTEFREGRTY YYISKPIHYH GET.CMRLRV HVSGRTT.PP PVNVHTPRSH
hephrin-A3  GYEFHA.GHE YYYISTPTHN LHWKCLRMKV FVCCASTSHS GEKPVPTLPQ
mephrin-A3  GYEFHA.GQE YYYISTPTHN LHWKCLRMKV FVCCASTSHS GEKPVPTLPQ
Xephrin-A3  GYEFHARGHE YYYISTGTHN HRRSCLKMKV FVSCASTSHS GEKHSPTLPQ
hephrin-A5  GFEFRPGREY FYISSAIPDN GRRSCLKLKV FVRPTNSCMK TIGVHDRVFD
mephrin-A5  GFEFRPGREY FYISSAIPDN GRRSCLKLKV FVRPTNSCMK TIGVHDRVFD
rephrin-A5  GFEFRPGREY FYISSAIPDN GRRSCLKLKV FVRPTNSCMK TIGVRDRVFD
cephrin-A5  GFEFRPGREY FYISSAIPDN GRRSCLKLKV FVRPANSCMK TIGVHDRVFD
zephrin-A5  GFEFRPGREY YYISSMITET GRRSCLKLKV FVRPPNGCEK TIGVHDRVF.
cephrin-A2  GFEFRPGHEY YYISASPLNV VDRPCLKLKV YVRPTNDSL. .YESPEPIFT
mephrin-A2  GFEFRPGHEY YYISATPPNL VDRPCLRLKV YVRPTNETL. .YEAPEPIFT
zephrin-A2  GFEFRPGHEY YYISSPHPNH AGKPCLKLKV YVKPTSSG.. .YESPEPFLT

                201                                         250
hephrin-A4  GESGTSGWRG GDTPSPLCLL LLLLLLILRL LRIL~~~~~~ ~~~~~~~~~~
mephrin-A4  GESGTSGWRG GHAPSPLCLL LLLLLPILRL LRVL~~~~~~ ~~~~~~~~~~
mephrin-A1  LQADDPEVQ. ..VLHSIGYS AAPRLFPLVW AVLLLPLLLL QSQ~~~~~~~
rephrin-A1  LQADDPEVQ. ..VLHSIGHS AAPRLFPLVW AVLLLPLLLL QTQ~~~~~~~
hephrin-A1  LAADDPEVR. ..VLHSIGHS AAPRLFPLAW TVLLLPLLLL QTP~~~~~~~
xephrin-A1  IQSDEPEVPL PGVMKSVAGN SAAPGTPCTL YGLLLAALLL RL~~~~~~~~
hephrin-A3  FTMGPNVKIN VLEDFEGENP QVPKLEKSIS GTSP.KREHL PLAVGIAFFL
mephrin-A3  FTMGPNVKIN VLEDFEGENP QVPKLEKSIS GTSP.KREHL PLAVGIAFFL
Xephrin-A3  FTIGPEVNIQ DLDNF...NP EIPKLEKSDQ WEQPHKREHL HLTVAVCLII
hephrin-A5  VNDKVENSLE PADDTVHESA EPSRGENAAQ TPRIPSR..L LAILLFLLAM
mephrin-A5  VNDKVENSLE PADDTVHESA EPSRGENAAQ TPRIPSR..L LAILLFLLAM
rephrin-A5  VNDKVENSLE PADDTVHESA EPSRGENAAQ TPRIPSR..L LAILLFLLAM
cephrin-A5  VNDKVENSLE PADDTVRESA EPSRGENAAQ TPRIPIR..L LATLLFLLAM
zephrin-A5  VDDKVDNALE PRDDTSHE.A EPSRSDVSTS GLRHQTSRPL LALLLLCISL
cephrin-A2  SNNSCCSLAV PRAVLVAAPV FWTLLGS~~~ ~~~~~~~~~~ ~~~~~~~~~~
mephrin-A2  SNSSCSGLGG CHLFLTTVPV LWSLLGS~~~ ~~~~~~~~~~ ~~~~~~~~~~
zephrin-A2  DQSQRCGADG PCLAVLMLLL VFLLAGV~~~ ~~~~~~~~~~ ~~~~~~~~~~

                251
hephrin-A3  MTFLAS~~~~
mephrin-A3  MTLLASDV~~
Xephrin-A3  MTLLAS~~~~
hephrin-A5  LLTL~~~~~~
mephrin-A5  LLTL~~~~~~
rephrin-A5  LLTL~~~~~~
cephrin-A5  LLIL~~~~~~
zephrin-A5  YLLL~~~~~~
```

Figure 3.9

vertebrate ephrin phylogenetic tree with Xephrin-A3

The tree indicates that Xephrin-A3 is most related to the ephrin-A3 family with closest homology to murine ephrin-A3.

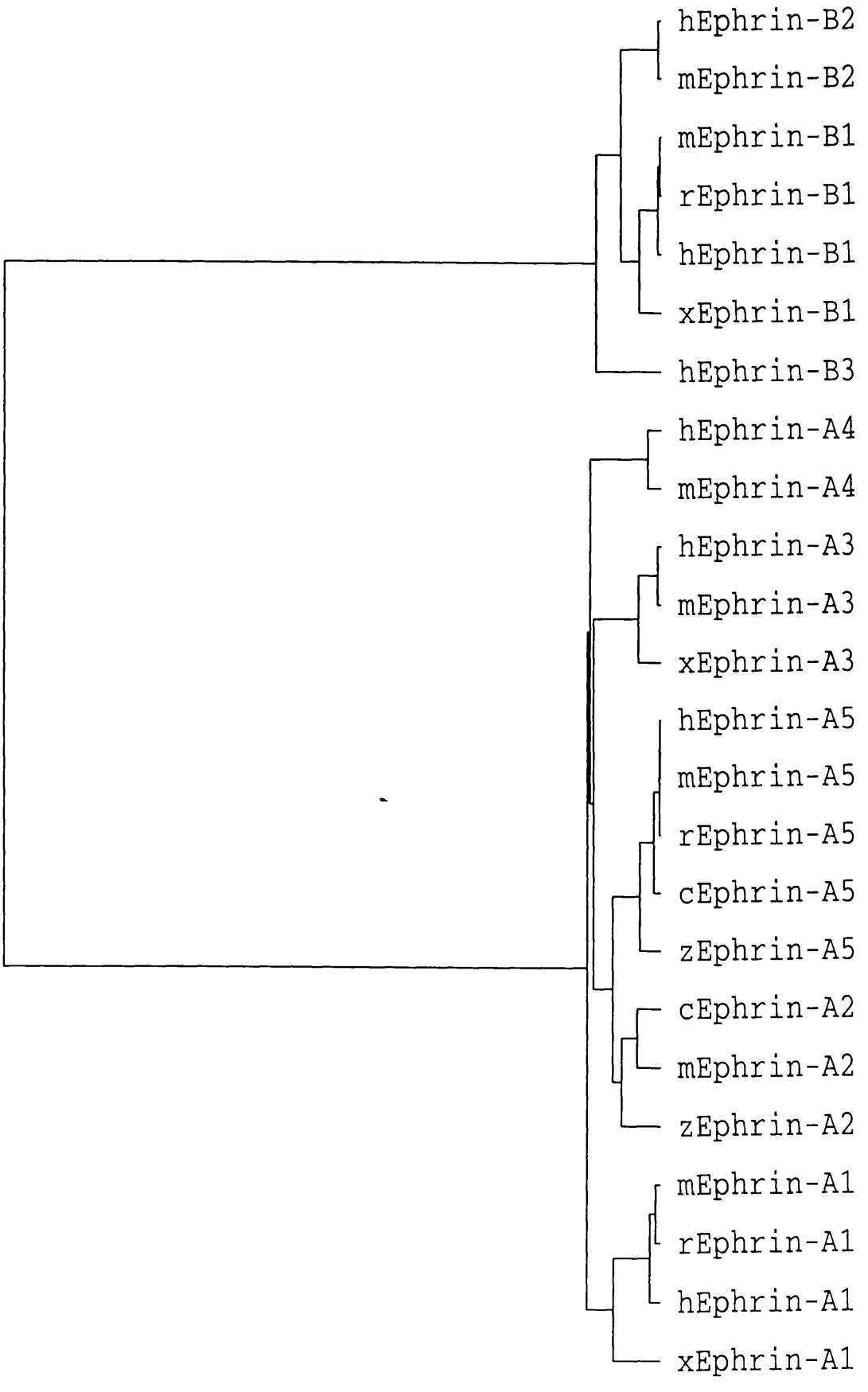
hEphrin-B2
mEphrin-B2
mEphrin-B1
rEphrin-B1
hEphrin-B1
xEphrin-B1
hEphrin-B3
hEphrin-A4
mEphrin-A4
hEphrin-A3
mEphrin-A3
xEphrin-A3
hEphrin-A5
mEphrin-A5
rEphrin-A5
cEphrin-A5
zEphrin-A5
cEphrin-A2
mEphrin-A2
zEphrin-A2
mEphrin-A1
rEphrin-A1
hEphrin-A1
xEphrin-A1

EPHRIN GROUP	XLIG4 cDNA PROTEIN IDENTITY %					
	M	X	R	H	C	Z
ephrin-A1	50.7	50.0	50.0	50.3	-	-
ephrin-A2	60.0	-	-	-	60.6	54.5
ephrin-A3	71.9	100	-	71.8	-	-
ephrin-A4	44.6	-	-	46.9	-	-
ephrin-A5	59.9	-	59.9	55.6	57.6	59.1

Table 4

Peptide Identities between the XLIG4 cDNA clone and all other cloned ephrin-A ligands

m-mouse, x-*Xenopus*, r-rat, h-human, c-chick and z-zebrafish

Figure 3.10

Peptide alignment of XLIG4 with murine ephrin-A3

The regions of peptide homology of XLIG4 with its closest family member, mephrin-A3.

Percent Similarity: 76.374 Percent Identity: 71.978

XLIG4.pep x mephrin-A3.pep

```
 34 LRRDGYTVQVDVNDYLDIYCPHYNESVVEHKMEQYILYMVSYEGLPTCNI
    |||:||||||.|||||||||||||| |      |||:||| .  |  |||
  1 LRREGYTVQVNVNDYLDIYCPHYNSSGPGGGAEQYVLYM.NLSGYRTCNA
             .         .         .         .         .
 84 SQGFKRWECNRP.APHSPIKFSEKFQRYSAFSLGYEFHARGHEYYYISTG
    ||| |||||||  | ||||||||||||||||||||||| | |||||||
 50 SQGSKRWECNRQHASHSPIKFSEKFQRYSAFSLGYEFHA.GQEYYYISTP
             .         .         .         .         .
133 THNHRRSCLKMKVFVSCASTSHSGEKHSPTLPQFTIGPEVNIQDLDNF..
    |||    ||:||||| |||||||||  |||||||.|| | |  |:.|
 99 THNLHWKCLRMKVFVCCASTSHSGEKPVPTLPQFTMGPNVKINVLEDFEG
             .         .         .
181 .NPEIPKLEKSDQWEQPHKREHLHLTVAVCLIIMTLLAS 218
     ||::||||||     | ||||| | | :   :||||||
149 ENPQVPKLEKSISGTSP.KREHLPLAVGIAFFLMTLLAS 186
```

Figure 3.11

Nucleotide alignment of XLIG4 with murine ephrin-A3

The regions of homology of XLIG4 with its closest family member, mephrin-A3.

Percent Similarity: 78.767 Percent Identity: 78.767

Xephrin-A3.DNA x mephrin-A3.DNA

```
  93 CTACCACCTGCGGCGGGACGGCTACACGGTGCAGGTGGATGTGAACGATT
     | ||  ||||||||| || |||||||| ||||||||| | |||||||| |
 920 CCACAGCCTGCGGCGAGAGGGCTACACCGTGCAGGTGAACGTGAACGACT
              .         .         .         .         .
 143 ACCTGGATATCTATTGCCCCCACTACAATGAGTCGGTGGTGGAGCACAAG
     | |||||||| || || || ||||||||    || | |   |    | |
 970 ATCTGGATATTTACTGTCCGCACTACAACAGCTCAGGGCCTGGCGGCGGG
              .         .         .         .         .
 193 ATGGAGCAGTACATCCTCTATATGGTGAGCTACGAGGGGCTACCG.ACCT
       |||||||||| | || || ||||||| |   ||| |||||||| ||||
1020 GCGGAGCAGTACGTGCTGTACATGGTGAAC.CTGAGCGGCTACCGCACCT
              .         .         .         .         .
 242 GCAACATCAGCCAGGGCTTCAAGCGCTGGGAGTGTAACCG...CCCCGCC
     |||||  |||||| |||| |||||||||||| || |||||    | ||||
1069 GCAACGCCAGCCAAGGCTCCAAGCGCTGGGAATGCAACCGGCAGCACGCC
              .         .         .         .         .
 289 CCCCACAGTCCAATCAAATTCTCCGAGAAGTTCCAGCGGTACAGTGCCTT
      | ||||| || ||||| |||||||||||||||||||| ||||| |||||
1119 TCGCACAGCCCCATCAAGTTCTCCGAGAAGTTCCAGCGTTACAGCGCCTT
              .         .         .         .         .
 339 CTCCTTGGGCTACGAGTTCCACGCTCGCGGCCACGAGTACTACTATATCT
     |||  ||||||| || ||||| ||   |||||| || |||||||| ||||
1169 CTCGCTGGGCTATGAATTCCATGC...CGGCCAAGAATACTACTACATCT
```

Initial expression data (see Chapter 4) indicated that XLIG4 and XLIG5 had dynamic expression in the early *Xenopus* embryo. An attempt was made to obtain cDNA clones for these two classes. A cDNA clone for XLIG4 was obtained. The sequence of XLIG4 cDNA sequence confirmed that an ephrin A-class member had been cloned, since the conserved cysteine residues, sequence motifs and sequence encoding the GPI-anchored region indicative of the group were present.

3.3.1 XLIG Classes

The sequence identities between the XLIG classes and their possible homologues detailed in Table 3, and phylogenetic tree data, suggests that the PCR screen identified homologues of three previously cloned members of the ephrin-A class. Sequence comparisons and family alignments indicate that XLIG3 may represent an ephrin-A1 homologue, XLIG2 an ephrin-A2 homologue and the XLIG1 and XLIG4 classes, members of the ephrin-A3 group.

The homology of the XLIG3 class to the ephrin-A1 group at 90.3%, is a distinctly greater sequence identity than to the other cloned ephrins (see Table 3). This high sequence identity to only one ephrin group is not shared by the XLIG2, XLIG1 and XLIG4 PCR classes. Although, XLIG2 has the greatest sequence identity to the ephrin-A2 group (80.0%), this ligand class also has a similar high sequence identity to the ephrin-A5 group (78.3%). XLIG1 and XLIG4 have high sequence identities to the ephrin-A3 group, 78.2% and 70.6%, respectively. However these classes also have high sequence identities to the ephrin-A2 group at 70.9% and 63.3% respectively.

The subsequent cloning of full length XLIG4 sequence (see 3.3.2) shows that the full length sequence is much more similar to ephrin-A3 members than to any other ephrins. For example, the XLIG4 cDNA sequence has 71.8% sequence identity to human ephrin-A3 (the XLIG4 PCR clone has 70.6% sequence identity), and the sequence identity between XLIG4 cDNA sequence and chick ephrin-A2 has fallen to 60.6% (XLIG4 PCR clone had an sequence identity of 63.3) (see Tables 3 and 4). Therefore, it is important to note that although the XLIG classes identified have apparent homologies to ephrins identified in other species, their true homologues cannot be certain until their full length cDNA's are obtained.

The XLIG5 PCR product contained a cysteine residue not previously seen in ephrins at this particular nucleotide position. Only one clone representing the XLIG5 class was obtained and therefore the significance of the cysteine residue cannot be judged. It seems most probable that the cysteine amino acid is PCR error. This is a plausible explanation since a cysteine codon [UG(U/C)] becomes an arginine codon [CGN] by a single nucleotide change.

XLIG5 shared a low sequence homology to every ephrin cloned. The highest sequence identity observed was 56.7% between XLIG5 and the ephrin-A3 group (Table 3). This result is reflected in the position of XLIG5 in the phylogenetic tree (Fig 3.9). However, further sequence analysis indicated that XLIG5 has a 55% homology with the ephrin-A5 group (Table 3). The homologies of XLIG5 with XLIG1, XLIG4, XLIG2 and XLIG3 are 50.0%, 47.4%, 49.1% and 33.9% respectively. These data indicate that XLIG5 has no clear homology to these classes. This may suggest that XLIG5 is a new ephrin. This can only be proved when a longer cDNA for XLIG5 is cloned. It is possible that XLIG5 homologues have not been identified in other species because they do not have an equivalent ephrin or the transcript is very rare. The latter might be the case since XLIG5 was only cloned once in my PCR screen.

3.3.2 The XLIG4 cDNA analysis

In the phylogenetic tree, the cDNA clone of XLIG4 is placed in the ephrin-A3 group. This clone has a highest peptide sequence homology to murine ephrin-A3 (71.9%).

To support the hypothesis that the full length XLIG4 sequence is a *Xenopus* homologue of the ephrin-A3 group, the following BestFit sequence analyses were carried out. First, the peptide sequence of the XLIG4 cDNA sequence was compared with all cloned ephrins (see Table 4), to indicate the relatedness of this cDNA to them. Second, a similar analyses with mouse ephrin-A5 (Table 5) and chick ephrin-A2 were carried out, to indicate the relatedness of other ephrins to all cloned ephrins. Third, the sequence identities between Xephrin-A1 (Table 6) and all other ephrins was carried out, also as a basis to discuss relatedness between ephrins.

Table 4 shows that the XLIG4 cDNA sequence has its highest sequence identity with murine ephrin-A3 which is 71.9%. This is closely followed by an sequence identity with

EPHRIN GROUP	mEphrin-A5 PROTEIN IDENTITY %					
	M	X	R	H	C	Z
ephrin-A1	50.5	53.1	48.4	54.1	-	-
ephrin-A2	62.9	-	-	-	67.5	62.9
ephrin-A3	54.8	59.8	-	53.3	-	-
ephrin-A4	49.3	-	-	48.7	-	-
ephrin-A5	100	-	99.1	99.1	90.8	76.9

Table 5

Peptide Identities between murine ephrin-A5 and all other cloned ephrin-A ligands

m-mouse, x-*Xenopus*, r-rat, h-human, c-chick and z-zebrafish

EPHRIN GROUP	xEphrin-A1 PROTEIN IDENTITY %					
	M	X	R	H	C	Z
ephrin-A1	56.3	100	58.6	57.5	-	-
ephrin-A2	50.0	-	-	-	46.9	56.3
ephrin-A3	46.9	50.0	-	48.5	-	-
ephrin-A4	45.2	-	-	48.2	-	-
ephrin-A5	53.1	-	52.3	52.3	52.6	49.0

Table 6

Peptide Identities between *Xenopus* ephrin-A1 and all other cloned ephrin-A ligands

m-mouse, x-*Xenopus*, r-rat, h-human, c-chick and z-zebrafish

human ephrin-A3 of 71.8%. Both the ephrin-A2 and ephrin-A5 groups had a highest peptide identity with the XLIG4 cDNA sequence of 60.6% and 59.9% respectively. The lowest peptide identity was found between full length XLIG4 sequence and the ephrin-A4 group (46.9%). The findings of this analysis indicate that the XLIG4 cDNA sequence has greatest homology to the ephrin-A3 group.

The sequence analysis can be taken further by comparing the sequence identities between recognised orthologues within a specific ephrin group. In support of the percentage sequence identities of full length XLIG4 sequence with its prospective homologue mouse ephrin-A3, I found that a sequence identity of 73.0% was present between chick ephrin-A5 and zebrafish ephrin-A5 and second, a 76.9% sequence identity was present between zebrafish ephrin-A5 and murine ephrin-A5. Additionally, the sequence identity between chick ephrin-A2 and murine ephrin-A2 is 75%.

Higher sequence identities do exist such as those shown in Table 5, where BestFit comparisons have been constructed between murine ephrin-A5 and all cloned ephrins. Murine ephrin-A5 was chosen since clones of all the known ephrin groups have been isolated from the mouse and second, since the ephrin-A5 group has representative clones from the most species. This ephrin is 99.1% identical to rat and human ephrin-A5.

Lower sequence identities were identified within the same ephrin group when *Xenopus* ephrin-A1 (the only other cloned *Xenopus* ephrin), was also compared with all the other cloned ephrins (Table 6). This ephrin had a highest sequence identity of 58.6% with rat ephrin-A1. This percentage is less than some sequence identities revealed between different ephrin groups such as murine ephrin-A5 with all the cloned ephrin-A2 members (Table 5).

The data from Tables 4, 5 and 6 indicate that within the same ephrin group, sequence identities can range between 99.1% (ephrin-A5 group) and 58.6% (ephrin-A1 group). These data also indicate that sequence identities between members of the same group are not always very high (Table 6). Additionally, the sequence comparisons show that sequence identities between individual ephrins of different ephrin groups may also be similar. For example, the sequence identity between *Xenopus* ephrin-A1 and rat ephrin-

A1 is 58.6% (Table 6) and between mouse ephrin-A5 and mouse ephrin-A3 is 54.8% (Table 5).

Therefore, the sequence identities found between the full length XLIG4 sequence and the ephrin-A3 group support the proposition that XLIG4 cDNA sequence represents a *Xenopus* ephrin-A3.

3.3.3 Pseudotetraploidy

Due to the presence of XLIG1 from the PCR screen, in addition to XLIG4, it is possible that this clone is another *Xenopus* homologue of the ephrin-A3 family. Sequence comparisons indicate that the XLIG1 class has greater sequence homology to the ephrin-A3 group that the XLIG4 class (see Table 3).This presence of a second ephrin-A3 gene would be due to pseudotetraploidy in *Xenopus.*

The cloning of the XLIG3 class is another potential example of pseudotetraploidy. The only other *Xenopus* ephrin to have a published sequence is *Xenopus* ephrin-A1 (Weinstein *et al.,* 1996), which has a significantly lower homology to other ephrin-A1 members than the XLIG3 class (see Table 3). Therefore, XLIG3 may represent the second *Xenopus* ephrin-A1 gene.

Presently, five ligands of the ephrin A-class have been cloned across five species. Assuming all these five groups are represented in *Xenopus*, one would expect 10 ephrins to be eventually cloned. The same is true of zebrafish where already two forms of ephrin-A5 have been identified (Brennan, unpublished data). If XLIG5 does represent a new ephrin group, it would increase the number of ephrin groups to six. Therefore, 12 ephrins would be expected to be found in *Xenopus.*

In summary, the XLIG class sequences suggest they have homology to existing ephrin groups. Only when longer cDNA's of XLIG1, XLIG2, XLIG3 and XLIG5 are cloned will their homologues be known. The nucleotide and protein sequence identities of the XLIG4 cDNA sequence to murine ephrin-A3, and comparisons with all cloned ephrins, strongly suggests that this XLIG4 cDNA is a *Xenopus* homologue of ephrin-A3 and therefore, the XLIG4 cDNA sequence will now be referred to as Xephrin-A3.

CHAPTER FOUR

4.1 INTRODUCTION

The expression pattern of a gene can suggest its sites of action and the role it may play in development. By comparing this pattern with the expression of other genes, information regarding possible interactions can be inferred. Several methods were used to analyse the developmental patterns of classes XLIG1-5. Initially RNAase protection was used to analyse the temporal expression of the XLIG classes. This technique allows the expression of the ephrins to be visualised sensitively and quantitatively. Northern Blot analysis was used to calculate the size of Xephrin-A3 mRNA. Finally, whole mount *in situ* hybridisation was employed to determine the spatial expression pattern of Xephrin-A3.

4.2 RESULTS

4.2.1 Temporal Profile of XLIG1-5 Classes

Initial expression analysis using the RNAase protection technique was carried out with a 200 bp PCR product from each ephrin class described in Chapter 3. An antisense probe was transcribed for each class of ephrin. 30μg of total RNA was analysed at stages 10, 13 and 17 which encompassed mesoderm induction, early and mid-late neurulation. Stage 10 and 17 total RNA had also been used as source material for the original RT-PCR procedure. EF-1α was used as a loading control (Krieg *et al.*, 1989).

Reproducible results were obtained for ephrin classes Xephrin-A3 and XLIG5. Fig. 4.1 shows the results of the RNAase protection experiments for Xephrin-A3 and XLIG5. Xephrin-A3 was found to be expressed strongly at stage 10 with decreased expression at stage 13 and strong expression again at stage 17. XLIG5, had very low expression at stage 10, strong expression at stage 13 and equally strong expression at stage 17.

RNAase protection data for the XLIG1, XLIG2 or XLIG3 classes was not obtained. This was due to the inability to make the antisense RNA probe necessary for the technique. It was possible that severe secondary structures within the 200 bp PCR clones for XLIG1, XLIG2 and XLIG3, prevented the RNA polymerase from creating a probe. To address

Figure 4.1

Temporal profile of Xephrin-A3 and XLIG5

RNA was extracted from the indicated stages and probed with Xephrin-A3 or XLIG5. Transfer RNA (tRNA) was used as an internal control to ensure that the protection results were only due to the embryo RNA. EF1-α was used as a loading control (Krieg *et al.*, 1989). Seven days of exposure was required to visualise Xephrin-A3 and XLIG5 expression. EF-1α was exposed for 20 hours.

Due to the length of exposure required to visualise Xephrin-A3 and XLIG5, EF-1α is over exposed. Therefore, visual quantification of the amount of expression of these ephrins is not possible

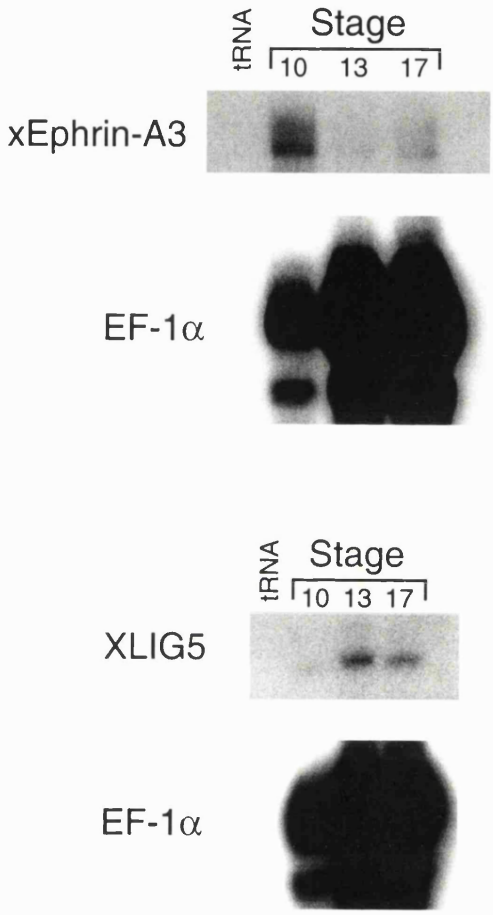
tRNA
Stage
10 13 17
xEphrin-A3
EF-1α
tRNA
Stage
10 13 17
XLIG5
EF-1α

this possibility the StemLoop GCG programme was used. StemLoop finds stems (inverted repeats) within a sequence. When the representatives of all the XLIG classes were assessed, all were found to exhibit secondary structure, but there were no regions of secondary structure particular to XLIG1-3 classes only. The possibility exists that the collective secondary structures of only the affected classes affects RNA polymerase action.

4.2.2 Expression Analysis of Xephrin-A3

Having isolated a longer clone of Xephrin-A3, it was decided to investigate the expression pattern of this ephrin during early *Xenopus* development in more detail.

Due to the strong expression of Xephrin-A3 at stage 10 in the RNAase protection experiments, the spatial expression of Xephrin-A3 could be investigated. In this experiment, an additional RNAase protection was carried out using whole embryo RNA obtained from 20 embryos at stage 10.5. These embryos were dissected into the following regions; animal pole, vegetal pole, dorsal marginal zone, lateral marginal zone and ventral marginal zone. The results show that Xephrin-A3 is uniformly expressed throughout the embryo at this stage (Fig. 4.2).

To obtain a more comprehensive profile of the temporal expression of ephrin Xephrin-A3, 12 embryonic developmental stages were assessed. The stages encompassed maternal RNA expression, the oocyte, gastrulation through neurulation and further into the tailbud stages of *Xenopus* development. In this RNAase protection 40µg of total RNA was used. The results are shown in Fig. 4.3. Xephrin-A3 was seen to be highly expressed at stage 0, the unfertilised egg[2], where only maternal RNA is present. This strong expression was maintained at stage 1, the fertilised egg and stage 3, the 4-cell stage embryo. By stage 6, the 32-cell stage, expression had fallen significantly. Expression then remained at a lower level between stages 10 to 46.

4.2.3 Northern Blot Analysis

In order to discover if the variations in expression level encountered in the developmental RNAase protection were due to single or alternatively spliced transcripts of Xephrin-A3 and to find the size of the Xephrin-A3 mRNA, Northern Blot analysis was carried out. Spliced variants have previously been noted for the ephrin-A class

Figure 4.2

Spatial localisation of Xephrin-A3 transcripts

An Range protection was performed on dissected pieces from 20, stage 10.5 embryos. RNA is present in all lanes, consistent with the whole mount *in situ* hybridisation data at this stage, where Xephrin-A3 is shown to have expression throughout the whole embryo.

This Xephrin-A3 expression was seen after the gel had been exposed for 3 days. The EF-1α was exposed for 12 hours.

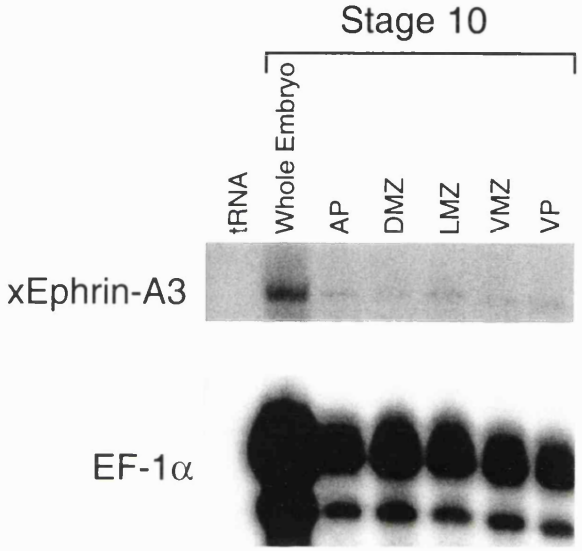
Stage 10
tRNA
Whole Embryo
AP
DMZ
LMZ
VMZ
VP
xEphrin-A3
EF-1α

Figure 4.3

Developmental RNAase protection

An RNAase protection was performed on the embryo stages shown. Strong expression of Xephrin-A3 is noted particularly during the early blastula stages. The loading control is ornithine decarboxylase (ODC) (Isaacs *et al.*, 1992).

The upper Xephrin-A3 expression on the gel was visualised after 2 days exposure. The ODC was exposed for 12 hours.

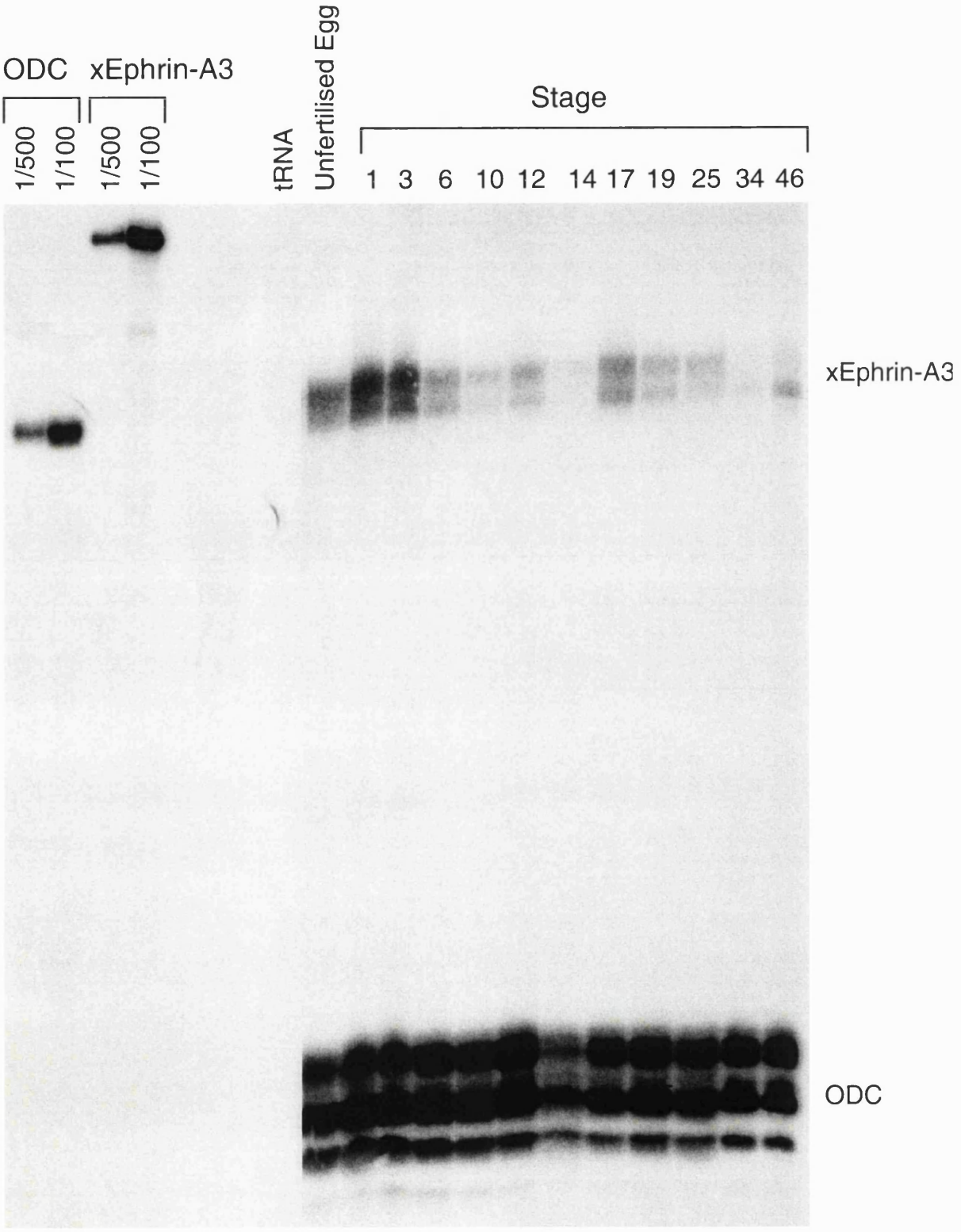
ODC
xEphrin-A3
1/500
1/100
1/500
1/100
tRNA
Unfertilised Egg
Stage
1 3 6 10 12 14 17 19 25 34 46
xEphrin-A3
ODC

members ephrin-A5 (Flenniken *et al.,* 1996; Winslow *et al.,* 1995) and ephrin-A3 (Davis *et al.,* 1994).

Stages 6 and 12 were chosen as representatives of stages, where in the developmental RNAase protection, Xephrin-A3 was equally expressed.

10mg of total RNA from these stages was used in Northern analysis. This is shown in Fig. 4.4. Using the coding region of Xephrin-A3 as a probe, one band is seen in both RNA samples which runs at the same location equivalent to 3.1 Kb. This is confirmed by the second gel which is the same Northern Blot at a lower exposure.

4.2.4 Whole Mount *in situ* Hybridisation

In order to visualise the expression pattern of Xephrin-A3, whole mount *in situ* hybridisation was carried out. The *Xenopus* embryos were analysed from early neurula (stage 15) to tail bud stages (stage 34). This procedure was carried out at least six times at each stage.

4.2.4.1 Early Neurula Stage Expression

At stage 15, diffuse Xephrin-A3 expression is present in the neural folds and throughout the neural plate (Fig. 4.5A). A region of increased expression is observed in a group of cells within the neural plate in the prospective hindbrain region (high-lighted in Fig. 4.5A by white arrows). By stage 16, Xephrin-A3 expression remains in the neural folds and neural plate (Fig. 4.5B). The heightened Xephrin-A3 expression observed in some cells within the posterior hindbrain is more discrete than at stage 15. At stage 18, the previous Xephrin-A3 expression pattern is maintained where strong expression continues along the midline, in the region of the neural folds and in the neural plate (Fig. 4.5C). The Xephrin-A3 expression in the presumptive r5/r6 hindbrain region can be more easily visualised by comparing the stage 18 embryo with a line diagram showing the position of neural crest cell masses in *Xenopus* at this developmental time (Fig. 4.5D). Additionally, two faint lines of expression appear to bisect the embryo within the presumptive hindbrain.

Figure 4.4

Northern Blot

Xenopus total RNA from stages 6 and 12 was probed with the 727 bp cDNA of Xephrin-A3. This revealed a single mRNA transcript running at 3.1 Kb after a 15 hour exposure.

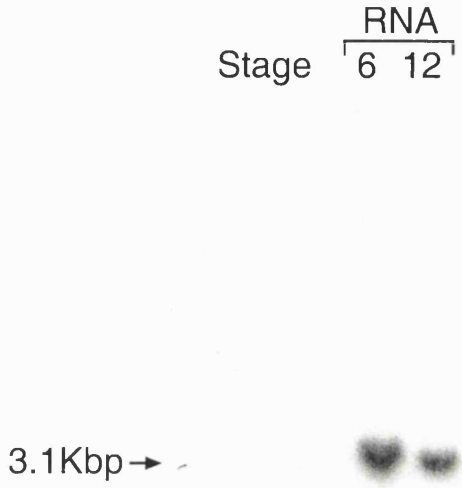
RNA
Stage 6 12
3.1Kbp

Figure 4.5

Whole mount *in situ* hybridisation of Xephrin-A3 at early neurula stages

(A) Dorsal view of the stage 15 embryo. Diffuse Xephrin-A3 expression is present in the neural folds and throughout the neural plate. A region of increased expression is observed in a group of cells within the neural plate in the prospective hindbrain region (white arrows). (B) Stage 15 expression is maintained in the stage 16 embryo. The expression of Xephrin-A3 appears to be more restricted to the neural plate and folds of the neural tube. Heightened Xephrin-A3 expression is observed in some cells within the posterior hindbrain. (C) A dorsal view of the stage 18 embryo shows that Xephrin-A3 expression remains in the neural fold and appears to compartmentalise the neural plate. The position of Xephrin-A3 expression in presumptive r5/r6 is indicated.

The Xephrin-A3 expression in the presumptive r5/r6 hindbrain region can be more easily visualised by comparing the stage 18 embryo with the line diagram D , which shows the position of neural crest cell masses in *Xenopus* at this developmental time.

An-anterior. P-posterior. pr5/r6- presumptive r5/r6. nc1-first arch neural crest. nc3-third arch neural crest. nc4-fourth arch neural crest. nc3/4-third and fourth arch neural crest. m3-mesoderm of the third branchial arch. B-blastopore. r3-rhombomere 3. r5-rhombomere 5.

Scale bar represents actual size of embryo where 1mm represents 100μm

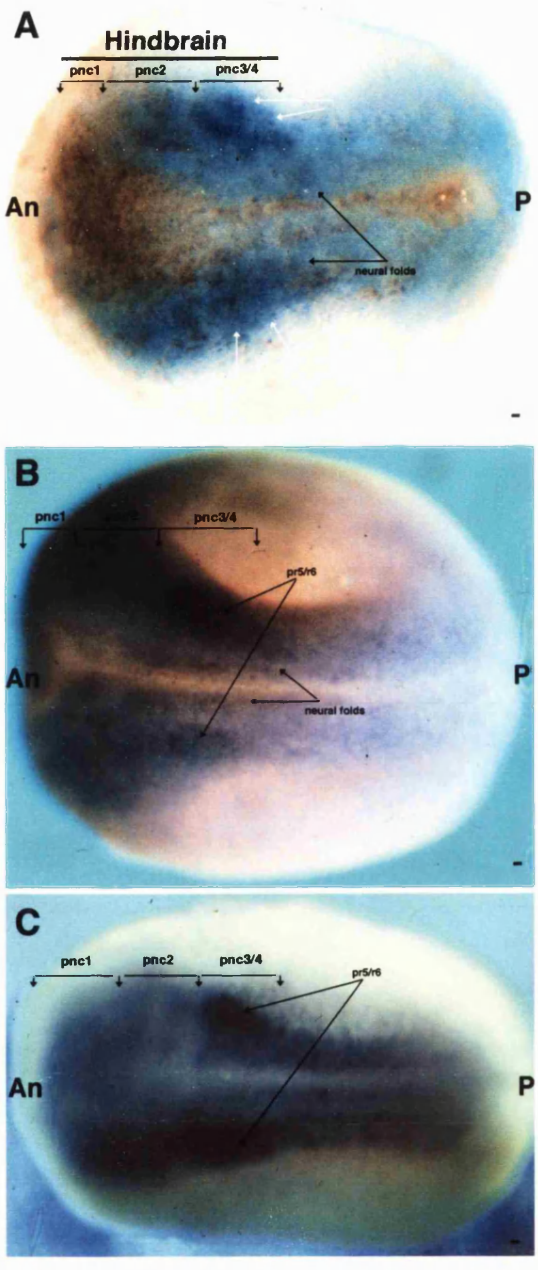
A
Hindbrain
pnc1
pnc2
pnc3/4
An
P
neural folds
B
pnc1
pnc3/4
pr5/r6
An
P
neural folds
C
pnc1
pnc2
pnc3/4
pr5/r6
An
P

D

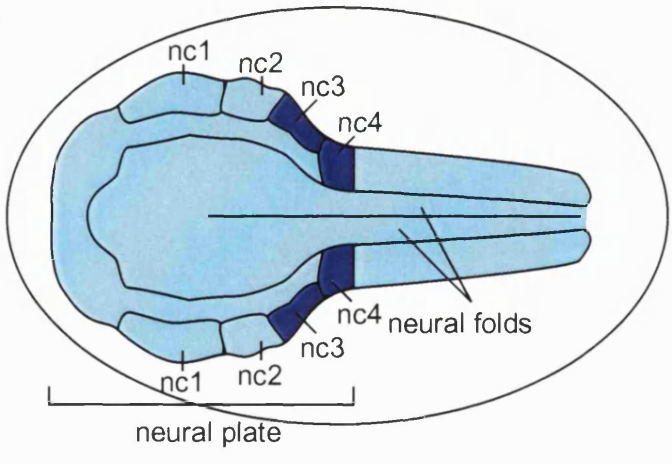
nc1
nc2
nc3
nc4
nc4
neural folds
nc3
nc1
nc2
neural plate

4.2.4.2 Late Neurula to Tailbud Stage Expression

By stage 19 Xephrin-A3 is expressed around the dorsal part of the eye and faintly in the mesoderm of the third arch (Fig 4.6A). Significant Xephrin-A3 expression is present in the neural crest migrating from the prospective region of rhombomeres 5 and 6. This expression is maintained at stage 20, except Xephrin-A3 expression now completely surrounds the eye (Fig 4.6B). A longitudinal section shows that this expression is in the first arch neural crest cells (Fig.4.6C).

At stage 21 and subsequent stages (21-23) represented in Fig 4.6D-G, Xephrin-A3 expression is maintained along the dorsal midline, at the blastopore and in the anterior head region. It is at these stages that strong Xephrin-A3 expression is observed in the joint mass of third and fourth arch neural crest cells emanating from the r5/r6 region of the hindbrain.

There is no fourth arch neural crest cell stream marker, so evidence that both these neural crest streams express Xephrin-A3 is supported in the following two ways. First, Xephrin-A3 expression occupies an area greater than that for the fourth arch neural crest cell stream alone (Fig. 4.6E). This is shown by comparing Xephrin-A3 expression with two markers *XKrox20* (Bradley *et al.,* 1992) and *XAP2* (Winning *et al.,* 1991). During neurulation stages, whole mount *in situ* hybridisation indicates *XKrox20* is expressed in rhombomeres 3 and 5 and in the third arch neural crest cells. *XAP2* is expressed in all cranial neural crest cells. By comparing the areas occupied by the third arch neural crest stream alone, (shown by *XKrox20*, Fig. 5.7A, Chapter Five), and the third and fourth arch neural crest streams together, (*XAP2* analysis, Fig. 5.9F, Chapter Five), Xephrin-A3 is expressed in third and fourth arch neural crest cells. Second, a double whole mount *in situ* hybridisation of *XKrox20* (dark blue) and Xephrin-A3 (lilac) shows Xephrin-A3 expression in the fourth arch neural crest, posterior to *XKrox20* expression in the third arch neural crest (Fig. 4.6F).

Xephrin-A3 expression in the combined, migrating third and fourth arch neural crest cells, appears to be maintained at a similar level (Fig. 4.6 B, D and E). However, at stage 23, after this neural crest stream splits apart (see Introduction 1.7), to produce the autonomous third and fourth arch neural crest cell streams, Xephrin-A3 expression in the fourth arch neural crest stream is significantly higher than that in the

Figure 4.6

Whole mount *in situ* hybridisation of Xephrin-A3 during branchial neural crest migration

(A) Side view of a stage 19 embryo. Xephrin-A3 expression is seen around the dorsal eye, faintly in the lateral mesoderm of the third arch and the neural crest cells migrating from adjacent to r5 and r6. (B) Side view (anterior) of a stage 20 embryo. Xephrin-A3 expression is present surrounding the eye, in the mesoderm of the third arch and in migrating neural crest cells. (C) Longitudinal section of the stage 20 embryo indicating Xephrin-A3 expression in the first arch neural crest. (D) The expression seen at stage 20 is maintained in the stage 21 embryo. Xephrin-A3 expression is present in third and fourth arch neural crest. This is more obvious at stage 22 (E), where Xephrin-A3 expression occupies a region greater than that for the fourth arch neural crest alone. (F) A dorsal view of the stage 22 embryo. Here, the embryo has undergone whole mount *in situ* hybridisation with both *XKrox20* (dark blue colour) and Xephrin-A3 (light purple colour). The expression of Xephrin-A3 in the fourth arch neural crest is observed. (G) Side view of the stage 23 embryo. Xephrin-A3 expression is seen in the eye, the third and fourth arch neural crest, the mesoderm of the third arch, along the midline and at the blastopore.

An-anterior. P-posterior. pr5/r6- presumptive r5/r6. nc1-first arch neural crest. nc3-third arch neural crest. nc4-fourth arch neural crest. nc3/4-third and fourth arch neural crest. m3-mesoderm of the third branchial arch. B-blastopore. r3-rhombomere 3. r5-rhombomere 5.

Scale bar represents actual size of embryo where 1mm represents 100μm

Neural Crest Stream

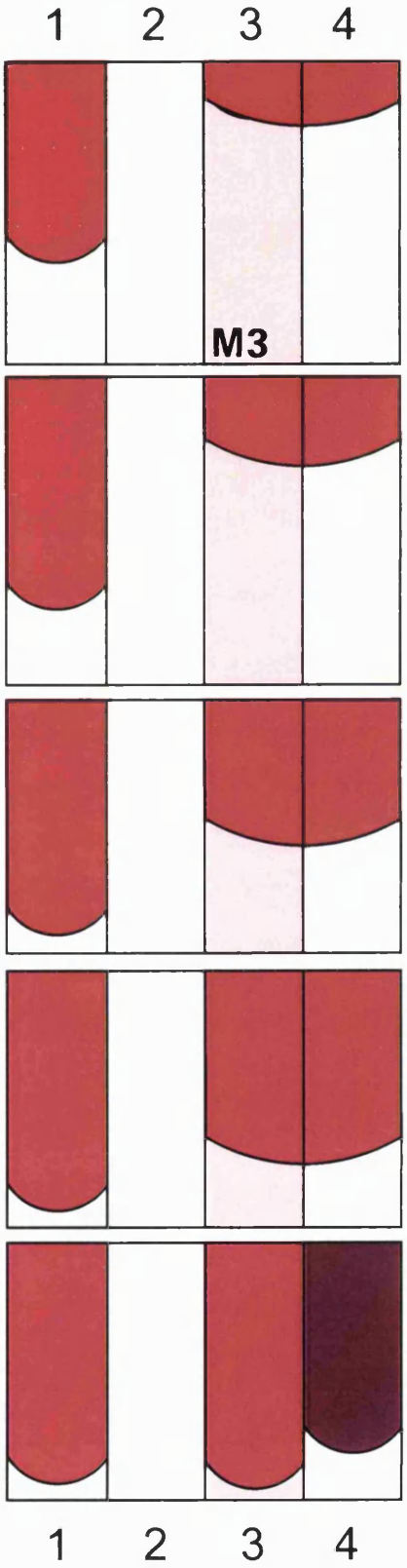

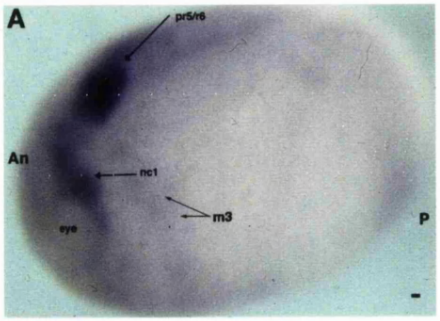

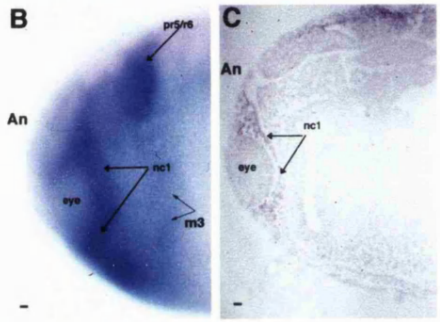

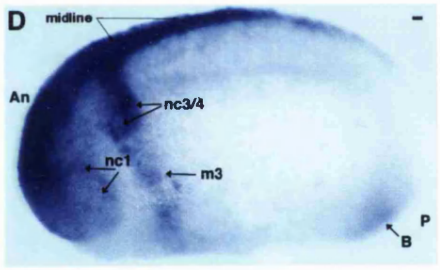

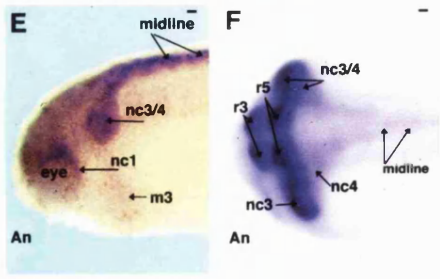

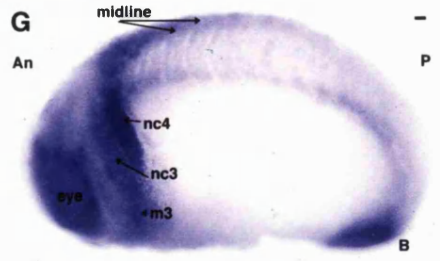

third arch neural crest stream. This is shown in Fig. 4.6G. Xephrin-A3 expression in the eye, blastopore, the mesoderm of the third arch and at the midline remains.

4.2.4.2.1 Summary

The change in Xephrin-A3 expression within the neural crest is summarised in line diagrams adjacent to Fig. 4.6. At stage 20 Xephrin-A3 is expressed in the migrating first arch neural crest cells and the initially non-migratory third arch neural crest cells (Fig. 4.6A). As neurulation continues, Xephrin-A3 expression continues in the first arch neural crest cells and remains in the migrating third arch neural crest cells (Fig. 4.6 B,D,F). Once the third arch neural crest cells have split into the third and fourth arch neural crest streams, Xephrin-A3 expression appears greater in the fourth arch neural crest cells than in the third arch neural crest cells while a constant level of expression appears to be maintained in the first arch neural crest cells (Fig. 4.6G). Low Xephrin-A3 expression is maintained in the mesoderm of the third arch throughout these stages.

4.2.4.3 Late Tailbud Stage Expression

At stage 30, additional expression is seen in the pronephros and the pronephric duct (Fig. 4.7A). Xephrin-A3 expression in the fourth arch neural crest cells is maintained but now appears to be substantially greater than in the third arch neural crest cells. A transverse section through the region of the third/fourth arch indicates that expression is maintained in the third/fourth arch neural crest, the lateral mesoderm of the third arch and surrounding the otic vesicle (Fig. 4.7B). A horizontal section at this stage through the dorsal head region shows that Xephrin-A3 expression is low in the posterior forebrain and present within the inner lumen walls of the otic vesicles (Fig. 4.7C). However, this expression may be caused by trapping since expression is not found within the otic vesicle itself. It is important to note that confirmation of the accuracy of the dissection requires the use of regional markers.

4.3 DISCUSSION

This chapter details the temporal and spatial expression of Xephrin-A3 in the early *Xenopus* embryo. Xephrin-A3 is represented by a single transcript of approximately 3.1Kb.

Figure 4.7

Whole mount *in situ* hybridisation of Xephrin-A3 at late tailbud stages

(A) At stage 30 Xephrin-A3 expression is present in the pronephros, the pronephric duct. the third and fourth arch neural crest cells and surrounding the eye and otic vesicle. (B) A transverse section through the region of the third arch indicates that expression is maintained in the neural crest, the lateral mesoderm of the third arch and surrounding the otic vesicle. (C) A horizontal section through the dorsal head region, shows that expression is low in the posterior fore-brain, encircles the otic vesicles but is negligible within the eye.

ov-otic vesicle. pn-pronephros, nc1-first arch neural crest. nc3-third arch neural crest. nc4-fourth arch neural crest. m3-mesoderm of the third branchial arch.

Scale bar represents actual size of embryo where 1mm represents 100μm

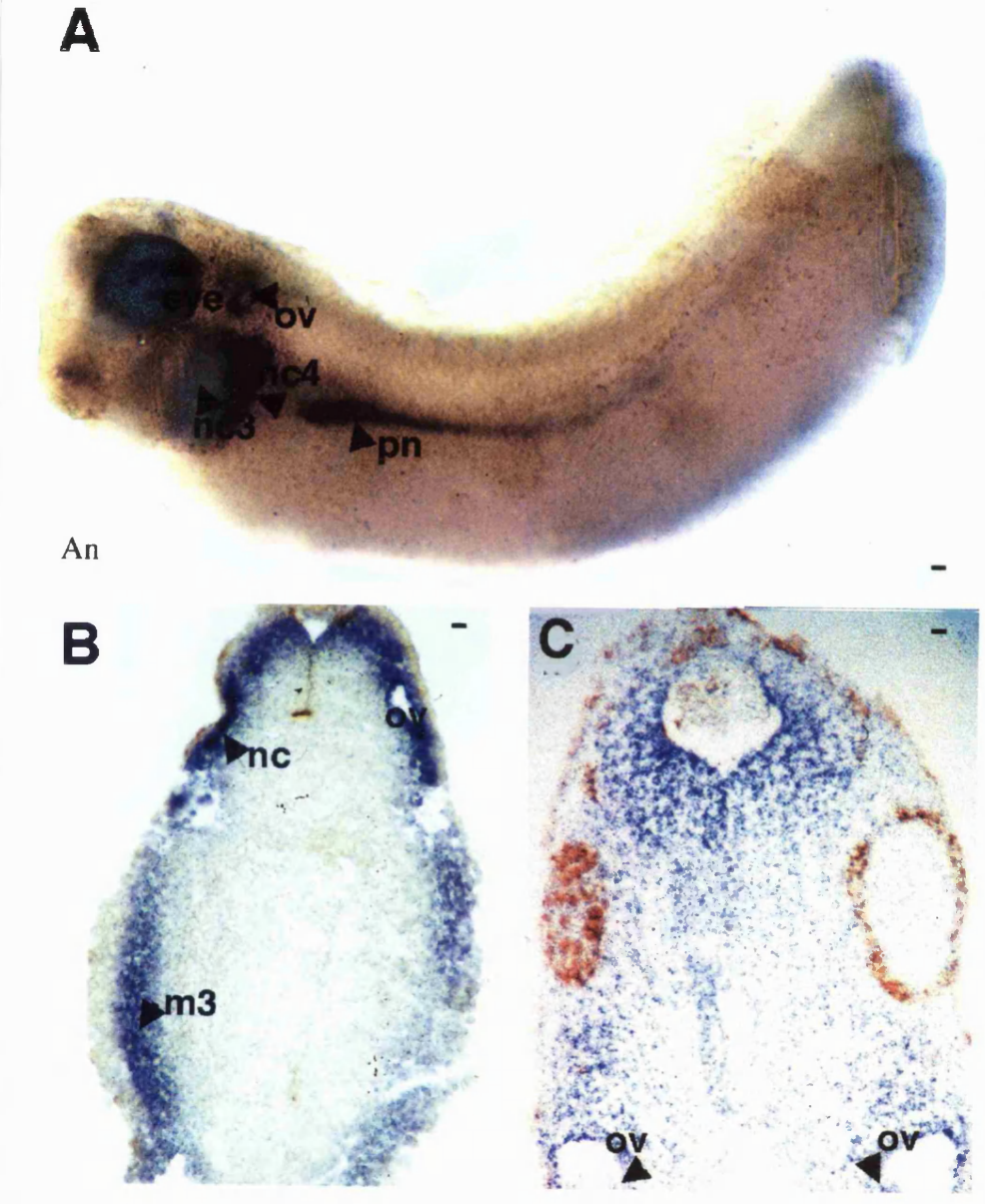

An

RNAase protection analysis identified dynamic Xephrin-A3 expression throughout the developmental stages assessed: very strong expression was found at blastula stages which fell significantly on reaching the gastrula stages. The lower expression persisted through to the later tailbud stages where fluctuations in expression were observed.

Spatial expression was revealed by whole mount *in situ* hybridisation analysis. Generally, Xephrin-A3 expression is present in several tissues: the anterior head, the first, third and fourth arch neural crest, the lateral mesoderm of the third branchial arch, the dorsal midline and at the blastopore. Expression in the blastopore region is maintained throughout all the stages analysed by whole mount *in situ* hybridisation.

4.3.1 Xephrin-A3 Expression in Neural Crest

During *Xenopus* neurulation, neural crest cells form at the border of the neural plate and epidermis. The neural crest cells remain at this border as a continuous mass for a period, prior to initiating migration into ventral regions. By stage 19, the branchial neural crest cells begin to migrate in streams that are initially in contact with one another: the most anterior neural crest cell stream moves towards the eye and the first branchial arch, the second stream towards the second branchial arch and the third stream towards the third and fourth branchial arches (see Fig. 1.7). By stage 24, the third neural crest cell stream splits into distinct third and fourth arch neural crest cell streams.

The Xephrin-A3 expression was particularly dynamic in neural crest. Expression was found in the pre-migratory and migrating neural crest. Of particular interest was the observation that during the migration of the third plus fourth arch neural crest (stages 20-22) Xephrin-A3 expression appears to be at the same level in each stream. However, by stage 23 after third and fourth neural crest cell streams have split into discrete streams, Xephrin-A3 expression has increased in the fourth arch crest, relative to third arch neural crest expression.

This change in expression exhibited by Xephrin-A3 is of great interest, since this could be involved in guiding the migration of individual neural crest streams.

4.3.2 Role of the Eph Family in Neural Crest Migration

It has been shown that members of the Eph family are expressed in *Xenopus* neural crest, and some contribute to neural crest cell migration (Helbling *et al.,* 1998; Smith *et al.,* 1997). The Eph family members expressed in *Xenopus* neural crest include the receptors, EphA4 (Xu *et al.,* 1995), EphB1 (Smith *et al.,* 1997) and EphA2 (Helbling *et al.,* 1998), and the ephrins, ephrin-B2 (Smith *et al.,* 1997) and the ephrin-A class (Helbling *et al.,* 1998). Figure 4.8 shows the expression of these Eph family members and the expression data provided by Xephrin-A3. This figure indicates the overlapping and complementary nature of Eph family expression.

It is believed that complementary and overlapping expression of Eph receptors in neural crest underlies the correct migration of these tissues by providing local, directional cues and prevent intermingling of different neural crest cell populations. Evidence for this was provided when the expression of ectopic truncated EphA2 receptor leads to aberrant migration of the third arch neural crest cells (Helbling *et al.,* 1998). Additionally, the overexpression of truncated forms of EphB1 and EphA4 caused disruption of third arch neural crest cell migration (Smith *et al.,* 1997). Here, the complementary expression between EphB1 and EphA4 and an interacting ephrin, ephrin-B2 (expressed in second arch neural crest), restricts the intermingling between the second and third arch neural crest streams, which allows the correct targeting of the third arch neural crest cells.

By virtue of its ephrin-A class status, Xephrin-A3 is likely to interact with EphA4 and EphA2. EphA4 is expressed in both rhombomeres 3 and 5 and also the third arch neural crest. This is complementary to Xephrin-A3 expression in the fourth arch neural crest and overlapping with Xephrin-A3 expression in the third arch neural crest. Complementary expression is also present between EphA2 and Xephrin-A3. EphA2 is expressed in the second arch neural crest and Xephrin-A3 is expressed in the third arch neural crest.

With these data in mind, the Xephrin-A3 expression in the third and fourth arch neural crest cells and the likely interaction with EphA4 and EphA2, it is possible that this ephrin might also contribute to the correct migration of neural crest.

Figure 4.8

Eph family expression in *Xenopus* branchial neural crest

This summary diagram shows the expression patterns of members of the Eph family in *Xenopus* branchial neural crest.

Ephrin-B2 is placed adjacent to EphB1 since it will bind to this receptor. EphA4 can bind both ephrin-B and ephrin-A class members, therefore it is placed between the ephrin-A and ephrin-B subgroups. Xephrin-A3, an ephrin-A class member, is likely to bind EphA4 and EphA2. Xephrin-A3 has complementary and overlapping expression to EphA4 and only complementary expression to EphA2. It was shown that ephrin-A ligands are expressed in all branchial arches (Helbling *et al.*, 1998). , by using receptor-tagged probes.

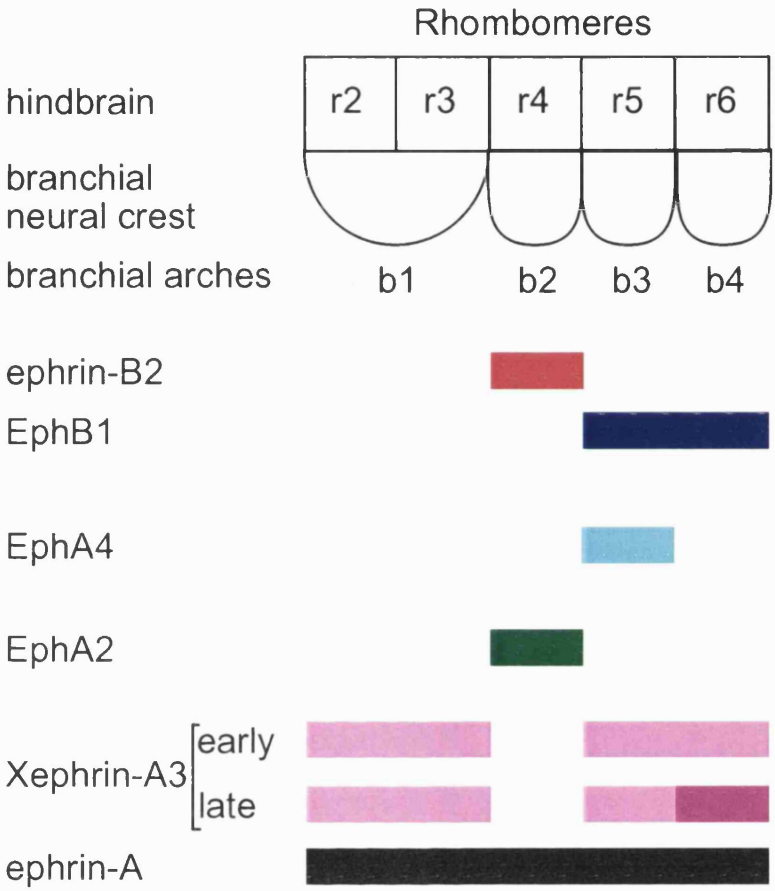
Rhombomeres
hindbrain
r2
r3
r4
r5
r6
branchial
neural crest
branchial arches
b1
b2
b3
b4
ephrin-B2
EphB1
EphA4
EphA2
Xephrin-A3
early
late
ephrin-A

4.3.3 Ephrin-A3 In Other Species

Ephrin-A3 has been cloned in two species other than *Xenopus*: a human cell line (Davis *et al.,* 1994) and in the mouse (Cerretti *et al.,* 1998). The only expression data available is from Northern Blot analysis, where human ephrin-A3 is shown to be expressed in the skin, but almost exclusively in the CNS. This expression included the brain, spinal cord and retina (Davis *et al.,* 1994). However, even if the spatial expression of human/mouse ephrin-A3 was known, it is possible that this expression will not be conserved in *Xenopus*. For example, two different ephrins, chick ephrin-B1 and rat ephrin-B2 are expressed in the posterior half of each somite (Krull *et al.,* 1997; Wang and Anderson, 1997). A similar use of different Eph receptor and ephrin family members in specific tissues has been observed in a number of other cases, arguing for a functional interchange-ability. Therefore, one would predict that Xephrin-A3 expression in some, but not all tissues, will be shared by other ephrin-A3 in other species.

4.3.4 Non-Neuronal Xephrin-A3 Expression

Xephrin-A3 was notably expressed, from the earliest stages of development, in the tissue surrounding the blastopore, along the midline, and at later stages in the pronephros. Of these tissues, EphA4 is also expressed in *Xenopus* pronephros (Xu *et al.,* 1995). However, there has been no further analysis of this expression in other species, and therefore the significance of this expression is not known.

CHAPTER FIVE

1.1 INTRODUCTION

It has been previously shown that overexpression of ephrin-B2, an ephrin-B class member which is expressed in *Xenopus* second arch neural crest, causes disruptions in the migration of third arch neural crest (Smith *et al.,* 1997). Additionally, blocking of Eph A-class receptors that can interact with Xephrin-A3 (Gale *et al.,* 1996), has also been shown to cause aberrant neural crest migration (Helbling *et al.,* 1998; Smith *et al.,* 1997). It is therefore a possibility that Xephrin-A3, a ephrin-A class ligand, may play a role in mediating cell interactions in specific streams of the neural crest.

To test the function of Xephrin-A3, the effects of overexpression of the full length ephrin and a soluble form of the ephrin, where the GPI-linkage motif is absent, were performed. Ectopic overexpression should activate the receptors that might not normally be activated due to the restricted location of endogenous Xephrin-A3 expression and second, increase the activation of receptors with endogenous overlapping expression. Previously it has been shown that soluble forms of ephrin-A1, ephrin-A3 and ephrin-B1 bind to, but not promote, the dimerisation of Eph receptors, since autophosphorylation of the receptor does not occur (Davis *et al.,* 1994). Indeed soluble receptors have been used as blocking agents (Davis *et al.,* 1994; Krull *et al.,* 1997; Winslow *et al.,* 1995). Therefore, overexpression of the soluble form of Xephrin-A3 may interfere with the activation of receptors for Xephrin-A3.

5.2 RESULTS

5.2.1 Subcloning the full length and soluble forms of Xephrin-A3

The full length and soluble forms of Xephrin-A3 were created by PCR as detailed in Chapter 2. The PCR fragments were subcloned into pSP64T (Krieg and Melton, 1984). This vector provides 5' untranslated sequences of β-globin, stop codons to terminate the truncated coding region followed by the 3' untranslated regions of the *Xenopus* β-globin gene. It has been shown that the untranslated regions enhance the translational efficiency and stability of the mRNA (Krieg and Melton, 1984). Fig. 5.1 shows the amino acid sequence of the full length Xephrin-A3 injection construct. The amino acids in red type

Figure 5.1

The amino acid sequences of the full length and soluble forms of Xephrin-A3 injection constructs

This figure indicates the full length and soluble forms of Xephrin-A3 used in the injection experiments. The soluble form of Xephrin-A3 is denoted by the red type. The * signifies the position of the stop codon.

RIMALVFALI LPLLSLFPRS GANRHSVYWN SSNYHLRRDG YTVQVDVNDY
RIMALVFALI LPLLSLFPRS GANRHSVYWN SSNYHLRRDG YTVQVDVNDY

LDIYCPHYNE SVVEHKMEQY ILYMVSYEGL PTCNISQGFK RWECNRPAPH
LDIYCPHYNE SVVEHKMEQY ILYMVSYEGL PTCNISQGFK RWECNRPAPH

SPIKFSEKFQ RYSAFSLGYE FHARGHEYYY ISTGTHNHRR SCLKMKVFVS
SPIKFSEKFQ RYSAFSLGYE FHARGHEYYY ISTGTHNHRR SCLKMKVFVS

CASTSHSGEK HSPTLPQFTI GPEVNIQDLD NFNPEIPKLE KSDQWEQPHK
CASTSHSGEK HSPTLPQFTI GPEVNIQDLD NFNPEIPKLE KSDQWEQPHK

REHLHLTVAV CLIIMTLLAS *
REHLH*

constitute the amino acid sequence used to create the soluble Xephrin-A3 injection construct.

To ensure that the ephrin constructs within the pSP64T vector were translated within the *Xenopus* embryo, *in vitro* transcription and translation of the full length and truncated Xephrin-A3 cDNA using the rabbit reticulocyte lysate system were carried out. Subsequent SDS-PAGE gel analysis showed that the resultant proteins of full length and soluble Xephrin-A3 had a size of 23 and 24 KDa respectively (Fig. 5.2). The soluble protein ran at an aberrant size as compared with the full length protein.

5.2.2 Microinjection of Full Length and Soluble Xephrin-A3

In most injections, RNA encoding full length or soluble Xephrin-A3 was microinjected together with fluorescein dextran, a lineage tracer into one cell of the two cell stage *Xenopus* embryo. This technique allows for an internal control for the injections as only one side of the embryo expresses the ephrin whereas the other side acts as an uninjected control. β-globin RNA which has been previously reported to have no specific effects on the development of *Xenopus* embryos, was injected into the embryos of every batch and used as a control for the non-specific effects of RNA injection. Using *XKrox20* as a marker, third arch neural crest was visualised by whole mount *in situ* hybridisation. An example of a control embryo is shown in Fig. 5.3A-B.

5.2.2.1 Microinjection of Full Length Xephrin-A3

The injected mRNA was titrated, such that within a single batch, embryos received 3ng, 2ng, 1ng, 500pg and 100pg of RNA. The concentration range will identify the minimum amount of RNA required to see a phenotype and demonstrate if the severity of the phenotype changed with RNA concentration. The higher mRNA concentrations injected had previously been shown to cause neural crest phenotypes in experiments with other Eph receptor/ephrin reagents (Helbling *et al.*, 1998; Smith *et al.*, 1997). 3ng can be a toxic amount of mRNA to inject into the *Xenopus* embryo since it can cause developmental defects especially during gastrulation. Therefore embryos from Xephrin-A3 or control injections with disrupted gastrulation phenotypes were removed from the overexpression analysis. These phenotypes were however distinguishable from gastrulation defects described later.

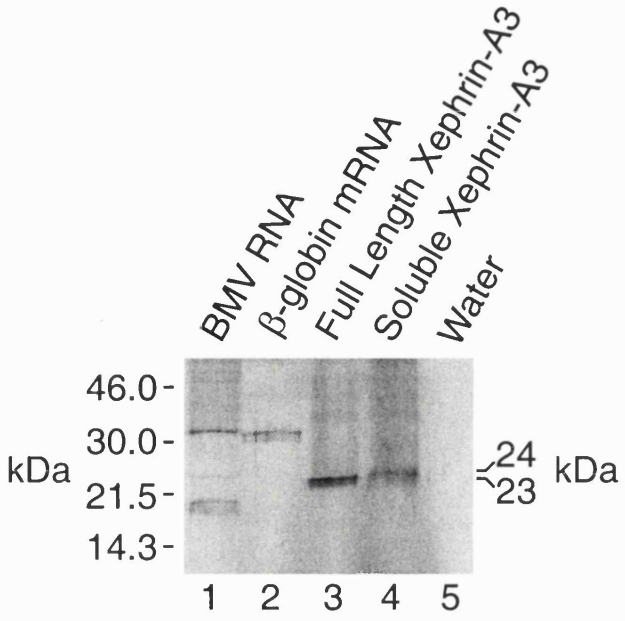
BMV RNA
β-globin mRNA
Full Length Xephrin-A3
Soluble Xephrin-A3
Water
kDa
46.0
30.0
21.5
14.3
24
23
kDa
1
2
3
4
5

Figure 5.2

***In vitro* translation of full length and soluble Xephrin-A3**

Autoradiograph of the ^{35}S labelled *in vitro* translation products of full length and soluble forms of Xephrin-A3. Adjacent lanes include β-globin, DNA and water controls. The cDNA was electrophoresed against rainbow markers on an SDS polyacrylamide gel.

Figure 5.3

***XKrox20* analysis: Overexpression of 3-2ng Xephrin-A3**

(A) Dorsal view of a control embryo at stage 22, injected with 2ng β-globin. (B) Side view of control embryo, indicating the normal migration of third arch neural crest. (C)-(F) Dorsal views of four examples of the failure of migration phenotype; the control uninjected sides indicate how the third arch neural crest stream migration should have occurred.

The red colour of the embryo denotes co-injection of fluorescein dextran to indicate the site of injection. Some embryos were not co-injected with the marker, but it was clear which sides of the embryo had been injected from the phenotypes observed.

C-control side. I-injected side. r3-rhombomere 3. r5-rhombomere 5. nc3-third arch neural crest.

Scale bar represents actual size of embryo where 1mm represents 100μm

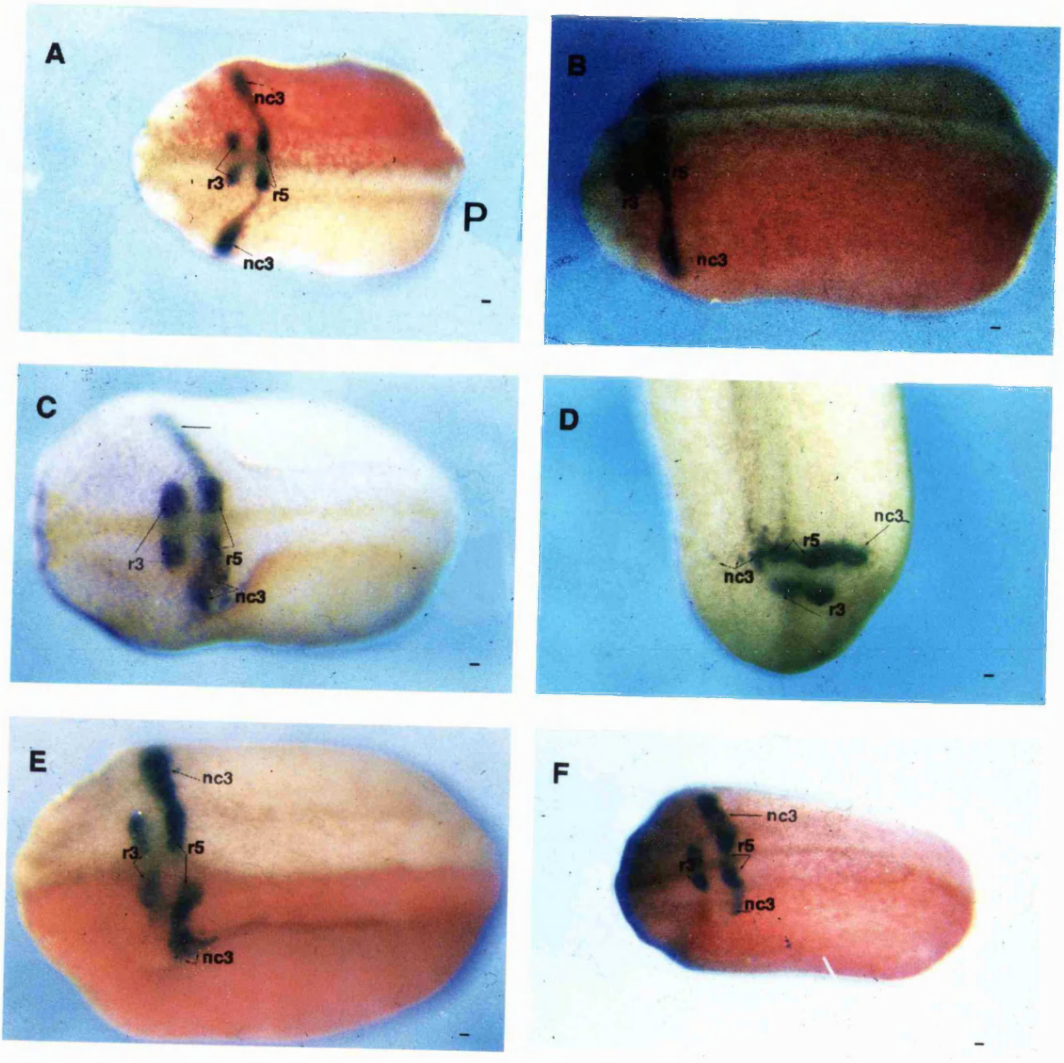
A
nc3
r3
r5
P
nc3
B
r5
r3
nc3
C
r3
r5
nc3
D
nc3
r5
nc3
r3
E
nc3
r3
r5
nc3
F
nc3
r5
r3
nc3

Since Xephrin-A3 showed expression in the first, third and fourth arch neural crest streams, it was decided to analyse injected embryos with neural crest markers to see if any neural crest phenotypes were discernible. The principal markers chosen were *XKrox20* (Bradley *et al.,* 1992), *XAP2* (Winning *et al.,* 1991) and EphA2 (Xu *et al.,* 1995). The transcription factor *XKrox20* is expressed in the third and fifth rhombomeres of the developing hindbrain and also in the third arch neural crest. *XAP2* is a pan neural crest marker which is expressed in the four neural crest streams in *Xenopus*: at the stages analysed, the neural crest streams are individually identifiable since the streams are discrete. EphA2 as mentioned in Chapter Four, is a marker for rhombomere four and the second arch neural crest stream (Xu *et al.,* 1995).

Xenopus embryos injected with full length Xephrin-A3 into the one cell at the two cell stage, were allowed to develop to stage 22-23 when neural crest migration is fairly advanced. Embryos were fixed and prepared for whole mount *in situ* hybridisation. Embryos injected with mRNA encoding full length Xephrin-A3 show aberrant migration of the third arch neural crest cells. The phenotype alters depending on the concentration of the mRNA injected.

5.2.2.1.1 *XKrox20* Analysis: Overexpression of 3-2ng Xephrin-A3

It was found with the higher concentrations of injected RNA 3-2ng, that there was an apparent failure of the migration of the third arch stream of neural crest cells. Whole mount *in situ* hybridisation with *XKrox20* showed third arch neural crest cells in the injected side of the embryos appearing as a mass of cells adjacent to their site of emergence from rhombomere 5 (Fig. 5.3C-F). The cells had failed to migrate compared with the uninjected side of the embryos (Fig. 5.3C-F). In addition to the cessation of migration, it appeared that the total area occupied by *XKrox20* expressing cells was reduced. There are three possibilities for these observations: first, third arch neural crest cells are migrating into deeper tissues and are therefore out of sight; second, there is reduced expression of *XKrox20* in the neural crest cells, or third, increased compactness is present between the neural crest cells. Horizontal serial sections were performed to address this question: the third arch neural crest cells remain at the edge of the neural plate as a mass of cells, and no migration is evident into deeper tissues compared with the uninjected side (Fig. 5.4A-L). The area occupied by the *XKrox20* expressing cells in

Figure 5.4

Serial sections indicating the absence of third arch neural crest cell migration

(A)-(L) Horizontal serial sections of embryo where the right hand side of each section indicates the control side of the embryo and the left hand side, the injected side. Overexpression of Xephrin-A3 has caused a failure of third arch neural crest cell migration on the injected side visualised by the absence of *XKrox20* expressing cells in ventral regions.

I-injected side. C-control side.

Scale bar represents actual size of embryo where 1mm represents 100μm

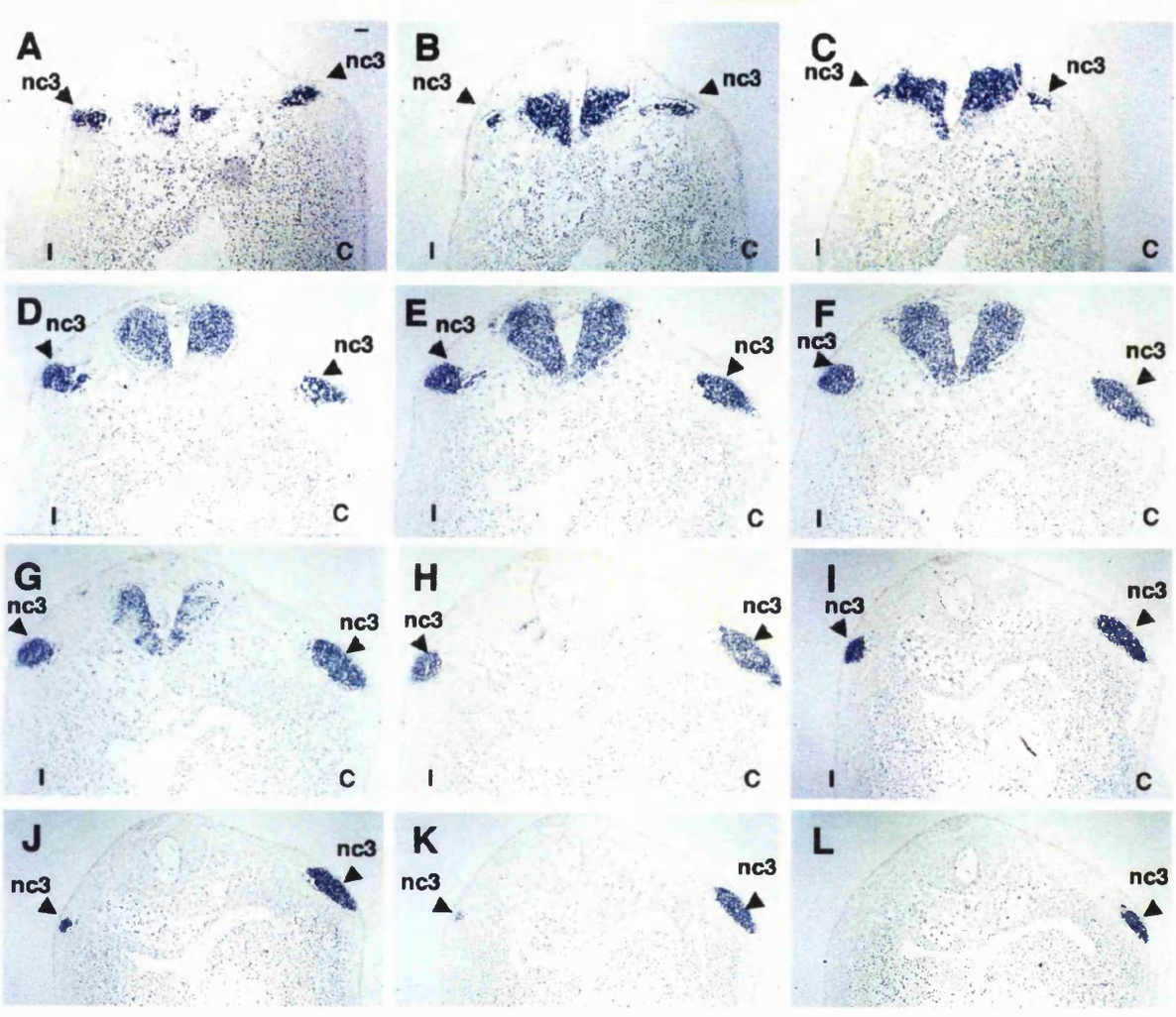
A
nc3
nc3
I
C
B
nc3
nc3
I
C
C
nc3
nc3
I
C
D
nc3
nc3
I
C
E
nc3
nc3
I
C
F
nc3
nc3
I
C
G
nc3
nc3
I
C
H
nc3
nc3
I
C
I
nc3
nc3
I
C
J
nc3
nc3
K
nc3
nc3
L
nc3

the sections suggest that the initial number of cells emanating from the neural plate region is similar.

5.2.2.1.2 *XKrox20* Analysis: Overexpression of 2-1ng Xephrin-A3

As the concentration of Xephrin-A3 RNA injected was decreased, the phenotype of the third arch crest migration appeared less severe. This lesser degree of severity was seen as several phenotypes.

It was observed that *XKrox20* expressing third arch neural cells in embryos overexpressing 2ng Xephrin-A3 mRNA had a less extensive migration than the third arch neural crest cells on the uninjected side of the embryo (Fig. 5.5A-B). Although migration was taking place, the pathway followed by the neural crest cells was abnormal; *XKrox20* expressing cells were positioned caudal to those observed in the normal pattern of migration, causing the neural crest cells to lie in positions across and posterior to the presumptive fourth arch crest region (Fig. 5.5C) (see later, section 5.2.2.1.4). In some cases, the posterior localisation included the whole length of the migrating neural crest cell stream. However, in other embryos, the third arch neural crest cell migration appeared to initially follow the normal migration pathway but with some cells singularly, or in groups, dissociating themselves from the main stream body and migrating into posterior positions (Fig. 5.5D). In all cases the aberrant migration was posterior to the normal migration route i.e. third arch neural crest cells encroach into fourth arch territory and beyond. Horizontal sections of the Figure 5.5A/B embryo show that some *XKrox20* positive cells migrated into deeper tissues of the embryo as small groups of cells (Fig. 5.6C-F). A section of a control embryo, injected with 2ng of β-globin is provided for comparison (Fig. 5.6A-B); here the regions occupied by the *XKrox20* positive cells on both sides of the embryo are the same.

The phenotypes with embryos that have been injected with 1ng of Xephrin-A3 mRNA also exhibit some slight retardation of third arch neural crest migration though not to the extent seem in previous embryos. There is however, a general greater incidence of cell scattering posterior to the normal migration pathway of the crest stream (Fig. 5.7A-F). For example, an extreme example of cell scattering is found (Fig. 5.7D). Both single cells and streams of cells are present in aberrant positions.

Figure 5.5

***XKrox20* Analysis: Overexpression of 2ng Xephrin-A3**

(A) Side view of normal migration of the third arch neural crest. (B) Dorsal view of (A) indicating the migration of the third arch neural crest on the injected side of the embryo, has not extended as far as that on the corresponding uninjected side of the embryo. (C) Dorsal view of an embryo where partial migration of the neural crest is indicated, but the pathway followed by the neural crest cells is abnormal: *XKrox20* expressing cells lie in positions across and posterior to the fourth arch crest region. (D) The third arch neural crest cell migration initially follows the wildtype pathway, but groups of *XKrox20* positive cells lie in ectopic caudal regions.

C-control side. I-injected side. r3-rhombomere 3. r5-rhombomere 5. nc3-third arch neural crest. An-anterior. P-posterior.

Scale bar represents actual size of embryo where 1mm represents 100μm

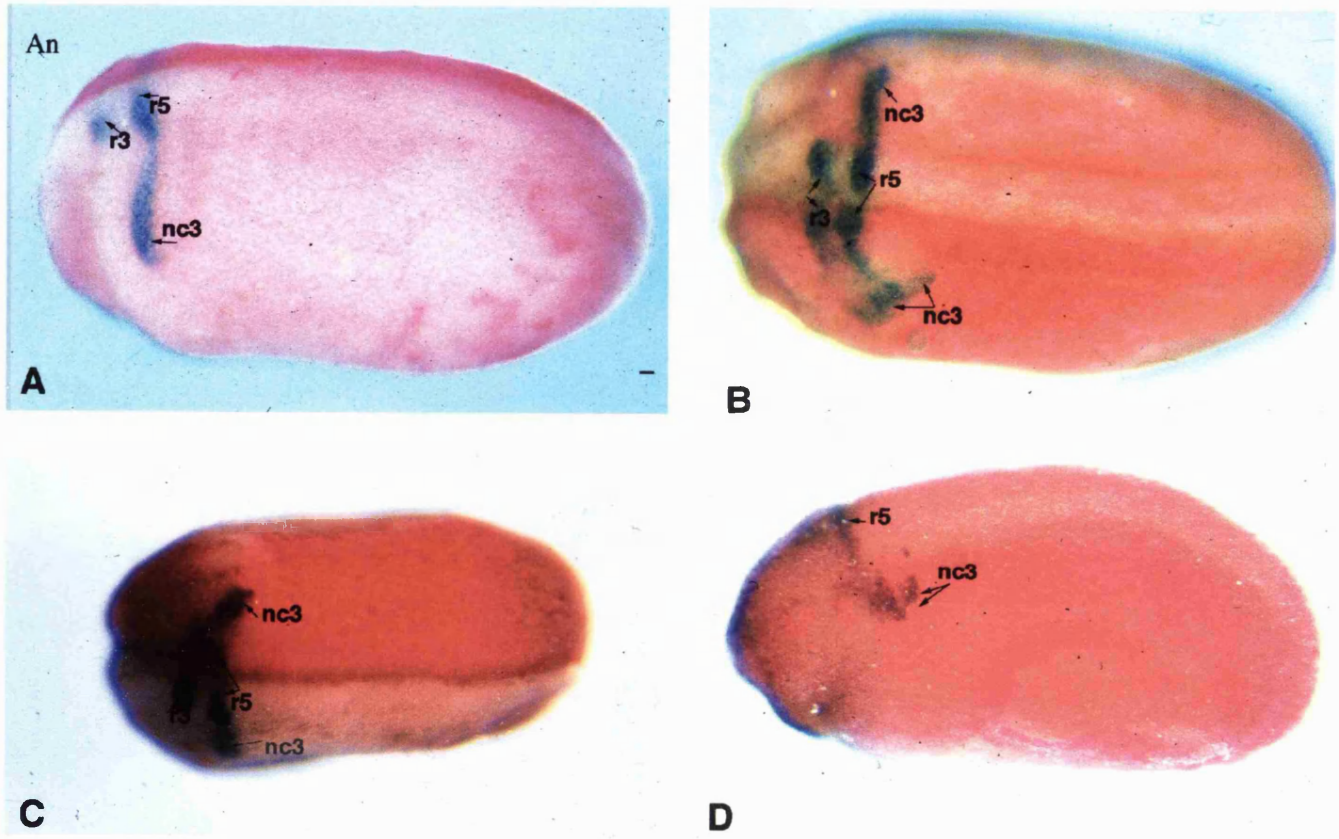
An
r5
r3
nc3
A
nc3
r5
r3
nc3
B
nc3
r5
nc3
C
r5
nc3
D

Figure 5.6

Horizontal sections of *XKrox20* hybridised third arch neural crest cells of 2ng injected embryos

(A)-(B) Two control sections are shown from a β-globin injected embryo. Both the regions occupied by the *XKrox20* positive cells and their position are the same. (C)-(F) Horizontal serial sections of an Xephrin-A3 injected embryo. The right hand side of each section indicates the injected side; *XKrox20* expression is found in groups of cells within deeper tissues of the embryo in comparison to the left hand, control side of the embryo.

C-control side. I-injected side. nc3-third arch neural crest cells.

Scale bar represents actual size of embryo where 1mm represents 100μm

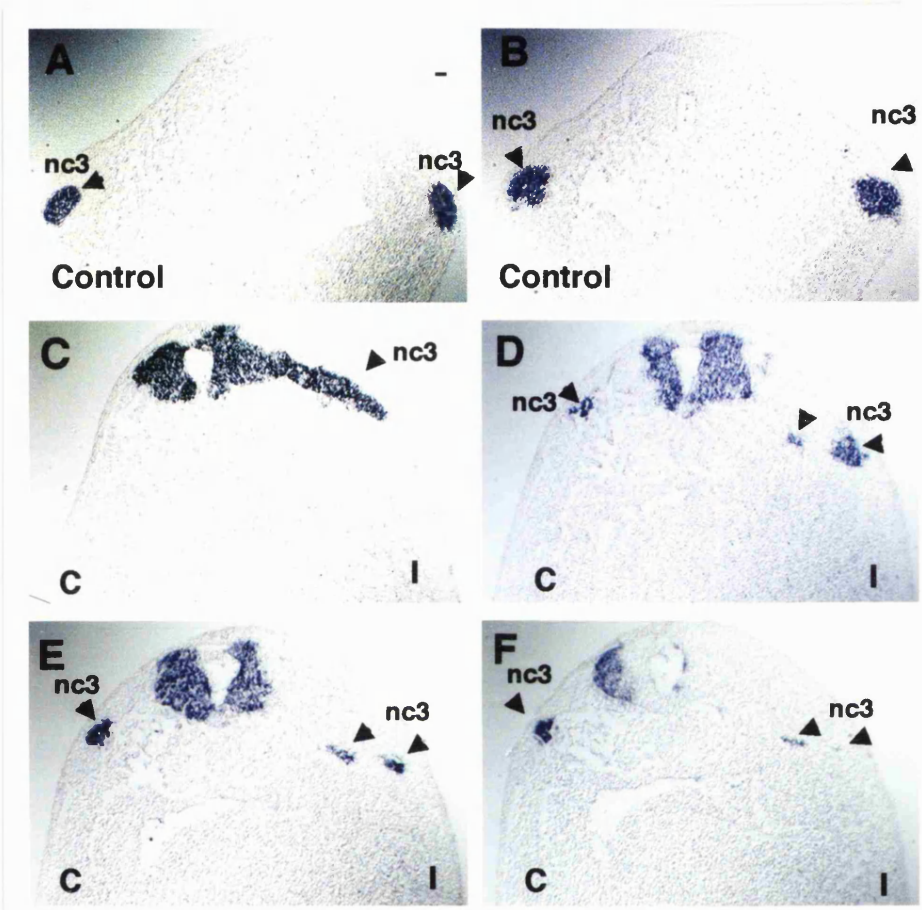
A
nc3
nc3
Control
B
nc3
nc3
Control
C
nc3
C
I
D
nc3
nc3
C
I
E
nc3
nc3
C
I
F
nc3
nc3
C
I

Figure 5.7

***XKrox20* Analysis: Overexpression of 1ng Xephrin-A3**

(A) Side view of the control side of a stage 23 embryo. (B) Side view of the injected side of (A). (C)-(F) Variations of the phenotype obtained from injections of 1ng of Xephrin-A3. An ectopic scattering of cells is evident in all examples to various extents. The cell scattering is posterior to the normal migration route of the third arch neural crest cells.

r3-rhombomere 3. r5-rhombomere 5. nc3-third arch neural crest. An-anterior. P-posterior.

Scale bar represents actual size of embryo where 1mm represents 100μm

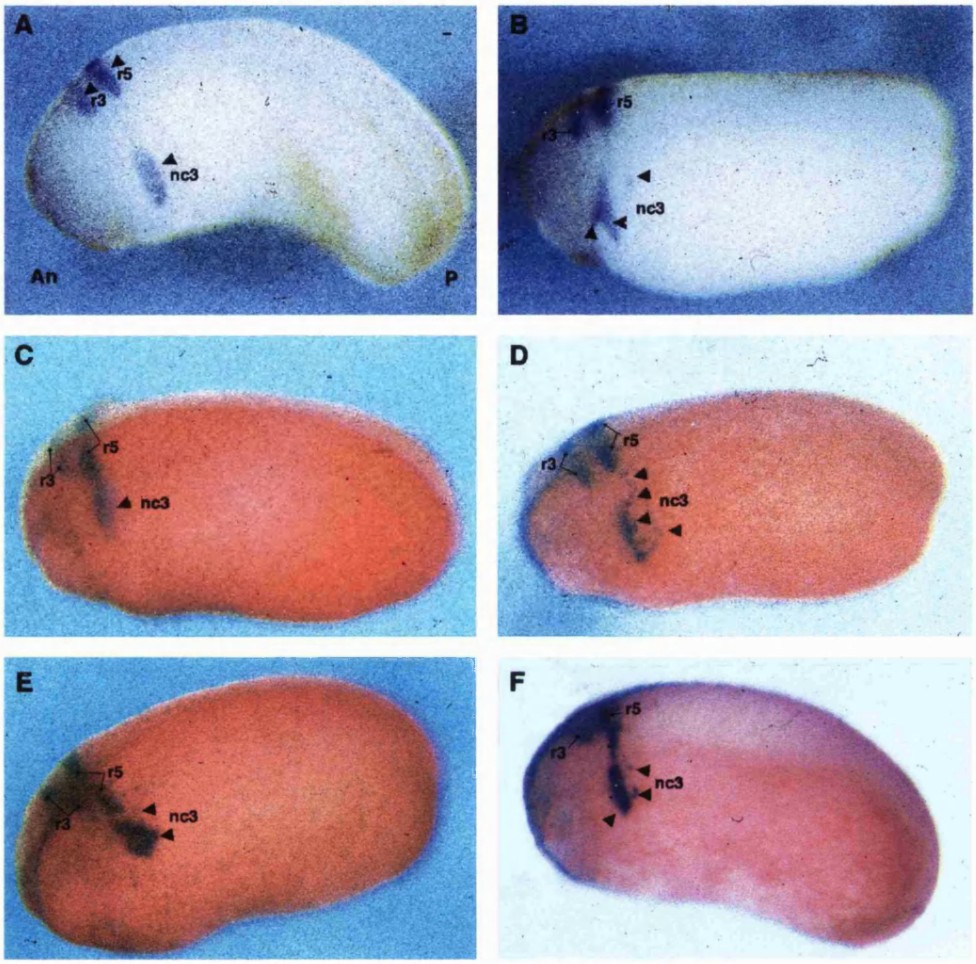
A
r5
r3
nc3
An
P
B
r5
r3
nc3
C
r5
r3
nc3
D
r5
r3
nc3
E
r5
r3
nc3
F
r5
r3
nc3

5.2.2.1.3 *XKrox20* Analysis: Overexpression of 0.5-0.1ng Xephrin-A3

The phenotypes exhibited by *Xenopus* embryos injected with 0.5ng-0.1ng mRNA have much less severe phenotypes compared to their siblings. The extent of migration of the third arch neural crest streams on the injected sides of the embryos is the same as on the uninjected control sides. The distribution of the cells within the stream however remains abnormal. In these cases, some streams have small tendril-like groups of cells along the entire length of the main stream body. These encroach into fourth arch territory but not anteriorly (Fig. 5.8A). This phenotype is also present in an example of a double whole mount *in situ* hybridisation with *XKrox20* and EphA2 (Fig. 5.8B; see next section). The control and injected sides of an embryo are seen in Fig. 5.8C-D respectively. The control side shows the expected third arch neural crest cell migration, whereas on the injected side there are tendrils of *XKrox20* third arch neural crest cells projecting from the body of the migrating crest stream (Fig. 5.8D).

5.2.2.1.4 *XAP2* and EphA2 Analysis

Since Xephrin-A3 is expressed in the fourth arch neural crest, it was possible that these cells might also be affected by Xephrin-A3 overexpression. In addition, complementary expression between Xephrin-A3 in the third arch neural crest and EphA2 in the second arch neural crest raised the question as to whether second arch neural crest migration is affected. Therefore, injected embryos were analysed by whole mount *in situ* hybridisation with the pan neural crest marker *XAP2* (Winning *et al.,* 1991) and EphA2.

As with the observations with *XKrox20*, the severity of phenotypes observed with *XAP2* lessened with decreasing amounts of injected mRNA: phenotypes were stronger in embryos injected with high concentrations of mRNA. Embryos injected with 3ng of Xephrin-A3 mRNA had two phenotypes; in the first *XAP2* expressing cells lie in ectopic posterior locations, parallel to the dorsal midline (Fig. 5.9A-B). Coincident with this phenotype there appeared to be a merging of all the streams of neural crest cells that had begun migration from the neural plate; the neural crest cells on the injected side of the embryo appear as a continual mass of cells extending from the position of the first arch neural crest to the region of the fourth arch neural crest and beyond (Fig. 5.9C,E). This phenotype is exhibited by 6 out of 55 embryos analysed by whole mount *in situ*

Figure 5.8

***XKrox20* Analysis: Overexpression of 0.5-0.1ng Xephrin-A3**

(A) Dorsal-anterior view of a stage 22 embryo; ectopic posterior localisation of *XKrox20* labelled cells along the length of the migrating neural crest cells. (B) Double *in situ* hybridisation with EphA2 indicating the wildtype migration of the second arch neural crest stream (purple colour) and the mis-migration of the third arch neural crest cells with *XKrox20* (Blue colour). (C) A control side and (D) the injected side of an embryo. Mis-migrating cells cause tendril-like processes especially at the more ventral portion of the neural crest stream. Arrows point to tendrils caused by the mis-migration of third arch neural crest cells.
C-control. I-injected. r3-rhombomere 3. r5-rhombomere 5. nc2- second arch neural crest. nc3-third arch neural crest.

Scale bar represents actual size of embryo where 1mm represents 100μm

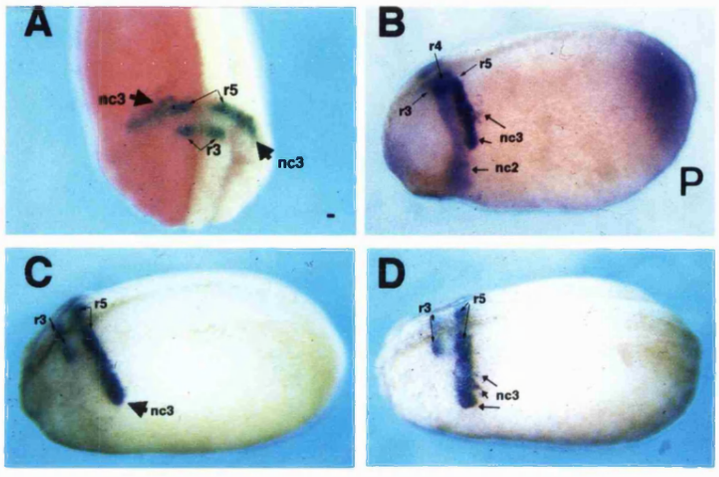
A
nc3
r5
r3
nc3
B
r4
r5
r3
nc3
nc2
P
C
r3
r5
nc3
D
r3
r5
nc3

Figure 5.9

XAP2 Analysis of Xephrin-A3 injected embryos

(A)-(B) Two dorsal view examples of *XAP2* analysis of 3ng Xephrin-A3 injected embryos. Increased posterior migration of neural crest cells parallel to the dorsal midline is observed in both examples. (C) Dorsal view of a 3ng injected embryo. The neural crest streams of the injected side of the embryo are merged into one mass. The migration of the first arch neural crest streams still encircles the eye but there are no apparent gaps separating the individual streams. The extent of migration compared to the control side is less. (D)-(E) Side views of the control and injected sides of (C). (F)-(I) 2ng injected embryos: (F)-(G) side views of control and injected sides of the same embryo; migration of the neural crest is slower on the injected side and the third and fourth arch neural crest streams intermingle. (H)-(I) In these embryos, migration is similar on both sides but there is no separation between the third and fourth arch neural crest cells.

C- control side. I-injected side. nc-neural crest. nc1- first arch neural crest. nc-2 second arch neural crest. nc3-third arch neural crest. nc4-fourth arch neural crest.

Scale bar represents actual size of embryo where 1mm represents 100μm

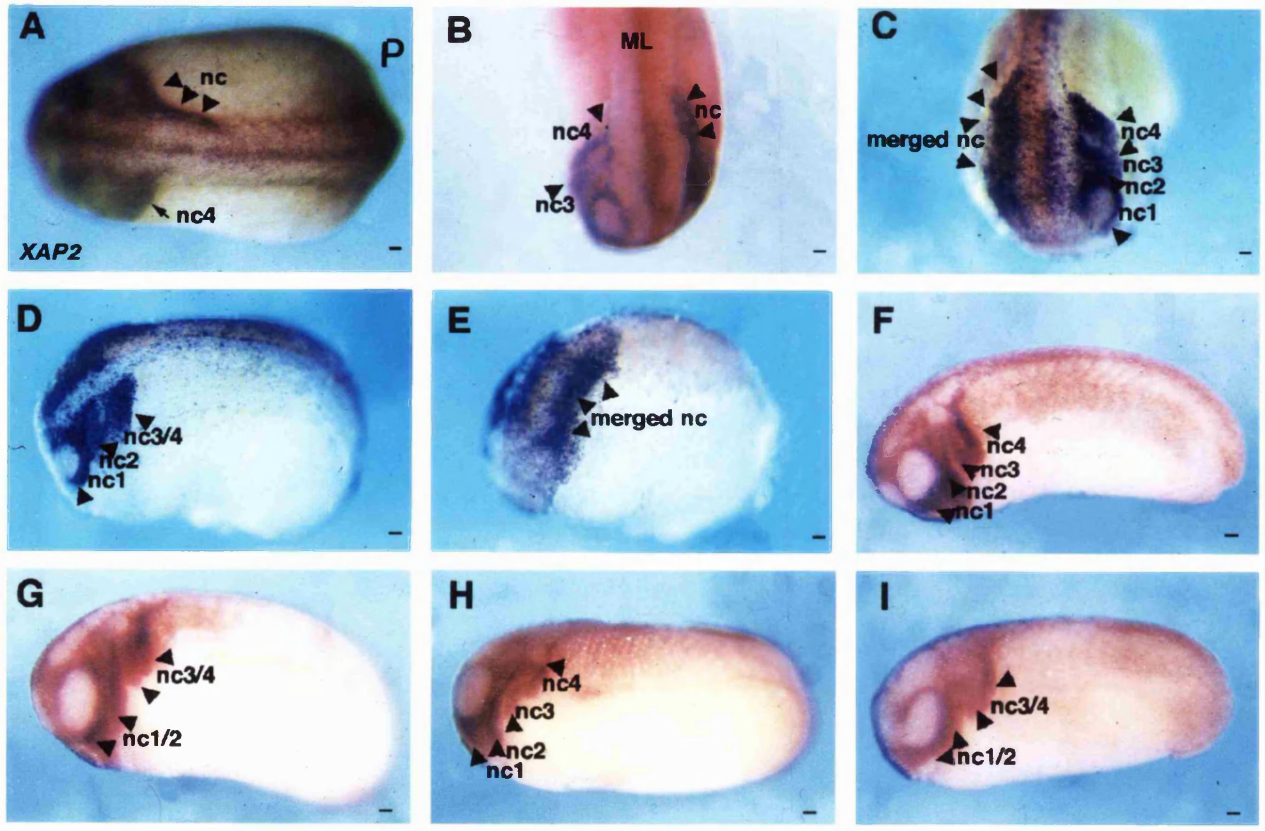
A
P
nc
nc4
XAP2
B
ML
nc
nc4
nc3
C
merged nc
nc4
nc3
nc2
nc1
D
nc3/4
nc2
nc1
E
merged nc
F
nc4
nc3
nc2
nc1
G
nc3/4
nc1/2
H
nc4
nc3
nc2
nc1
I
nc3/4
nc1/2

hybridisation with *XAP2*, but it was not observed in control or non-injected sibling embryos.

At the same concentration of the injected Xephrin-A3 mRNA, a second but less severe phenotype is revealed: a merging of the third and fourth arch crest streams and a delay in their migration relative to the migration on the uninjected control side of the embryo (Fig. 5.9F-I). Phenotypes were not observed in the first or second arch neural crest cell migration pathways.

All the neural crest cell migration phenotypes exhibited by embryos overexpressing full length Xephrin-A3 had defective migration posterior to the normal migration pathway. Third arch neural crest cells were not seen to enter second arch territory. To further investigate this, whole mount *in situ* hybridisation of injected embryos with *Xenopus* EphA2 (Xu *et al.*, 1995) was carried out. As previously noted, EphA2 is expressed in rhombomere 4 and the second arch neural crest. EphA2 has been shown to be an high affinity receptor for mouse ephrin-A3, the closest putative homologue for Xephrin-A3 and therefore, it was possible that there could be disruption of cells expressing EphA2 (Gale *et al.*, 1996).

The injected embryos did not show any change to the distribution of neural crest cells expressing EphA2. A double *in situ* hybridisation of EphA2 and *XKrox20* of a 0.5ng injected embryo shows aberrant third arch neural crest cell migration without an effect on the migration of the second arch neural crest stream. EphA2 is not expressed as strongly as *XKrox20* and there is a slight colour reaction difference which enables the second and third arch neural crest streams to be distinguished (Fig. 5.8B).

In summary, the over-expression of full length Xephrin-A3 caused aberrant migration of third arch neural crest cells. Ectopic migration of these cells was always posterior to the normal migration pathway, into fourth arch territory.

5.2.2.2 Microinjection of Soluble Xephrin-A3

Embryos were injected with mRNA encoding soluble Xephrin-A3 into the *Xenopus* embryo in one cell at the two cell stage. Again the injected RNA was titrated, such that within a single batch, embryos received 3ng, 2ng, 1ng, 500pg and 100pg of RNA. As with the full length Xephrin-A3 injections, injection of 3ng of soluble Xephrin-A3 can

cause non-specific gastrulation phenotypes. These embryos were removed from the analysis.

The phenotypes produced by soluble Xephrin-A3 overexpression were very similar to those observed with full length Xephrin-A3 overexpression (see Fig. 5.10). There were no discernible differences within the phenotypes themselves but the number of embryos exhibiting the phenotypes was less. The trend observed was that embryos injected with high titres of Xephrin-A3 mRNA (3-2ng), showed a greater incidence of the less severe phenotypes (Fig. 5.10A-D). Here, migration of the third arch neural crest took place but seemed to occupy greater areas of the migration pathway and ectopic cells were seen in the fourth arch region (Fig. 5.10A-D). Embryos injected with lower Xephrin-A3 mRNA (1-0.1ng) concentrations displayed fewer phenotypes and subsequently, larger numbers of embryos showed normal third arch neural crest migration on their injected sides. Injections of 100pg of soluble Xephrin-A3 were indistinguishable from control RNA injected embryos or their uninjected siblings.

The soluble Xephrin-A3 injected embryos were also analysed with the pan neural crest marker *XAP2* and with EphA2. Similar neural crest phenotypes were observed with *XAP2* analysis as had been observed with the full length Xephrin-A3 injections: migration of the first and second arch neural crest appeared unaffected by ectopic expression of soluble Xephrin-A3 but the migration of the third and fourth arch neural crest streams was delayed and the separation of these streams was lessened (Fig. 5.10E-F). EphA2 expression analysis did not show any disruption of second arch neural crest migration (data not shown). Both results were indistinguishable from phenotypes exhibited following full length Xephrin-A3 injections.

All the overexpression results with either full length or soluble Xephrin-A3 were tabulated (see Table 7). The table shows the number of experiments performed with each Xephrin-A3 construct, the numbers of embryos injected and the spread of phenotypes. Table 8 is an example of a typical injection experiment. It includes the numbers of embryos that die pre- and post- gastrulation. Usually the loss of embryos at gastrulation is related to the concentration of mRNA injected; however, the loss of control β-globin injected embryos injected with the same mRNA concentrations as Xephrin-A3 injected embryos, did not produce the same degree of embryo loss. Further investigation into these observations is described below.

Figure 5.10

Ectopic soluble Xephrin-A3 expression

(A) Side view of the control side and (B) injected side of an embryo injected with 3-2ng of soluble Xephrin-A3. *XKrox20* expressing cells occupy a wider area along the migration pathway of third arch neural crest. (C)-(D) Side view of two further examples *XKrox20* analysed embryos injected with 2ng of soluble Xephrin-A3; (C) ectopic cells of the third arch neural crest are present in more caudal positions than normal and (D) a retardation in migration of the third arch neural crest cells. (E)-(F) Control and injected side views respectively of an *XAP2* analysed embryo injected with 3ng of soluble Xephrin-A3; (E) The control side indicates normal *XAP2* expression in the four neural crest streams. (F) The injected side of the embryo indicates a normal migration of the first and second arch neural crest streams. The third and fourth arch crest streams have not migrated as far as those on the control side of the embryo.

r3-rhombomere 3. r5-rhombomere 5. nc1-first arch neural crest. nc2-second arch neural crest. nc3-third arch neural crest. nc4-fourth arch neural crest.

Scale bar represents actual size of embryo where 1mm represents 100μm

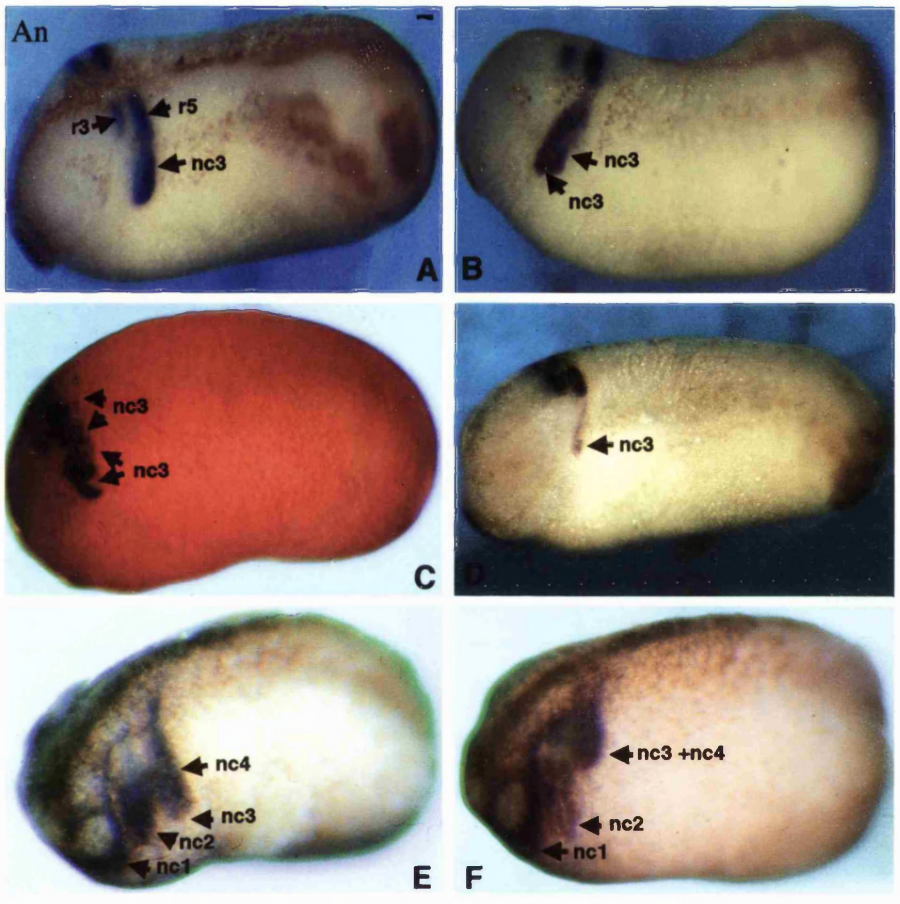
An
r3
r5
nc3
A
nc3
nc3
B
nc3
nc3
C
nc3
D
nc4
nc3
nc2
nc1
E
nc3 +nc4
nc2
nc1
F

Table 7

Composite table of injections performed in 1 cell of the 2 cell stage *Xenopus* embryo

This table indicates the number of embryos exhibiting each phenotype in relation to the concentration of mRNA encoding β-globin, full length Xephrin-A3 or soluble Xephrin-A3 injected into the 1 cell of the two cell stage *Xenopus* embryo.

The following terms are used;

β-globin - β-globin; Xephrin-A3 - Full length Xephrin-A3; ΔXephrin-A3 - soluble Xephrin-A3; No. of expts - number of experiments; (N) - number of embryos; No Mig. - No migration of the third arch neural crest cells; Delay - delay in the migration of either the third arch or the third arch plus fourth arch neural crest in respect to the uninjected control side; Aberrant - Migration occurs but incorrectly; Ectopic Spot - single spot of marker expression is separated from the main crest stream being investigated; Merged - Intermingling between the third and fourth arch neural crest cell streams; WT - the percentage of injected embryos exhibiting neural crest migration that is similar to uninjected siblings.

The figures in brackets represent the percentage phenotype the figure represents.

Construct	RNA injected (ng)	No. of Expts	(N)	No. Mig (N)	Delay (N)	Aberrant (N)	Ectopic Spot (N)	Merged (N)	WT %
β-globin	4	1	9	--	--	--	--	--	100
	3	3	21	--	2 (10)	--	--	--	90
	2	4	28	--	--	--	--	--	100
	1	3	14	--	--	--	--	--	100
	0.5	3	32	--	--	--	--	--	100
	0.1	2	4	--	--	--	--	--	100
Xephrin-A3	4	1	6	5 (83)	--	--	--	1 (17)	0
	3	4	46	15 (33)	--	16 (35)	--	6 (13)	19
	2	5	98	13 (13)	--	52 (21)	--	7 (7)	27
	1	3	51	--	4 (8)	19 (33)	--	4 (8)	27
	0.5	3	58	--	3 (5)	26 (22)	3 (5)	--	45
	0.1	2	27	--	2 (7)	11 (41)	5 (19)	--	33
ΔXephrin-A3	3	3	23	6 (26)	--	5 (9)	--	3 (22)	30
	2	4	78	7 (9)	--	13 (13)	--	--	76
	1	2	25	10 (40)	2 (8)	--	--	--	52
	0.5	2	26	--	--	--	--	--	100
	0.1	2	15	--	--	7 (13)	--	3 (20)	33

Table 8

Data for a typical injection experiment with reference to gastrula stage embryo death

Included in this table are numbers of embryos that are die at pre-gastrula (from fertilisation inclusive of stage 10) and post gastrula (stage 11 until collection).

* relates to *XKrox20* whole mount *in situ* hybridisations.

" relates to *XAP2* whole mount *in situ* hybridisations.

Construct 1/2	RNA injected (ng)	No. Dead Pre-Gastrula	No. Dead Post-Gastrula	*XKrox20* Analysis	*XAP2* Analysis	*XKrox20*/EphA2"* Analysis	% Phenotype
Experiment 6							
β-globin	3	20	3	3/3 WT	3/3 WT	--	**100 WT**
	0.5	8	6	14/14 WT	9/9 WT	2/4 WT 2/4 Not analysed	**92.3 WT**
Xephrin-A3	3	25	55	3/5 No mig. 2/5 WT	4/8 Aberrant 1/8 WT 3/8 Not analysed	--	**23.1 No mig.** **30.8 Aberrant** **23.1 WT**
	1	34	16	12/15 Aberrant 3/15 Not analysed	4/9 Merged 1/9 WT 4/9 Not analysed	4/4 Aberrant* 4/4 WT"	**14.3 Aberrant** **17.9 WT**
	0.5	11	29	15/25 Aberrant 4/25 WT 6/25 Not analysed	5/8 Merged 2/8 WT 1/8 Not analysed	4/4 Aberrant* 4/4 WT"	**13.5 Merged** **51.3 Aberrant** **27 WT**
ΔXephrin-A3	3	27	26	3/6 No mig. 3/6 Not analysed	--	--	**50 No mig.**
	1	11	17	7/13 Aberrant 6/13 Not analysed	2/3 Aberrant 1/3 WT	1/4 Aberrant* 3/4 Not analysed	**50 Aberrant** **5 WT**
	0.5	23	13	7/8 Aberrant 1/8 Not analysed	3/4 Merged 1/4 WT	1/4 WT*" 3/4 Not analysed	**44 Aberrant** **19 Merged** **12.5 WT**

5.2.2.3 Targeted Blastomere Injections of Full Length and Soluble Xephrin-A3

Since Xephrin-A3 is expressed in both first, third and fourth arch neural crest and the underlying mesoderm of the third branchial arch, it is of interest to discover whether the migration phenotypes of third arch neural crest are due to expression in the neural crest cells themselves or expression in the underlying mesoderm over which they migrate or to both. To address this question, injections using both forms of Xephrin-A3 mRNA were targeted to blastomere cells fated to become neural crest. Fate maps of the 32 cell stage *Xenopus* embryo have been established (Dale and Slack, 1987; Moody *et al.*, 1997). The maps indicate that the A-tier blastomeres, A1 or A2, have a high probability of giving rise to head neural tissue and not to mesoderm. These blastomeres were targeted. The lineage tracer fluorescein dextran was co-injected with the mRNAs to detect correct targeting.

200pg of full length and soluble Xephrin-A3 were each injected into A1 or A2 blastomeres. Then embryos for both sets of injections were analysed by whole mount *in situ* hybridisation with *XKrox20*. Only a few embryos with abnormal phenotypes were obtained and they are similar to phenotypes associated with 1ng-500pg Xephrin-A3 injections in one cell of the two cell stage embryo (Fig. 5.11A-C). Table 9 displays the results from the targeted injections.

5.2.2.4 Observations of Gastrulation

As previously mentioned, some gastrulation defects were observed. These defects, like the third arch neural crest phenotypes, had greater severity in embryos that had been injected with the higher mRNA concentrations of full length and soluble Xephrin-A3. In some injection experiments, especially with the higher injection concentrations, 50% of the injected embryos died at the time of gastrulation and this suggested that Xephrin-A3 was having an effect during gastrulation. For example, stage 10 embryos that overexpress β-globin visually appear normal when compared to non-injected control siblings at gastrulation stages (Fig 5.12A). However, Xephrin-A3 injected embryos at gastrulation stages show lesions on their apical and ventral ectodermal surfaces. The apical lesions initially appear as patches of black discoloration amongst the brown animal pole ectodermal tissue. On the lighter ventral surface the lesions appear as spaces in the ectodermal tissue (Fig 5.12B-D). The lesions expose the sub-ectodermal tissues of the

Figure 5.11

Targeted injections in the 32 cell stage *Xenopus* embryo

Top: A schematic representation of the 32 cell stage *Xenopus* embryo. The two cells injected in these experiments, A1 and A2, are coloured red.

Below: (A)-(E) Variations of third arch neural crest mis-migration shown by *XKrox20 in situ* hybridisation. Ectopically migrating third arch neural crest cells are seen in locations posterior to the normal pathway. The red fluorescein dextran is seen in the anterior head regions, corresponding to A1 and A2 cell injections. (D)-(E) The injected and control sides respectively, of an embryo where the 200pg injection was concentrated on one side of the embryo. The *XKrox20* marked neural crest cells exhibit a retarded migration compared to the uninjected side of the embryo.

red colour-fluorescein dextran, r3-rhombomere 3. r5-rhombomere 5. nc3-third arch neural crest.

Scale bar represents actual size of embryo where 1mm represents 100μm

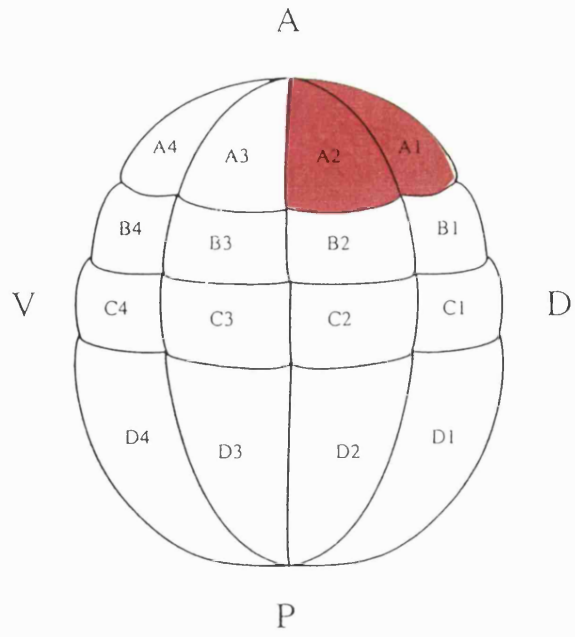
A
A4
A3
A2
A1
B4
B3
B2
B1
V
C4
C3
C2
C1
D
D4
D3
D2
D1
P

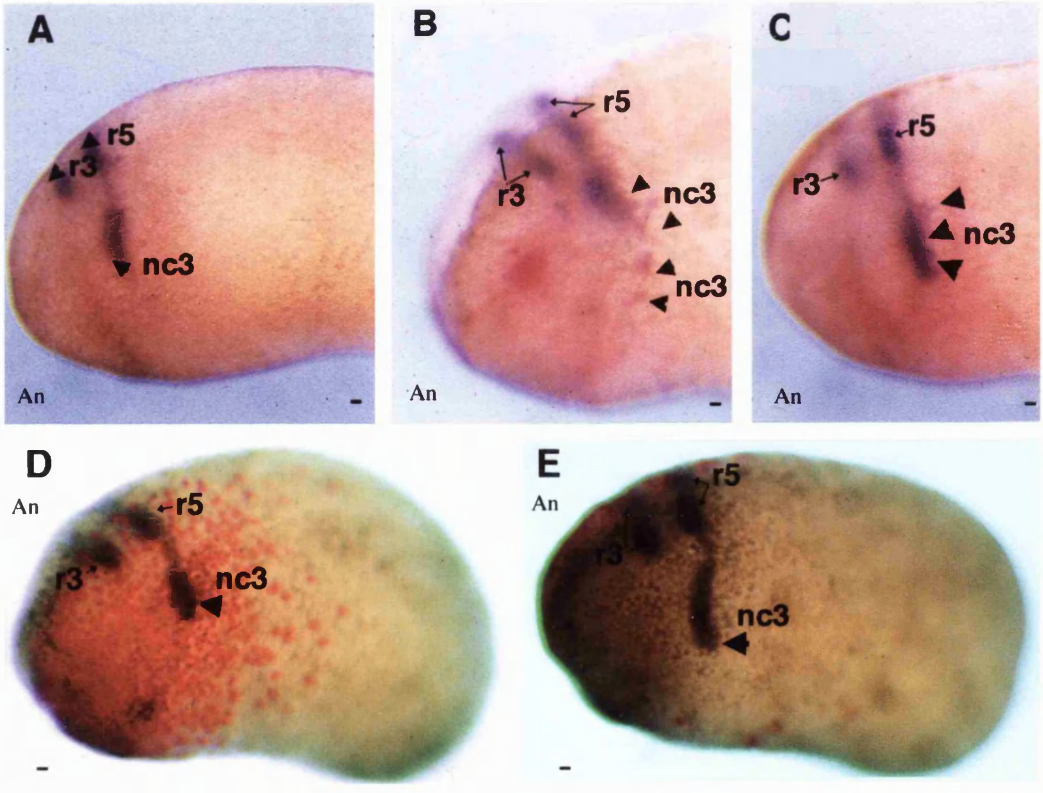
A
r5
r3
nc3
An
B
r5
r3
nc3
nc3
An
C
r5
r3
nc3
An
D
An
r5
r3
nc3
E
An
r5
r3
nc3

Construct 1/32	RNA Injected (ng)	No. Dead Pre-gastrula	No. Dead Post-gastrula	*XKrox20* Analysis	*AP2* Analysis
Experiment 9					
β-globin	0.2	5	6	16/16 WT	16/16 WT
Xephrin-A3	0.2	14	8	21/21 WT	21/21 WT
Xephrin-A3	0.2	21	9	26/26 WT	26/26 WT
Experiment 10					
β-globin	0.2	15	4	23/23 WT	7/14 WT 3/14 Not analysed 4/14 No Mig.
Xephrin-A3	0.2	24	2	5/37 (C2) Delay 32/37 WT	1/20 Delay 19/20 WT
Xephrin-A3	0.2	24	3	7/35 (C2) Delay 28/35 WT	1/17 Delay 16/17 WT
Stage 34					
β-globin	0.2	-	-	3/3 WT	3/3 WT
Xephrin-A3	0.2	-	-	9/9 WT	4/4 WT
Xephrin-A3	0.2	-	-	8/8 WT	5/5 WT

Table 9

Data for the targeted overexpression injections

This table gives the details for the 1 cell in 32 cell stage *Xenopus* embryo injections. Some embryos were allowed to develop to stage 34. Visually these embryos appeared as their uninjected siblings and no phenotypes were observed with whole mount in situ hybridisation with *XKrox20* or *XAP2*.

Xephrin-A3-full length Xephrin-A3; ΔXephrin-A3 - soluble Xephrin-A3.

embryo. The embryos maintain this physical appearance but rarely continue to develop: they turn white and die. Embryos that are not so severely affected do continue to develop but often have posterior neural tube closure defects. At stages 22-23 these embryos are unanalysable.

To examine the effects of Xephrin-A3 injection on mesoderm formation, *Xenopus* embryos were collected at stage 10 at all mRNA injection concentrations and whole mount *in situ* hybridisation with Brachyury (*XBra*) was carried out. This would indicate if the ectodermal lesions elicited changes in expression, strength or presence, of the mesodermal marker (Smith *et al.*, 1991). Control embryos are shown with *XBra* expression present as a ring of expression surrounding the involuting mesoderm (Fig 5.12E). No differences in expression pattern or degree of expression of *XBra* was seen in either embryos injected with full length or soluble Xephrin-A3 (Fig 5.12F). Table 10 summarises data from the *XBra* analyses.

5.3 DISCUSSION

The ectopic expression of full length and soluble Xephrin-A3 in the early *Xenopus* embryo leads to the aberrant migration of third arch neural crest which is RNA concentration-dependent. The data presented suggests that Xephrin-A3 is required to prevent the third arch neural crest mixing with the adjacent fourth arch neural crest. The second arch neural crest is not affected by Xephrin-A3 overexpression.

5.3.1 The Effect of Ectopic Expression of Xephrin-A3 on Neural Crest Cell Migration

The phenotype resulting from ectopic full length Xephrin-A3 expression can be subdivided into three categories: the first which is observed at the highest concentrations (3ng-2ng) of ectopic Xephrin-A3 expression shows that third arch neural crest cells are prevented from migrating ventrally down the *Xenopus* embryo. Sectioning indicated that a few groups of cells did migrate into deeper tissues in the *Xenopus* embryo but generally cells remained at the site of third arch neural crest emanation. Embryos injected with equivalent concentrations of RNA but assessed with *XAP2* showed three phenotypes: first, neural crest cells were present in posterior positions adjacent to the dorsal midline of the embryo, second; the merging of all neural crest cell streams, or third; a merging of

Figure 5.12

Ectodermal lesions in gastrula stage embryos

(A) Control embryos injected with 3ng β-globin. Ectodermal lesions are not present. (B) Animal pole view of a group of gastrula stage embryos injected with 3ng Xephrin-A3 mRNA. Lesions are visible white regions due to the exposure of sub-ectodermal tissues. Black discoloration of some embryo cells is also visible. (C) Four embryos from the (B) group showing the ectodermal lesions and black discoloration. (D) Ventral view of a single embryo of (A) at higher magnification. (E)-(F) Ventral view of control β-globin-injected (E) and Xephrin-A3 injected embryos (F) hybridised with *Xbra* (Smith *et al.*, 1991). No variation in expression pattern or strength between (E) or (F) was seen.

Scale bar represents actual size of embryo where 1mm represents 100μm

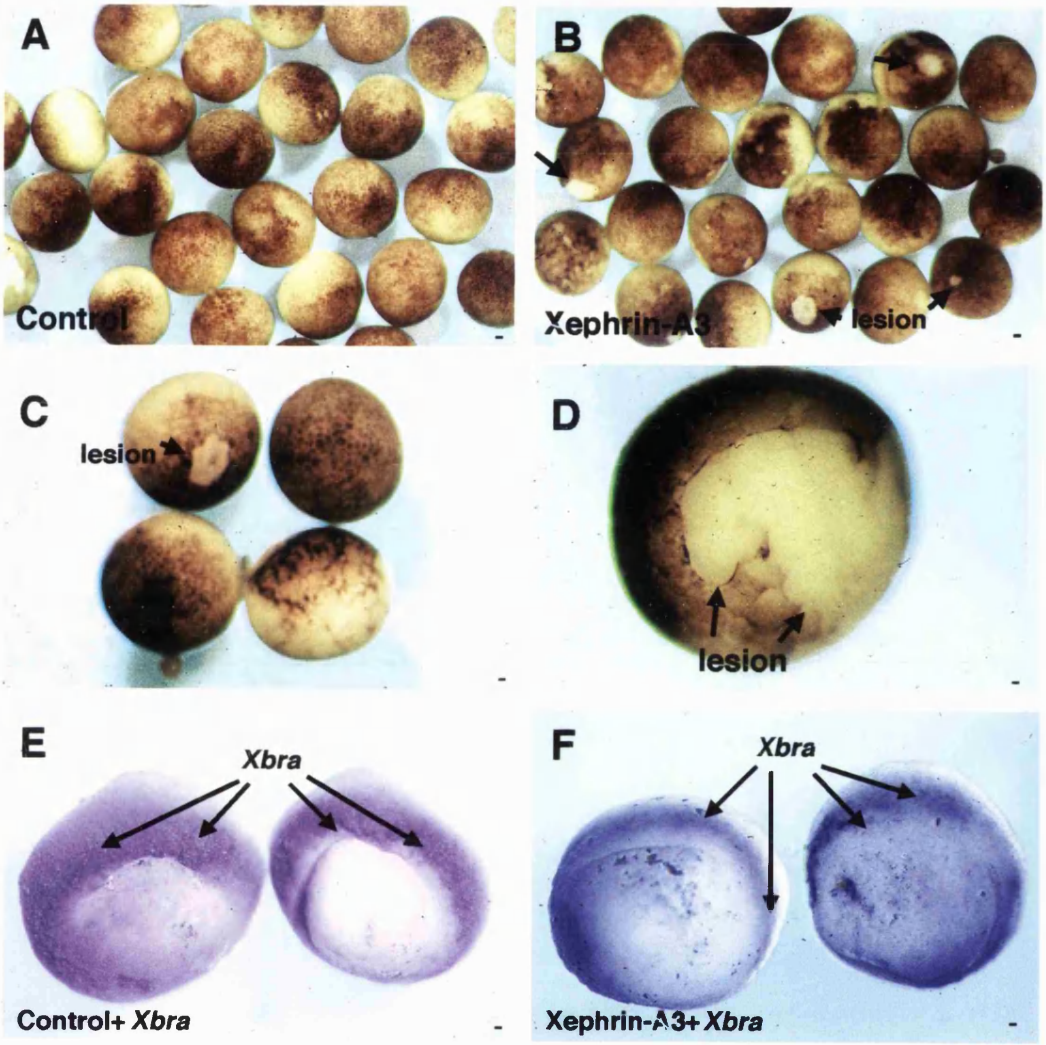
A
Control
B
Xephrin-A3
lesion
C
lesion
D
lesion
E
Xbra
Control+ Xbra
F
Xbra
Xephrin-A3+ Xbra

Construct 1/2	RNA Injected (ng)	*Xbra* Analysis
Experiment 11		
β-globin	3	8/8 WT
	2	12/12 WT
	1	8/8 WT
	0.5	11/11 WT
	0.1	10/10 WT
	3	34/34 WT
	2	28/28 WT
	1	26/26 WT
	0.5	30/30 WT
	0.1	23/23 WT
Experiment 12		
Xephrin-A3	3	25/25 WT
Xephrin-A3	3	24/24 WT
Experiment 13		
Xephrin-A3	3	9/9 WT
Xephrin-A3	3	12/12 WT

Table 10

***Xbra* expression in stage 10 embryos ectopically expressing full length and soluble Xephrin-A3**

This table provides the data for three experiments to assess any differences between the expression of Brachyury (*Xbra*) in full length Xephrin-A3 or soluble Xephrin-A3 injected embryos. As the table shows, no variations could be seen.

Xephrin-A3-full length Xephrin-A3; ΔXephrin-A3 - soluble Xephrin-A3.

the third and fourth arch crest streams only, with a delay in their migration relative to the migration on the uninjected control side of the embryo.

The second observation was the migration of some third arch neural crest cells in a direction more caudal than wildtype. This took place when the concentration of injected Xephrin-A3 RNA was lowered (2ng-1ng). In these embryos, third arch neural crest cells lie in abnormal positions across and posterior to the fourth arch crest region. The further dilution of Xephrin-A3 injected RNA (0.5ng-0.1ng) showed that neural crest migration was similar on the injected and non-injected sides of the embryo. However, a few groups of caudally located *XKrox20* expressing cells were observed branching out from the main body of the migrating third arch neural crest stream.

The ectopic expression of decreasing concentrations of soluble Xephrin-A3 produced the same phenotypes as embryos injected with full length Xephrin-A3 expression. However, fewer numbers of these phenotypes were observed.

5.3.2 The Role Of Overlapping and Complementary Expression in Xephrin-A3 Function

Eph receptors and ephrins are expressed in complementary and overlapping expression patterns (Flenniken *et al.,* 1996; Gale *et al.,* 1996). Xephrin-A3 expression is both overlapping and complementary to interacting EphA receptors in the neural crest. During their initial migration, Xephrin-A3 expression is equal in the first, third and fourth arch neural crest streams. At this time, expression studies indicate that overlapping expression exists between Xephrin-A3 and EphA4 in the third arch neural crest and mesoderm of the third arch (Xu *et al.,* 1995). As migration proceeds however, Xephrin-A3 expression in the fourth arch neural crest is upregulated such that there is complementarity between EphA4 and elevated Xephrin-A3.

This finding raises questions as to whether the third arch neural crest cell disruptions found relate to a normal role of overlapping expression, complementary elevated expression, or both. These possibilities are discussed below.

5.3.2.1 The Role of Overlapping Expression in the Eph Family

In previous studies where it has been shown that ephrin and Eph receptor expression is overlapping, there is a role in adhesion has been shown (Pandey *et al.,* 1995c). Further

examples of this finding were shown in *in vitro* experiments, where increased cell adhesion occurred in cell mixing experiments between ephrin and Eph receptor expressing cells (Bohme *et al.,* 1996; Holash *et al.,* 1997). In 1998, Stein and co-workers showed that ephrin-B1 promoted the capillary-like assembly of renal endothelial cells *in vitro* (Stein *et al.,* 1998). In this work, they found that stimulating endothelial-derived and teratocarcinoma-derived cell lines with ephrin-B1 dimers and multimers (tetramers) each caused the phosphorylation of EphB1 and EphB2 receptors (Stein *et al.,* 1998). The higher order multimerisation of EphB1 and EphB2 led to with the recruitment of LMW-PTP (low molecular weight phosphotyrosine phosphatase protein) to the receptor complexes. The mechanistic role of LMW-PTP with Eph signalling has not been defined, but multimer formation led to increased cell attachment between receptor and ligand expressing cells.

Examples of overlapping expression are also present in the retinotectal system where the uniform expression of EphA4 and EphA5 in the retina (Connor et al., 1998; Monschau et al., 1997) overlaps with ephrin-A5 and ephrin-A2 which are expressed in a decreasing gradient from nasal to temporal retina (Brennan et al., 1997; Hornberger et al., 1999; Marcus et al., 1996). Hornberger *et al* (1999) showed by the stripe assay that the ectopic expression of ephrin-A ligands in temporal axons disrupts the normal repulsion of these axons. Usually restricted to the anterior tectal tissue (containing low ephrin levels), the temporal axons aberrantly migrated on posterior tectal tissue (high ephrin levels) (Hornberger *et al.,* 1999). Conversely, the removal of ephrin-A ligands from nasal axons which usually can migrate on posterior tectal tissue, allowed these axons to exhibit striped outgrowth on anterior tectal tissue, indicating an increased sensitivity to repulsive cues from the posterior tectum.

This change in migration behaviour by these axons is thought to involve the persistent activation of EphA receptors. Normally, Eph receptors within the nasal axon are activated by overlapping ephrins also expressed within the same axon. This overlapping expression causes the persistent activation of the EphA receptors and a desensitisation of the repulsion response. The removal of these ephrins prevents persistent activation occurring, so when the nasal axon migrates over the extrinsic ephrins located on the posterior tectum, a repulsive response is elicited in the nasal axon (Hornberger *et al.,* 1999; Wilkinson, 1999). In the temporal axons, the concentration of ephrins are lower

compared to those in the nasal axons. Therefore, the extent of migration of the temporal axons is restricted by extrinsic ephrins in the posterior tectum. However, when ephrin-A ligands are ectopically expressed in the temporal axons, EphA receptors within the axon are persistently activated. This causes a desensitisation of the EphA receptors, similar to the normal situation in the nasal axon, causing repulsion cues from extrinsic ligands to have a reduced effect. This allows the temporal axon to aberrantly migrate on posterior tectal tissue (Hornberger *et al.*, 1999).

These findings can be applied to the neural crest migration phenotypes I observe. High concentrations of ectopic Xephrin-A3 expression activates endogenous Eph-A receptors, causing persistent activation of these receptors. In the severest phenotypes I observe, where migration of the third arch neural crest cells appears to cease, it is thought that the persistent activation of EphA receptors may cause a desensitisation of these receptors, leading to increased cell-cell adhesion. As the concentration of ectopically expressed Xephrin-A3 is lowered, the degree of receptor desensitisation falls and the migration phenotypes exhibited by the third arch neural crest cell stream are less severe.

5.3.2.2 The Potential Role of Xephrin-A3 Expression in the First Arch Neural Crest Cells

Overlapping expression of Xephrin-A3 with EphA receptors may also play a role in the migration of the first arch neural crest. Embryos ectopically expressing high concentrations of Xephrin-A3 and analysed with the *XAP2* marker, exhibit a merging of all the neural crest cell streams, suggesting the aberrant migration of first arch neural crest. Expression analysis of Xephrin-A3 (see Chapter 4) indicates the ephrin is also expressed in the first arch neural crest. Murine EphA3 and EphA7 are expressed in this neural crest stream (Becker *et al.*, 1994; Ellis *et al.*, 1995), and therefore it is possible that *Xenopus* EphA receptors may also be expressed in this tissue. If this situation does occur, then the overlapping expression of Xephrin-A3 in the first arch neural crest may contribute to the migration of this tissue. This however, cannot be confirmed due the absence of a first arch neural crest cell marker in *Xenopus*. In addition, no *Xenopus* EphA receptors are reported to be expressed in this tissue.

The possibility also exists that complementary expression of Xephrin-A3 with EphA receptors plays a role in the migration of the first, third and fourth arch neural crest. This is discussed below.

5.3.2.3 The Role of Complementary Expression in the Eph Family

In embryos analysed by detection of *XAP2* expression after the ectopic expression of 3ng of Xephrin-A3, neural crest cells were observed positioned adjacent to the dorsal midline, migrating more posteriorly than the control side of the embryo. This observation suggested a loss of repulsion which normally restricts migration of these cells. It is not certain from which neural crest stream these caudally-located cells originate, but it is possible that both third and fourth arch neural crest cells migrate aberrantly. The aberrant migration of fourth arch neural crest cannot be confirmed, since there is no marker for this crest stream.

A similar migration phenotype was observed after blocking the action of EphA4 and EphB1 receptors. Smith *et al* (1997), found that the expression of truncated EphA4 and EphB1 caused the ectopic localisation of third arch neural crest (Smith *et al.,* 1997). These observations were believed to result from the inability of neural crest cells to perceive a guidance cue: either a positive cue expressed along the third arch pathway or a negative cue that prevents neural crest cell migration into adjacent pathways.

In some of the severe phenotypes I observed with the *XAP2* marker, all the neural crest cell streams merge. Analysis with *XKrox20* and EphA2 shows that third arch neural crest cells move to aberrant caudal positions and that the second arch neural crest cells are unaffected. These observations would account for the merging of the third and fourth arch neural crest cell streams. The apparent merging of the first and second neural crest cell stream suggests the aberrant caudal migration of first arch neural crest cells; the merging of the second and third arch neural crest cells would indicate a spreading of the third arch neural crest stream towards the second arch neural crest cell stream without entering second arch territory. Therefore, it is possible that neural crest cells originating from the first, third and fourth arches may migrate aberrantly causing the phenotype observed. Without the appropriate markers, it is not possible to know how the migration of the first and fourth arch neural crest cells is affected in this phenotype.

However, the majority of embryos exhibited a phenotype where a merging of only the third and fourth arch neural crest cell streams occurs. Xephrin-A3 is upregulated in fourth arch neural crest cells. This complementary expression with EphA4 may serve a role in third and fourth arch neural crest cell stream segregation.

A clue as to why the merging occurs emerges from work by Mellitzer *et al* (1999). It was found that when cells expressing full length EphB2 (or EphA4) receptor were juxtaposed with cells expressing full length ephrin-B2, there is a restriction of the intermingling between these cell populations. In this situation, bi-directional signalling between receptor and ligand expressing cells takes place. In contrast, unidirectional EphB/ephrin-B signalling between juxtaposed zebrafish animal caps, allows the migration of cells into adjacent territories. This finding is explained by a model in which cells that express full length Eph receptor or ephrin are repelled from those expressing a ligand (truncated ephrin or Eph receptor, respectively). However, the cells expressing truncated Eph receptor or ephrin are not repelled since they cannot receive the signal. In the context of Xephrin-A3 overexpression, when EphA4 is desensitised, third arch neural crest cells no longer perceive a repulsion signal and therefore invade fourth arch territory, causing these neural crest streams to merge.

Additional investigations by Xu *et al* (1999) revealed a role for the Eph family in preventing inappropriate intermingling between cell populations. In order to assess a possible role for EphA4 and EphB receptors in cell sorting, ephrin-B2, an interacting ligand, was expressed mosaically in one cell of the 8 cell stage zebrafish embryo (Xu *et al.,* 1999). Ephrin-B2 expressing cells aligned together at the boundaries of rhombomeres 3 and 5 (that express EphA4 and EphB2), and did not intermingle with other cells. A similar cell sorting occurs after the mosaic expression of truncated ephrin-B2. Additionally, the mosaic expression of truncated EphA4, leads to cell sorting in rhombomeres 2, 4 and 6 (that express ephrin-B proteins), indicating that the activation of ephrin-B ligands may cause a similar response to Eph receptor activation. It is believed that this cell sorting involves a repulsion or de-adhesion between adjacent cells.

5.3.3 The Effects of Lower Ectopic Xephrin-A3 Expression

As the ectopic expression of Xephrin-A3 is lowered further, the phenotypes exhibited by *XKrox20* and *XAP2* expressing cells are less severe. This is likely to be due to a

decreased persistent activation of Xephrin-A3 interacting receptors. *XKrox20* expressing cells are positioned in fourth arch neural crest cell territory and the third and fourth arch neural crest streams are merged. This suggests that repulsion cues elicited by ephrins in fourth arch neural crest/mesoderm are still subdued allowing mis-migration of third arch neural crest cells.

When the ectopic expression of Xephrin-A3 was lowered further migration of the third arch neural crest was barely affected. A few groups of cells were ectopically caudally located. Therefore in this situation, repulsive cues provided by complementary expressed Eph receptors may be only slightly compromised by persistent receptor activation.

5.3.4 Soluble Xephrin-A3 Ectopic Expression

Previously it had been shown that the soluble form of an ephrin does not induce phosphorylation of its interacting receptor(s) (Davis *et al.*, 1994; Stein *et al.*, 1998). The ectopic expression of soluble Xephrin-A3 was predicted to serve as a blocking reagent which could produce the following effects: first, to block repulsion by complementary Eph/ephrin expression and therefore allow mixing between adjacent streams of neural crest cells and second, to block Eph receptor activation due to overlapping expression with Xephrin-A3, which may cause loss of adhesion (if normal overlapping expression between Eph receptors and ephrins leads to increased adhesion).

These predictions fit with the phenotypes exhibited by the expression of low concentrations of ectopic Xephrin-A3 leading to a blocking of repulsion. Unexpectedly, there an arrest of migration after overexpression of high concentrations of soluble Xephrin-A3. One explanation might come from studies involving the ECM (extracellular cell matrix). It is already known that the ECM and mesoderm are important for the migration of neural crest cells. This was shown when the injection of antibodies against fibronectin and laminin caused a build-up of neural crest cells within the lumen of the avian neural tube (Bronner-Fraser, 1986).

Evidence provided by (Miao *et al.*, 2000) show links between Eph receptors and the ECM (Miao *et al.*, 2000). This research shows that activated Eph receptors induce an inactive conformation of integrins that inhibits integrin-mediated adhesion in PE-3 cells (prostate epithelial cells). Integrins are the primary receptors for ECM molecules. On

binding ECM ligands, integrins initiate multiple intracellular signalling pathways. When EphA2 is activated, this suppresses integrin function and induces FAK (focal adhesion kinase) de-phosphorylation and inactivation. FAK inactivation causes focal adhesion disassembly, resulting in the loss of PC-3 cell adhesion, spreading and migration on a fibronectin substratum. Therefore it is possible that in the context of soluble Xephrin-A3 overexpression, the ligand blocks activation of EphA receptors. This would prevent the suppression of integrin function and the uncoupling of focal adhesion complexes, and therefore contribute to the increased arrested migration phenotype observed here. It is believed that only when the appropriate balance of repulsion and adhesion is restored, as less EphA receptors are blocked with decreasing ectopic Xephrin-A3 overexpression, will correct migration of the third arch neural crest cells resume.

5.3.5 Gastrulation Defects

5.3.5.1 Xephrin-A3 Ectopic Expression

In the experiments where one cell at the two-cell stage *Xenopus* embryo was injected with full length or soluble Xephrin-A3, it was noted that many embryos died before or during gastrulation. These phenotypes were typified by ectodermal lesions on the embryo surface which revealed sub-ectodermal tissue layers.

Northern Blot analyses have shown that the EphA receptors EphA4 and EphA2, are expressed maternally in the *Xenopus* oocyte and blastula stages (Winning *et al.,* 1994; Helbing *et al.,* 1999). Therefore, the ectopic expression of Xephrin-A3 might activate interacting receptors causing receptor activation, leading to de-adhesion of ectodermal cells. The apparent loss of adhesion in epidermal gastrula cells has been observed in previous work where an activated form of EGFR-XEphA4 was injected into *Xenopus* embryos (Winning *et al.,* 1996). There was a kinase-dependent dissociation of embryonic tissue believed to be a result of interference with the adhesive properties of the cells. Additionally, it was shown that the ectopic expression of *Xenopus* ephrin-B1 causes disaggregation of blastomeres (Jones *et al.,* 1998).

It is likely that some loss of adhesion will interfere with the process of gastrulation but it is difficult to deduce whether this reflects a normal role of Xephrin-A3. Indeed, the effects observed may not indicate a normal role for Xephrin-A3 in gastrulation; rather, ectopic activation of Eph receptors may lead to loss of adhesion which interferes with

gastrulation. However, since Xephrin-A3 is expressed in the Xenopus oocyte and early blastula stages as indicated in Chapter 4, a role during gastrulation cannot be ruled out. Interestingly, observations in the zebrafish embryo implicate a requirement for Eph-ephrin interactions in the cellular movements of convergence during gastrulation (Oates *et al.*, 1999).

5.3.5.2 Targeted Injections of Xephrin-A3

At the 32-cell stage, RNA encoding full length or soluble Xephrin-A3 was microinjected together with fluorescein dextran, a lineage tracer enabling the location of injected Xephrin-A3 to be visualised, into the A1 and A2 blastomeres of *Xenopus* embryos. These blastomeres are fated to become brain tissue, including neural crest (Dale and Slack, 1987). The phenotypes arising from these injections indicated a less extensive migration of the third arch neural crest cells with respect to the normal migration of these cells non-injected sibling embryos. These phenotypes were very similar to the phenotypes exhibited when one cell of the two cell stage *Xenopus* embryo was injected with lower amounts of Xephrin-A3 RNA.

The less severe migration phenotypes observed might be attributed partly to the loss of overexpression in the branchial arch mesoderm. Expression in the mesoderm could affect the migration of neural crest cells as they migrate through mesoderm, by Xephrin-A3 acting as a repellent or desensitising EphA receptors by persistent activation. It remains possible that alterations to the organisation or properties of the branchial arch mesoderm might also be involved. However, there are no good markers at present to investigate this.

5.3.5.3 Fate change of Injected Blastomeres

The possibility exists that the fate of injected blastomeres changes on ectopic expression of Xephrin-A3. Xu *et al* (1999) and unpublished work (Xu and Wilkinson) has shown that ephrin expression in zebrafish embryos affects patterns of cell intermingling, but does not alter the identity of cells. As previously noted, this was shown when ephrin-B2 was mosaically expressed in the zebrafish embryo, cell sorting was observed. However, ephrins expressed ubiquitously, showed no loss or gain of any specific tissue - only a disruption to cell organisation. So far, no one has found a role for Eph receptors in

controlling cell type in any system - the principal roles seem to be in controlling cell movements.

5.3.6 Similarity of Full Length and Soluble Xephrin-A3 Overexpression Phenotypes

The similarity of the phenotypes observed after ectopic expression of full length and soluble forms of Xephrin-A3 is not unique. It has previously been observed that similar phenotypes may be produced after the overexpression of both activating and blocking Eph reagents both *in vitro* (Krull *et al.,* 1997) and *in vivo* (Krull *et al.,* 1997; Smith *et al.,* 1997; Xu *et al.,* 1999). For example, trunk neural crest entering the caudal half of somites (Krull *et al.,* 1997), third arch neural crest cells entering second arch territory (Smith *et al.,* 1997) and the disruption of hindbrain patterning (Xu *et al.,* 1999). These results can be explained as ephrins acting as repulsive cues at boundaries such that Eph receptor-expressing cells will enter ephrin-expressing territory if Eph receptor is blocked (soluble ephrin) or non-directionally activated (membrane-bound ephrin). In addition, the persistent activation of Eph receptor due to overlapping expression with membrane-bound ephrin has recently been shown to desensitise repulsion, so that the cells enter adjacent ephrin-expressing territory (Hornberger *et al.,* 1999).

5.3.7 Comparing and Contrasting the Effect of Dominant-Negative EphA Receptors in *Xenopus* Neural Crest Migration with Xephrin-A3

The action of soluble Eph receptors on the migration of *Xenopus* neural crest has previously been investigated. Smith *et al* (1997), found that the overexpression of dominant negative EphA4 led to the mis-migration of the third arch neural crest cell stream into adjacent second and fourth arch territory (Smith *et al.,* 1997). This phenotype was reproduced when the same group ectopically expressed ephrin-B2, a ligand for EphA4. A second study by Helbing *et al* (1999), expressed truncated EphA2, a receptor expressed in rhombomere 4 and second arch neural crest. *XKrox20* analysis indicated the aberrant migration of the third arch neural crest cell stream. Similarly to my results, the third arch neural crest cells entered fourth arch territory only. Additional analysis with *XAP2* indicated the merging of the third and fourth arch neural crest cell streams (Helbing *et al.,* 1999).

From the observations of Smith *et al* (1997), it is believed that ephrinB2/EphB1 + EphA4 interactions may restrict the migration of second and third arch neural crest cell streams. Therefore blocking EphA4 or EphA2 with Xephrin-A3 will not cause mixing between these neural crest cell streams since the ephrin-B2/EphB1 interactions are still present. It appears that ephrin-A/EphA receptor interactions may provide the main mechanism for maintaining the third and fourth arch neural crest cell boundary. This is supported by my findings and those of Helbing *et al* (1999), where the ectopic expression of truncated EphA2 causes the mismigration of third arch neural crest cells into fourth arch territory but not into second arch territory.

CHAPTER SIX

The mechanisms employed by some species to control the segregation and pathfinding of neural crest cells have been shown to involve members of the Eph family (Krull *et al.*, 1997; Smith *et al.*, 1997; Helbing *et al.*, 1998; Wang and Anderson 1997). This thesis has described the cloning and functional analysis of *Xenopus* ephrin-A3, an Eph ligand. My findings suggest that Xephrin-A3 contributes to the correct migration of the *Xenopus* third arch neural crest stream.

6.1 Neural Crest Cell Migration

6.1.1 Generating Neural Crest Free Zones

Branchial neural crest migrates in segmental streams (Lumsden *et al.*, 1991), and several mechanisms have been associated with the formation of these streams: the presence of areas of neural crest free mesenchyme that separate individual neural crest streams (Anderson and Meier, 1981; Tan, 1985); the selective apoptosis of neural crest cells from rhombomeres 3 and 5 (Lumsden *et al.*, 1991) and neural crest cell guidance cues. The expression of the signalling molecule BMP4 in rhombomeres 3 and 5, which mediates the upregulation of msx2, was shown to be involved in the elimination of neural crest cells from these rhombomeres (Graham *et al.*, 1993; Graham *et al.*, 1994). In addition guidance mechanisms are used to prevent neural crest streams intermingling, since tracer injections identified some neural crest cells which originated from rhombomeres 3 and 5, and migrated along rostral and caudal routes to join cells arising from adjacent even-numbered rhombomeres (Kontges *et al.*, 1996; Lumsden *et al.*, 1991; Lee *et al.*, 1995; Birgbauer *et al.*, 1995; Sechrist *et al.*, 1993). Selective apoptosis and guidance mechanisms are thought to contribute to the formation of neural crest free zones.

6.1.2 Neural Crest Cell Guidance

The guidance of neural crest cells are thought to fall into three main categories: diffusible long range guidance cues which involve either attraction or repulsion between neural crest cells (Nieto, 1995; Sechrist, 1994; Lee *et al.*, 1995); short-range or contact-mediated attractive or repulsive cues involving laminin and fibronectin (Krotoski *et al.*,

1986; Bronner-Fraser, 1986); and finally, interactions between neural crest cells that co-ordinate their migration (Krull, 1995; Ring *et al.,* 1996; Debby-Brafman *et al.,* 1999).

Of these guidance categories, it is possible that the long and short range cues may arise from mesodermal ectoderm. The third category, the interactions between neural crest cells, has been especially important in understanding the migration of trunk neural crest. It has been shown that cues inherent in the somite impose this segmental pattern of neural crest migration (Bronner-Fraser and Stern, 1991). These cues include inhibitory molecules present in the caudal sclerotome which have been shown to inhibit trunk neural crest migration: a peanut lectin binding glycoprotein (PNA), collagen IX and F-spondin (Debby-Brafman *et al.,* 1999; Krull, 1995; Ring *et al.,* 1996).

In *Xenopus* embryos, the second, third and fourth arch neural crest cells migrate in contact with each other but during migration the third arch crest segregates into two, creating the third and fourth arch neural crest streams. Physical barriers between the migrating streams of crest only arise when the cells are permanently separated by the branchial clefts (Sadaghiani and Thiebaud, 1987). This is different from the situation in the chick or mouse, and raises the question as to whether different mechanisms are used to restrict mixing between adjacent streams compared with the formation of neural crest free zones.

6.1.3 The Role of the Eph Family

Several receptors and ligands of the Eph family are expressed in pre-migratory and migratory neural crest (Becker *et al.,* 1994; Cheng and Flanagan, 1994; Nieto *et al.,* 1992; Bergemann *et al.,* 1995; Flenniken *et al.,* 1996; Winning and Sargent, 1994; Xu *et al.,* 1995; Jones *et al.,* 1995; Scales *et al.,* 1995; Smith *et al.,* 1997; Helbling *et al.,* 1998). In *Xenopus*, previous studies have shown that EphA and EphB receptors in the cranial neural crest are involved in maintaining the cohesive, segmented, migration of the third arch neural crest cell streams (Smith *et al.,* 1997; Helbing *et al.,* 1998). Trunk neural crest, like cranial neural crest, migrates in a segmental manner and moves through the rostral half of each somitic sclerotome. Other members of the Eph family have been shown to regulate axon guidance and neural crest migration in the trunk (Wang and Anderson, 1997; Krull *et al.,* 1997).

Therefore, multiple guidance cues, incorporating those provided by members of the Eph family, contribute to the correct migration of neural crest. The Eph family are thought to mediate these cues by repulsion and adhesion interactions created between Eph receptor-expressing and ephrin-expressing cells (see below).

6.2 General Roles of Eph Receptors and Ephrins

Many studies of the developmental function of EphA receptors and ephrins implicate a role in cell repulsion, for example in the collapse of axonal growth cones (Meima *et al.,* 1997a; Meima *et al.,* 1997b). In addition, the autoactivation of EphA4 in *Xenopus* embryos caused the dissociation of cells, suggesting a possible role in the down-regulation of adhesion, independent of cytoskeletal interactions (Winning *et al.,* 1996). In contrast, the activation of Eph receptors can also promote cell adhesion in endothelial cells, myeloid cells and retinal cells (Stein *et al.,* 1998; Bohme *et al.,* 1996; Holash *et al.,* 1997).

The reason for either adhesive or repulsive responses from activated Eph receptors may be due to different cell types responding in different ways to the same extracellular signals. This may occur by Eph receptors using different intracellular pathways, or, by enabling higher-order Eph receptor clustering which is required to trigger cell adhesion (Stein *et al.,* 1998).

A model, based on retinal growth cones predicted by Rosentreter *et al* (1998), suggests that only if the activation of an Eph receptor exceeds a certain threshold, will repulsion occur (Rosentreter *et al.,* 1998). By its nature, a repulsion response allows only transient receptor activation and cell contact, preventing the establishment of high-order receptor multimers. If, however, the activation of an Eph receptor is below the repulsion threshold level, cell-cell contact is prolonged. This enables the formation of higher-order receptor multimers, which may promote cell adhesion.

In the functional analysis of Xephrin-A3, the ectopic expression of the ephrin causes a retardation in the migration of third arch neural crest. Therefore, increasing the activation levels of EphA receptors alters the response of the receptor, possibly by changing the signalling pathways the receptor utilises. This response may be aligned to Rosentreter's model, but when applied to the migration of cranial neural crest, the higher-order

receptor multimers can be substituted with persistent activation of receptors (Rosentreter *et al.,* 1998).

Eph receptors and ephrins are expressed in overlapping and complementary domains. Overlapping expression has been shown to promote increased cell adhesion (Bohme *et al.,* 1996; Holash *et al.,* 1997), cell migration (Pandey *et al.,* 1995c) and remodelling of cellular organisation (Stein *et al.,* 1998; Wang *et al.,* 1998). However, complementary expression between ephrins and Eph receptors has been shown to provide repulsive responses. For example, the targeting of retinal axons in the retinotectal system (Cheng *et al.,* 1995; Drescher *et al.,* 1995), the guidance of trunk neural crest cells by repulsion (Krull *et al.,* 1997; Wang and Anderson, 1997), the restriction of cell mixing in the rhombomeres of the hindbrain (Xu *et al.,* 1995) and the migration of branchial neural crest cells in the hindbrain (Smith *et al.,* 1997). Analogous processes of local adhesion and de-adhesion of endothelial cells may also underlie the remodelling of blood vessels and sprouting during angiogenesis (Gale and Yancopoulos, 1999).

Xephrin-A3 has both overlapping and complementary expression with interacting EphA receptors. Functional experiments with Xephrin-A3 has indicated that altering this situation disrupts the correct migration of third arch neural crest cells. These observations support a role of overlapping and complementary expression plays, perhaps by adhesion and repulsion effects, in the migration of cranial neural crest cells. A summary figure, Fig. 6.1, shows the Eph receptors and ephrins that are known to be expressed in *Xenopus* branchial neural crest. The likely overlapping and complementary interactions between individual members are indicated.

6.3 Xephrin-A3 Expression Patterns

Ephrin-A3 has been cloned in both the human and rat (Davis *et al.,* 1994). The spatial expression of these ephrin-A3 has not been reported therefore, it is not possible to comment directly on a conserved function between species. However, in *Xenopus*, in addition to the first, third and fourth arch neural crest, Xephrin-A3 is notably expressed in the branchial mesoderm of the third arch, the pronephros, along the midline and at the blastopore. The potential role of this expression is summarised below.

Xephrin-A3 expression in the presumptive third arch mesoderm may provide a pre-formed pathway to ensure the correct migration of the third arch neural crest stream. This

Figure 6.1

Eph family overlapping and complementary interactions in *Xenopus* branchial neural crest

This summary diagram shows the overlapping and complementary expression patterns of members of the Eph family in *Xenopus* branchial neural crest.

The small arrows indicate complementary expression between Eph receptors and ephrins. For example, late Xephrin-A3 expression in the fourth arch neural crest (purple arrow) has complementary expression with EphA4 (turquoise arrow). Overlapping expression is indicated by a double-headed arrow, therefore, early Xephrin-A3 expression in the third arch neural crest (pink arrow-head) has overlapping expression with EphA4 (turquoise arrow-head).

This model shows that Xephrin-A3 is expressed in complementary and overlapping patterns with EphA4, and has complementary expression with EphA2. These interactions are believed to play a role in the correct targeting of third arch neural crest migration.

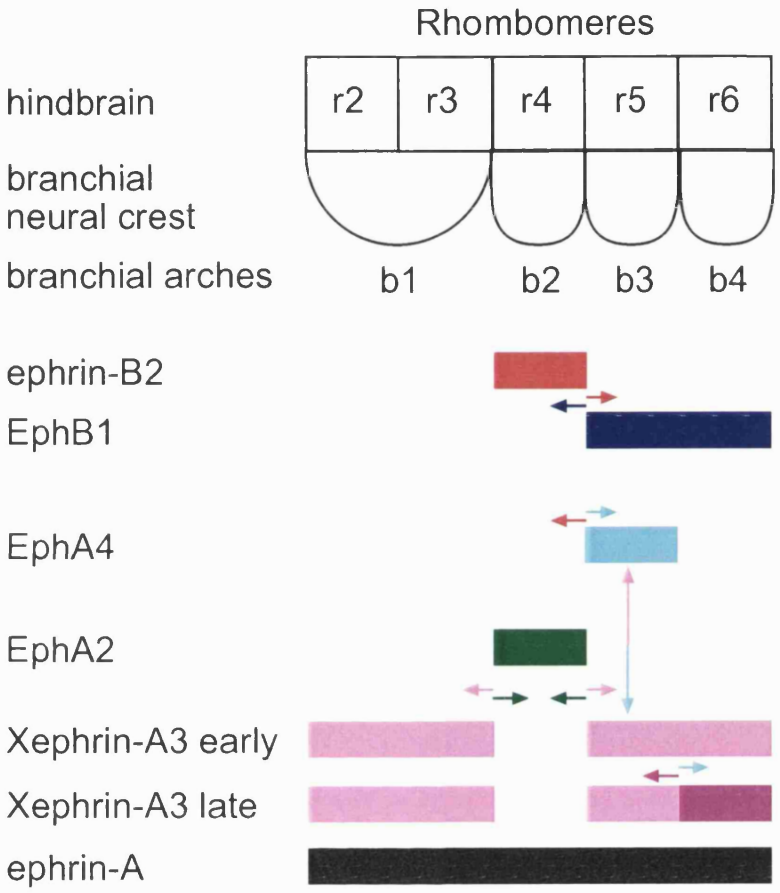
Rhombomeres
hindbrain
r2
r3
r4
r5
r6
branchial
neural crest
branchial arches
b1
b2
b3
b4
ephrin-B2
EphB1
EphA4
EphA2
Xephrin-A3 early
Xephrin-A3 late
ephrin-A

may be due to overlapping expression with EphA4, which may provide adhesive cues. Xephrin-A3 expression may also prevent the mixing of third and fourth arch neural crest cells by complementary expression with as yet undiscovered Eph family members in the fourth arch mesoderm. It has been shown that targeted injections of soluble and full length Xephrin-A3 into A-tier blastomeres of the 32-cell stage *Xenopus* embryo produce delayed migration, and some ectopic migration, of third arch neural crest cells. These are equivalent to phenotypes observed in embryos overexpressing medium/low levels of full length and soluble Xephrin-A3 where *Xenopus* embryos were injected at into one cell at the two cell stage. Therefore, a role for Xephrin-A3 mesoderm expression cannot be ruled out but cannot be confirmed.

The expression of ephrins other than Xephrin-A3 in the pronephros has not been reported, but the *Xenopus* EphA receptor, XEphA4 is expressed in this tissue (Xu *et al.*, 1995). However, a role for this expression has not been elucidated. It is suggested that the *Xenopus* pronephric duct (PD) is constructed in part by migration of PD cells using adhesion gradients (Cornish *et al.*, 1993). From evidence for the role of the Eph family in cell adhesion and in cell migration, it could be possible that the Eph family has a role in the migration of PD cells.

Previous expression analysis has indicated ephrin-A ligands expression along the midline (Cheng *et al.*, 1995). However, the identity of those ephrins are not known since the technique used for this visualisation, utilised IgG-Fc receptors which indicate regions of interacting ligand expression. The reason for the expression of Xephrin-A3 along the midline and at the blastopore is not known.

6.4 General Summary

Based on collective expression in all tissues and function studies, the Eph family may not have tissue-specific functions, but rather act in all tissues. Specific family members may act in a specific tissue, but in other cases different family members can function in a particular tissue in different species. What is emerging is that the Eph family work as key regulators of the repulsion and adhesion between cells: controlling cell and axon movement by acting as repellents and promoting adhesion in some contexts (Wilkinson, 2000). These are crucial properties required in the establishment and maintenance of patterns of cellular organisation.

The cloning of Xephrin-A3 has identified a new *Xenopus* ephrin. Expression and functional experiments indicate Xephrin-A3, with other EphA receptor and ephrin-A interactions, contributes to the controlled migration of third arch neural crest cells. Based on my findings and the emerging properties of complementary and overlapping Eph receptor and ephrin expression, Xephrin-A3 is believed to provide repulsive and adhesive cues that contribute to targeted neural crest cell migration.

6.5 Future Directions

There are several approaches which can be followed to further investigate the role of Xephrin-A3 in *Xenopus* cranial neural crest migration.

The first approach would be to identify other Eph receptors or ephrins that are expressed in the branchial neural crest. The expression profiles can be used to determine further incidence of overlapping and complementary expression and therefore investigate the influence of Eph family expression in neural crest migration. This work may uncover Xephrin-A3 interacting receptors present in the fourth arch mesoderm, the first arch neural crest and/or the first arch mesoderm. The isolation of these proteins and their ectopic expression could further define the role of Xephrin-A3, and of overlapping and complementary expression of Eph receptors and ephrins, in the neural crest.

Functional analysis indicates that Xephrin-A3 has a concentration dependent effect on third arch neural crest migration. Stripe assays can be used to assess this finding *in vitro*, by allowing neural crest cells, which can be easily and cleanly isolated from chick or *Xenopus* embryos, to migrate over stripes of varying concentrations of full length or soluble Xephrin-A3. This assay would confirm both the concentration dependent migrational defects and assess how similar the effects of full length and soluble Xephrin-A3 expression has on neural crest migration. An adaptation to this assay could utilise time lapse analysis. If a repulsion or indeed adhesive mechanism is being utilised by neural crest in contact with Xephrin-A3, the filopodia of the migrating neural crest cells may be seen to retract or adhere, confirming or disclaiming the roles of repulsion versus adhesion during complementary or overlapping Eph receptor or ephrin expression, respectively.

Recently, the interaction between EphA receptors and components of adhesion signalling pathways, has been highlighted (Miao *et al.,* 2000). Further analysis of the role of cell adhesion molecules and cell adhesion assays should be performed. Recently members of the semaphorin and integrin families have been shown to affect neural crest migration (Eickholt *et al.,* 1999; Kil *et al.,* 1998) and, associations of the Eph family with the integrins are currently being uncovered (Huynh-Do *et al.,* 1999; Miao *et al.,* 2000). To further study the effects of Xephrin-A3, if any, on integrin activation, I would transfect neural crest cells with interacting EphA receptors such as EphA4. These cells could then be stimulated with full length and soluble forms of Xephrin-A3. After harvesting these cells, their cell lysates could be analysed to indicate the phosphorylation status of integrins (or signalling molecules known to associate with integrins) to try to show biochemically if Xephrin-A3 can affect signalling through adhesion pathways.

Some adhesion molecules also affect neural crest cell migration. Preventing the action of NCAM or N-cadherin with function-blocking antibodies *in vivo* causes avian neural crest cells to accumulate in the neural tube or at its periphery (Bronner-Fraser *et al.,* 1992). Similarly, antibodies to tenasin create similar defects (Bronner-Fraser, 1988). Therefore, extracellular matrix molecules and adhesion molecules create a permissive environment for the migration of cranial neural crest cells. A role in neural crest cell guidance however has not been defined. N-CAM and N-cadherin adhesion molecules are expressed in *Xenopus* neural crest before and during migration. It would be interesting to see if N-CAM and N-cadherin expression or function is attenuated in anyway after ectopic expression of various concentrations of Xephrin-A3. This may give an indication of signalling downstream of Xephrin-A3 interacting receptors.

BIBLIOGRAPHY

Albano, R. M., Arkell, R., Beddington, R. S., and Smith, J. C. (1994). Expression of inhibin subunits and follistatin during postimplantation mouse development: decidual expression of activin and expression of follistatin in primitive streak, somites and hindbrain. *Development* **120,** 803-13.

Albers, B. (1987). Competence as the main factor determining the size of the neural plate. *Dev. Growth Differ,* **29,** 535-45.

Amaya, E., Musci, T. J., and Kirschner, M. W. (1993). FGF signalling in the early specification of mesoderm in *Xenopus*. *Development* **118,** 477-487.

Anderson, C. B., and Meier, S. (1981). The influence of the metameric pattern in the mesoderm on migration of cranial neural crest cells in the chick embryo. *Dev Biol* **85,** 385-402.

Baker, C. V. H., and Bronner-Fraser, M. (1997). The origins of the neural crest. Part 1: embryonic induction. *Mech Dev* **69,** 3-11.

Banin, S., Truong, O., Katz, D. R., Waterfield, M. D., Brickell, P. M., and Gout, I. (1996). Wiskott-Aldrich syndrome protein (WASp) is a binding partner for c-Src family protein-tyrosine kinases. *Curr Biol* **6,** 981-8.

Barbera, A. J. (1975). Adhesive recognition between developing retinal cells and the optic tecta of the chick embryo. *Dev Biol* **46,** 167-91.

Barbera, A. J., Marchase, R. B., and Roth, S. (1973). Adhesive recognition and retinotectal specificity. *Proc Natl Acad Sci U S A* **70,** 2482-6.

Barinaga-M. (1995). Receptors find work as guides. *Science* **269,** 1668-70.

Becker, N., Seitanidou, T., Murphy, P., Mattei, M. G., Topilko, P., Neito, M. A., Wilkinson, D. G., Charnay, P., and Gilardi-Hebenstreit, P. (1994). Several receptor tyrosine kinase genes of the Eph family are segmentally expressed in the developing hindbrain. *Mech-Dev* **47,** 3-17.

Bennett, B. D., Zeigler, F. C., Gu, Q., Fendly, B., Goddard, A. D., Gillett, N., and Matthews, W. (1995). Molecular cloning of a ligand for the EPH-related receptor protein- tyrosine kinase Htk. *Proc Natl Acad Sci U S A* **92,** 1866-70.

Bergemann, A. D., Cheng, H. J., Brambilla, R., Klein, R., and Flanagan, J. G. (1995). ELF-2, a new member of the Eph ligand family, is segmentally expressed in mouse embryos in the region of the hindbrain and newly forming somites. *Mol-Cell-Biol* **15,** 4921-9.

Birgbauer, E. (1995). Rhombomeric origin and rostrocaudal reassortment of neural crest cells revealed by intravital microscopy. *Development* **121,** 935-45.

Birgbauer, E., and Fraser, S. E. (1994). Violation of cell lineage restriction compartments in the chick hindbrain. *Development* **120,** 1347-1356.

Birge, R. B., Fajardo, J. E., Mayer, B. J., and Hanafusa, H. (1992). Tyrosine-phosphorylated epidermal growth factor receptor and cellular p130 provide high affinity binding substrates to analyse Crk-phosphotyrosine-dependent interactions in vitro. *J Biol Chem* **267,** 10588-95.

Blitz, I. L., and Cho, K. W. (1995). Anterior neurectoderm is progressively induced during gastrulation: the role of the *Xenopus* homeobox gene *orthodenticle*. *Development* **121,** 993-1004.

Bohme, B., VandenBos, T., Cerretti, D. P., Park, L. S., Holtrich, U., Rubsamen-Waigmann, H., and Strebhardt, K. (1996). Cell-cell adhesion mediated by binding of membrane-anchored ligand LERK- 2 to the EPH-related receptor human embryonal kinase 2 promotes tyrosine kinase activity. *J Biol Chem* **271,** 24747-52.

Bonstein, L., Elias, S., and Frank, D. (1998). Paraxial-fated mesoderm is required for neural crest induction in Xenopus embryos. *Dev Biol* **193,** 156-68.

Bouwmeester, T., Kim, S., Sasai, Y., Lu, B., and De Robertis, E. M. (1996). Cerberus is a head-inducing secreted factor expressed in the anterior endoderm of Spemann's organizer. *Nature* **382,** 595-601.

Boyd, A. W., Ward, L. D., Wicks, I. P., Simpson, R. J., Salvaris, E., Wilks, A., Welch, K., Loudovaris, M., Rockman, S., and Busmanis, I. (1992). Isolation and characterization of a novel receptor-type protein tyrosine kinase (hek) from a human pre-B cell line. *J Biol Chem* **267,** 3262-7.

Bradley, L., Snape, A., Bhatt, S., and Wilkinson, D. G. (1992). The structure and expression of the *Xenopus Krox-20* gene: conserved and divergent patterns of expression in rhombomeres and neural crest. *Mech Dev* **40,** 73-84.

Braisted, J. E., McLaughlin, T., Wang, H. U., Freidman, G. C., Anderson, D. J., and O'Leary, D. D. (1997). Graded and lamina-specific distributions of ligands of EphB recptor tyrosine kinases in the developing retinotectal system. *Dev Biol* **191,** 14-28.

Brambilla, R., Schnapp, A., Casagranda, F., Labrador, J. P., Bergemann, A. D., Flanagan, J. G., Pasquale, E. B., and Klein, R. (1995). Membrane-bound LERK2 ligand can signal through three different Eph- related receptor tyrosine kinases. *Embo J* **14,** 3116-26.

Brennan, C., Monschau, B., Lindberg, R., Guthrie, B., Drescher, U., Bonhoeffer, F., and Holder, N. (1997). Two Eph receptor tyrosine kinase ligands control axon growth and may be involved in the creation of the retinotectal map in the zebrafish. *Development* **124,** 655-64.

Bronner-Fraser, M. (1986). An antibody to a receptor for fibronectin and laminin perturbs cranial neural crest development in vivo. *Dev Biol* **117,** 528-36.

Bronner-Fraser, M. (1988). Distribution and function of tenascin during cranial neural crest development in the chick. *J Neurosci Res* **21,** 135-47.

Bronner-Fraser, M. (1995). Patterning of the vertebrate neural crest. *Perspect Dev Neurobiol* **3,** 53-62.

Bronner-Fraser, M., and Stern, C. (1991). Effects of mesodermal tissues on avian neural crest cell migration. *Dev Biol* **143,** 213-7.

Bronner-Fraser, M., Wolf, J. J., and Murray, B. A. (1992). Effects of antibodies against N-cadherin and N-CAM on the cranial neural crest and neural tube. *Dev Biol* **153,** 291-301.

Bruckner, K., Pasquale, E. B., and Klein, R. (1997). Tyrosine phosphorylation of transmembrane ligands for Eph receptors. *Science* **275,** 1640-3.

Bruckner, K. a., and Klein, R. (1998). Signaling by Eph receptors and their ephrin ligands. *Curr Opin Neurobiol* **8,** 375-82.

Brummendorf, T., Kenwrick, S., and Rathjen, F. G. (1998). Neural cell recognition molecule L1: from cell biology to human hereditary

brain malformations. *Curr Opin Neurobiol* **8,** 87-97.

Carpenter, C. L., Duckworth, B. C., Auger, K. R., Cohen, B., Schaffhausen, B. S., and Cantley, L. C. (1990). Purification and characterisation of phosphoinositide 3-kinase from rat liver. *J Biol Chem* **265,** 19704-11.

Cerretti, D. P., and Nelson, N. (1998). Characterization of the genes for mouse LERK-3/Ephrin-A3 (Epl3), mouse LERK-4/Ephrin-A4 (Epl4), and human LERK-6/Ephrin-A2 (EPLG6): conservation of intron/exon structure. *Genomics* **47,** 131-5.

Cheng, H.-J., Natamoto, M., Bergemann, A. D., and Flanagan, J. G. (1995). Complementary gradients in expression and binding of ELF-1 and Mek4 in development of the topographic retinotectal projection map. *Cell* **82,** 371-381.

Cheng, H. J. a., and Flanagan, J. G. (1994). Identification and cloning of ELF-1, a developmentally expressed ligand for the Mek4 and Sek receptor tyrosine kinases. *Cell* **79,** 157-68.

Chitnis, A. B. (1999). Control of neurogenesis - lessons from frogs, fish and flies. *Curr Opin Neurobiol* **9,** 18-25.

Chung, C. T., and Miller, R. H. (1988). A rapid and convenient method for the preparation and storage of competent bacterial cells. *Nuc Acids Res* **16,** 3580.

Ciossek, T., Millauer, B., and Ullrich, A. (1995). Identification of alternatively spliced mRNAs encoding variants of MDK1, a novel receptor tyrosine kinase expressed in the murine nervous system. *Oncogene* **9,** 97-108.

Clarke, J. D., and Lumsden, A. (1993). Segmental repetition of neuronal phenotype sets in the chick embryo hindbrain. *Development* **118,** 151-62.

Cohen, N. R., Taylor, J. S. H., Scott, L. B., Guillery, R. W., Soriano, P., and Furley, A. J. W. (1997). Errors in corticospinal axon guidance in mice lacking the neural cell adhesion molecule L1. *Curr Biol* **8,** 26-33.

Committee, E. N. (1997). Unified nomenclature for Eph family receptors and their ligands, the ephrins. Eph Nomenclature Committee. *Cell* **90,** 403-4.

Connor, R. J., Menzel, P., and Pasquale, E. B. (1998). Expression and tyrosine phosphorylation of Eph receptors suggest multiple mechanisms in patterning of the visual system. *Dev Biol* **193,** 21-35.

Connor, R. J. a., and Pasquale, E. B. (1995). Genomic organization and alternatively processed forms of Cek5, a receptor protein-tyrosine kinase of the Eph subfamily. *Oncogene* **11,** 2429-38.

Cook, M., Gould, A., Brand, N., Davies, J., Strutt, P., Shaknovich, R., Licht, J., Waxman, S., Chen, Z., Gluechsohn-Waelsch, S., Krumlauf, R., and Zelent, A. (1994). Expression of the zinc-finger gene *PLZF* at rhombomere boundaries in the vertebrate hindbrain. *Proc Natl Acad Sci* **92,** 2249-2253.

Cordes, S. P., and Barsch, G. S. (1994). The mouse segmentation gene *kr* encodes a novel basic domain-leucine zipper transcription factor. *Cell* **79,** 1025-1034.

Cornish JA, Etkin LD. (1993). The formation of the pronephric duct in Xenopus involves recruitment of posterior cells by migrating pronephric duct cells. *Dev Biol.* 159, 338-45.

Couly, G., and LeDourin, N. (1990). Head morphogenesis in embryonic chimeras: evidence for a segmental pattern in the ectoderm corresponding to the neuromeres. *Development* **108,** 543-558.

Cox, E. C., Muller, B., and Bonhoeffer, F. (1990). Axonal guidance in the chick visual system: Posterior tectal membranes induce collapse of growth cones from the temporal retina. *Neuron* **2,** 31-37.

Craven, S. E., and Bredt, D. S. (1998). PDZ proteins organise synaptic signaling pathways. *Cell* **93,** 495-498.

Cunliffe, V., and Smith, J. C. (1994). Specification of mesodermal pattern in *Xenopus laevis* by interactions between *Brachyury, noggin* and *Xwnt-8. EMBO J.* **13,** 349-359.

Dale, L., Howes, G., Price, B. M., and Smith, J. C. (1992). Bone morphogenetic protein 4: a ventralizing factor in early Xenopus development. *Development* **115,** 573-85.

Dale, L., and Slack, J. M. (1987). Fate map for the 32-cell stage of Xenopus laevis. *Development* **99,** 527-51.

Davenport, R. W., Thies, E., Zhou, R., and Nelson, P. G. (1998). Cellular localization of ephrin-A2, ephrin-A5, and other functional guidance cues underlies retinotopic development across species. *J Neurosci* **18,** 975-86.

Davis, S., Gale, N., Aldrich, T. H., Maisonpierre, P. C., Lhotak, V., Pawson, T., Goldfarb, M., and Yancopoulos, G. D. (1994). Ligands for EPH-related receptor tyrosine kinases that require membrane attachment or clustering for activity. *Science* **266,** 816-9.

Debby-Brafman, A., Burstyn-Cohen, T., Klar, A., and Kalcheim, C. (1999). F-Spondin, expressed in somite regions avoided by neural crest cells, mediates inhibition of distinct somite domains to neural crest migration. *Neuron* **22,** 475-88.

Derynck, R. (1994). TGF-beta-receptor-mediated signaling. *Trends. Biochem. Sci.* **19,** 548-53.

Drescher, U. (1997). The Eph family in the patterning of neural development. *Curr Biol* **7,** R799-807.

Drescher, U., Kremoser, C., Handwerker, C., Loschinger, J., Noda, M., and Bonhoeffer, F. (1995). In vitro guidance of retinal ganglion cell axons by RAGS a 25 kDa tectal protein related to ligands for Eph receptor tyrosine kinases. *Cell* **82,** 359-70.

Eickholt, B. J., Mackenzie, S. L., Graham, A., Walsh, F. S., and Doherty, P. (1999). Evidence for collapsin-1 functioning in the control of neural crest migration in both trunk and hindbrain regions. *Development* **126,** 2181-9.

Ellis, C., Kasmi, F., Ganju, P., Walls, E., Panaytou, G., and Reith, A. D. (1996). A juxtamembrane autophosphorylation site in the Eph family receptor tyrosine kinase, Sek, mediates high affinity interaction with p59fyn. *Oncogene* **12,** 1727-1736.

Fainsod, A., Steinbeisser, H., and De Robertis, E. M. (1995). On the function of BMP-4 in patterning the marginal zone of the *Xenopus* embryo. *EMBO J.* **13,** 5015-5025.

Flanagan, J. G. a., and Vanderhaeghen, P. (1998). The ephrins and Eph receptors in neural development. *Annu Rev Neurosci* **21,** 309-45.

Flenniken, A. M., Gale, N. W., Yancopoulos, G. D., and Wilkinson, D. G. (1996). Distinct and overlapping expression patterns of ligands for Eph-related receptor tyrosine kinases during mouse embryogensis. *Dev. Biol.* **In press.**

Fraser, S., Keynes, R., and Lumsden, A. (1990). Segmentation in the chick embryo is defined by cell lineage restrictions. *Nature* **344,** 431-5.

Frisen, J., Yates, P. A., McLaughlin, T., Friedman, G. C., O'Leary, D. D., and Barbacid, M. (1998). Ephrin-A5 (AL-1/RAGS) is essential for proper retinal axon guidance and topographic mapping in the mammalian visual system. *Neuron* **20,** 235-43.

Frohman, M. A., Martin, G. R., Cordes, S. P., Halamek, L. P., and Barsh, G. S. (1993). Altered rhombomere-specific gene expression and hyoid bone differentiation in the mouse segmentation mutant, *kreisler* (*kr*). *Development* **117,** 925-936.

Gale, N. W., Flenniken, A., Compton, D. C., Jenkins, N., Copeland, N. G., Gilbert, D. J., Davis, S., Wilkinson, D. G., and Yancopoulos, G. D. (1996a). Elk-L3, a novel transmembrane ligand for the Eph family of receptor tyrosine kinases, expressed in embryonic floor plate, roof plate and hindbrain segments. *Oncogene* **13,** 1343-52.

Gale, N. W., Holland, S. J., Valenzuela, D. M., Flenniken, A., Pan, L., Ryan, T. E., Henkemeyer, M., Strebhardt, K., Hirai, H., Wilkinson, D. G., Pawson, T., Davis, S., and Yancopoulos, G. D. (1996b). Eph receptors and ligands comprise two major specificity subclasses and are reciprocally compartmentalized during embryogenesis. *Neuron* **17,** 9-19.

Garrity, P. A., Rao, Y., Salecker, I., McGlade, J., Pawson, T., and Zipursky, S. L. (1996). Drosophila photoreceptor axon guidance and targeting requires the dreadlocks SH2/SH3 adapter protein. *Cell* **85,** 639-50.

George, S. E., Simokat, K., Hardin, J., and Chisholm, A. D. (1998). The VAB-1 Eph receptor tyrosine kinase functions in neural and epithelial morphogenesis in C. elegans. *Cell* **92,** 633-43.

Graham, A., Francis-West, P., Brickell, P., and Lumsden, A. (1994). The signalling molecule BMP4 mediates apoptosis in the rhombencephalic neural crest. *Nature* **372,** 684-6.

Graham, A., Heyman, I., and Lumsden, A. (1993). Even-numbered rhombomeres control the apoptotic elimination of neural crest cells from odd-numbered rhombomeres in the chick hindbrain. *Development* **119,** 233-45.

Green, J. B. A., and Smith, J. C. (1990). Graded changes in dose of a Xenopus activin A homologue elicit stepwise transitions in embryonic cell fate. *Nature* **347,** 391-394.

Gurniak, C. B. a., and Berg, L. J. (1996). A new member of the Eph family of receptors that lacks protein tyrosine kinase activity. *Oncogene* **13,** 777-86.

Guthrie, S. (1996). Patterning the hindbrain. *Curr Opin Neurobiol* **6,** 41-8.

Guthrie, S., Butcher, M., and Lumsden, A. (1991). Patterns of cell division and interkinetic nuclear migration in the chick embryo hindbrain. *J Neurobiol* **22,** 742-54.

Guthrie, S., Prince, V., and Lumsden, A. (1993). Selective dispersal of avian rhombomere cells in orthotopic and heterotopic grafts. *Development* **118,** 527-38.

Hall, A. (1998). Rho GTPases and the actin cytoskeleton. *Science* **279,** 509-14.

Hansen, C. S., Marion, C. D., Steele, K., George, S., and Smith, W., C. (1997). Direct neural induction and selective inhibition of mesoderm and epidermis inducers by Xnr-3. *Development* **124,** 483-92.

Harai, H., Maru, Y., Hagiwara, K., Nishida, J., and Takaku, F. (1987). A novel putative tyrosine kinase receptor encoded by the eph gene. *Science* **238,** 1717-1720.

Harland, R. a., and Gerhart, J. (1997). Formation and function of Spemann's organizer. *Annu Rev Cell Dev Biol* **13,** 611-67.

Harland, R. M. (1994). Neural induction in Xenopus. *Curr. Opin. Genet. Dev.* **4,** 543-549.

Harris, W. A., and Holt, C. E. (1995). From tags to RAGS: chemoaffinity finally has receptors and ligands. *Neuron* **15,** 241-4.

Hawley, S. H. B., Wunnenberg-Stapleton, K., Hashimoto, C., Laurent, M., Watabe, N., Blumberg, B. W., and Cho, K. W. Y. (1995). Disruption of BMP signals in embryonic Xenopus ectoderm leads to direct neural induction. *Genes Dev.* **9,** 2923-35.

Helbling, P. M., Tran, C. T., and Brandli, A. W. (1998). Requirement for EphA receptor signaling in the segregation of Xenopus third and fourth arch neural crest cells. *Mech Dev* **78,** 63-79.

Hemmati-Brivanlou, A., de la Torre, J. R., Holt, C., and Harland, R. M. (1991). Cephalic expression and molecular characterisation of Xenopus En-2. *Development* **111,** 715-24.

Hemmati-Brivanlou, A., Kelly, O. G., and Melton, D. A. (1994). Follistatin, an antagonist of activin, is expressed in the Spemann organizer and displays direct neuralizing activity. *Cell* **77,** 283-295.

Hemmati-Brivanlou, A., and Melton, D. (1997). Vertebrate embryonic cells will become nerve cells unless told otherwise. *Cell* **88,** 13-17.

Hemmati-Brivanlou, A., and Melton, D. A. (1992). A truncated activin receptor inhibits mesoderm induction and formation of axial structures in *Xenopus* embryos. *Nature* **359,** 609-614.

Hemmati-Brivanlou, A., and Melton, D. A. (1994). Inhibition of activin receptor signalling promotes neuralisation in *Xenopus*. *Cell* **77,** 273-81.

Hemmati-Brivanlou, A., and Thomsen, G. H. (1995). Ventral mesodermal patterning in Xenopus embryos: expression patterns and activities of BMP-2 and BMP-4. *Dev. Genet.* **17,** 78-89.

Henkemeyer, M., Marengere, L. E. M., McGlade, J., Olivier, J. P., Conlon, R. A., Holmyard, D. P., Letwin, K., and Pawson, T. (1994). Immunolocalisation of the Nuk receptor tyrosine kinase suggests roles in segmental patterning of the brain and angiogenesis. *Oncogene* **9,** 1001-1014.

Henkemeyer, M., Orioli, D., Henderson, J. T., Saxton, T. M., Roder, J., Pawson, T., and Klein, R. (1996). Nuk controls pathfinding of commissural axons in the mammalian central nervous system. *Cell* **86,** 35-46.

Heyman, I., Faissner, A., and Lumsden, A. (1995). Cell and matrix specialisations of rhombomere boundaries. *Dev Dyn* **204,** 301-15.

Himanen, J. P., Henkemeyer, M., and Nikolov, D. B. (1998). Crystal structure of the ligand-binding domain of the receptor tyrosine kinase EphB2. *Nature* **396,** 486-91.

Hock, B., Bohme, B., Karn, T., Feller, S., Rubsamen-Waigmann, H., and Strebhardt, K. (1998a). Tyrosine-614, the major autophosphorylation site of the receptor tyrosine kinase HEK2, functions as multi-docking site for SH2-domain mediated interactions. *Oncogene* **17,** 255-60.

Hock, B., Bohme, B., Karn, T., Yamamoto, T., Kaibuchi, K., Holtrich, U., Holland, S., Pawson, T., Rubsamen-Waigmann, H., and Strebhardt, K. (1998b). PDZ-domain-mediated interaction of the eph-related receptor tyrosine kinase EphB3 and the ras-binding protein AF6 depends on the kinase activity of the receptor . *Proc Natl Acad Sci U S A* **95,** 9779-84.

Holash, J. A., Soans, C., Chong, L. D., Shao, H., Dixit, V. M., and Pasquale, E. B. (1997). Reciprocal expression of the Eph receptor Cek5 and its ligand(s) in the early retina. *Dev Biol* **182,** 256-69.

Holash, J. A. a., and Pasquale, E. B. (1995). Polarized expression of the receptor protein tyrosine kinase Cek5 in the developing avian visual system. *Dev. Biol.* **172,** 683-693.

Holland, S. J., Gale, N. W., Gish, G. D., Roth, R. A., Songyang, Z., Cantley, L. C., Henkemeyer, M., Yancopoulos, G. D., and Pawson, T. (1997). Juxtamembrane tyrosine residues couple the Eph family receptor EphB2/Nuk to specific SH2 domain proteins in neuronal cells. *Embo J* **16,** 3877-88.

Holland, S. J., Gale, N. W., Mbamalu, G., Yancopoulos, G. D., Henkemeyer, M., and Pawson, T. (1996). Bidirectional signalling through the EPH-family receptor Nuk and its transmembrane ligands. *Nature* **383,** 722-5.

Holland, S. J., Peles, E., Pawson, T., and Schlessinger, J. (1998). Cell-contact-dependent signalling in axon growth and guidance: Eph receptor tyrosine kinases and receptor protein tyrosine phosphatase beta. *Curr Opin Neurobiol* **8,** 117-27.

Holt, C. E., and Harris, W. A. (1998). Target selection: invasion, mapping and cell choice. *Current Opinion in Neurobiology* **8,** 98-105.

Holtzman, L. B., Marks, R. M., and Dixit, V. M. (1990). A novel intermediate-early response gene of endothelium is induced by cytokines and encodes a secreted protein. *Mol.Cell.Biol.* **10,** 5830-5838.

Hopwood, N. D., Pluck, A., and Gurdon, J. B. (1989). A Xenopus mRNA related to Drosophila twist is expressed in response to induction in the mesoderm and the neural crest. *Cell* **59,** 893-903.

Hornberger, M. R., Dutting, D., Ciossek, T., Yamada, T., Handwerker, C., Lang, S., Weth, F., Huf, J., Wessel, R., Logan, C., Tanaka, H., and Drescher, U. (1999). Modulation of EphA receptor function by coexpressed ephrinA ligands on retinal ganglion cell axons. *Neuron* **22,** 731-42.

Hu, Q., Milfay, D., and Williams, L. T. (1995). Binding of NCK to SOS and activation of ras-dependent gene expression. *Mole Cell Biol* **15,** 1169-1174.

Huang, C., Ni, Y., Wang, T., Gao, Y., Haudenschild, C. C., and Zhan, X. (1997). Down-regualation of the filamentous actin cross-linking activity of cortactin by Src-mediated tryrosine phosphorylation. *J Biol Chem* **272,** 13911-13915.

Hunt, P., Gulisano, M., Cook, M., Sham, M. H., Faiella, A., Wilkinson, D., Boncinelli, E., and Krumlauf, R. (1991b). A distinct Hox code for the branchial region of the vertebrate head. *Nature* **353,** 861-4.

Hunt, P., and Krumlauf, R. (1992). Expression of Hox-2 genes and their relationship to regional diversity in the vertebrate head. *"Cell-cell signalling in vertebrate development" (E.Robertson, F.Maxfield, H.Vogel, Eds.), In press. Springer-Verlag, New York.* .

Hunt, P., Whiting, J., Muchamore, I., Marshall, H., and Krumlauf, R. (1991d). Homeobox genes and models for patterning the hindbrain and branchial arches. *Dev Suppl* **1,** 187-96.

Hunt, P., Whiting, J., Nonchev, S., Sham, M. H., Marshall, H., Graham, A., Cook, M., Allemann, R., Rigby, P. W., Gulisano, M., and et al. (1991c). The branchial Hox code and its implications for gene regulation, patterning of the nervous system and head evolution. *Development* **Suppl 2,** 63-77.

Hunt, P., Wilkinson, D., and Krumlauf, R. (1991a). Patterning the vertebrate head: murine Hox 2 genes mark distinct subpopulations of premigratory and migrating cranial neural crest. *Development* **112,** 43-50.

Huynh-Do, U., Stein, E., Lane, A. A., Liu, H., Cerretti, D. P., and Daniel, T. O. (1999). Surface densities of ephrin-B1 determine EphB1-coupled activation of cell attachment through alphavbeta3 and alpha5beta1 integrins. *Embo J* **18,** 2165-2173.

Irvine, R. (1998). Inositol phospholipids: translocation, translocation, translocation... *Curr Biol* **8,** R557-R559.

Irving, C., Nieto, M. A., DasGupta, R., Charnay, P., and Wilkinson, D. G. (1996). Progressive spatial restriction of *Sek-1* and *Krox-20* gene expression during hindbrain segmentation. *Dev Biol* **173,** 26-38.

Jones, C. M., Lyons, K. M., Lapan, P. M., Wright, C. V. E., and Hogan, B. L. M. (1992). DVR-4 (bone morphogenic protein 4) as a posterior-ventralising factor in *Xenopus* mesoderm induction. *Development* **115,** 639-647.

Jones, T. L., Chong, L. D., Kim, J., Xu, R. H., Kung, H. F., and Daar, I. O. (1998). Loss of cell adhesion in Xenopus laevis embryos mediated by the cytoplasmic domain of XLerk, an erythropoietin-producing hepatocellular ligand. *Proc Natl Acad Sci U S A* **95,** 576-81.

Jones, T. L., Karavanova, I., Chong, L., Zhou, R. P., and Daar, I. O. (1997). Identification of XLerk, an Eph family ligand regulated during mesoderm induction and neurogenesis in Xenopus laevis. *Oncogene* **14,** 2159-66.

Jones, T. L., Karavanova, I., Maeno, M., Ong, R. C., Kung, H. F., and Daar, I. O. (1995). Expression of an amphibian homolog of the Eph family of receptor tyrosine kinases is developmentally regulated. *Oncogene* **10,** 1111-7.

Jukes, and Cantor, a. (1969). "Evolution of Protein Molecules." Academic Press.

Kalcheim, C. a., and Teillet, M.-A. (1989). Consequences of somite manipulation on the pattern of dorsal root ganglion development. *Development* **106,** 85-93.

Kazlauskas, A. (1994). Receptor tyrosine kinases and their targets. *Curr. Opin. in Genetics and Development* **4,** 5-14.

Kengaku, M., and Okamoto, H. (1993). Basic fibroblast growth factor induces differnetiation of neural tube and neural crest lineages of cultured ectoderm cells from *Xenopus* gastrula. *Development* **119,** 1067-1078.

Kenny, D., Bronner-Fraser, M., and Marcelle, C. (1995). The receptor tyrosine kinase Qek5 mRNA is expressed in a gradient within the neural retina and the tectum. *Dev.Biol.* **172,** 708-716.

Kessler, D. S., and Melton, D. A. (1994). Vertebrate embryonic induction: mesodermal and neural patterning. *Science* **266,** 596-604.

Kil, S. H., Krull, C. E., Cann, G., Clegg, D., and Bronner-Fraser, M. (1998). The alpha4 subunit of integrin is important for neural crest migration. *Dev Biol* **202,** 29-42.

Kimmel, C. B., Metcalfe, W., and Schabtach, E. (1985). T reticular interneurons: a class of serially repeating cells in the zebrafish hindbrain. *J Comp Neurol* **15,** 365-76.

Kimura, M. (1980). A simple method for estimating evolutionary fates of base substitutions through comparative studies of nucleotide sequences. *J Mol Evol* **16,** 111-120.

Kinoshita, N., Minshull, J., and Kirschner, M. W. (1995). The identification of two novel ligands of the FGF receptor by a yeast screening method and their activity in Xenopus development. *Cell* **83,** 621-630.

Knecht, A. K., Good, P. J., Dawid, I. B., and Harland, R. M. (1995). Dorsal-ventral patterning and differentiation of noggin-induced neural tissue in the absence of mesoderm. *Development* **121,** 1927-35.

Koch, W. J., Inglese, J., Stone, W. C., and Lefkowitz, R. J. (1993). The binding site for the beta gamma subunits of heterotrimeric G proteins on the beta-adrenergic receptor kinase. *J Biol Chem* **268,** 8256-60.

Kontges, G. a. L., A. (1996). Rhombencephalic neural crest segmentation is preserved througout cranialfacial ontogeny. *Development* **122,** 329-3242.

Krieg, P. A., and Melton, D. A. (1984). Functional messenger RNAs are produced by SP6 in vitro transcription of cloned cDNAs. *Nucleic Acids Res* **12,** 7057-70.

Krieg, P. A., Varnum, S. M., Wormington, W. M., and Melton, D. A. (1989). The mRNA encoding elongation factor 1-alpha (EF-1 alpha) is a major transcript at the midblastula transition in Xenopus. *Dev Biol* **133,** 93-100.

Krotoski, D. M., Domingo, C., and Bronner-Fraser, M. (1986). Distribution of a putative cell surface receptor for fibronectin and laminin in the avian embryo. *J Cell Biol* **103,** 1061-71.

Krull, C. E. (1995). Segmental migration of trunk neural crest: time-lapse analysis reveals a role for PNA-binding molecules. *Development* **121,** 3733-43.

Krull, C. E., Lansford, R., Gale, N. W., Collazo, A., Marcelle, C., Yancopoulos, G. D., Fraser, S. E., and Bronner-Fraser, M. (1997). Interactions of Eph-related receptors and ligands confer rostrocaudal pattern to trunk neural crest migration. *Curr Biol* **7,** 62-74.

Kuo, K.-T., Hartz, J. A., Law, M. L., and Davidson, J. N. (1982). Isolation and chromosomal localisation of unique DNA sequences from a human genomic library. *Proc. Nat. Acad. Sci* **79,** 865-869.

LaBonne, C., and Bronner-Fraser, M. (1998). Neural crest induction in Xenopus: evidence for a two-signal model. *Development* **125,** 2403-14.

Labrador, J. P., Brambilla, R., and Klein, R. (1997). The N-terminal globular domain of Eph receptors is sufficient for ligand binding and receptor signaling. *EMBO* **16,** 3889-3897.

Lachmann, M., Oates, A. C., Dottori, M., Smith, F. M., Do, C., Power, M., Kravets, L., and Boyd, A. W. (1998). Distinct subdomains of the EphA3 receptor mediate ligand binding and receptor dimerisation. *J Biol Chem* **273,** 20228-20237.

Lackmann, M., Mann, R. J., Kravets, L., Smith, F. M., Bucci, T. A., Maxwell, K. F., Howlett, G. J., Olsson, J. E., Vanden Bos, T., Cerretti, D. P., and Boyd, A. W. (1997). Ligand for EPH-related kinase (LERK) 7 is the preferred high affinity ligand for the HEK receptor. *Biochem Biophys Res Commun* **235,** 487-92.

Lamb, T. M., Knecht, A. K., Smith, W. C., Stachel, S. E., Economides, A. N., Stahl, N., Yancopolous, G. D., and Harland, R. M. (1993). Neural induction by the secreted polypeptide noggin. *Science* **262,** 713-718.

Layer, P. G., and Alber, R. (1990). Patterning of the chick brain vesicles as revealed by peanut agglutinin and cholinesterases. *Development* **109,** 613-24.

Le Douarin, N. (1982). "The Neural Crest." Cambridge University Press, Cambridge.

Lee, Y. M., Osumi-Yamashita, N., Ninomiya, Y., Moon, C. K., Eriksson, U., and Eto, K. (1995). Retinoic acid stage-dependently alters the migration pattern and identity of hindbrain neural crest cells. *Development* **121,** 825-37.

Li, R. (1997). Bee1, a yeast protein with homology to Wiskott-Aldrich syndrome protein, is critical for the assembly of cortical actin cytoskeleton. *J Cell Biol* **136,** 649-658.

Lin, D., Gish, G. D., Songyang, Z., and Pawson, T. (1999). The carboxyl terminus of B class ephrins constitutes a PDZ domain binding motif. *J Biol Chem* **274,** 3726-33.

Lowenstein, E. J., Daly, R. J., Batzer, A. G., Li, W., Margolis, B., Lammers, R., Ullrich, A., Skolmik, E. Y., Bar-Sagi, D., and Schlessinger, J. (1992). The SH2 and SH3 domain-containing protein GRB2 links receptor tyrosine kinases to ras signalling. *Cell* **70,** 431-442.

Lu, w., Katz, s., Gupta, R., and Mayer, B. J. (1997). Activation of Pak by membrane localisation mediated by an Sh3 domain from the adaptor protein Nck. *Curr Biol* **7,** 85-94.

Lumsden, A., Sprawson, N., and Graham, A. (1991). Segmental origin and migration of neural crest cells in the hindbrain region of the chick embryo. *Development* **113,** 1281-1291.

Lumsden, A. a., and Keynes, R. (1989). Segmental patterns of neuronal development in the chick hindbrain. *Nature* **337,** 424-428.

Luo, L., Jan, L. Y., and Jan, Y. N. (1997). Rho family GTP-binding proteins in growth cone signalling. *Curr Opin Neurobiol* **7,** 81-6.

Luo, L., Liao, J., Jan, L. Y., and Jan, Y. N. (1994). Distinct morphogenic functions of similar small GTPases: *Drosophila* Drac1 is involved in axonal outgrowth and myoblast fusion. *Genes Dev* **8,** 1787-1802.

Mahmood, R., Keifer, P., and al, e. (1995). Multiple roles for Fgf-3 during cranial neural development in chicken. *Development* **121,** 1399-1410.

Maisonpierre, P. C., Barrezueta, N. X., and Yancopoulos, G. D. (1993). Ehk1 and Ehk2: two novel members of the Eph receptor-like tyrosine kinase family with distinctive structures and neuronal expression. *Oncogene* **8,** 3277-3288.

Mancilla, A., and Mayor, R. (1996). Neural crest formation in Xenopus laevis: mechanisms of Xslug induction. *Dev Biol* **177,** 580-9.

Manser, E., Huang, H.-Y., Loo, T.-H., Chen, X.-Q., Dong, J.-M., Leung, T., and Lim, L. (1997). Expression of constitutively active a-PAK reveals effects of the kinase on actin and focal complexes. *Mol Cell Biol* **17,** 1129-1143.

Manzanares, M., Cordes, S., Kwan, C. T., Sham, M. H., Barsh, G. S., and Krumlauf, R. (1997). Segmental regulation of Hoxb-3 by kreisler. *Nature* **387,** 191-5.

Manzanares, M., Trainor, P. A., Nonchev, S., Ariza-McNaughton, L., Brodie, J., Gould, A., Marshall, H., Morrison, A., Kwan, C. T., Sham, M. H., Wilkinson, D. G., and Krumlauf, R. (1999). The Role of kreisler in Segmentation during Hindbrain Development. *Dev Biol* **211,** 220-237.

Marchant, L., Linker, C., Ruiz, P., Guerrero, N., and Mayor, R. (1998). The inductive properties of mesoderm suggest that the neural crest cells are specified by a BMP gradient. *Dev Biol* **198,** 319-29.

Marchase, R. B., Meunier, J. C., Pierce, M., and Roth, S. (1977). Biochemical investigations of retinotectal specificity. *Prog Clin Biol Res* **15,** 73-9.

Marcus, R. C., Gale, N. W., Morrison, M. E., Mason, C. A., and Yancopoulos, G. D. (1996). Eph family receptors and their ligands distribute in opposing gradients in the developing mouse retina. *Dev Biol* **180,** 786-789.

Margolis, B., Bellot, F., Honegger, A. M., Ullrich, A., Schlessinger, J., and Zilberstein, A. (1990). Tyrosine kinase activity is essential for the association of phospholipase C-gamma with the epidermal growth factor receptor. *Mol Cell Biol* **10,** 435-41.

Marikovsky, M., Lavi, S., Pinkas-Kramarski, R., Karunagaran, D., Liu, N., Wen, D., and Yarden, Y. (1995). ErbB-3 mediates differential mitogenic effects of NDF/heregulin isoforms on mouse keratinocytes. *Oncogene* **10,** 1403-1411.

Marshall, C. J. (1995). Specificity of receptor tyrosine kinase signaling: Transient versus sustained signal-related kinase activation. *Cell* **80,** 179-185.

Matzuk, M. M., Lu, N., Vogel, H., Sellheyer, K., and Roop, D. R. (1995). Multiple defects and perinatal death in mice deficient in follistatin. *Nature* **374,** 360-63.

Mayor, R., Guerrero, N., and Martinez, C. (1997). Role of FGF and noggin in neural crest induction. *Dev. Biol.* **189,** 1-12.

Mayor, R., Morgan, R., and Sargent, M. G. (1995). Induction of the prospective neural crest of Xenopus. *Development* **121,** 767-777.

McKay, I. J., Muchamore, I., Krumlauf, R., Maden, M., Lumsden, A., and Lewis, J. (1994). The kreisler mouse: a hindbrain segmentation mutant that lacks two rhombomeres. *Development* **120,** 2199-211.

McMahon, J. A., Takada, S., Zimmerman, L. B., Fan, C. M., Harland, R. M., and McMahon, A. P. (1998). Noggin-mediated antagonism of BMP signaling is required for growth and patterning of the neural tube and somite. *Genes Dev* **12,** 1438-52.

Meima, L., Kljavin, I. J., Moran, P., Shih, A., Winslow, J. W., and Caras, I. W. (1997). AL-1-induced growth cone collapse of rat cortical neurons is correlated with REK7 expression and rearrangement of the actin cytoskeleton. *Eur J Neurosci* **9,** 177-88.

Meima L, Moran P, Matthews W, Caras IW. (1997). Lerk2 (ephrin-B1) is a collapsing factor for a subset of cortical growth cones and acts by a mechanism different from AL-1 (ephrin-A5). *Mol Cell Neurosci.* **9,** 314-28.

Meisenhelder, J., and Hunter, T. (1992). The SH2/SH3 domain-containing protein Nck is rcognised by certain anti-phospholipase C-gamma 1 monoclonal antibodies, and its phosphorylation on tyrosine is stimulated by platelet-derived growth factor and epidermal growth factor treatment. *Mol Cell Biol* **12,** 5843-56.

Mellitzer G, Xu Q, Wilkinson DG. (1999). Receptors and ephrins restrict cell intermingling and communication. *Nature* **400,** 77-81.

Metcalfe, W. K., Mendelson, B., and Kimmel, C. B. (1986). Segmental homologies among reticulospinal neurons in the hindbrain of the zebrafish larva. *J Comp Neurol* **251,** 147-159.

Miao H, Burnett E, Kinch M, Simon E, Wang B. (2000). Activation of EphA2 kinase suppresses integrin function and causes focal-adhesion-kinase dephosphorylation. *Nat Cell Biol.* **2,** 62-9.

Mizuseki, K., Kishi, M., Matsui, M., Nakanishi, S., and Sasai, Y. (1998). Xenopus Zic-related-1 and Sox-2, two factors induced by chordin, have distinct activities in the initiation of neural induction. *Development* **125,** 579-87.

Moans, C., Yan, Y.-L., and al, e. (1996). Valentino: A zebrafish gene required for normal hindbrain segmentation. *Development* **122,** 3981-3990.

Monschau, B., Kremoser, C., Ohta, K., Tanaka, H., Kaneko, T., Yamada, T., Handwerker, C., Hornberger, M. R., Loschinger, J., Pasquale, E. B., Siever, D. A., Verderame, M. F., Muller, B. K., Bonhoeffer, F., and Drescher, U. (1997). Shared and distinct functions of RAGS and ELF-1 in guiding retinal axons. *Embo J* **16,** 1258-67.

Moody, S. A. (1997). Analysis of heterologous gene expression in Xenopus blastomeres. *Methods Mol Biol* **62,** 271-84.

Moury, J. D., and Jacobson, A. G. (1990). The origins of neural crest cells in axolotl. *Dev. Biol.* **141,** 243-53.

Muller, B. K., Bonhoeffer, F., and Drescher, U. (1996a). Novel gene families involved in neural pathfinding. *Curr Opin Genet Dev* **6,** 469-74.

Muller, B. K., Bonhoffer, F., and Drescher, U. (1996b). Novel gene families involved in neural pathfinding. *Curr. Opinions in Genetics and Development* **6,** 469-474.

Nakamoto, M., Cheng, H. J., Friedman, G. C., McLaughlin, T., Hansen, M. J., Yoon, C. H., O'Leary, D. D., and Flanagan, J. G. (1996). Topographically specific effects of ELF-1 on retinal axon guidance in vitro and retinal axon mapping in vivo. *Cell* **86,** 755-66.

Nguyen, V. H., Schmid, B., Trout, J., Conners, S. A., Ekker, M., and Mullins, M. C. (1998). Ventral and lateral regions of the zebrafish gastrula, including the neural crest progenitors, are established by a bmp2b/swirl pathway of genes. *Dev Biol* **199,** 93-110.

Nieto, M. A. (1995). Relationship between spatially restricted Krox-20 gene expression in the branchial neural crest and segmantation in the chick embryo hindbrain. *EMBO J* **14,** 1697-710.

Nieto, M. A., Bradley, L., and Wilkinson, D. G. (1991). Conserved segmental expression of *Krox-20* in the vertebrate hindbrain and its relationship to lineage restriction. *Development* **113,** 59-62.

Nieto, M. A., Gilardi-Hebenstreit, P., Charnay, P., and Wilkinson, D. G. (1992). A receptor protein tyrosine kinase implicated in the segmental patterning of the hindbrain and mesoderm. *Development* **116,** 1137-1150.

Nieto, M. A., Sargent, M. G., Wilkinson, D. G., and Cooke, J. (1994). Control of cell behaviour during vertebrate development by *Slug*, a zinc finger gene. *Science* **264,** 835-839.

Nieuwkoop, P. D., and Albers, B. (1990). The role of competence in the cranio-caudal segregation of the nervous system. *Dev. Growth Differ.* **32,** 23-31.

Nieuwkoop, P. D., and Faber, J. (1975). "Normal Table of *Xenopus laevis* (Daudin)." North Holland, Amsterdam.

Nieuwkoop, P. D., and Koster, K. (1995). Vertical versus planar induction in early amphibian development. *Dev. Growth Differ.* **37,** 653-68.

Nishibe, S., Wahl, M. I., Hernandez-Sotomayor, S. M. T., Tonks, N. K., Rhee, S. G., and Carpenter, G. (1990). Increase in the catalytic activity of phospholipase C-g1 by tyrosine phosphorylation. *Science* **250,** 1253-56.

Noden, D. M. (1983). The role of the neural crest in patterning of avian cranial skeletal, connective, and muscle tissues. *Dev Biol* **96,** 144-65.

Noden, D. M. (1988). Interactions and fates of avian craniofacial mesenchyme. *Development* **103 Suppl,** 121-40.

Nonchev, S., Maconochie, M., Vesque, C., Aparicio, S., Ariza-McNaughton, L., Manzanares, M., Maruthainar, K., Kuroiwa, A., Brenner, S., Charnay, P., and Krumlauf, R. (1996). The conserved role of *Krox-20* in directing *Hox* gene expression during vertebrate hindbrain expression. *Proc Natl Acad Sci* **95,** 9339-9345.

O'Leary, D. D. M. a., and Wilkinson, D. G. (1999). Eph receptors and ephrins in neural development. *Curr Opin Neur Biol* **9,** 65-73.

Oates, A. C., Lackmann, M., Power, M. A., Brennan, C., Smith, F. M., Do, C., Evans, B., Holder, N., and Boyd, A. W. (1999). An early developmental role for Eph-ephrin interaction during vertebrate gastrulation. *Mech Dev* **83,** 77-94.

Ooi, J., Yajnik, V., Immanuel, D., Gordon, M., Moscow, J. J., Buchberg, A. M., and Margolis, B. (1995). The cloning of Grb-10 reveals a new family of SH2 domain proteins. *Oncogene* **10,** 1621-1630.

Orike, N., and Pini, A. (1996). Axon guidance: Following the Eph plan. *Curr. Biol* **6,** 108-110.

Orioli, D., Henkemeyer, M., Lemke, G., Klein, R., and Pawson, T. (1996). Sek4 and Nuk receptors cooperate in guidance of commissural axons and in palate formation. *Embo J* **15,** 6035-49.

Orioli, D., and Klein, R. (1997). The Eph receptor family: axonal guidance by contact repulsion. *Trends Genet* **13,** 354-9.

Oxtoby, E., and and Jowett, T. (1993). Cloning of the zebrafish *krox-20* gene (*krx-20*) and its expression during hindbrain development. *Nucleic Acids Res* **21,** 1087-1095.

Pandey, A., Duan, H., and Dixit, V. M. (1995a). Characterization of a novel Src-like adapter protein that associates with the Eck receptor tyrosine kinase. *J Biol Chem* **270,** 19201-4.

Pandey, A., Lazar, D. F., Saltiel, A. R., and Dixit, V. M. (1994). Activation of the eck receptor protein tyrosine kinase stimulates phosphatidyl-inositol-3-kinase. *J.Biol.Chem* **269,** 30154-30157.

Pandey, A., Lindberg, R. A., and Dixit, V. M. (1995b). Receptor orphans find a family. *Curr-Biol.* **5,** 986-9.

Pandey, A., Shoa, H., Marks, R. M., Polverini, P. J., and Dixit, V. M. (1995c). Role of B61, the Ligand for the Eck Receptor Tyrosine Kinase, in TNF-a-induced Angiogenesis. *Science* **268,** 567-569.

Pasquale, E. B. (1997). The Eph family of receptors. *Curr Opin Cell Biol* **9,** 608-15.

Pelicci, G., Lanfrancone, L., Grignani, F., McGlade, J., Cavallo, F., and al., e. (1992). A novel transforming protein (SHC) with an SH2 domain is implicated in mitogenic signal transduction. *Cell* **70,** 93-104.

Piccolo, S., Agius, E., Leyns, L., Bhattacharyya, S., Grunz, H., Bouwmeester, T., and De Robertis, E. M. (1999). The head inducer Cerberus is a multifunctional antagonist of Nodal, BMP and Wnt signals. *Nature* **397,** 707-710.

Piccolo, S., Sasai, Y., Lu, B., and De Robertis, E. M. (1996). Dorsoventral patterning in Xenopus: inhibition of ventral signals by direct binding of chordin to BMP-4. *Cell* **86,** 589-598.

Rickmann, M., Fawcett, J. W., and Keynes, R. J. (1985). The migration of neural crest cells and the growth of motor axons throught the rostral half of the chick somite. *J Embryol Exp Morphol* **90,** 437-455.

Rijli, F. M., Mark, M., Lakkaraju, S., Dierich, A., Dolle, P., and Chambon, P. (1993). A homeotic transformation is generated in the rostral branchial region of the head by disruption of Hoxa-2, which acts as a selector gene. *Cell* **75,** 1333-49.

Ring, C., Hassel, H., and Halfter, W. (1996). Expression pattern of collagen IX and potential role in the segmentation of the peripheral nervous system. *Dev Biol* **180,** 41-53.

Rivero-Lezcano, O. M., Marcilla, A., Sameshima, J. H., and Robbins, K. C. (1995). Wiskott-Aldrich syndrome protein physically associates with Nck through Src homology 3 domains. *Mol Cell Biol* **15,** 5725-31.

Roche, S., Alonso, G., Kazlauskas, A., Dixit, V. M., Courtneidge, S. A., and Pandey, A. (1998). Src-like adaptor protein (Slap) is a negative regulator of mitogenesis. *Curr Biol* **8,** 975-978.

Rodriguez-Viciana, P., Warne, P. H., Khwaja, A., Marte, B. M., Pappin, D., Das, P., Waterfield, M. D., Ridley, A., and Downward, J. (1997). Role of phosphoinositide 3-OH kinase in cell transformation and control of the actin cytoskeleton by Ras. *Cell* **89,** 457-467.

Rosentreter, S. M., Davenport, R. W., Loschinger, J., Huf, J., Jung, J., and Bonhoeffer, F. (1998). Response of retinal ganglion cell axons to striped linear gradients of repellent guidance molecules. *J. Neurobiol* **37,** 541-62.

Sadaghiani, B. a., and Thiebaud, C. H. (1987). Neural crest development in the Xenopus laevis embryo, studied by interspecific transplantation and scanning electron microscopy. *Dev Biol* **124,** 91-110.

Sajjadi, F. G., Pasquale, E. B., and Subramani, S. (1991). Identification of a new eph-related receptor tyrosine kinase gene from mouse and chicken that is developmentally regulated and encodes at least two forms of the receptor. *New Biol* **3,** 769-78.

Sajjadi, F. G. a., and Pasquale, E. B. (1993). Five novel avian Eph-related tyrosine kinases are differentially expressed. *Oncogene* **8,** 1807-1813.

Sasai, Y., Lu, B., Piccolo, S., and De Robertis, E. M. (1996). Endoderm induction by the organizer-secreted factors chordin and noggin in *Xenopus* animal caps. *EMBO J.* **15,** 4547-4555.

Sasai, Y., Lu, B., Steinbeisser, H., and De Robertis, E. M. (1995). Regulation of neural induction by the Chd and Bmp-4 antagonistic patterning signals in *Xenopus*. *Nature* **376,** 333-336.

Sasai, Y., Lu, B., Steinbeisser, H., Geisssert, D., Gont, L. K., and De Robertis, E. M. (1994). Xenopus *chordin*: a novel dorsalizing factor activated by organizer-specific homeobox genes. *Cell* **79,** 779-790.

Scales, J. B., Winning, R. S., Renaud, C. S., Shea, L. J., and Sargent, T. D. (1995). Novel members of the eph receptor tyrosine kinase subfamily expressed during Xenopus development. *Oncogene* **11,** 1745-1752.

Schlessinger, J., and Ullrich, A. (1992). Growth factor signaling by receptor tyrosine kinases. *Neuron* **9,** 383-91.

Schmidt, J. E., Suzuki, A., Ueno, N., and Kimelman, D. (1995). Localised BMP-4 mediates dorsal/ventral patterning in the early *Xenopus* embryo. *Dev Biol* **169,** 37-50.

Schneider-Maunoury, S., Topilko, P., Seitandou, T., Levi, G., Cohen-Tannoudji, M., and al., e. (1993). Disruption of Krox-20 results in alteration of rhombomeres 3 and 5 in the developing hindbrain. *cell* **75,** 1199-1214.

Schulte-Merker, S., McMahon, A. P., and Hammerschmidt, M. (1997). The *dino* phenotype is caused by a mutation in the zebrafish *chordin* gene. .

Schulte-Merker, S., Smith, J. C., and Dale, L. (1994). Effects of truncated activin and FGF receptors and of follistatin on the inducing activities of BVg1 and activin: does activin play a role in mesoderm induction? *EMBO J.* **15,** 3533-3541.

Schultz, J., Ponting, C. P., Hofmann, K., and Bork, P. (1997). SAM as a protein interaction domain involved in developmental regulation. *Protein Sci* **6,** 249-53.

Scott, M. P. (1992). Vertebrate homeobox gene nomemclature. *Cell* **71,** 551-553.

Sechrist, J. (1993). Segmental migration of the hindbrain neural crest does not arise from its segmental generation. *Development* **118,** 691-703.

Sechrist, J. (1994). Rhombomere rotation reveals that multiple mechanisms contribute to the segmental pattern of hindbrain neural crest migration. *Development* **120,** 1777-90.

Sefton, M., Araujo, M., and Nieto, M. A. (1997). Novel expression gradients of Eph-like receptor tyrosine kinases in the developing chick retina. *Dev Biol* **188,** 363-8.

Selleck, M. A. J., and and Bronner-Fraser, M. (1995). Origins of the avian neural crest: the role of neural plate-epidermal interactions. *Development* **121,** 525-38.

Sham, M. H., Vesque, C., Nonchev, S., Marshall, H., Frain, M., and al., e. (1993). The zinc finger *krox20* regulates *HoxB2* (*Hox 2.8*) during hindbrain segmentation. *Cell* **72,** 183-86.

Sheng, M. (1996). PDZs and receptor/channel clustering: rounding up the latest suspects. *Neuron* **17,** 575-578.

Smith, A., Robinson, V., Patel, K., and Wilkinson, D. G. (1997). The EphA4 and EphB1 receptor tyrosine kinases and ephrin-B2 ligand regulate targeted migration of branchial neural crest cells. *Curr Biol* **7,** 561-70.

Smith, J. C. (1995). Mesoderm-inducing factors and mesodermal patterning. *Curr Opin Cell Biol* **7,** 856-861.

Smith, J. C., Price, B. M. J., Green, J. B. A., Weigel, D., and Herrmann, B. G. (1991). Expression of a Xenopus homolog of *Brachyury (T)* is an immediate-early response to mesoderm induction. *Cell* **67,** 79-87.

Smith, J. C., and Slack, J. M. W. (1983). Dorsalization and neural induction: properties of the organizer in *Xenopus laevis*. *J. Embryol. Exp. Morph.* **78,** 299-317.

Smith, W. C., and Harland, R. M. (1992). Expression cloning of noggin, a new dorsalizing factor localized to the Spemann organizer in Xenopus embryos. *Cell* **70,** 829-840.

Smith, W. C., Knecht, A. K., Wu, M., and Harland, R. M. (1993). Secreted noggin protein mimics the Spemann organiser in dorsalising *Xenopus* mesoderm. *Nature* **361,** 547-49.

Sobieszczuk DF, Wilkinson DG. (1999). Masking of Eph receptors and ephrins. *Curr Biol.* **9** R469-70.

Songyang, Z., Fanning, A., Fu, C., Xu, J., Marfatia, S., Chishti, A., Crompton, A., Chan, A., Anderson, J., and Cantley, L. (1997). Recognition of unique carboxyl-terminal motifs by distinct PDZ domains. *Science* **275,** 73-76.

Spemann, H. a., and Mangold, H. (1924). Uber induktion von embryonanlagen durch implantation artfremder organistoren. *Arch mikr Anat EntwMech* **100,** 599-638.

Stein, E., Cerretti, D. P., and Daniel, T. O. (1996). Ligand activation of ELK receptor tyrosine kinase promotes its association with Grb10 and Grb2 in vascular endothelial cells. *J Biol Chem* **271,** 23588-93.

Stein, E., Huynh-Do, U., Lane, A. A., Cerretti, D. P., and Daniel, T. O. (1998a). Nck recruitment to Eph receptor, EphB1/ELK, couples ligand activation to c-Jun kinase. *J Biol Chem* **273,** 1303-8.

Stein, E., Lane, A. A., Cerretti, D. P., Schoecklmann, H. O., Schroff, A. D., Van Etten, R. L., and Daniel, T. O. (1998b). Eph receptors discriminate specific ligand oligomers to determine alternative signaling complexes, attachment, and assembly responses. *Genes Dev* **12,** 667-78.

Streit, A., Lee, K. J., Woo, I., Roberts, C., T.M., J., and Stern, C. D. (1998). Chordin regulates primitive streak development and the stability of induced neural cells, but is not sufficient for neural induction in the chick embryo. *Development* **125,** 507-19.

Suter, D. M., and Forscher, P. (1998). An emerging link between cytoskeletal dynamics and cell adhesion molecules in growth cone guidance. *Current Opinion in Neurobiology* **8.**

Swiatek, P. J. a., and Gridley, T. (1993). Perinatal lethality and defects in hindbrain development in mice and homozygousfor a targeted mutation of the zinc finger gene Krox20. *Genes Dev* **7,** 2071-84.

Symons, M., Derry, J. M., Karlak, B., Jiang, S., Lemahieu, V., McCormick, F., Francke, U., and Abo, A. (1996). Wiskott-Aldrich syndrome protein, a novel effector for the GTPase CDC42Hs, is implicated in actin polymerization. *Cell* **84,** 723-34.

Tan, S. S. a. M.-K., G. (1985). The development and distribution of the cranial neural crest in the rat embryo. *Cell Tissue Res.* **240,** 403-416.

Tang, X. X., Pleasure, D. E., Brodeur, G. M., and Ikegaki, N. (1998). A varient transcript encoding an isoform of the human protein tyrosine kinase EPHB2 is generated by alternative splicing and alternative use of polyadenylation signals. *Oncogene* **17,** 521-26.

Tessier-Lavigne, M. (1995). Eph receptor tyrosine kinases, axon repulsion, and the development of topograghic maps. *Cell* **82,** 345-8.

Thanos, C. D., Goodwill, K. E., and Bowie, J. U. (1999). Oligomeric structure of the human EphB2 receptor SAM domain. *Science* **283,** 833-6.

Torres, R., Firestein, B. L., Dong, H., Staudinger, J., Olsen, E. N., Huganir, R. L., Bredt, D. S., Gale, N. W., and Yancopoulos, G. D. (1998). PDZ proteins bind, cluster and synaptically colocalise with Eph receptors and their ephrin ligands. *Neuron* **21,** 1453-63.

Ullrich, A., and Schlessinger, J. (1990). Signal transduction by receptors with tyrosine kinase activity. *Cell* **61,** 203-212.

Valenzuela, D. M., Rojas, E., Griffiths, J. A., Compton, D. L., Gisser, M., Ip, N. Y., Goldfarb, M., and Yancopoulos, G. D. (1995). Identification of the full-length and truncated forms of Ehk-3, a novel member of the Eph receptor tyrosine kinase family. *Oncogene* **10,** 1573-1580.

van der Geer, P., Hunter, T., and Lindberg, R. A. (1994). Receptor protein tyrosine kinases and their signal transduction pathways. *Ann. Rev. Cell Biol.* **10,** 251-337.

Van Vactor, D. (1998). Adhesion and signaling in axonal fasciculation. *Current Opinion in Neurobiology* **8,** 80-86.

Vogel, U. S., Dixon, R. A. F., Schaber, M. D., Diehl, R. E., Marshall, M. S., and al., e. (1988). Clonong of bovine GAP and its interaction with oncogenic *ras* p21. *Nature* **335,** 90-93.

Walter, J., Henke-Fahle, S., and Bonhoeffer, F. (1987a). Avoidance of posterior tectal membranes by temporal retinal axons. *Development* **101,** 909-913.

Walter, J., Kern-Veits, B., Huf, J., Stolze, B., and Bonhoeffer, F. (1987b). Recognition of position-specific properties of tectal cell membranes by retinal axons *in vitro*. *development* **101,** 685-696.

Wang, H. U., Chen, Z.-F., and Anderson, D. J. (1998). Molecular distinction and angiogenic interaction between embryonic arteries and veins revealed by ephrin-B2 and its receptor Eph-B4. *Cell* **93,** 741-753.

Wang, H. U. a., and Anderson, D. J. (1997). Eph family transmembrane ligands can mediate repulsive guidance of trunk neural crest migration and motor axon outgrowth. *Neuron* **18,** 383-96.

Weinstein, D. C., Rahman, S. M., Ruiz, J. C., and Hemmati-Brivanlou, A. (1996). Embryonic expression of *eph* signalling factors in *Xenopus*. *Mech. Dev.* **57,** 133-44.

Wilkinson, D. G. (1994). *Whole Mount In Situ Hybridisation of Vertebrate Embryos. Oxford,UK: Oxford University Press.* .

Wilkinson, D. G. (1995). Genetic control of segmentation in the vertebrate hindbrain. *Perspectives on Dev.Neurobiology* **3,** 29-38.

Wilkinson, D.G. (2000). Eph receptors and ephrins: regulators of guidance and assembly. *Int Rev Cytol.* **196**:177-244.

Wilkinson, D. G., Bhatt, S., Chavrier, P., Bravo, R., and Krumlauf, R. (1989). Segment-specific expression of a zinc-finger gene in the developing nervous system of the mouse. *Nature* **337,** 461-464.

Wilson, P. A., and Hemmati-Brivanlou, A. (1995). Induction of epidermis and inhibition of neural fate by Bmp-4. *Nature* **376,** 331-33.

Winning, R. S., and Sargent, T. D. (1994). *Pagliaccio*, a member of the Eph family of receptor tyrosine kinase genes, has localised expression in a subset of neural crest and neural tissues in *Xenopus laevis* embryos. *Mech-Dev* **46,** 219-29.

Winning, R. S., Scales, J. B., and Sargent, T. D. (1996). Disruption of cell adhesion in Xenopus embryos by Pagliaccio, an Eph- class receptor tyrosine kinase. *Dev Biol* **179,** 309-19.

Winning, R. S., Shea, L. J., Marcus, S. J., and Sargent, T. D. (1991). Developmental regulation of transcription factor AP2 during *Xenopus laevis* embryogenesis. *Nuc. Acids. Res.* **19,** 3709-3714.

Winslow, J. W., Moran, P., Valverde, J., Shih, A., Yuan, J. Q., Wong, S. C., Tsai, S. P., Goddard, A., Henzel, W., Hefti, F., and et-al. (1995). Cloning of AL-1, a ligand for an Eph-related tyrosine kinase receptor involved in axon bundle formation. *Neuron* **14,** 973-81.

Wizenmann, A. a., and Lumsden, A. (1997). Segregation of rhombomeres by differential chemoaffinity. *Mol Cell Neurosci* **9,** 448-59.

Xu, Q., Alldus, G., Holder, N., and Wilkinson, D. G. (1995). Expression of truncated Sek-1 receptor tyrosine kinase disrupts the segmental restriction of gene expression in the Xenopus and zebrafish hindbrain. *Development* **121,** 4005-16.

Xu, Q., Alldus, G., Macdonald, R., Wilkinson, D. G., and Holder, N. (1996). Function of the Eph-related kinase rtk1 in patternng of the zebrafish forebrain. *Nature* **381,** 319-322.

Xu, Q., Mellitzer, G., Robinson, V., and Wilkinson, D. W. (1999). *In vivo* cell sorting in complementary segmental domains mediated by Eph receptors and ephrins. *Nature* **399,** 267-270.

Yamanashi, Y., and Baltimore, D. (1997). Identification of the Abl- and rasGAP-associated 62 kDa protein as a docking protein, Dok. *Cell* **88,** 205-211.

Zimmerman, L. B., De Jesus Escobar, J. M., and Harland, R. M. (1996). The Spemann organizer signal noggin binds and inactivates bone morphogenetic protein 4. *Cell* **86,** 599-606.

Zipkin, I. D., Kindt, R. M., and Kenyou, C. J. (1997). Role of a new Rho family member in cell migration and axon guidance in C.elegans. *Cell* **90,** 883-894.

Zisch, A. H. (1998). Complex formation between EphB2 and Src requires phosphorylation of tyrosine 611 in the EphB2 juxtamembrane region. *Oncogene* **16,** 2657-70.

Zisch, A. H., Stallcup, W. B., Chong, L. D., Dahlin-Huppe, K., Voshol, J., Schachner, M., and Pasquale, E. B. (1997). Tyrosine phosphorylation of L1 family *adhesion* molecules: implication of the Eph kinase Cek5. *J Neurosci Res* **47,** 655-65.

Stern CD, Sisodiya SM, Keynes RJ.: Interactions between neurites and somite cells: inhibition and stimulation of nerve growth in the chick embryo, *J Embryol Exp Morphol.* (1986): 91:209-26.

ACKNOWLEDGEMENTS

'...It was a magnificent car; it could hold the road like a boat holds on water..."Think if you and I had a car like this what we could do. Do you know there's a road that goes down Mexico and all the way to Panama?-and maybe all the way to the bottom of South America where the Indians are seven feet tall and eat cocaine on the mountainside? Yes! You and I Sal, we'd dig the whole world with a car like this because, man, the road must eventually lead to the whole world. Ain't nowhere else it can go-right?""

On The Road, Jack Kerouac.

These past years have been great. Gifted people in excellent labs-my cup has indeed runneth over! Thanks to all my lab colleagues who have been sources of inspiration, advice, humour, kindness, insults, parties and the loss of my sanity.

My supervisors, Dr. Jim Smith and Dr. David Wilkinson, have had a hard time. Yours truly is endowed with the ability to frustrate even the most patient and sympathetic of souls, in my case, Jim and Dave. Thank you both for providing me with the opportunities I have had, for your help, your perseverance and for giving me the chance to be a member of your respective labs .
Kathy, Emmanuel, Nina and "MuzZ-BomB" - thanks for your friendship, common-sense and honesty. Not forgetting the sunshine given by my lab neighbours: Simon "bad jokes" Bullock, Mehul "the smile" Dattani, Tristan "Lionel Ritchie" Rodriguez and Sven "Kaleidoscopic Encounters of the Turing Kind" Pfeiffer. Thanks to you all for putting up with my moods, incessant rambling and in your collective opinions, my appalling humour.

A sigh of relief to/from Meera "please don't mention your old school again" Ravel and Geoffrey "big feet" Ingram. Thanks to my oldest and manic-depressive mates who have suffered with me for years: my severest critics and my kindest critics who forever remind me to remember reality.

My two erstwhile lab co-habitees - sweet Elena "smug-girl/ don't talk to me, I'm in a bad mood" Casey and M.A.D. (Magnificent Austrian Doctor) Walter "space cadet" Lerchner. You have both given me hours of insanity and laughter in our happy, stimulating and madcap lab. I will remember your relentless whinging usually due to my apparently terrible music taste: R.E.M are wonderful. Your intellectual inability to accept this has made me a better person and sympathetic to your imperfections.

Elena: thanks for the lab advice, wanted or not. I prostrate before your stratospheric intellect and cower to NIMR's resident 'Hello' magazine gossip queen. Keep smiling and thanks - it's been a pleasure.

Kind, thoughtful, messy and infuriating Walter: I won't mention radioactivity - it upsets me. I shall miss your ethereal presence and those masterful attempts, amid Earth's chaos, to maintain the serenity of your parallel world. This feat was rarely obvious when you were attempting experiments or racing, literally, to international meetings. Past shouts of "Walter!" being screamed down the corridor still echo in my ears. But Walter don't change: you are irreplaceable...and irredeemable - Elena and I tried but Vienna said "NO!"

Finally, thanks to my family. To my brother Adam for providing the (I'm sure) kindly meant torment, exasperation and frustration....and some timely comedy: the jokes, the fashion attempts and erratic dancing - You are priceless. Most thanks however, are for my parents. They have always been there, providing me with both stability and support. I hope that this thesis is a small testament for their years of selflessness, care and enthusiasm.

I guess I got here in the end!

Thank you to Sir John Skehel and the National Institute for Medical Research, The Ridgeway, Mill Hill, London NW7 1AA, UK. Financial support was received from the Medical Research Council.